THE INTERACTION BETWEEN WATER MOVEMENT, DIFFUSION BOUNDARY LAYERS, PHOSPHATE UPTAKE AND PHOSPHATE LIMITED GROWTH OF *Ulva australis*.

Patrick William Hone B.Sc. (Hons)

Botany Department

The University of Adelaide

Submitted for the degree of

Doctor of Philosophy, October, 1988.

To my wife, my best friend, Susan.

DECLARATION

This thesis contains no material which has been accepted for the award of any other degree or diploma in any University. To the best of my knowledge and belief this thesis contains no material previously published or written by any other person except where due reference is made in the text.

Patrick William Hone.

ACKNOWLEDGEMENTS

I would like to thank Dr. F.A. Smith for his patience, supervision and advice, which was not always easy considering the nature of the student. I should also like to thank Dr. G.G. Ganf for the time he devoted for some very helpful discussion and objective critism. Further, the members of the FAS lab over the period of this thesis have all contributed to stimulating discussions and helpful advice on a wide range of topics, they include Jane Bromely, Mark Tester, Robert Reid, John Whitington and Alan Walker. The technical staff in the Botany Department have also given freely of their time, in particular, Brian Rowland's considerable and underestimated skills in helping to construct some wonderful equipment and Anthony Fox for all his help in procuring the right equipment. This thesis would not have materialised or been attempted if not for the wonderful support I received from my parents. Finally, to my wife, Susan, for the hours correcting, collating, preparing graphs, for an incredible amount of moral support, and believing that I could do it.

ABSTRACT

The processes of phosphate transport to the thallus surface of *Ulva australis* and across the plant membrane have been studied in conjunction with the changes in its growth rate and variations in the diffusion boundary layer resistance, which was manipulated by altering the water velocity relative to the plants. Further, the growth of *U. australis*, in conditions where phosphate was growth limiting, was empirically modelled in an attempt to provide a predictive means of quantifying the observed results and the resultant interactions between the different processes studied. The short term phosphate influx was found to be affected by the rate of water movement, and could be predicted by the Briggs-Maskell equation which combined the phosphate transport processes through the diffusion boundary layer and across the plant membrane. Originally it was hypothesized that diffusion limitation of $H_2PO_4^-$ would control the overall phosphate transport, but the predicted values underestimated the observed results. It was concluded that the simultaneous diffusive flux of HPO_4^{2-} was effectively increasing the concentration of $H_2PO_4^-$ at the plant's surface, short circuiting the mass transport resistance for $H_2PO_4^-$. The observed effect of water movement on short term phosphate influx was predicted to effect the growth rate of *U. australis*, however, field collected plants with limited preconditioning did not show a significant difference in growth rate with changes in water movement. It was concluded that plants collected from the field were not sufficiently starved of phosphate to make their growth dependent on phosphate influx, and further, the growth variation inherent in field collected plants made it difficult to establish the growth response of plants to water movement. By preconditioning plants in a more controlled environment and only selecting plants for experimental use that had approximately

uniform growth rates, it was found that a significant increase in growth rate was observed between different water movement treatments. A combination of the Droop growth equation and the Briggs-Maskell equation approximately predicted the observed results, however, they could not explain the variation in phosphate uptake which correlated with the observed changes in the cellular total phosphate concentration. Short term phosphate influx was found to increase when the cellular total phosphate concentration decreased, however, phosphate uptake (averaged phosphate uptake between experimental growth measurement times) varied in its response to phosphate starvation. The enhancement of phosphate influx by phosphate starvation could be modelled empirically by either an exponential model or an un-competitive enzymic model, both based on the observed concurrent increase in Km and Vm with increasing phosphate starvation. The results have been discussed in relation to the problems that occur in trying to empirically derive models for singular processes without taking into account the interactive effects between different processes.

CHAPTER 1. INTRODUCTION

The usual approach in the field of biophysics has been to study one mechanism in relation to metabolism for a relatively "simple" biological system. This approach has resulted in the elucidation of the mechanics of metabolism that constitute the life processes of a variety of organisms. However, it fails to comprehend how the interaction of various physical and metabolic mechanisms can lead to a modification of the overall mechanics of the system being studied; for example, by studying the mechanics of nutrient uptake without reference as to how the growth rate can influence its kinetics. This approach has often led to broad based assumptions about the significance these mechanisms have in an ecological context, which often goes far beyond the experimental conditions under which the mechanisms were elucidated.

The disadvantages of this approach also apply to the advances in mathematical analogs of living processes through computer modelling. These analogs require a more detailed understanding of the inter-relationships between the different metabolic processes, as the models become more precise, wider in their application and provide a greater predictive tool in understanding what will occur given a specific set of conditions.

An understanding of plant nutrition requires a knowledge of the controlling effect that nutrient transport up to and into the cells has on the growth rate. Previous research has shown that the rate of diffusion to the cell's surface through the external solution can limit the rate of nutrient uptake (Smith and Walker, 1980). The magnitude of this resistance to nutrient diffusion and its comparative limitation on nutrient uptake, requires a knowledge of the physical processes external to the cell which control its rate. Increasing the water or air movement

relative to the plant's surface can decrease the resistance associated with the diffusion transport, and therefore can exert a controlling influence on plant growth (for examples see Gavis, 1976; Grace,1977). For plants growing in water the effect is more pronounced because of the slower rate of diffusion compared to air (Leyton, 1975).

By studying in tandem the mechanisms of phoshate diffusion, phosphate uptake and growth, and also the effect of increasing water movement on these mechanisms for *Ulva australis*, it is the aim of this thesis to determine how these processes interact and what significance this interaction has to the overall process of plant nutrition. Before detailing the effects of these processes on plant growth rate, the mechanical concepts of nutrient diffusion limitation and uptake in series will be introduced.

1.1 TERMINOLOGY

Water movement can be divided into two components: firstly forced convection, which results when the fluid is moved by an external force (e.g. wind, tidal forces, or mechanical disturbance); secondly, free convection results when the fluid or individual molecules are moved by variations in density which can occur as a result of a concentration and or temperature gradient (Tobias, Eisenberg and Wilke, 1952; Leyton, 1975). For the purposes of this thesis it is assumed that no variations in temperature occur within the fluid. The consequence of this is that free convection is then equivalent to the diffusive flux.

The term transport is used here to indicate the movement of nutrients, reactants or products between any two points.

For convenience and consistency, Levich's (1962) terminology to describe boundary layers is used.

1.2 THE BOUNDARY LAYER CONCEPT

Anyone who has ever had a bath will be aware of the phenomenon whereby the water immediately adjacent to your body is cooler than the surrounding water. However, by mixing the water by moving your body you can effectively increase the apparent temperature of the water. This phenomenon of zoning in fluids adjacent to objects can occur for different processes (e.g. temperature, momentum, concentration) all with their own physical attributes, and all of different importance as to how the object perceives and reacts to their presence.

This zone adjacent to the object is termed the boundary layer. For an overview of the boundary layer phenomenon as it applies to the various fields of biological science see the reviews by Briggs and Robertson (1948), Munk and Riley (1952), Levich (1962), Dainty and House (1966), Engaser and Horvath (1974), Leyton (1975), Gavis (1976), Thomson and Dietschy (1977), Smith and Walker (1980), Vogel (1981), Barry and Diamond (1984) and LaBarbera (1984).

1.2.1. DESCRIPTION OF THE HYDRODYNAMIC BOUNDARY LAYER

As any fluid passes over an object there is a zone next to the object where the fluid's velocity is retarded by the shearing forces associated with the fluid-object boundary. This zone of reduced velocity is termed the hydrodynamic boundary layer (H.B.L.), due to its association with a loss of fluid particle momentum. Outside the H.B.L. the bulk fluid acts as if it is an ideal fluid passing the object.

At the surface of the fluid-object boundary the fluid velocity is zero relative to the object, because the fluid particles attain the same velocity as the object (the no-slip condition associated with continuum flow). The result of this condition is the development of a velocity gradient between the object's surface and the bulk flow.

For the case of a flat plate parallel to the direction of flow (Figure 1.1), at the leading edge there is a sharp transition between the bulk-flow velocity and that of the plate's, creating a steep velocity gradient. As the flow proceeds downstream along both sides of the plate the shearing force will retard the fluid particles at the object's surface and these particles in turn will retard other adjacent particles further out. Therefore the H.B.L. will grow in thickness on both sides of the plate in the downstream direction with a consequent reduction in the steepness of the velocity gradient (Figure 1.1). The H.B.L. will continue to thicken until its thickness becomes unstable with the result that the flow develops turbulence. The advent of turbulence reduces the shearing stress, hence the H.B.L. thickness increases at this point (Figure 1.1).

From the above description the H.B.L. can exist in either of two states, namely laminar or turbulent. The development of turbulence depends on; firstly, the flow characteristics of the bulk solution (that is, whether it is laminar or turbulent); secondly, the magnitude of the Reynolds number (1883)

$$Re = \frac{U_b x}{\nu} \qquad \text{Equ-1.1}$$

where U_b is the velocity of the bulk flow, x is the downstream length from the leading edge of the plate and ν is the kinematic viscosity of fluid. Thirdly, the roughness of the plate can induce turbulence depending on the height the projections extend into the flow.

The important point about the Reynolds number is that it works out to be the ratio of inertial and viscous forces, and as a consequence it is dimensionless (Vogel, 1981). The onset of turbulence occurs when the inertial force predominates over the viscous force. When this occurs the Reynolds number reaches a critical magnitude (Recr). When the bulk flow turbulence is low and the object's surface is smooth, transition may not

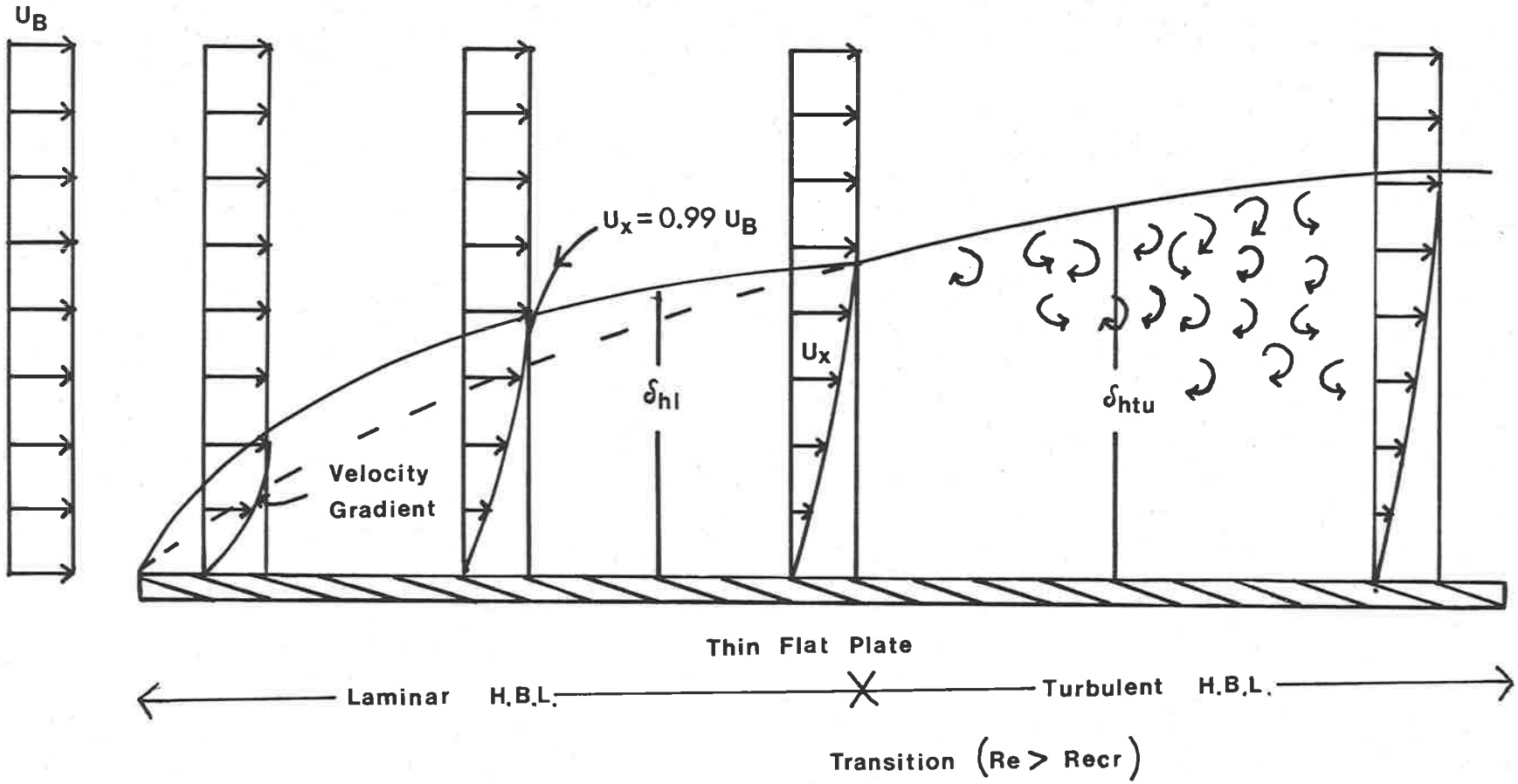

Figure 1.1. The H.B.L. over the top side of a flat plate showing the change from laminar to turbulent flow. Where the arrows represent the magnitude of the water velocity, U_x is the water velocity x distance from the plate's surface.

occur until Recr > 10^6 to 3 x 10^6 (Levich, 1962). This in reality is often not the case, as the bulk flow is always turbulent to some degree under natural conditions, and the surface rarely smooth. A more workable condition is when Recr > 1 x 10^5 (Leyton, 1975; Vogel, 1981).

The next two sections deal quantitatively with the H.B.L. for the cases when it is either laminar or turbulent.

1.2.1.1. LAMINAR HYDRODYNAMIC BOUNDARY LAYER FOR A FLAT PLATE

Prandtl (1905) in 1904 first postulated the essence of the H.B.L., but it was not until 1908 that Blasius (1908), a student of Prandtl's, obtained a solution for the thickness of a laminar H.B.L. along a flat plate (assuming a zero pressure gradient).

$$\delta_{hl} = 5 \times Re^{-\frac{1}{2}} \qquad \text{Equ-1.2}$$

where δ_{hl} represents the thickness of the laminar H.B.L. When by convention the laminar H.B.L. velocity is 99% that of the bulk flow velocity (U_b), and x is the downstream length, this solution has been shown to be valid experimentally, except very near the leading edge (Levich, 1962).

1.2.1.2. TURBULENT HYDRODYNAMIC BOUNDARY LAYER FOR A FLAT PLATE

The problem with trying to find a relationship that adequately describes the turbulent H.B.L. is that no expression can as yet fit the experimentally derived velocity distribution within the turbulent H.B.L. The reason for this is the flow characteristics of turbulence, and the modifying influence the boundary between the fluid and the object has on dampening the scale of turbulence.

To account for this Von Karman (1954) proposed three phases within the turbulent H.B.L.: (1) the outer turbulent flow which comprises 90% of the effective thickness of the turbulent H.B.L., (2) a buffer layer in which the large scale eddies associated with turbulence are damaged, (3) the laminar sublayer, where according to Von Karman the flow is purely laminar (Figure 1.2a).

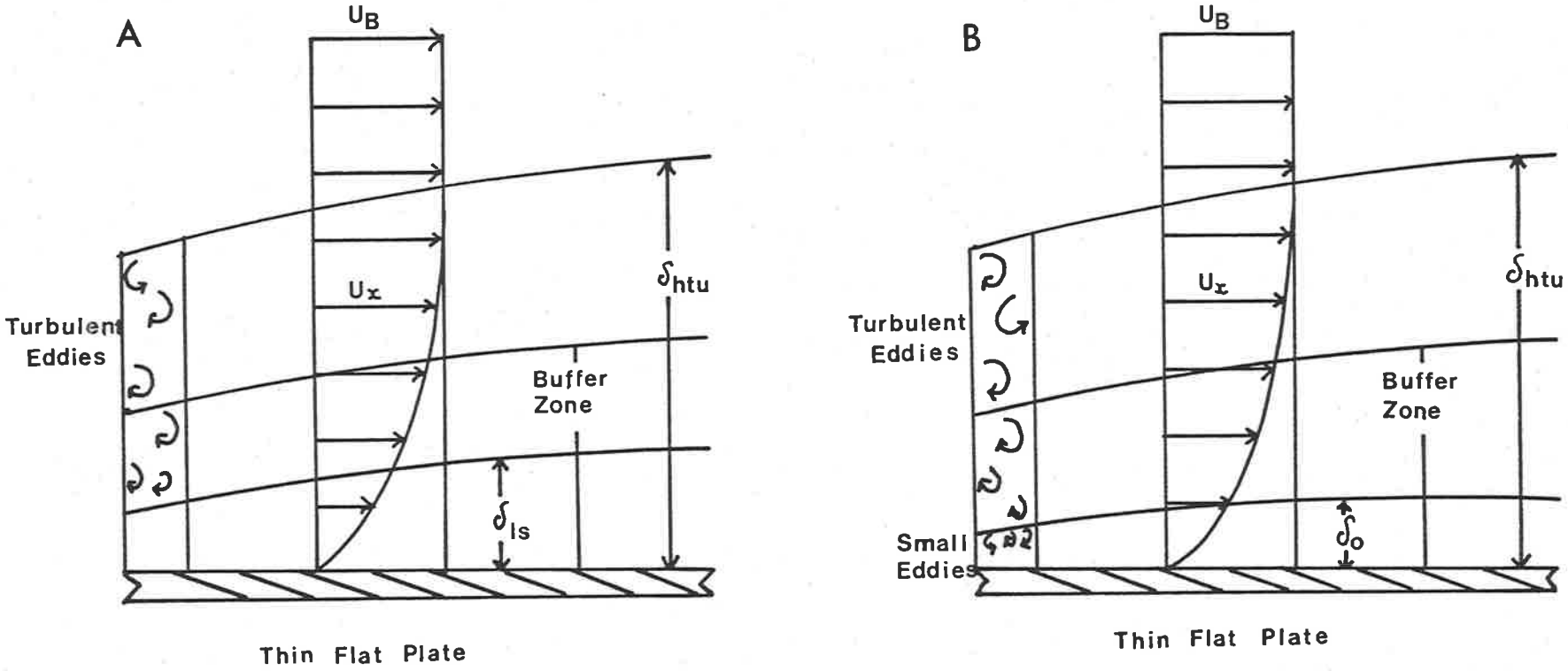

Figure 1.2. (A) Von Karman (1954) model of turbulent flow next to a flat plate. The buffer zone represents the region where the turbulent eddies are completely damped.
(B) Levich (1962) model of turbulent flow next to a flat plate. δo is the region in which the small turbulent eddies are damped (figure adapted from Levich, 1962).

The overall thickness of the turbulent H.B.L. (δ_{htu}) over a flat plate is given by Leyton (1975) and Roberson and Crowe (1980)

$$\delta_{htu} = 0.376\ x_{tu}\ Re^{-0.20} \qquad \text{Equ-1.3}$$

where x_{tu} is the distance from the beginning of the turbulence.

Leyton (1975) has derived an expression for the thickness of the laminar sublayer (δ_{ls}) based on

$$Uo = (\tau\rho^{-1})^{\frac{1}{2}} \qquad \text{Equ-1.4}$$

where Uo is the shear velocity, τ is the local shear stress and ρ is the density of the fluid. The local shear stress can be expressed as

$$\tau = 0.029\ \rho\ U_b^2\ Re^{-0.20} \qquad \text{Equ-1.5}$$

Substituting equations 1.4 and 1.5 into the expression for δ_{ls}

$$\delta_{ls} = \frac{10\nu}{Uo} \qquad \text{Equ-1.6}$$

the result is

$$\delta_{ls} = 58\ x\ Re^{-0.9} \qquad \text{Equ-1.7}$$

The problem with Equation 1.7 is that it applies to the inside of a pipe which Leyton (1975) thought was a reasonable approximation. Roberson and Crowe (1980) give an alternative expression for Equation 1.6 for the case of a flat plate

$$\delta_{ls} = \frac{5\nu}{Uo} \qquad \text{Equ-1.8}$$

which is simplified in the same manner, to

$$\delta_{ls} = 29\ x\ Re^{-0.9} \qquad \text{Equ-1.9}$$

Levich (1962) opposes the concept that the laminar sublayer is in fact laminar. Levich's theory is that the small scale eddies associated with turbulence extend into the laminar sublayer. To account for this Levich (1962) defined a more realistic layer termed the viscous sublayer (Figure 1.2b). To determine the thickness of the viscous sublayer (δo) the Reynolds number for the eddies (Re) must be approximately unity

$$Re_l = \frac{Uo\ l}{\nu} = \frac{Uo\delta o}{\nu} \cong 1 \qquad \text{Equ-1.10}$$

where l is the characteristic length of the eddies.

Therefore

$$\delta o = a \frac{Uo}{\nu} \qquad \text{Equ-1.11}$$

Equation 1.1. is similar to equations 1.8 and 1.6, except for the proportionality constant a. The value of a, relates to the slope of the logarithmic velocity profile and was determined experimentally to be approximately unity (Levich, 1962). However as the external bulk flow increases in turbulence the value of a increases.

Equation 1.9 then according to Levich (1962) is better expressed as

$$\delta o = 5.8 \times Re^{0.9} \qquad \text{Equ-1.12}$$

The next section deals with the extent to which the laminar H.B.L. and viscous sublayer effect molecular movement to the object's surface, and also the limitations this effect has on a reaction at the object's surface.

1.2.2. DESCRIPTION OF THE DIFFUSION BOUNDARY LAYER

The foregoing descriptions of the laminar and turbulent H.B.L. has introduced the concept that next to each object's surface is a zone where the forced convection is purely laminar in nature. The streamlines associated with forced convective laminar flow do not cross, and by definition no molecular transfer occurs normal to the flow direction.

If we generalize to a liquid solution containing a single dissolved solute flowing over a flat plate, at the surface of which an infinitely fast heterogeneous reaction is removing the solute from solution.

This results in a concentration gradient developing normal to the object's surface and as a consequence a molecular diffusive flux (free convection) normal to the surface. As shown in Figure 1.1 the velocity gradient at the leading edge is extremely abrupt, consequently the concentration at this point is essentially that of the bulk solution. Further downstream the H.B.L. increases in width and the concentration

gradient becomes less steep (Figure 1.1), resulting in a zone of reduced concentration within the H.B.L. This zone is called the diffusion boundary layer (D.B.L.) (Levich, 1962) and ranges in thickness from 5 to 500 μm, for well stirred to calm solutions (Dainty, 1963; Dainty and House, 1966; Sha'afi, Rich, Sidel, Bossert and Solomon, 1967; Everitt, Redwood and Haydon, 1969; Green and Otori, 1970; Wilson and Dietschy, 1974). Originally this zone was considered to be static with regard to flow (Nernst, 1904; Barry and Diamond, 1984) which led to the use of the term "unstirred layer" to describe this phenomenon. In fact laminar motion has been observed to persist to within 0.625 μm (Fage and Townend, 1932) of the surface, well within the D.B.L. This has led to the more accepted description that flow within the D.B.L. is very slow and laminar (Dainty, 1963; Smith and Walker, 1980).

We can simplify this description, by firstly considering molecular transport by force convection separately from free convection. The rate of forced convection (molecular transport) parallel and next to the surface (x direction, Figure 1.3) is insufficient with regard to the surface reaction. The solute concentration in the forced convection streamlines next to the object's surface, will be increasingly reduced downstream from the leading edge. At some point along the surface, if only this flow process was to occur, the concentration of the solute would equal zero. However, if this process is then coupled with the molecular diffusive flux normal to the surface (Figure 1.3), the solute will be depleted from streamlines further from the surface. As the flow proceeds downstream over the plate, the thickness of the depleted zone will increase as the two flow mechanisms provide solute for the reaction at the surface. Equilibrium will be eventually established over the plate between the two flow processes with a concentration gradient

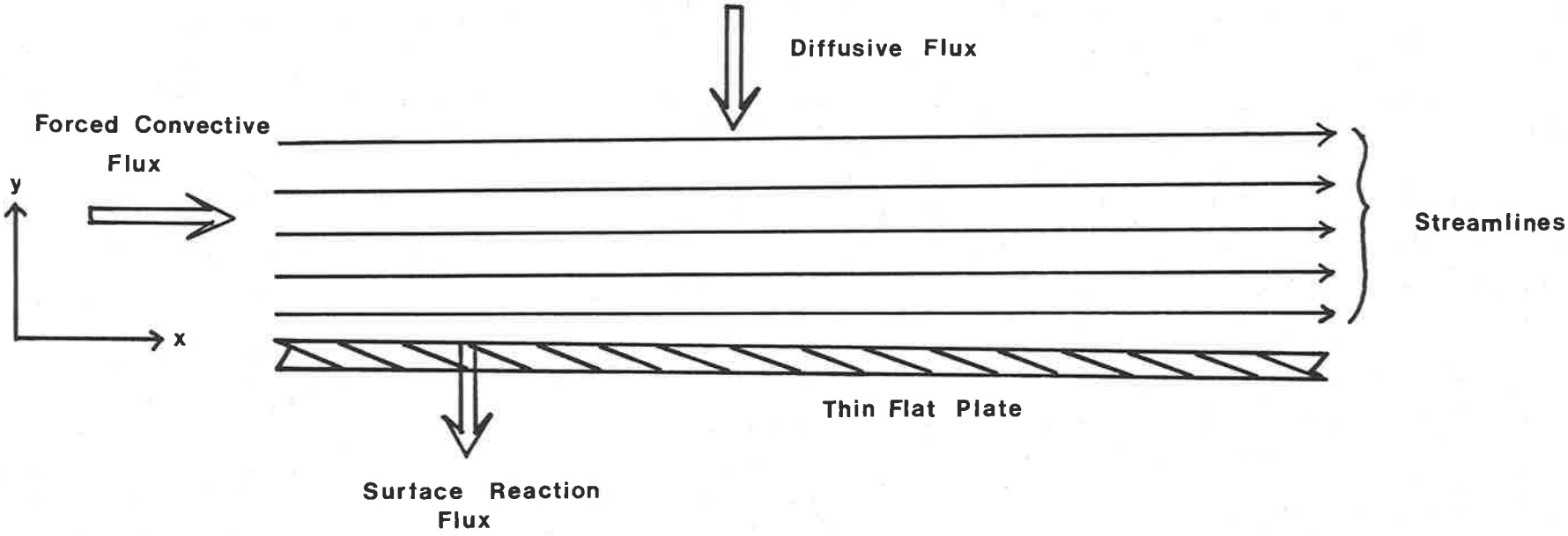

Figure 1.3. A diagrammatic representation of water flow flow close to the surface of a flat plate within the D.B.L.. The plate is shown as having a reaction at its surface which is removing solute from the surrounding medium, and the solute is being replaced at the surface by a combination of the forced convective flux (parallel) and the the diffusive flux (normal).

developing in the same for as the H.B.L. The time (t) required for equilibrium to be established is expressed as

$$t = \text{constant } \frac{\delta^2}{D} \qquad \text{Equ-1.13}$$

where δ is the thickness of the D.B.L., D is the diffusion coefficient, and the constant varies from 1 (Levich, 1962) to 0.37 (Smulders and Wright, 1971; Wilson and Dietschy, 1974). The thickness of the D.B.L. over the flat plate is then determined by the magnitude of the two flow processes.

Analagous to the Reynolds number for forced convection is the Peclet number (Pe) for free convection

$$Pe = \frac{U_b x}{D} \qquad \text{Equ-1.14}$$

The ratio of these two dimensionless quantities determines which of the two flow processes has the most significant effect on the reaction at the surface. This ratio is called the Schmidt number (Sc)

$$Re : Pe = \frac{V}{D} = Sc \qquad \text{Equ-1.15}$$

or sometimes referred to as the Prandtl number[1] (Leyton, 1975). When $V \cong D$ as is the case for air [$V = 1.51 \times 10^{-5}$ m^2 s^{-1} at 20°C, $D = 1.59 \times 10^{-5}$ m^2 s^{-1} at 20°C (Leyton, 1975)] the rate of molecular transport due to forced convection and the diffusive flux are equivalent. The H.B.L. and D.B.L. coincide in thickness for this case.

However for water the diffusion coefficient is 10,000 times slower than in air and 1,000 times slower than the kinematic viscosity for water. Consequently forced convection is far more important for molecular transport in liquids. That is, even small disturbances due to

---

(1) Interchanged because of the direct analogy between heat and mass transfer.

forced convection are far more effective in transporting solute than the diffusive flux in liquids. This has the effect of reducing the thickness of the D.B.L. relative to the H.B.L. or viscous sublayer.

The above description of the D.B.L.'s development depends on certain assumptions about the boundary conditions at the plate's surface and in the bulk solution. The next section deals with the quantitative basis of these boundary conditions. The successive three sections deal with the physical determinates controlling the thickness of the D.B.L. under laminar, turbulent or stationary conditions.

1.2.2.1. QUANTITATIVE DESCRIPTION OF THE BOUNDARY CONDITIONS FOR THE DIFFUSION BOUNDARY LAYER

The concentration in the bulk of the solution (Cb) is considered homogeneous and is described by the following conditions:

$$C \rightarrow Cb \quad \text{as} \quad y \rightarrow \delta \qquad \text{Equ-1.16}$$

or

$$C = Cb \quad \text{as} \quad y \rightarrow \infty \qquad \text{Equ-1.17}$$

where C is the concentration y distance from the reaction surface.

The boundary conditions at the reacting surface are more complex, being determined by either the rate of the reaction or the flux due to diffusion. To determine the surface boundary conditions, the diffusive flux across the D.B.L. can be expressed using a combination of Fick's first law (1855) and Nernst's theory (1904) as

$$J = \frac{d\ (Cb - Cs)}{\delta} \qquad \text{Equ-1.18}$$

where J is the diffusive flux from the bulk concentration (Cb) to the concentration at the object's surface (Cs). Simplifying Equation 1.18 in terms of a rate constant,

$$J = Kt\ (Cb - Cs) \qquad \text{Equ-1.19}$$

where Kt $(= \frac{D}{\delta})$ is the mass transfer coefficient $(m\ s^{-1})$, and its reciprocal is the mass transfer resistance, Rt $(s\ m^{-1})$.

For a heterogeneous chemical reaction at the surface, the rate of the reaction (Vc) is described by the general reaction low,

$$Vc = Kc\ (Cs)^n \qquad \text{Equ-1.20}$$

where Kc is the reaction velocity constant for the given physical conditions and n refers to the order of the chemical reaction.

When equations 1.19 and 1.20 are at a steady state and the chemical reaction is first order (n = 1) then,

$$Kt\ (Cb - Cs) = Kc\ (Cs) \qquad \text{Equ-1.21}$$

solving for Cs

$$Cs = \frac{Kt\ \ Cb}{Kc + Kt} \qquad \text{Equ-1.22}$$

and substituting Equation 1.22 into Equation 1.19

$$J = Kt\ \left(Cb - \frac{Kt\ Cb}{Kc + Kt}\right) \qquad \text{Equ-1.23}$$

which can be simplified to

$$J = \left(\frac{KtKc}{Kt + Kc}\right) Cb \qquad \text{Equ-1.24}$$

or $$J = Kapp\ (Cb) \qquad \text{Equ-1.25}$$

where $$Kapp = \left(\frac{KtKc}{Kt + Kc}\right)$$

is the apparent overall reaction velocity constant.

The importance of this type of expression (Equation 1.25) is that the three possible rate limiting steps can be distinguished and also the surface boundary conditions (Bircumshaw and Riddiford, 1952; Levich, 1962; MacFarlane, 1985; MacFarlane and Raven, 1985).

(1) When Kt >> Kc (slow chemical reaction velocity) therefore Kapp ≅ Kc, and the overall reaction rate is determined by the rate of the chemical reaction. Under this condition $\frac{dC}{dy} \cong 0$ at the boundary surface, (that is the concentration in the entire solution) is constant, therefore

$$Cs = Cb \qquad \text{Equ-1.26}$$

(2) The converse case when Kc >> Kt then Kapp ≅ Kt and the overall reaction rate is determined by the diffusive flux to the surface. The surface boundary condition becomes

$$Cs = 0 \qquad \text{Equ-1.27}$$

It is under this condition that a fully developed D.B.L. occurs, and the overall reaction rate depends on the thickness of the D.B.L. which can be manipulated by the external velocity. The quantitative dependence of δ on the external velocity will be examined in Section 1.2.2.2.

(3) For the intermediate case where Kt ≅ Kc, then neither the heterogeneous chemical reaction nor the diffusive flux selectively control the overall rate process. Rather a combined resistance equal to 1/Kapp controls the overall process. The surface boundary condition becomes

$$Cb > Cs > 0 \qquad \text{Equ-1.28}$$

Under this condition the thickness of the D.B.L. is not only dependent on the external physical factors but also on the velocity of the chemical reaction (Levich, 1962).

This type of analysis will be extended later for the case where the reaction at the surface is of the Michaelis-Menten type (Section 1.3).

1.2.2.2. QUANTITATIVE DESCRIPTION OF THE DIFFUSION BOUNDARY LAYER FOR A FLAT PLATE

1.2.2.2.1. LAMINAR FLOW

As previously mentioned the D.B.L. is related to the H.B.L. by the Schmidt number,

$$\delta_l \cong \delta_{hl} (S_c)^{-0.33} = \delta_{hl} \left(\frac{\upsilon}{D}\right)^{-0.33} \qquad \text{Equ-1.29}$$

where δ_l is the thickness of the laminar D.B.L. Substituting Equation 1.2 for δ_{hl}

$$\delta_l \cong 5\, x^{0.5}\, \upsilon^{0.166}\, D^{0.33}\, U_b^{-0.5} \qquad \text{Equ-1.30}$$

or in terms of the dimensionless Reynolds and Prandtl numbers,

$$\delta_l \cong 5 \times Re^{-0.5} Sc^{-0.33} \qquad \text{Equ-1.31}$$

Levich (1962) has solved δ_l more exactly for the case of a flat plate,

$$\delta_l \cong 3 \times Re^{-0.5} Sc^{-0.33} \qquad \text{Equ-1.32}$$

where the boundary condition at the surface is given by Cs = 0. The consequence of Equation 1.32, is that for liquids the laminar D.B.L. thickness is far smaller than the laminar H.B.L. thickness. Further δ_l is inversely related to the square root of U_b, so by altering U_b the diffusive flux can be manipulated. The expression for the diffusive flux under laminar (J_l) conditions is developed by substituting Equation 1.32 into Equation 1.18 ($C_s = 0$)

$$J_l \cong 0.34 \, x^{-1} \, D \, Cb \, Sc^{-0.33} \, Re^{-0.5} \qquad \text{Equ-1.33}$$

The average thickness of the laminar D.B.L. $\bar{\delta}_{lx}$, for a flat plate of length x is given by 0.5 δ_{lx} where δ_{lx} is the thickness of the laminar D.B.L. at a distance x along the plate (MacFarlane, 1985).

1.2.2.2.2. TURBULENT FLOW

The development of the D.B.L. under turbulent conditions is dependent on that area within the turbulent H.B.L. that is characterized by laminar flow. The problem with this is that as mentioned in section 1.2.1.2 there are two differing theories on the extent to which the turbulent eddies approach the plate's surface. As a result the thickness of the turbulent D.B.L. (δ_{tu}) varies depending on the theory used.

The first theory states that in the laminar sublayer, turbulent eddies disappear altogether so that mass transport normal to the surface is by diffusion only (Table 1a). The thickness of the turbulent D.B.L. (δ_{tu}) is then given approximately by

$$\delta_{tu} \cong \delta_{ls} \left(\frac{\nu}{D} \right)^{-0.33} \qquad \text{Equ-1.34}$$

TABLE 1.1a.[a] Von Karmen (1954) model of turbulent flow

Zone Number	Value of the normal coordinate y	Characteristics of the zone	Mechanism of transfer		Law of concentration distribution[b]
			of momentum	of mass	
I	$y > \delta_{htu}$	Developed turbulence	Turbulent	Turbulent	$C_I = C_b = \text{constant}$
II	$\delta_\lambda < y < \delta_{htu}$	Turbulent H.B.L.	Turbulent	Turbulent	$C_{II} = \frac{J}{\beta V_o} \ln \frac{y}{\delta_{htu}} + c_b$
III	$0 < y > \delta_{hs}$	Laminar sublayer	Molecular viscosity	Molecular diffusion	$C_{III} = \frac{J}{\Delta} y$

(a) Table adapted from Levich (1962).
(b) Where C_I, C_{II}, and C_{III} refer to the concentration distribution for their associated zones.
(c) β is a constant ($\simeq 1$).

TABLE 1.1b.[a] Levich (1962) model of turbulent flow

Zone Number	Value of the normal coordinate y	Characteristics of the zone	Mechanism of transfer of momentum	Mechanism of transfer of mass	Law of concentration distribution[b]
I	$y > \delta_{htu}$	Developed turbulence	Turbulent	Turbulent	$C_I = C_b = \text{constant}$
II	$\delta_o < y < \delta_{htu}$	Turbulent H.B.L.	Turbulent	Turbulent	$C_{II} = \frac{J}{\beta V_o} \ln \frac{y}{\delta_{htu}} + C_b$
III	$\delta < y < \delta_o$	Viscous sublayer	Small scale turbulent eddies	Small scale turbulent eddies	$C_{III} = -\frac{J\delta_o^3}{3\gamma V_o} \frac{1}{y^3} + a_2$
IV	$0 < y < \delta$	Turbulent D.B.L.	Molecular viscosity	Molecular diffusion	$C_{IV} = \frac{J}{\Delta} y$

(a) Table adapted from Levich (1962).
(b) a_2 is a constant of integration, β is a constant ($\simeq 1$) and γ is a constant ($\simeq 1$).

The second theory by Levich (1962) disagrees with the view that the turbulent eddies suddenly disappear (Table 1b). Levich's relationship between δ_{tu} and δo is then given by

$$\delta_{tu} \cong \delta o \left(\frac{\upsilon}{D} \right)^{-0.25} \qquad \text{Equ-1.35}$$

Experimental evidence points to the second theory being a more accurate description of turbulent motion (Levich, 1962; Schlichting, 1968; Cebeci and Smith, 1974).

Substituting Equation 1.12 into Equation 1.35 we obtain

$$\delta_{tu} \cong 5.8 \; a \; x \; Re^{-0.9} \; Sc^{-0.25} \qquad \text{Equ-1.36}$$

Levich (1962) has solved Equation 1.35 for the case of a flat plate[1] ($C_s = 0$),

$$\delta_{tu} = 5.24 \; \alpha \; D^{0.25} \; U_b^{-0.9} \; \upsilon^{0.65} \; x^{0.1} \qquad \text{Equ-1.37}$$

and the diffusive flux

$$J_{tu} = 0.19 \; \alpha^{-1} \; Cb \; D^{0.75} \; U_b^{0.9} \; \upsilon^{-0.65} \; x^{-0.1} \qquad \text{Equ-1.38}$$

where α is a proportionality constant approximately equal to unity.

Using the first theory, Vielstich (1953) obtained the following solution for δ_{tu}

$$\delta_{tu} \cong D^{0.33} \; \upsilon^{0.567} \; U_b^{-0.9} \; x^{0.1} \qquad \text{Equ-1.39}$$

The difference between the two theories is not great, being only a difference of 1/12 in the exponent on the Schmidt number. The implication of δ_{tu} being proportional to $U_b^{-0.9}$ and $x^{0.1}$, is that the thickness of the D.B.L. is considerably reduced by the advent of turbulence, and changes very little in the downstream direction. A consequence of this last point is that the diffusive flux decreases very slowly in the downstream direction. The average thickness of the D.B.L.

---

(1) Equation 1.37 is essentially the same as that used by Wheeler (1980), except that the latter, taken from Levich (1962), refers to the case for the inside of a pipe.

($\bar{\delta}_{tux}$) (for either Equation 1.37 or 1.39) is given by

$$\bar{\delta}_{tux} = 0.9\ \delta_{tux} \qquad \text{Equ-1.40}$$

where δ_{tux} is the δ_{tu} at a distance x along a flat plate.

The major complication of Equation 1.40 is that it assumes that turbulence develops at the leading edge. For the case where transition from laminar to turbulent flow develops downstream from the leading edge, the average D.B.L. thickness is a combination of the two flow types. To overcome this a dimensional analysis (Bircumshaw and Riddiford, 1952; Bird, Stewart and Lightford, 1960; Leyton, 1975; MacFarlane, 1985) can be used to develop a power function

$$\delta_{tu} = \text{constant}\ D^{1-p}\ U_b^{-q}\ x^{1-q}\ \upsilon^{q-(1-p)} \qquad \text{Equ-1.41}$$

The power factors p and q increase with increasing turbulence. The range for p varies from 0.66 to 0.75, and for q from 0.5 to 0.9 (Levich, 1962; Leyton, 1975). When the power factors take their minimum values (i.e. negligible turbulence) Equation 1.41 approximates to that for laminar flow over a flat plate (Equation 1.32). Alternatively, the use of the maximum range values (i.e. high degree of turbulence) makes Equation 1.41 similar in form to Equation 1.37. The constant for Equation 1.41 also varies depending on what theory of turbulence is used in the viscous sublayer and the degree of turbulence. Values for the constant range from 43 (Leyton, 1975), 33 (Rohsenow and Choi, 1961) to 5.3 (Levich, 1962).

1.2.2.2.3. FREE CONVECTIVE FLOW

There is one other flow type that can occur, other than forced laminar or turbulent flow, and that is free convection. This type of flow is important for mass transport when the solution is "stagnant".[1]

---

[1] In reality a stagnant solution is very difficult to achieve because of the likelihood of temperature and or concentration variations.

It occurs as a result of density gradient developed from variations in temperature and or concentration within the solution.

To determine the diffusional flow to a flat plate it is necessary to make the following assumptions: firstly, that a fast reaction is occurring at the surface (Cs = 0); secondly, that the temperature is constant; and thirdly, that mass transport within the solution is due to free convection only, which from the previous assumption reduces to the diffusion flow. This flow then only occurs within the D.B.L. where the concentration gradient exists. Such that the flow velocity in the x, y and z coordinates is zero at the surface and also at the limiting thickness of the D.B.L. (Ux = Uy = Uz = 0 at y = 0 and at y = δ, where δ is the thickness of the free convection D.B.L.) One further point is that under these conditions the D.B.L. coincides with the H.B.L.

Because of the mathematical difficulties associated with determining the free convectional flow associated with a horizontal flat plate, the following analysis applies to a vertical flat plate. The effective thickness of the D.B.L. is then given by Levich (1947), Agar (1949) and Wilke, Eisenberg and Tobias (1953).

$$\delta = \frac{x^{0.25}}{\text{constant } Sc^{0.25} \left[\frac{g\ Cb}{\upsilon^2\ \rho_b} \left(\frac{\partial \rho}{\partial C} \right) \right]^{0.25}} \qquad \text{Equ-1.42}$$

which simplifies to (Vetter, 1967),

$$\delta = \frac{1}{\text{constant}} \left[\frac{D\ \upsilon x}{g\ Cb\ \alpha} \right]^{0.25} \qquad \text{Equ-1.43}$$

where g is the acceleration due to gravity and α is the density coefficient ($m^3\ mol^{-1}$)

$$\alpha = \frac{1}{\rho_b} \left(\frac{\partial \rho}{\partial c} \right) \qquad \text{Equ-1.44}$$

expressing the relationship between the change in density (ρ) and con concentration (c) to the bulk solution density (ρ_b). Agar (1949)

calculated α to be 40 x 10^{-6} m^3 mol^{-1} as typical for salts such as KCl and indicated that α increased as the molecular weight of the salt increased. The value of the constant varies from 0.51 (Levich, 1947), 0.525 (Agar, 1949) to 0.677 (Tobias, Eisenberg and Wilke, 1952). As a result of δ being proportional to $Cb^{-0.25}$ as the thickness is reduced by increasing concentration (i.e. increasing diffusive flux).

1.2.2.3. CONCLUSION

The ability to determine the D.B.L. thickness from the external physical parameters provides an *a priori* method of measuring the mass transfer coefficient. It also facilitates the computation of the diffusive flux for the experimental situation. A drawback is the dependence for these expressions on the concentration at the surface being zero. For the situation where neither the surface reaction nor the diffusive flux rate limits the overall transport process ($Cs \neq 0$) then the D.B.L. thickness is reduced depending on the magnitudes of the two fluxes. Levich (1962) showed that the laminar D.B.L. thickness under intermediate kinetics is given approximately by

$$\delta_l \cong 2.15\, x^{0.5}\, D^{0.33}\, \upsilon^{0.167}\, U_b^{-0.5} \qquad \text{Equ-1.45}$$

Equation 1.45 effectively reduces the thickness by 2/3 compared to Equation 1.32.

By altering the external flow velocity it is possible to manipulate the mass transfer coefficient (Kt) so that the overall transport kinetics go from being diffusion controlled to reaction controlled.

Finally, because the D.B.L. thickness depends on the diffusion coefficient of the reacting solute, it is obvious that for different surface reactions there will be a corresponding D.B.L. for the associated reactants. Also it is possible that where more than one reaction occurs at the surface there can be more than one D.B.L. surrounding the object.

1.3 TRANSPORT KINETICS FOR A DIFFUSIVE FLUX IN SERIES WITH AN ENZYMIC REACTION

The influx of nutrients into plant cells often equates to that of a first-order enzymic reaction as described by Michaelis and Menten (1911), and modified by Briggs and Haldane (1925) to account for the rate of formation of the enzyme-substrate intermediate. Hence,

$$V = \frac{Vm \quad Cs}{Km + Cs} \qquad \text{Equ-1.46}$$

where V is the reaction-velocity, Vm the maximum reaction velocity, and Km[1] the Michaelis constant (Km is the concentration[2] when V = Vm/2). As previously shown for the case of a heterogeneous reaction at the surface (Section 1.2.2.1) an expression for the diffusive flux[3] through the D.B.L. in series with the Briggs-Haldane equation can be calculated.

Equation 1.19 is rearranged to obtain Cs in terms of Cb

$$Cs = Cb - \frac{J}{Kt} \qquad \text{Equ-1.47}$$

Substituting Equation 1.47 into Equation 1.46 and rearranging (V = J, at steady state),

$$V^2 - V\,(Km\ Kt + Cb\ Kt + Vm) + Km\ Kt\ Cb = 0 \qquad \text{Equ-1.48}$$

---

(1) Km as described by Briggs and Haldane (1925) is not a simple equilibrium constant, but has also a kinetic element incorporated which is referred to in Chapter 6.

(2) No account has been taken of the activity for the concentration of the reactants in Equation 1.46, which is more accurately expressed as (MacFarlane, 1985)

$$V = Vm\ \frac{Cs\ \gamma}{Km + Cs\ \gamma} = Vm\ \frac{Cs}{Km/\gamma + Cs}$$

where γ is the molal activity coefficient, which by definition is equal to the activity/molal concentration (Morris, 1968). For the case of $H_2PO_4^-$ in seawater (T = 25°C) the activity coefficient varies from 0.523 - $^{-2}$ 0.483 for the following range of total ionic strength, 0.6 - 0.8 kmol m^{-3} (Whitfield, 1975). For the purpose of this thesis Km will be expressed in terms of the activity, the assumption being that the temperature and ionic strength are constant throughout.

(3) Equation 1.19 for diffusive flux does not necessarily apply to the transport of ions as there is no electrical component to account for the charge on the ions or the membrane potential difference.

This is a quadratic equation of the form $ax^2 + bx + c = 0$, for which the general solution is

$$x = \frac{-b \pm \sqrt{b^2 - 4ac}}{2a}$$

Using this solution, Equation 1.48 becomes

$$V = 0.5\ [Km\ Kt + Cb\ Kt + Vm - \sqrt{(Km\ Kt + Cb\ Kt + Vm)^2 - 4\ Km\ Kt\ Cb}]$$

Equ-1.49

Only the negative root has any physical meaning as the positive root requires a negative concentration (Maskell, 1928; Hill and Whittingham, 1955; Lommen, Schwintzer, Yocum and Gates, 1971; Winne, 1973; Pasciak and Gavis, 1974; Wilson and Dietschy, 1974; Markl, 1977; Thomson and Dietschy, 1977; Dromgoole, 1978; Wheeler, 1980; Livansky, 1982; MacFarlane, 1985; Mierle, 1985). MacFarlane (1985) is correct in attributing Equation 1.49 to Briggs and Maskell, and hereafter it will be referred to as the Briggs-Maskell equation.

The Briggs-Maskell equation can be used to predict the limitations of the D.B.L. resistance (Rt) on the experimentally determined uptake parameter, Km. Because the surface concentration is less than the bulk solution concentration, in the presence of a D.B.L., the experimentally determined value of Km will be an over-estimation of the true Km at the object's surface (Figure 1.4). An expression for the apparent Km (Km*) is obtained by substituting V = Vm/2 into the Briggs-Maskell equation and solving for Cb (Pasciak and Gavis, 1974; MacFarlane, 1985; Mierle, 1985)

$$Km^* = Km + \frac{Vm}{2Kt} \qquad \text{Equ-1.50}$$

where Cb = Km* when V = Vm/2. When Km >> Vm/2 Kt (i.e. Kt >> Vm/2Km, Km* ≅ Km) then the reaction kinetics are controlled by the enzymic reaction, and the Briggs-Maskell equation reduces to the Briggs-Haldane equation (Figure 1.4, curve A). This occurs when the resistance to transport through the D.B.L. (Rt = 1/Kt) is small, and can be brought about by increasing the water velocity.

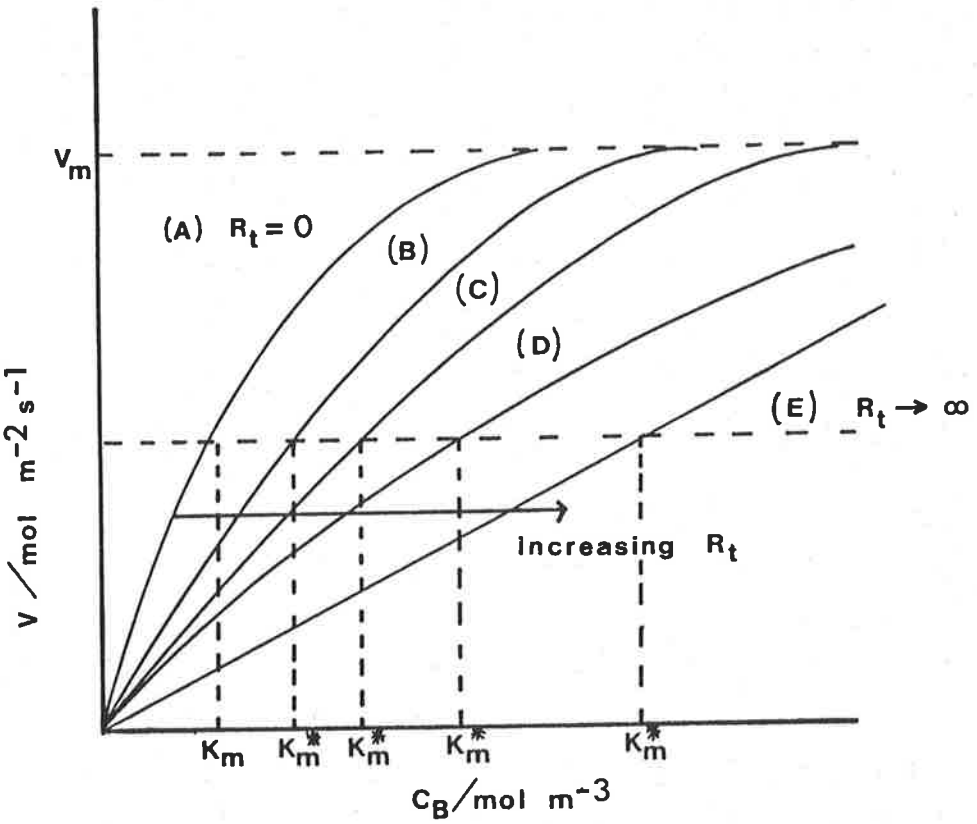

Figure 1.4. Theoretical solute uptake (V) versus solute concentration (Cb) for increasing D.B.L. resistance. The changes in Km indicated along the X-axis show the effect of increasing D.B.L. thickness on the true value of Km (K_m^* is the apparent Km).

When Km << Vm/2Kt (i.e. Kt << Vm/2Km, Km* ≅ Vm/2Kt), then the Briggs-Maskell equation reduces to the linear Equation 1.19 for the diffusive flux (Figure 1.4, curve E). Therefore as the external resistance decreases by increasing the water velocity the relationship between V versus Cb goes from a straight line to a rectangular hyperbole (Figure 1.4).

Experimentally, Equation 1.50 predicts that the presence of a D.B.L. resistance can lead to an overestimation of Km for the enzymic reaction (Winne, 1973; Lieb and Stein, 1974; Thomson, 1979; Smith and Walker, 1980). This problem can be overcome to a degree by measuring the Km under well stirred conditions; however even rapid stirring does not completely remove the D.B.L.[(1)] (Dainty, 1963; Dainty and House, 1966; Wilson and Dietschy, 1974; MacFarlane and Raven, 1985; Williams and Kutchai, 1986). Thomson and Dietschy (1977) showed that a plot of Km* versus Rt is a straight line with the intercept on the abscissa being the true Km at zero Rt. Thomson and Dietschy (1977) showed three important results when they altered separately the parameters in the Briggs-Maskell equation: (1) when Rt is low and the true Km is altered then there is little difference between Km and Km* over a wide range of Km values. However, when Rt is high the error associated with Km* is far greater (830%) when the Km is low (1.0 mol m^{-3}), than the error (166%) when Km is high (5.0 mol m^{-3}), (2) as Vm is lowered, Km* also decreases and approaches the true Km, this effect is even more pronounced when Rt is high, (3) in an experimental situation that causes a change in Km* and Vm, it can be predicted that the change was predominantly due to a change in Vm. If, on the other hand, Km* is changed but Vm stays constant then the most probable explanation is a change in Km or Rt.

---

(1) By definition (no slip condition) there must always exist a zone of fluid adjacent to the surface in which a velocity gradient develops with a concentration gradient also associated with it.

Another effect associated with the presence of a D.B.L. is its capability to alter the surface chemical environment which can lead to the diffusing solute undergoing chemical reactions. Gutknecht and Tosteson (1973) have shown that this effect is especially important for the case uptake of weak acids. They found that as the concentration of CO_2 decreases within the D.B.L. there is an increased rate of production of CO_2 from HCO_3^- and H_2CO_3 to maintain the equilibrium concentration, effectively "short circuiting" (Walker, Smith and Cathers, 1980) the diffusion resistance. For CO_2 the overall rate of transport is then dependent on the breaking of covalent bonds ($H_2CO_3 \rightleftharpoons CO_2 + H_2O$ and $HCO_3^- \rightleftharpoons CO_2 + OH^-$) which have relatively slow rate constants (Gutknecht and Tosteson, 1973; Gutknecht, Bisson and Tosteson, 1977; Walker, Smith and Cathers, 1980). This is further compounded by the pH of the D.B.L. [which can differ from that of the bulk solution by an order of magnitude (Walker, Smith and Cathers, 1980)], which can alter the equilibrium concentration of the reacting solute species.

In conclusion, for a complete understanding of the mechanics of solute influx through a D.B.L. in series with a membrane, it is necessary to know firstly the chemical pathway from the bulk solution into the cell, and secondly the transport rates associated with the D.B.L. and the membrane. The possibility of the transport resistance within the D.B.L. being rate limiting to growth or uptake is increased considerably when the plant is at its metabolic optimum [with respect to factors such as temperature or light (Wheeler, 1980)].

1.4 PREVIOUS RESEARCH ON THE EFFECTS OF WATER MOVEMENT ON THE RATE OF GROWTH OR UPTAKE FOR AQUATIC PLANTS

Previous research has shown that increasing water movement increases the rate of growth or uptake in diatoms (Canelli and Fuhs, 1976; Parslow, Harrison and Thompson, 1985), microalgae and bacteria (Myers, 1944; McIntire, 1966a,b; Hartman, 1967; Sperling and Grunewald, 1969; Sperling and Hale, 1973; Falco, Kerr, Barron and Brockway, 1975; Pasciak and Gavis, 1975; Markl, 1977; Mierle, 1985; Vilenkin and Pertsov, 1985), freshwater macroalgae (Ruttner, 1926; Whitford, 1960; Whitford and Schumacher, 1961, 1964; Schumacher and Whitford, 1965; Thirb and Benson-Evans, 1982; MacFarlane and Raven, 1985), submerged macrophytes (Darwin and Pertz, 1896; James, 1928; Owens and Maris, 1964; Westlake, 1967; Werner and Weise, 1982; Madsen and Sondergaard, 1983) and marine macroalgae (Jones, 1959; Matsumoto, 1959; Boalch, 1961; Whitford and Kim, 1966; Conover, 1968; Doty, 1971a,b; Wheeler, 1976, 1977, 1980; Dromgoole, 1978; Lapointe and Ryther, 1979; Littler, 1979; Andrake, 1980; Bottom, 1981; Cousens, 1981, 1982; Parker, 1981, 1982; Gerard, 1982a,b; Kain, 1982; Fujita and Goldman, 1985; MacFarlane, 1985).

The increases in growth or uptake in these plants are attributed to the decrease in the D.B.L. thickness with increasing water movement. The results of this previous research have shown some dramatic increases in uptake or growth rate. For example, Whitford and Schumacher (1964) found a 16-fold increase in phosphate uptake upon increasing the water movement (0 - 20 cm s^{-1}) around *Oedogonium kurzii*. This has led many ecological researchers to erroneously assume that plants living in higher water movement environments will have an increased productivity compared to those habitating calmer waters. The reason for this is that water movement can have many different effects on a plant's metabolism, form and life history. This was shown by Jones (1959) on the effect of water movement on the growth of *Gracilaria verrucosa*, who found that the most

important effect of water movement is to orientate the plants' thallus normal to the incident light. Jones concluded that only the minimal water movement above stagnant conditions was required to saturate any increases in growth rate. Gerard and Mann (1979) found that of two populations of *Laminaria longicruris* inhabiting different water movement intensities, the population in the lower water movement environment had the higher productivity. This is attributed to the morphological differences necessitated to survival in the high intensity water movement. In a more recent study, Gerard (1987) concluded that productivity was similar for *Laminaria saccharina* inhabiting low and high mechanical stress (water movement), and that increasing mechanical stress caused enhanced hydrodynamic streamlining of the thallus.

Therefore, apart from decreasing the thickness of the D.B.L., other effects which can be attributed to water movement in the marine environment are:

(1) Morphological streamlining, whereby plants alter their morphology (form) to reduce drag and therefore increase their persistence within areas of high water movement (Sundene, 1962, 1964; Norton, 1969; Mann, 1971; Ramus, 1972; Chapman, 1973; Terekhove, 1973; Koehl and Wainwright, 1977; Gerard and Mann, 1979, Mshigeni, 1979; Andrake, 1980; Littler and Littler, 1980; Santelices, Castilla, Cancino and Schmiede, 1980; Clarke and Womersley, 1981; Hay, 1981; Kain, 1982; Mshigeni and Magingo, 1982; Fonseca, Zieman, Thayer and Fisher, 1983; Littler, Littler and Taylor, 1983; Vogel and London, 1985; Gerard, 1987).

(2) Dispersal and settlement - water movement is important in dispersing the spores of the next generation and in determining the environment in which successful settlement can occur (Coon, Neushul and Charters, 1972; Charters, Neushul and Coon, 1973; Norton and Fettler, 1981; Eckman, 1983; Rees and Jones, 1984).

(3) Disturbance - the development and timing of clear patches during periods of extreme water movement is important in sustaining the integrity of aquatic plant communities (Dayton, 1971; Doty, 1971; Sousa, 1979a,b; Pain and Levin, 1981; Cowen, Agegian and Foster, 1982; Peckol and Searles, 1983; Dayton, Currie, Gerrodette, Keller, Rosenthal and VenTresca, 1984; Dethier, 1984; Ebeling, Laur and Rowley, 1985).

(4) Orientation - the concept that water movement can increase light interception through orientating plants has had very little research (Jones, 1959; Hanisak, 1987). More work has been done on animals, especially corals, with regard to drag reduction and light interception (Riedl, 1971; Chamberlain and Graus, 1975; Graus, Chamberlain and Boker, 1977).

(5) Predation - the swaying motion of plants by the action of water movement can have a beneficial effect by physically sweeping away predators in the plant's vicinity (Velimirov and Griffiths, 1979; Santelices and Ojeda, 1984).

The relative importance of the effects attributed to water movement depends also on the scale of the plant; that is, small plants (e.g. microalgae) experience a completely different environment (low Reynolds number) from that of larger plants (high Reynolds number, e.g., macroalgae) in the same environmental conditions (Allen, 1977; Purcell, 1977; Sourina, 1982). The consequence of a low Reynolds number for micro-plants is that they are far more susceptible to diffusion limitations which probably explains the elaborate methods they have developed to move within the water column (Purcell, 1977). It is therefore apparent that researchers must be cautious in extrapolating results from one scale to another.

Another aspect of scale results from the development of the H.B.L. over the substrate the plant is attached to. Depending on the size of the plant it can experience relatively little water movement or extreme

water movement when attached to the same substrate (Neushul, 1972). Also as the plant develops throughout its life history, it will experience varying water movement velocities in the same environment. Therefore scale can be used by aquatic plants as a way of avoiding the destructive potential of water movement, but this can lead to other negative effects (e.g. diffusional limitations, shading).

These effects attributed to water movement are more physical in nature than the physiological response to decreased thickness of the D.B.L. The important point is that the effects are not independent as they all contribute to the persistence and productivity within the selected environment.

Little quantitative research has been done on determining the relationship between transport through the D.B.L. and the rate of growth or uptake for marine macroalgae. Several workers have found a positive relationship between increasing water velocity and the rate of growth or uptake for marine macroalgae (Conover, 1968; Wheeler, 1980; Parker, 1981, 1982; Fujita and Goldman, 1985). This response was shown to saturate with further increases in water velocity, and in some cases high water velocities had a negative effect on the rate of growth and uptake (Parker, 1981, 1982). Parker (1981, 1982) found that the enhancement in the rate of growth or uptake was achieved at the lowest water velocity (7.5 cm s^{-1}) used; Hone (1982) concluded that the rate of growth of *Ulva rigida* saturated at the minimum water velocity tried (0.85 cm s^{-1}). Other workers have also concluded that very little water movement is required to overcome any diffusional limitations for macroalgae (Jones, 1959; Wheeler, 1980; Gerard, 1982). Munk and Riley (1952) developed a theoretical expression to determine the water velocity required to overcome diffusional limitations. They gave as an example the case of phosphate uptake (Table 1.2) and found that a water velocity of 37 cm s^{-1} would be required to overcome any diffusional limitations. As shown in Table 1.2, any variations in the membrane flux or external concentration

TABLE 1.2. Water velocity required to overcome the effect of diffusion limitations on phosphate uptake, based on Munk and Riley's (1952) formula.

	Munk & Riley's Example	Case 1	Case 2
Membrane flux, ϕ, nmol m^{-2} s^{-1} (a)	32.3	10	10
Bulk solution concentration, Cb, mol m^{-3}	1×10^{-3}	1×10^{-3}	0.5×10^{-3}
Length along plate, l, m	4×10^{-2}	4×10^{-2}	4×10^{-2}
Constant, K^1, m^{-2} s^{-1} (b)	4.5×10^{-10}	4.5×10^{-10}	4.5×10^{-10}
Water velocity, U_b m s^{-1} (c)	37	3.6	14

(a) The units of flux used by Munk and Riley (1952) were g s^{-1} cm^{-2}, therefore a phosphate flux of 10^{-10} x g s^{-1} cm^{-2} = 32.3 nmol m^{-2} s^{-1}.

(b) $K^1 = 1.8\ D^{1.33}\ \upsilon^{-0.33}$, took $D = 2.5 \times 10^{-9}$ m^2 s^{-1} for phosphate and $\upsilon = 1.0 \times 10^{-6}$ m^2 s^{-1}.

(c) The formula used to determine the water velocity required for the observed flux was determined by Munk and Riley (1952) as:

$$U_b = \frac{(2\ \phi)^2\ l}{Cb^2 1.8\ D^{1.33}\ \upsilon^{-0.33}} = (2\ J)^2 \frac{l}{Cb^2\ K^1}$$

This formula was derived from an equation similar to Equation 1.33 [$J = 0.67\ Sc^{0.33}\ Re^{0.5}\ D\ Cb\ l^{-1}$] and ϕ is equivalent to Cb - Cs.

have a large effect on the required velocity (Table 1.2, case 1,2). Munk and Riley concluded that attached plants must inhabit areas of high water movement or high concentration of nutrients to overcome the diffusional limitation.

The water velocities that occur in the marine environment have a considerable range depending on the locality (Milgram, 1978). Raymont (1963) found surge and current velocities along the coast to range from 1 to 2 m s^{-1}, Roberts and Suhayda (1983) measured wave velocities and currents over a reef and found the average flow velocity to be 10-20 cm s^{-1} while wave surges increased this to 1.8 m s^{-1}. Wheeler (1981) and Jackson (1983) have measured water velocities less than 5 cm s^{-1} and frequently less than 1 cm s^{-1} outside kelp beds in Southern California; Jackson has further shown that within the kelp beds currents are about a third those outside. Charters, Neushul and Barilotti (1969) computed from the results of Jones and Demetropoulos (1968) the maximum surge velocity of 14 m s^{-1} which they calculated was equivalent to a wind velocity of 400 m s^{-1} (to achieve similar drag forces).

From the description of the D.B.L., its thickness is dependent on the bulk water velocity and whether the flow is laminar or turbulent. At low water velocities (0-20 cm s^{-1}) the development of turbulence has a drastic effect on the thickness of the D.B.L. For *Macrocystis pyrifera*, Wheeler (1980) found turbulence to develop at Reynolds numbers of 10^4 or less, as did Charters (1940). Other research has found turbulence to develop for macroalgae at Reynolds numbers less than 10^3 (Charters and Anderson, 1980; Wheeler and Neushul, 1981). The development of turbulence at such low Reynolds numbers is due to the surface roughness of the plants or the inherent turbulence of the external flow (Levich, 1962; Schlichting, 1968; Wheeler, 1980). Wheeler (1980) has pointed out that a plant which has diffusional limitations can overcome this to a degree, by inducing turbulence to occur over its thallus by altering its morphology.

1.5 THESIS AIMS.

The aim of this thesis was to study the interaction between water movement, phosphate uptake and growth of *Ulva australis* for the conditions where the concentration of phosphate was limiting to growth. The main hypothesis was that altering the water velocity relative to the plant would result in a change in both the phosphate uptake rate and growth rate as predicted by the D.B.L. theory. The magnitude of the growth and uptake response to changes in water movement will be related to the predicted changes in phosphate uptake based on the Briggs-Maskell equation.

By definition, Rt (1/Kt) as used in the Briggs-Maskell equation, refers to the transport resistance through the D.B.L. and cell wall in series (effective Rt). MacFarlane (1985) found for *Ulva rigida*, that the cell wall had a negligible effect on the effective Rt for phosphate transport. Further, MacFarlane found that the internal phosphate resistance in parallel with the D.B.L. resistance did not influence the magnitude of the effective Rt calculated from only the D.B.L. resistance. This was similar to the result found by Shaw (1960) for iodide uptake by *Laminaria digitata*. Therefore it was assumed that the effective transport resistance was approximated by the D.B.L. resistance.

Particular emphasis was given to the growth status of the plants prior to the start of the experiments. Growth status refers to the capacity of *Ulva australis* to change its growth rate when the growth conditions are altered. Significantly, variations in the plant's internal total phosphate concentration will be measured to determine its interaction with both the rate of growth and phosphate uptake.

Finally, an attempt was made to formulate an empirical model capable of predicting the interactions between water movements, phosphate uptake, internal phosphate concentration and growth rate.

CHAPTER 2. METHODS

2.1.1. PLANT COLLECTION

Ulva australis Areschoug collected from Saint Kilda, South Australia was used in all experiments. This taxa was selected because: (1) its geometry resembled that of a flat plate (Figure 2.1; Table 2.1), which simplified the calculations involving boundary layers, (2) it had been found previously (Hone, 1982) to be extremely robust for experimental purposes and to be able to be kept in culture for long periods, and (3) it is an extremely fast growing alga and there is much previous research on this genus. For comparison, *U. australis* is similar in morphology and physiology to *U. rigida*, *U. lactuca* and *U. curvata* (Steffensen, 1976; Rosenberg and Ramus, 1981; MacFarlane, 1985; Hone, 1982). Previously, in southern Australian waters *U. lactuca* was used as the name to describe the three species *U. lactuca*, *U. australis* and *U. rigida*. Womersley (1984) has distinguished the morphological differences required to identify each species, though there still exists some confusion arising from the considerable morphological plasticity that this taxa exhibits. Also, no attempt has been made to distinguish between the isomorphic generations of *U. australis*, as the only apparent difference is in the number of chromosomes (2N or N).

Because of the need for a large amount of uniformly pre-conditioned tissue, large amounts of *U. australis* (up to 50 plants) were collected each time. In the field, plants were selected on the basis of size (approximately 0.25 m^2) and the lack of visible epiphytic fauna and flora. To keep plants healthy they were transported in plastic bags, filled with local seawater, and placed in a styrofoam container which was kept cool with crushed ice, kept separate from the plants.

Immediately on arrival in the laboratory the plants were individually checked to confirm their taxonomic status and any small

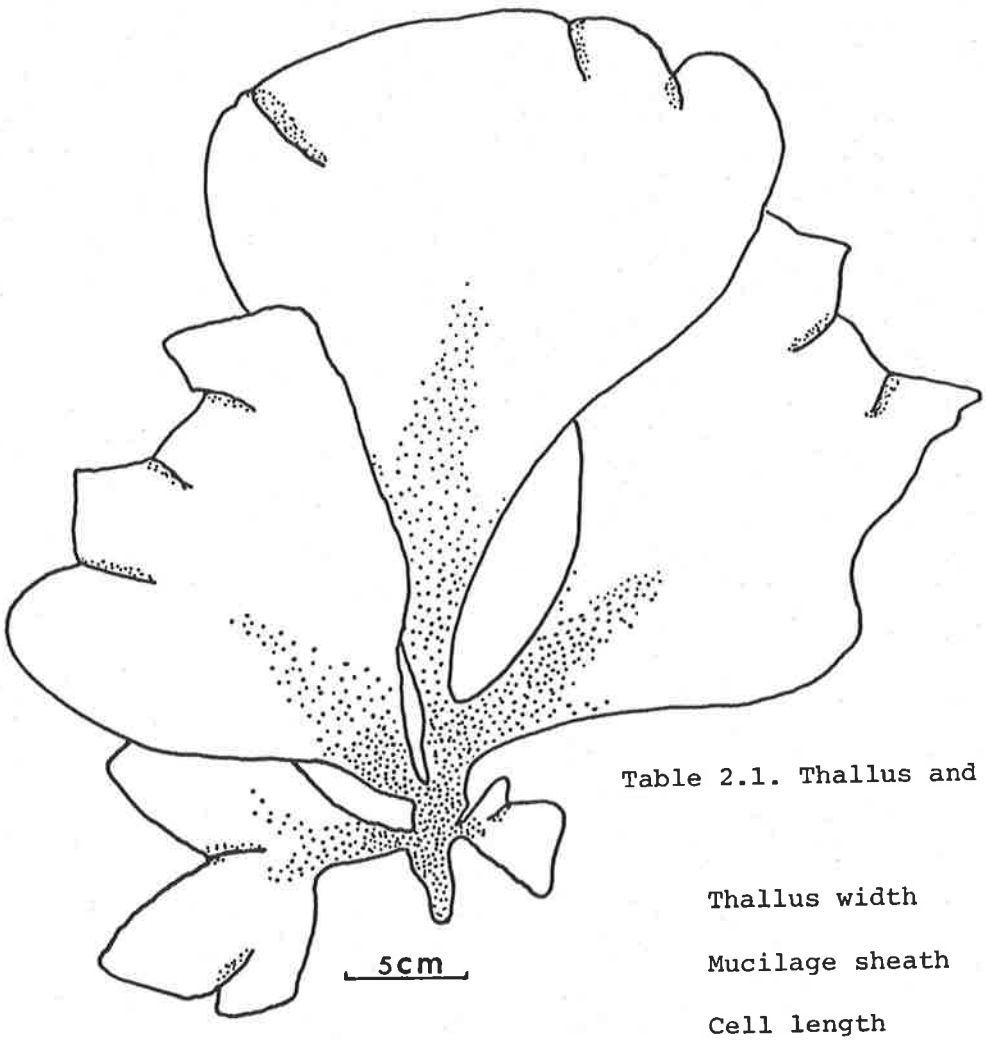

Table 2.1. Thallus and cell dimensions

	Size µm
Thallus width	74 ± 6
Mucilage sheath	4.8 ± 0.9
Cell length	28 ± 2.5
Cell width	12.5 ± 1.1

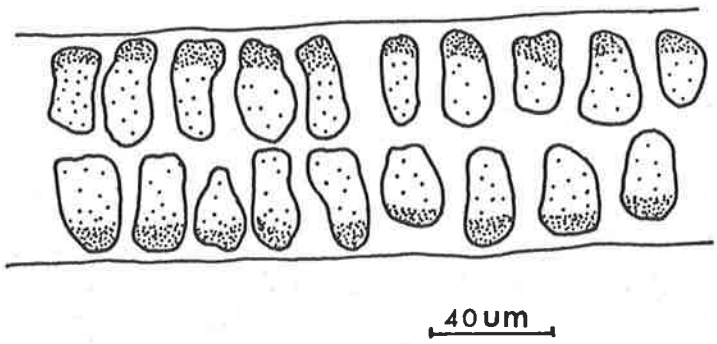

Figure 2.1. (A) Habit sketch of *Ulva australis*. (B) Cross-sectional view of thallus showing cells embedded in mucilaginous sheath. The region of darker shading within each cell represents the position of the chloroplast.

gastropods or crustaceans removed. The plants were also gently brushed by hand, using the fingertips to dislodge any microscopic organisms and washed in filtered seawater. It was found that this cleaning procedure was very important as it increased the time that it was possible to keep the plants in a healthy condition in culture.

2.1.2. CULTURE CONDITIONS

The cleaned *U. australis* plants were placed in 30 litre glass aquaria filled with filtered seawater (see Section 2.2.2.), and vigorously bubbled with air. Light was provided by four overhead fluorescent tubes (120 cm Sylvania F40/GRO-LUX) which gave a light flux of 50-60 µmol m^{-2} s^{-1} (P.A.R.) at the seawater surface, with a 14 hour light/10 hour dark cycle. The aquaria were kept in a constant temperature room at 15 ± 1°C. By replacing the filtered seawater every week and allowing only a low biomass of *U. australis* in each aquarium, it was possible to keep the plants healthy for up to three months.

For the short term pre-loading uptake experiments, disks of *U. australis* were placed in 500 ml of artificial seawater (see Section 2.2.3.) in one litre acid-washed conical flasks, bubbled with air and kept under the same conditions as the aquaria.

2.1.3. DESCRIPTION OF COLLECTION SITE

Saint Kilda is a sheltered bay (maximum depth two metres) 26 km north of Adelaide on the eastern shore of the Gulf of Saint Vincent. The bay is surrounded by mangroves on its northern and southern shores and the dominant flora in the bay are an association of *Heterozostera tasmanica*, *Zostera* sp. and *Ulva australis*.

The *U. australis* plants recruit initially on small shells and stones but as they grow they break free and become a free-floating entity. The abundance of *U. australis* in the bay varies seasonally, peaking in the summer months where it creates at times a severe pollution problem. One

of the local reasons given for the prevalence of *U. australis* in this location is the existence of the nearby sewage treatment plant's outlet into the bay. The annual range of total phosphate is 1.3 to 3.9 mmol m^{-3}, and for total nitrogen 57.1 to 92.8 mmol m^{-3} (South Australian Engineering and Water Supply report, 1982). A more likely explanation is that the life cycle and growth requirements of *U. australis* are well adapted to the physical characteristics of the bay. The bay is protected from all but the most severe storm waves, with a limited fetch in all directions. The most frequent source of water movement is the daily tidal action, which at extreme low tides reduces the seawater depth to approximately 10-20 cm.

2.2.1. SOLUTION PREPARATION

All chemicals used in experiments were of a laboratory standard. The glassware used where the concentration of phosphate was critical, was acid-washed and triple rinsed in distilled water. The problem with bacterial contamination of growth chambers requires the use of axenic culture techniques to maintain clean cultures. Provasoli (1958) found that the growth of *Ulva* in axenic cutures produced abnormal morphologies which could be corrected by adding plant hormones and algal extracts. To avoid the technical and time difficulties associated with axenic cultures it was the aim of this study to control the bacterial growth. This was achieved by rigorous cleaning of equipment and replacing the media daily.

2.2.2. SEAWATER COLLECTION

Seawater was collected from Brighton beach using a battery operated pump which passed the water through a two stage filtering device (Hatcher, 1977), the minimum particle size retention was 0.45 µm. The filtered seawater was stored in acid washed 25 litre plastic containers in the dark, for a minimum of one month before use. The annual chemical analysis for the seawater from this site is given in Table 2.2.

TABLE 2.2

	Minimum	Maximum	Mean
Phosphate (mmol m^{-3})	<0.16	1.4	0.67 ± 0.28
Salinity (o/oo)	35	39	37 ± 1.64
Nitrate (mmol m^{-3})	<0.7	120.9	12.8 ± 9.4
Carbon (mol m^{-3})	2.0	2.3	2.2 ± 0.07
pH	8.1	8.3	8.2 ± 0.06
Na (mol m^{-3})	470	530	492 ± 24
K (mol m^{-3})	9.4	10.0	9.7 ± 0.3

[Phosphate refers to total inorganic phosphate, see Section 3.1. Nitrate refers to the total inorganic nitrate, obtained from the Engineering and Water Supply report for the southern coast (1984). Salinity, carbon, pH, Na and K were measured using the methods outlined in the sections on nutrient analysis. Errors are standard deviations.]

Seawater was collected during periods of calm weather to minimize the concentration of phosphate and nitrogen.

2.2.3. ARTIFICIAL SEAWATER (A.S.W.)

Artificial seawater was made using the method of Findlay, Hope, Pitman, Smith and Walker (1971). It consisted of glass distilled water containing 490 mol m^{-3} NaCl, 10 mol m^{-3} KCl, 11.5 mol m^{-3} $CaCl_2$, 25 mol m^{-3} $MgCl_2$, 25 mol m^{-3} $MgSO_4$, 2.5 mol m^{-3} $NaHCO_3$. The final pH was buffered using 10 mol m^{-3} TAPS (Zwitterionic buffer, pKa 8.4 at 25°C) and 10 kmol m^{-3} NaOH to give a pH of 8.2, and a ionic strength of 0.7. All A.S.W. was stored in the dark in sealed 2 litre glass flasks.

2.2.4. GROWTH NUTRIENTS

Hoagland's solution consisted of glass distilled water, macronutrients (5 mol m^{-3} KNO_3, 5 mol m^{-3} $Ca(NO_3)$, 2 mol m^{-3} $MgSO_4$, 1 mol m^{-3} KCl), micronutrients (46.27 mmol m^{-3} H_3BO_3, 9.15 mmol m^{-3} $MnCl_2.4H_2O$,

0.77 mmol m^{-3} $ZnSO_4.7H_2O$, 0.32 mmol m^{-3} $CuSO_4.5H_2O$, 0.11 mmol m^{-3} $NaMoO_4.2H_2O$), and Fe.E.D.T.A (5mg of Fe/litre or, 89.5mmol/m^3). Where Hoagland's solution was used, the amount added achieved a final concentration of 42 mmol m^{-3} with respect to total nitrogen. This was based on the results of Waite and Mitchell (1972) and Steffensen (1976) who found that *Ulva lactuca's* growth rate was maximium at a nitrogen concentration of 42 mmol m^{-3}. Phosphate stock solution was made up using KH_2PO^4 to a concentration of 2 mol m^{-3}. Both solutions were refrigerated (4°C) and kept in the dark. The use of Hoagland's solution is appropriate, based on the results of previous research into the nutrient factors limiting algal growth (Provasoli, McLaughlin and Droop, 1957; Green, 1977; Oza and Rao, 1977; Dufkova, 1984). It also reduced the problem associated with sporulation during growth, probably due to the lack of vitamins added (Oza and Rao, 1977).

2.2.5. pH

The pH of all solutions was measured using an Activon glass pH electrode connected to an Orion research digital meter (model 701A).

2.2.6. INORGANIC CARBON

Total inorganic carbon was measured using the method of Strickland and Parsons (1965).

2.2.7. TOTAL SALINITY

Total salinity was calculated by measuring the electrical conductivity of seawater.

2.2.8. SODIUM AND POTASSIUM

A flame photometer was used to measure the concentration of sodium and potassium both in filtered seawater and plant tissue. For plant tissue the weighed sample was first thoroughly digested in 20 ml of 100 mol m^{-3} nitric acid (20 minutes), and the decanted solution measured.

2.3. GROWTH MEASUREMENTS

2.3.1 AREA

The area of each disk was determined by placing the disks between clear plastic sheets divided into numbered squares (for identification). This was then photocopied on a Minolta copier. Care was taken that only the central 60% of the photocopier's area was used as distortion occurs at the periphery of most copiers. This method produced a quick non-destructive permanent record of the area of each disk. Each disk was then transfered quickly to an individually labelled glass vial containing 5ml of A.S.W. and kept in the dark until it could be weighed.

The area of each disk was later measured using a Houston instrument Hipad digitizer connected to a Digital PDP-11 mini computer. The program allowed for statistical analysis of the areas measured, which were expressed as cm^2 plus or minus 95% confidence limits. To reduce error, it was necessary prior to measurement of disk areas, to practice with the digitizer using shapes of known size, until the error between successive measurements was less than 0.5%.

2.3.2. FRESH AND DRY WEIGHT

Each disk was blotted dry using paper towelling (keeping the method constant) and weighed on a Mettler AE-163 balance. The disks were then placed on aluminium foil in 12 cm diameter petri dishes, which were

divided into sections for disk identification. The petri dishes were placed in a Labmaster drying oven at 90°C for 48 hours (time required to achieve constant weight). The petri dishes were then placed in a desiccator and subsequently each disk was removed and re-weighed on the Mettler AE-163. The disks were finally stored in glass vials for future total phosphate and C.H.N. (carbon, hydrogen and nitrogen) analysis.

2.4. *ULVA* COMPOSITION

2.4.1. TOTAL PHOSPHATE

A combined modified method was used to determine total phosphate content of *U. australis* (Murphy and Riley, 1962; Menzel and Corwin, 1965).

The area, fresh and dry weight of the *U. australis* disks were measured. The dried disks were then transferred to separate 50 ml pyrex flasks containing 25 ml of distilled water and approximately 1 g of potassium persulphate (Menzel and Corwin, 1965). All flasks were weighed (Mettler PC 2200) to monitor liquid loss and then sealed with aluminium foil and placed randomly in either of two pressure cookers (Namco). Two flasks containing only distilled water and 1 g of potassium persulphate were used as reference blanks. Also a duplicated set of standards containing 1.6, 3.2, 4.8 and 6.4 mmol m^{-3} phosphate were made up each time. It was important to determine a standard curve for each run, as fresh batches of prepared chemicals caused a slight variation between time periods. The pressure cookers were heated to 15 pounds per square inch (units as specified on the Namco pressure gauge) for one hour and then allowed to cool for 20-30 minutes.

After each flask had cooled sufficiently to be handled, 2 drops of phenolphthalein [1 g phenolphthalein per 100 μm^{-3} ethyl alcohol (90%) and 100 ml distilled water] were added and then titrated with 10 kmol m^{-3}

NaOH until a stable pale pink colour was achieved. This was then titrated back to neutral pH (clear colour) by adding a few drops of 4 kmol m^{-3} HCl. The reason for neutralizing the digested solution was that it produced a more stable development of the phosphomolybdenum blue complex. The flasks were then re-weighed and distilled water added to make up the volume to the initial weight. If the weight was greater than the original this was taken into account in the final calculations.

Each flask had 4 cm^3 of freshly prepared mixed reagent (Murphy and Riley, 1962) added and allowed 20 minutes, with gentle shaking, for the blue colour to develop. The absorption was then measured at 665 nm using 4 cm glass cuvettes (necessary due to the small amount of tissue used). For the purpose of this thesis, 3 different spectrometers were used as they became available, each one enabling an improvement in speed and accuracy. They were, in order of use, the Beckman D.B., the Beckman Acta CIII, and the Philips PU8800.

The results were expressed as µmoles (total phosphate) per disk, µmoles (total phosphate) per g fresh weight and µmoles (total phosphate) per g dry weight.

The inorganic phosphate concentration of seawater (50 cm^3 samples) was measured using the method of Murphy and Riley (1962).

2.4.2. CHLOROPHYLL

Individual disks were homogenized using a mortar and pestle in approximately 3-5 cm^3 of 80% acetone and approximately 10 mg of acid washed sand. The acetone extract was then poured into graduated centrifuge tubes (volume recorded) and centrifuged at 2500-3000 r.p.m. for 10 minutes. The absorbance was measured at 645 nm and 663 nm using 1 cm glass cuvettes and 80% acetone as the reference. Total chlorophyll was calculated using the formula of Arnon (1949), and expressed as either µg total chlorophyll per disk or mg total chlorophyll per g fresh weight.

2.4.3. CARBON,HYDROGEN AND NITROGEN (C.H.N.)

C.H.N. was measured using a Hewlett-Packard (model 185) Carbon, Hydrogen and Nitrogen Gas Analyzer. To reduce the errors it was found to be important to keep all disks and all chemicals used in a desiccator. Because only a small sample (1-2 mg, Cahn ratio electrobalance) was necessary for each measurement, it was possible to have replicate measurements for each disk. Results are expressed as percentages on a dry weight basis.

2.5. GROWTH EXPERIMENTS

2.5.1. GROWTH CHAMBER

2.5.1.1. INTRODUCTION

One of the problems with previous attempts to measure the growth of aquatic algae has been the use of systems that inadequately represented the water movement of the natural environment. Too often air bubbling has been used to alleviate a lack of water movement. More recently, as the importance of water movement has unfolded, more emphasis has been placed on simulating water movement characteristics of the habitat preference of the plants.

The design (Figure 2.2) adopted here was similar to that of Matsumoto's (1959) except that instead of the plants being attached to the arms which rotate around the chambers, the plants were stationary within the chambers and the water was moved past them. This was achieved by means of paddles attached to overhead circulating arms. The reason for the adoption of this design was that the increased biomass per chamber allowed for increased replication and experimental duration. It also overcame the difficult hydrodynamic calculations associated with flow around plant holders if they had been attached to the arms.

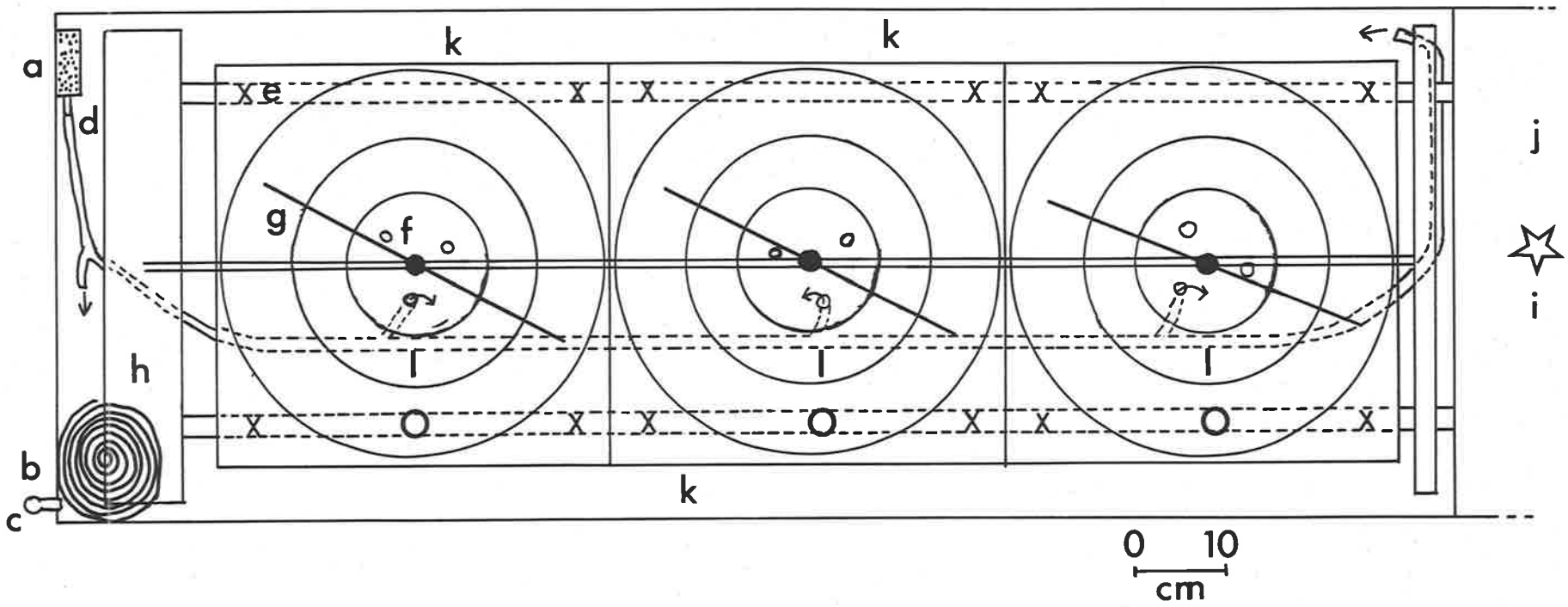

Figure 2.2. An over-head view of the water movement simulator showing the position of the three containers consisting of two annular chambers. (a) heater-stirrer, (b) cooler coil, (c) drainage plug, (d) plastic tube used to direct water flow output from the heater-stirrer, (e) position of wingnuts used to attach containers to aluminium base frame, (f) drainage holes in the centre of the containers used to increase water circulation, (g) over-head rotating arms, (h) aluminium base frame, (i) position of cog used to drive the chain, which in turn drives the rotating arms, (j) heat shield and (k) water bath.

The approach used by Matsumoto (1959) to simulate water movement has also been used to a similar extent by Parker (1981, 1982). In both cases, no reference was given to the problem associated with water stirring, that is, that the water movement experienced by the plant is the vectorial sum of the arm velocity and the velocity of the stirred water. The importance of this is only apparent if the results are applied to boundary layer theory, where as near as possible accurate measurement of the water velocity is required. To overcome this problem a calibration method was required that accounted for all possible sources of water movement surrounding the plant (this will be extended in Section 2.7).

Finally it was important to differentiate between experimental methodologies of those who have manipulated water movement in an attempt to increase the productivity of large quantities of alga, and of those interested in the mechanisms that are involved in this increase, as the two approaches require different economies of scale.

2.5.1.2. CONSTRUCTION

Three circular containers were constructed out of non toxic P.V.C., with a base thickness of 5 mm and a side thickness of 2 mm. The joints were welded using a hot air gun (Figure 2.2). Each container consisted of two annular chambers and a central chamber. On opposite sides of each annular chamber a 1.5 mm stainless steel pipe was set flush with the base for the purpose of aeration.

The three circular containers were placed within a rectangular perspex water bath, and secured to an aluminium frame (Figure 2.2). The temperature within the water bath was kept constant by using a Grant's cooling coil and a Heidolph heater-stirrer. The homogeneity of the temperature within the water bath was improved by connecting plastic tubing to the stirrer outlet and distributing the water throughout the water bath. The central chamber had three holes (1 cm diameter) drilled

in it so that it was connected to the water bath, and was further supplemented by pumped water. This resulted in both annular chambers being adjacent to the influence of the water bath.

To hold the disks of *U. australis* stationary within each annular chamber, U-shaped disk holders were constructed out of P.V.C. (Figure 2.4). Along the top of each arm of the U, holes were drilled through which fine nylon line was interwoven. At each open end of the disk holder three stainless steel screws were evenly spaced, bolted and covered with thin plastic tubing. Disks were held in place on the nylon line by stretching thin rubber bands between the screws, and pushing them down until the disks were sandwiched between the line and the rubber bands. This method was used as it combined speed of use with minimum interference with the disks and also kept the disks parallel to the water movement. A further reason for using this method was that previous use of the method (Hone, 1982) whereby disks were propelled along by the arms found that the vibration associated with this mechanical system altered the morphology of the disks.

The water movement within the containers was created by overhead horizontal revolving arms which had vertical paddles (paddle area was 11.5 and 4.83 cm^2 for the outer and inner chambers respectively) suspended in each annular chamber (Figure 2.3). The depth to which the paddles were suspended was such that they were just below the surface of the media. These arms were supported on a shaft located on a central pin within the containers. The arms were rotated by connecting them up via a chain drive which was turned by 240 volt induction motor with a reduction gearbox (9.68 r.p.m.). As shown in Figure 2.5 the speed at which the arms turned could be altered by changing the cog ratios, by either altering the position of the motor or by changing the cog connected to the drive cog. The motor was housed within an aluminium heat shield with a 1.5 cm layer of rockwool insulation between the shield and the water bath.

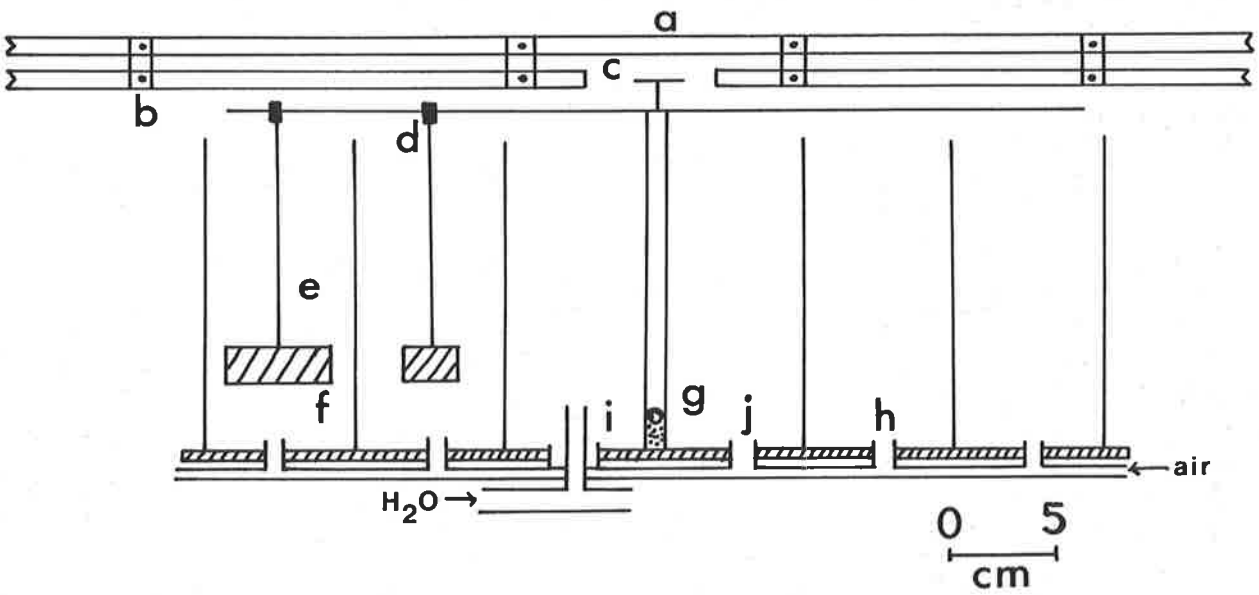

Figure 2.3. Cross-sectional view of one growth container. (a) chain support bar, (b) chain guard, (c) 15 toothed cog, (d) rotating arm, (e) paddle support rod, (f) paddle, (g) central support rod and brass pivot screw, (h) air inlet, (i) inlet pipe for recirculated water from heater-stirrer, (j) drainage holes connecting the central chamber with the temperature regulated water bath.

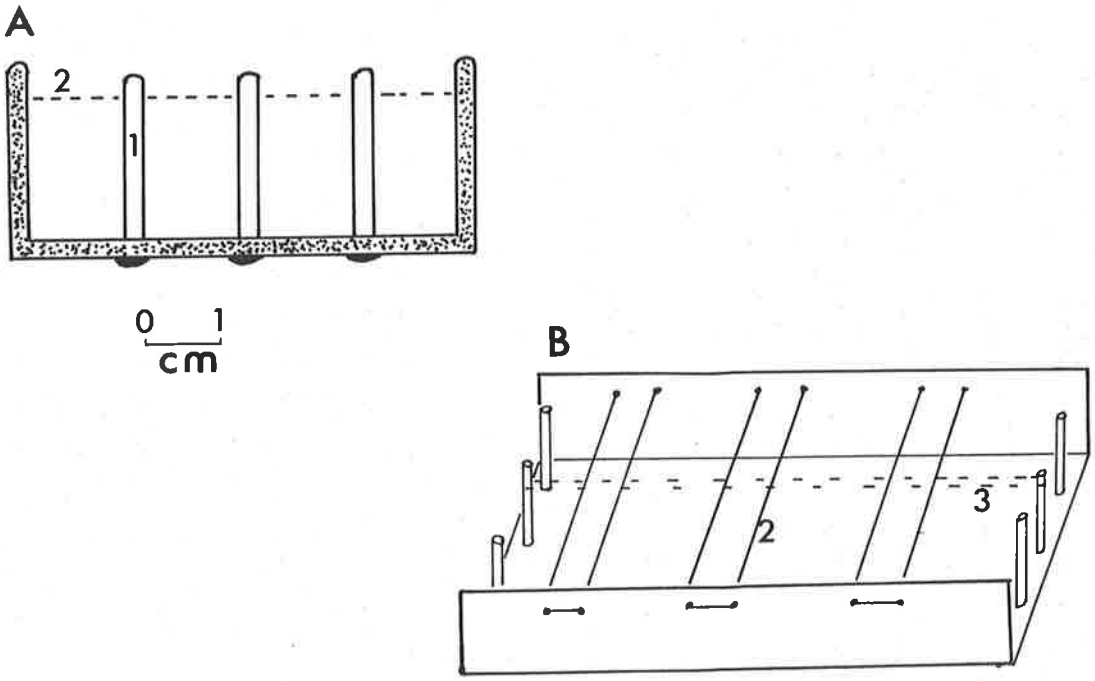

Figure 2.4. Disk holder showing the nylon lines (2), and rubber band (3) stretched between the screws (1) used to hold the disks in position, (A) end view, (B) top view.

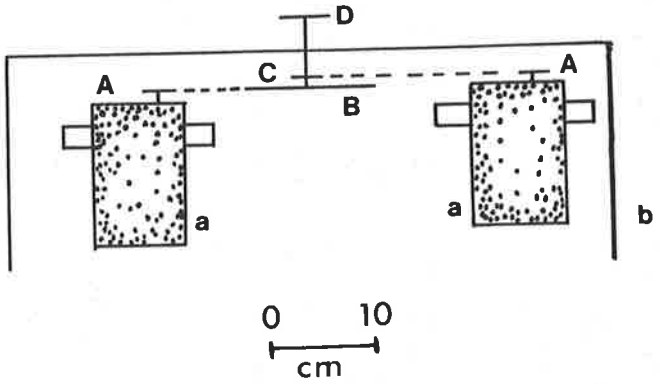

Figure 2.5. End view of motor chamber connected to water bath, showing position of drive cogs and two positions for motor (a). (A) engine cog = 12 teeth, (B) 48 teeth, (C) 12 teeth, (D) 10 or 15 teeth.

A light bank was constructed out of nine, 40 Watt, 120 cm long fluorescent tubes (three Sylvania F40/GRO-LUX, three Philips white TL 40 and three NEC 40W Bio-Lux-A) connected parallel to each other with a further two 40 Watt, 59 cm fluorescent tubes (Philips white TL 40) attached normally at each end. Aluminium foil was placed behind the tubes to increase the light intensity projected downwards. This whole structure was supported by metal legs with castors (to facilitate access) at 40 cm above the base of the containers.

To avoid possible problems associated with interactions between the materials used in construction and the plant material, all materials used were pre-soaked for 48 hours in seawater and then thoroughly cleaned (Schonbeck and Norton, 1980).

2.5.2. EXPERIMENTAL CONDITIONS

2.5.2.1. TEMPERATURE

The temperature within the chambers was maintained at 15± 0.5°C by use of a water bath. The selection of this temperature was used because Steffensen (1976) and Fortes and Leuning (1980) found that the growth of *Ulva lactuca* was maximized at 15 and 16°C respectively and, also because the temperature of the coastal waters of the Gulf of Saint Vincent average approximately 15-17°C (Bye, 1976).

2.5.2.2. LIGHT

The light flux necessary to maximize the growth rate of *Ulva* sp. has been found to range from 50- 100 µmol m^{-2} s^{-1} (Mohsen, Nasr and Metwalli, 1973; Fortes and Leuning, 1980; Parker, 1981). The light flux measured just below the water surface (using a Lambda underwater quantum sensor (LI-1855) and meter (LI-0192)), at the side and centre of each experimental chamber, varied from 100-120 µmol m^{-2} s^{-1}.

The light cycle was set at 12 hours light/ 12 hours dark. To maintain the light intensity achieved it was necessary to replace the fluorescent tubes regularly, as their output decays with time.

2.5.2.3. AERATION

Aeration was supplied using a small aquarium pump with clamps to control the flow rate. It was found that the aeration supplied was adequate to maintain dissolved oxygen levels at saturation for the duration of all experiments. This was measured by placing a 1 cm layer of liquid paraffin on the seawater surface and measuring the oxygen concentration using a Clark oxygen electrode coupled to a chart recorder. It was concluded that the gas exchange from the aeration coupled with the gas exchange at the seawater surface was more than that required for plant growth.

2.5.2.4. VOLUME OF MEDIUM

Because of the variation in size of the inner and outer annular chambers it was necessary to have the volume of medium non-limiting to the smaller of the chambers based on the volume of plant tissue present [0.3-0.6 g (fresh weight) per litre]. This was based on a daily schedule of media replacement and the concentration of the limiting nutrient, in this case phosphate. The required volume of the outer and inner chambers were 3.848 and 2.309 litres respectively. This gave a depth of medium in each chamber of 5 cm. Evaporation was compensated for daily by adding distilled water to maintain this depth.

2.5.3. EXPERIMENTAL PROCEDURE

Two types of experimental procedure were used to determine the rate of plant growth.

2.5.3.1. THE ONE CUT METHOD

In the first type, called the one cut method, disks were cut using a number seven cork borer (approximately 110 mm^2) from preconditioned *U. australis* thalli (see Section 2.1.2.). The disks were cut from the expanding region of the frond, avoiding the area 5 cm from the periphery and the thicker basal area (Steffensen, 1976). The disks from this region are uniform in cell size and the problem of sporulation is considerably reduced.

A large quantity of plants were used for each experiment because of the large number of disks required (300-400). The rationale for using many rather than an individual plant, was firstly to incorporate a large population sample in any one experiment, thereby reducing the variation in any experiments due to individual plant differences. Secondly, it had previously been found that a growth period of greater than six days was needed to obtain significantly different growth rates between treatments (Hone, 1982). Also, coupled with Hunt's (1982) reasoning, that to observe any variations in growth rate it was better to measure as frequently as possible, rather than from one initial and final measurement, this meant that a lot of disks were required.

Disks were kept in A.S.W. overnight (within the experimental water bath) to allow time for any wound response to occur. The next morning approximately 20 disks were put aside for later measurement of the experimental parameters, to give the initial growth status of the plants. Care was taken to handle the disks only with clean stainless steel tweezers to avoid contamination and bruising of the tissue. The remaining disks were randomly placed on the plant holders then placed randomly in any of the experimental chambers until sufficient disks had been added. This allowed an extra ten percent of disks for any losses occurring during the course of the experiment.

Before the experiment started the chambers were acid-washed (see Section 2.2.1.) and then filled with the appropriate medium. The whole system was turned on the previous day to allow the system to equilibrate. During the experiment disks were removed from the appropriate chambers according to the experimental schedule (usually every two or three days) and measured using the procedures outlined in Sections 2.3 and 2.4.

2.5.3.2. THE TWO CUT METHOD

The second type of experiment, called the two cut method, developed out of the observation that there was a large amount of variation within each treatment for all of the measured parameters. It was concluded that a lot of this variation was due to the growth status of the plant tissue at the beginning of the experiment. It was assumed that this occurred because the pre-conditioning culture conditions were not adequate to overcome individual plant differences in the time allowed. This was most probably a result of the lack of growth that occurred during the pre-conditioning. To overcome this a larger number of disks than required (400-500) were cut and placed on the plant holders, and placed in the same sized chambers (equivalent water movement) for a two week pre-conditioning period . The medium used was filtered seawater which was monitored and replaced as outlined in the next section.

After two weeks the disks were placed in a large dish filled with filtered seawater, and divided into two groups. Firstly those that had increased in size by greater than 100% (using a template), and secondly those that had grown less than this. This second group of disks was discarded, as were all disks which had sporulated or been damaged in any way. The first group of disks, which were to be used in the subsequent experiment, were re-cut using the number seven cork borer. These re-cut disks were treated in the same fashion as those used in the one cut method outlined above.

2.5.4. EXPERIMENTAL UPKEEP

The medium within the chambers was replaced daily with more of the same medium, which had been allowed to equilibrate to the experimental conditions. This was achieved by transferring the disk holders to a dish filled with their experimental medium, the chamber was then siphoned dry and wiped clean. The required amount of fresh medium was then added and the disk holders returned after a quick rinse in A.S.W.. This was repeated for each chamber. The whole process took less than 15 minutes and was done first thing in the morning, so as to avoid disturbing the disks during the light period. At the same time water samples were taken of the old and new media to monitor inorganic phosphate concentration and pH (see Sections 2.4.1 and 2.2.5).

2.6. FLOW TANK CONSTRUCTION

The design adopted was similar to one developed by Vogel and LaBarbera (1978). The flow trough was made out of a molded piece of 1 cm thick clear perspex (1.4 m long, 16.8 cm wide, 20.0 cm high). The final cross-section of the test region was 16.8 cm by 16 cm, and was located in the middle of the flow trough. The liquid volume was 78 litres. The water flow was created using a small pitch propeller (10 cm diameter, 1 cm wide) connected to a variable speed electric motor.

Material was held horizontally within the test region by supporting it on a nylon line rack and securing it with the use of rubber bands. The rack was held in place using thin stainless steel rods suspended from the edge of the flow tank.

2.7. CALIBRATION OF WATER MOVEMENT

Two methods were used, firstly a method using dye and secondly by a zinc dissolution method.

2.7.1 DYE METHOD

The dye was made using a mixture of milk and green vegetable dye (Merzkirch, 1974), which approximated the density of seawater. It was injected into the flow in a thin stream, and the time it took to pass along a marked distance (10 or 5 cm) measured. This method was not suitable for use in the shaker bath.

2.7.2. ZINC DISSOLUTION METHOD

King and Braverman (1932) found that the rate at which zinc dissolves in HCl was linearly related to the fluid velocity of the HCl. They concluded that this was caused by the reaction at the zinc surface being limited by the rate of diffusion of the HCl. Using this principle it is possible to measure the appropriate value of Kt for a particular water velocity using the relationship Kt = Vt/Cb (see Equation 1.19, Section 1.2.2.1.), where Vt is the rate of loss of zinc, and Cb is the concentration of HCl in the bulk solution. This formula assumes that the concentration of the HCl at the zinc surface is zero, which holds when diffusion boundary layer limitations occur and the bulk concentration does not saturate the reaction.

Zinc disks (133 mm^2) were punched from zinc foil (380 µm thick), and levelled by compressing between two blocks of wood. The disks were then gently sanded, etched for 5-10s in 5 kmol m^{-3} HCl, washed in distilled water, then in ethanol, and dried. The initial weight was recorded (measured to 4 significant figures in grams) and the disks placed in either the growth chambers, shaker bath or flow tank. 10 mol m^{-3} HCl and 50 mol m^{-3} KNO_3 were also added (used as a depolarizer since it eliminates hydrogen evolution and increases the rate of dissolution). The disks were removed at 10 minute intervals and reweighed. Four replicate disks were used per time period. To avoid oxidation, disks were kept in distilled water until used. The technique used for the shaker bath was

TABLE 2.3 Results of zinc calibration of the different flow treatments. The calculated D.B.L. thickness from the formulae of Chapter 1 are also given (S.E.)

Cog Ratio Engine/top	Growth-1	Growth-2 Inner 9/10	Growth-3 Inner 12/15	Growth-4 Outer 9/10	Growth-5 Outer 12/15	Shaker-S Slow	Shaker-F Fast
Dye Velocity U_b cm s^{-1}		1.31±0.03	2.50±0.04	3.07±0.06	3.33±0.07	-(a)	(4.33)(a)
Kt x 10^{-5} m s^{-1}	0.394	0.855	1.373	1.556	2.593	0.385	3.591
Rt x 10^{-5} s m^{-1}	2.54	1.17	0.73	0.64	0.39	2.59	0.28
δ = D/Kt(b) µm	583	269(c)	168(c)	148(c)	89(c)	597	64
$\bar{\delta}$lx(d) µm	579(e)	217(f)	157(f)	142(f)	136(f)	579(e)	120(f)
$\bar{\delta}$tux(g) µm	-	146	82	68	63	-	45

(a) The apparent velocity for the shaker treatments can be calculated using $Kt = 0.15e^{0.5}U_b$ (r^2 = .96) determined from the growth treatments. The velocity for Shaker-S is less than zero.

(b) The diffusion coefficient of HCl is 2.3 x 10^{-9} m^2s^{-1} at 15°C (see Table 3.1 for determination).

(c) Data was fitted to Equation 1.41 for constant, p and Q. Result was $\delta = 9.19\ U_b^{-0.88}\ \upsilon^{0.62}\ D^{0.27}\ x^{0.12}$ (r^2 = 0.91).

(d) $\bar{\delta}lx = 0.5\ \delta lu$ which is the average D.B.L. thickness for laminar flow.

(e) Used the equation (1.43) for free convection, $\delta = 2.02\left(\frac{x\ \upsilon\ D}{g\Delta\ c\alpha}\right)^{\frac{1}{4}}$ where α = 40 cm^2 mol^{-1}, g = 9.8 x 10^2 cms^{-1}, υ = 1.15 x 10^{-2} cm^2 s^{-1}, D = 2.3 x 10^{-5} cm^2s^{-1}, x = 1cm, Δc = 10 x 10^{-6} mol cm^{-3}.

(f) $\delta l = 3\ Sc^{-0.33}\ Re^{-0.5}\ x$ (Equation 1.32) for laminar flow.

(g) $\bar{\delta}tux = 0.9\ \delta tu$, where $\delta tu = 5.24\ D^{0.25}\ \upsilon^{0.65}\ x^{0.1}\ U_b^{-0.9}$, is the average D.B.L. thickness for turbulent flow.

slightly different as only one side of the disks was exposed to the acid solution. To reduce the error the downward side was coated in petroleum jelly to stop any dissolution that could occur.

The value of Kt for each water velocity was calculated using,

$$Kt\ (m/s) = ((W/\ A.W.)/t)/A)/[HCl] \qquad \text{Equ-2.1}$$

Equ. 2.1 where W is the change in zinc weight (g), A.W. is the atomic weight of zinc, t is the elapsed time (s), A is the disk area, either 265.5 or 132.7 μm^2, and [HCl] is the concentration of HCl (mol m^{-3}).

This technique was also used to determine the diffusion boundary layer profile over a flat plate in the flow tank. To do this a clean sheet of zinc (20 cm long by 10 cm wide) was placed on the holder within the flow tank. The solution was 20 mol m^{-3} HCl and 50 mol m^{-3} KNO_3, and the temperature 19°C. The sheet was removed after 6-8 hours, and 4 replicate disks punched at increasing distances from the leading edge, these disks weighed. The long time span was necessary to overcome the variation in disk size associated with punching out the disks from the sheet.

The value of Kt determined using this method takes into account any variations that occur in fluid velocity and character, and as such represents an average value for the flow situation measured.

2.7.2.1. RESULTS

The rate of zinc dissolution was linear with time as shown in Figure 2.6. The value of Kt for each flow situation is presented in Table 2.3. Also calculated were the effective diffusion boundary layer (D.B.L.) thicknesses based on the values of Kt or the external conditions. The thickness of the D.B.L. as measured using the zinc technique is an average value for the length of the disk. Therefore the predictive formulas for calculating the thickness of the D.B.L. need to be based on average formulae. There is a good agreement between the zinc and formula D.B.L. thicknesses for all except the Growth-5 and Shaker-F

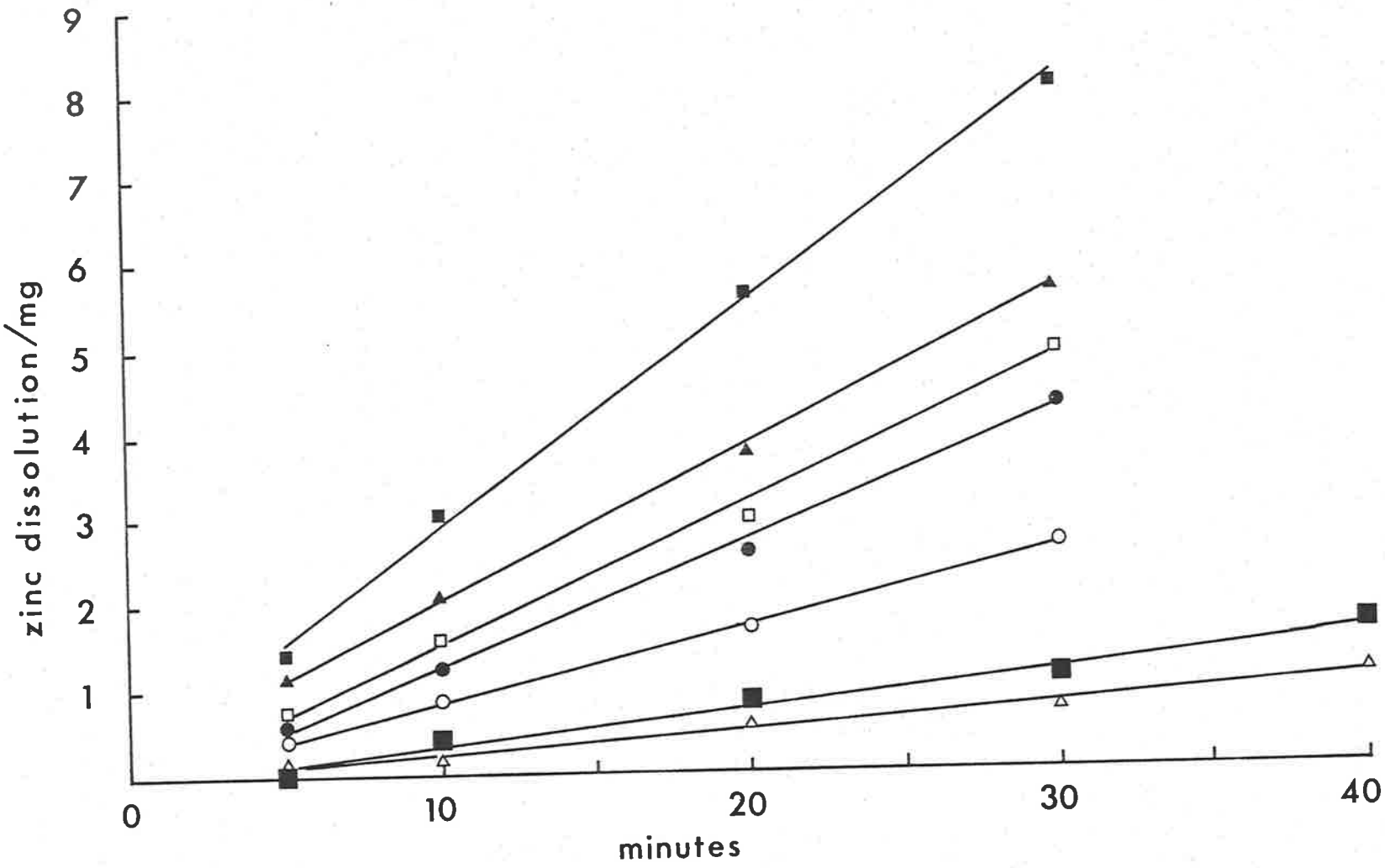

Figure 2.6. Change in weight of zinc disks versus time for the Shaker-S (△, r^2 = 0.99), Shaker-F (▲, r^2 = 0.99), Growth-1 (■, r^2 = 0.99), Growth-2 (○, r^2 = 0.99), Growth-3 (●, r^2 = 0.99), Growth-4 (□, r^2 =0.99) and Growth-5 (■, r^2 = 0.99) (each point is the average of 10 values)

treatments. These treatments have a far better fit with the turbulent formula for D.B.L.. The conclusion, based on the observed devolopment of turbulence (dye experiment) in Growth-5, is that the D.B.L. is turbulent for these two treatments. One of the problems with equating the formulae for the thickness of the D.B.L. and the apparent measured values is that if turbulence develops at some distance from the leading edge then the average thickness is a combination of the two predictive formulae.

2.8. MEASURMENT OF SHORT TERM PHOSPHATE INFLUX

2.8.1 TYPES OF EXPERIMENTS

Two major types of experimental methodology were used, which can be identified on the basis of the apparatus in each.

2.8.1.1. TYPE 1

2.8.1.1.2. APPARATUS

This consisted of a Labmaster shaker bath fitted with a rack capable of holding 16, 50 ml pyrex flasks. The temperature of the water bath was kept constant at 15°C by recirculating water from a constant temperature water bath fitted with a Heidolph heater/stirrer and a Grant cooler. An overhead light bank consisting of four fluorescent tubes (Philips TL 40 cool white) provided a light intensity of 100-110 µmol m^{-2} s^{-1}.

All experiments used acid washed glassware. The various phosphate concentrations were achieved using 2 mol m^{-3} KH_2PO_4 stock solution added to A.S.W.. Radioactive super-32P was added to give a concentration of 0.3 µCi m^{-3}, and a final volume of 25 μm^{-3}. The final pH of all solutions was 8.2. All solutions were handled using the appropriately calibrated Gilsen Pipette, and appropriate radiation safety precautions were observed. Once the solutions had been made up they were placed in the water bath for the temperature to equilibrate.

2.8.1.1.3. STANDARD METHOD AND SCHEDULE

The experimental procedure (variations of which are outlined below) involved placing individual disks in their allotted flasks at staggered intervals (1 minute). The velocity control of the shaker bath was set to the same determined two settings for each experiment (slow velocity is Shaker-S, fast velocity is Shaker-F). After 10 minutes the disk was removed, blotted dry and then placed in a separate beaker filled with 50 μm^{-3} of A.S.W. for 5 minutes, occasionally agitating by hand. The reason was to rinse the labelled phosphate from the free space, so that the influx measured truly reflected the amount of label that had crossed the plasmalemma. Each disk was then blotted dry and placed in an individual scintillation vial containing 10 μm^{-3} of the standard toluene/detergent/PPO/POPOP scintillation liquid and 100 nm^{-3} of 3 kmol m^{-3} HNO_3. The vials were allowed to stand for 2 hours, as this allowed the disk which had sunk into the layer of nitric acid at the bottom of the vial to be partly digested, facilitating the release of the labelled phosphate. The vials were then shaken to mix the contents, and the labelled phosphate counted using a Packard Tri-Carb Liquid Scintillation Spectrometer (Model 3330) for 5 to 10 minutes (depending on the specific activity of the radioactive solutions).

From each radioactive flask, two replicate 40 µl aliquots were taken so that specific activities [counts min^{-1} (mol of phosphate)$^{-1}$] could be measured. The results were expressed in a variety of ways, as nmol (of incorporated phosphate) m^{-2} (surface area, both sides) s^{-1}, as nmol g^{-1} (fresh or dry weight of tissue) s^{-1}, or finally as specific influx μs^{-1} [nmol g^{-1} s^{-1} nmol g^{-1}(internal phosphate concentration)].

This experimental technique was used for four main variations on the above theme.

2.8.1.1.4. PHOSPHATE INFLUX VERSUS TIME

The temperature was set at 15°C. The disks (total tissue area per disk was 1.72 cm^2, number five cork borer) were placed in individual flasks containing three phosphate concentrations (0.25, 1.0, 10.0 mmol m^{-3}) and removed after 10, 20, 40, or 80 minutes. There were four replicates per concentration per time period, and the speed selected was shaker-F.

2.8.1.1.5. PHOSPHATE INFLUX VERSUS PHOSPHATE CONCENTRATION

The temperature was set at 15°C. The amount of labelled phosphate added was 0.3 µCi μm^{-3}, and the shaker bath speed set to shaker-S or shaker-F. Replicate measurements (n = 3-5) for each concentration were made.

2.8.1.1.6. GROWTH EXPERIMENTS

Sixteen acid washed flasks were prepared for each experimental growth treatment, which allowed for 8 phosphate concentrations (0.25, 0.5, 1, 2, 3, 5, 10, 20 mmol m^{-3}) replicated twice. The equivalent number of beakers were prepared for the final rinse, and all solutions kept at 15°C. All growth influx experiments started at 0900 hours with the random removal of 16 disks from each experimental treatment (from the growth chambers). Their area and fresh weight was recorded and then each disk was divided in half using a circular template. One half was put aside for measurement of dry weight and internal total phosphate content. The remaining half of each disk was kept in an individual vial containing A.S.W., and then used to determine phosphate influx. The reasoning behind this technique was that influx for each disk could be associated with its internal phosphate content.

The phosphate influx was then determined for the various concentrations using the standard method outlined above, with the speed set to shaker-F. This speed was appropriate as it was shown (Chapter 3)

that it overcame any diffusional limitations, therefore the measured influx was a reflection of the influx kinetics at the plasmalemna surface.

2.8.1.1.7. PHOSPHATE LOADING

Disks (number 7 cork borer, two times area = 2.24 cm^2) were placed in 500 cm^3 beakers of A.S.W. with known concentrations of KH_2PO_4 (0, 5, 10, 20 mmol m^{-3}). They were placed in a shaker bath kept at 15°C, light intensity 40 µmol m^{-2} s^{-1}, bubbled with air and shaken prior to the experiment starting. The disks were left for various time periods to take up non-labelled phosphate prior to the experiment starting, and during the experiment. At increasing loading times, four replicate disks were removed and divided in half, and their ^{32}P influx measured at a single phosphate concentration using the standard method (temperature of shaker bath was 15°C, shaker speed was shaker-F).

2.8.1.2. TYPE 2

2.8.1.2.1. FLOW TANK

The flow tank contained 78 litres of filtered seawater to which radioactive ^{32}P phospate (67 µCi m^{-3}) was added to give a phosphate concentration of 0.29 mmol m^{-3}. Temperature was constant at 19 ± 1°C, light intensity 40 µmol m^{-2} s^{-1}, pH 8.2 ± 0.07, and water velocity varied. The experimental technique required placing rectangular sheets of *U. australis* on a nylon line rack parallel to the flow and normal to the irradiance. The sheet was removed after 2 hours and approximately 7 replicate disks (number 7 cork borer) cut from measured distances (every 2 cm) from the leading edge. The disks were washed for 5 minutes and then placed in scintillation vials and counted using the technique previously explained . Results for phosphate influx were either expressed as µmol m^{-2} s^{-1} or µmol g^{-1} (fresh weight) s^{-1}.

2.9. DATA PRESENTATION AND ANALYSIS

All results are expressed as the mean plus or minus the 95% confidence levels, except where otherwise stated. For growth analysis the programs of Parsons and Hunt (1981) and Hunt (1982) have been used to curve fit the data, calculate the confidence levels, and the relative growth rates (R.G.R.). The R.G.R. has also been calculated from the raw data, using the relationship

$$R.G.R. = \ln(W2/W1)(t2 - t1)^{-1} \quad \text{Equ. 2.1}$$

where W1 and W2 are the dry weights at times t1 and t2 respectively (note natural logarithms). The units of R.G.R. are expressed as day^{-1} ($g\ g^{-1}\ day^{-1}$). The term specific growth rate is often used in the literature, and is equivalent to 100 times the R.G.R..

The data from the influx experiments were analysed using the FORTRAN-4 program INFLUX-P.FOR, which took into account the isotopic decay of ^{32}P.

The values of Vm and Km were obtained using the Basic-M program NONLIN.BAS (Duggleby, 1981), which uses a least squares method of calculation to obtain the parameters from the Briggs-Haldane equation (Equation 46). The determination of the constant values (Vm, Km, and Kt) was achieved using a FORTRAN-4 program developed by N. A. Walker (FVKUP.FOR). This was based on the subroutine written by M. Bell using the pattern-search method of Hookes and Jeeves (1961) and described in Colquhoun (1971). This pattern-search method was further adapted to fit the appropriate values in other equations used by the author. All programs were run on a Kaypro-4 micro-computer.

Where possible the problems associated with pseudo-replication, as described by Hurlbert (1984), have been avoided. In the case of the growth chambers a compromise had to be reached between false replication and the logistics of creating a suitable system.

CHAPTER 3. THE EFFECT OF WATER MOVEMENT ON SHORT TERM PHOSPHATE INFLUX.

3.1 INTRODUCTION

Phosphorus plays a crucial role in plant metabolism, especially with regard to energy transfer. The plant's phosphorus status is therefore closely linked to the phenomena of growth, development and reproduction (Kuhl, 1974). When the plant's internal phosphorus content declines to below a critical level then the plant is said to be phosphorus limited. The concept of a limiting nutrient is based on Liebig's Law, that the rate of growth depends on the nutrient in least supply (Droop, 1973). Under this condition the rate of metabolism is directly related to the equilibrium between the external phosphorus content and the internal phosphorus status. The concentration of inorganic phosphorus in seawater often limits the growth of algae (Kuwabara and North, 1980; Birch, Gordon and McComb, 1981; Myers and Iverson, 1981; Raven, 1981; Manley and North, 1984; Smith, 1984; Lapointe, 1985, 1986, 1987; Lapointe and Hanisak, 1985). The concentration of inorganic phosphorus in most coastal surface waters ranges from unmeasurabe to 2 mmol m^{-3} with the majority of waters less than 1 mmol m^{-3} (Cooper, 1937; Smith, 1984). Therefore it is of interest to know what resistances are associated with the various steps in the pathway from the external phosphorus concentration to internally available phosphorus, and the overall kinetics of the process.

Phosphorus in seawater can exist in one of four states: (1) incorporated into living systems, (2) particulate phosphorus (PP), (3) dissolved organic phosphorus (DOP), (4) dissolved inorganic phosphorus (DIP) (Strickland and Parsons, 1965). Excluding the living systems, PP is the most abundant form (60-70%), then either DOP or DIP depending on the biomass of the flora present (Valiela, 1984). Within the marine environment DIP is the form of phosphorus which is utilized by algae (Raven, 1980).

Inorganic phosphorus exists in the aquatic environment almost always as orthophosphates (abbreviated to phosphate, Stumm and Morgan, 1970), which includes phosphoric acid (H_3PO_4) and the products of its dissociation ($H_2PO_4^-$, HPO_4^{2-}, PO_4^{3-}; Table 3.1), all of which can form various complexes with other compounds present in the seawater (Kuwabara, Davis and Chang, 1986). This is of considerable importance as $H_2PO_4^-$ binds with $CaCO_3$ (Hanisak, 1987) decreasing the available phosphate for plant metabolism. In seawater with a pH of 8.2, the percentages of phosphate species are 86.1%, 13.3% and 0.6% for HPO_4^{2-}, PO_4^{3-} and $H_2PO_4^-$ respectively, while H_3PO_4 virtually does not exist (Figure 3.1).

The question of which species of phosphate is taken up by plants is not easily resolved. Energetically it is far cheaper for the plant to take up $H_2PO_4^-$ over HPO_4^{2-}, because of the single negative charge opposed by the electrical potential difference of the cell (see Section 3.2.4.). However the former is two orders of magnitude lower in concentration. Ecological reasoning would suggest then that HPO_4^{2-} could be of more importance. The majority of experimental evidence points to $H_2PO_4^-$ being the species taken up (see Bieleski, 1973) though there is some evidence for the uptake of HPO_4^{2-} in higher plants (Hagen and Hopkins, 1955). Experimental variation of the external pH provides inconclusive evidence. For higher plants the optima ranges from pH 4 to pH 6 ([$H_2PO_4^-$] 95%, Hagen and Hopkins, 1955; Dunlop and Bowling, 1978; Sentenac and Grignon, 1985). In the aquatic environment, for most algae the optimum exists between pH 7 and pH 9 ([$H_2PO_4^-$] 1%, Ullrich-Eberius and Yingchol, 1974; MacFarlane, 1985). This conflicts with the downward shift in the pH optima for each phosphate species compared to weak buffered solutions (Sober, 1968).

TABLE 3.1. Physical attributes of phosphate[1] and the diffusion coefficient of hydrogen (in seawater 35 °/oo).

PARAMETER	VALUE (°C)	REFERENCE
DISSOCIATION CONSTANTS		
pK'_{a1} of PHOSPHORIC ACID	1.54(25)	Millero (1983)
	1.61(25)	Kester and Pytkowicz (1967)
	1.53(15)	
	1.62(25)	Dickson and Riley (1979)
	1.60(15)	
pK'_{a2} of PHOSPHORIC ACID	5.90(25)	Millero (1983)
	6.06(25)	Kester and Pytkowicz (1967)
	6.13(15)	
	5.94(25)	Dickson and Riley (1979)
	6.03(15)	
	6.03(15)	Johansson and Wedborg (1979)
pK'_{a3} of PHOSPHORIC ACID	8.63(25)	Millero (1983)
	8.56(25)	Kester and Pytkowicz (1967)
	9.08(15)	
	8.93(25)	Dickson and Riley (1979)
	9.08(15)	
	9.19(15)	Johansson and Wedborg (1979)
DIFFUSION COEFFICIENTS		
$H_2PO_4^-$ m^2 s^{-1}	8.27×10^{-10}(25)	Krom and Berner (1980)
	6.56×10^{-10}(15)	(at infinite dilution)
	6.88×10^{-10}(25)	MacFarlane (1986)
	4.75×10^{-10}(15)[2]	
HPO_4^{2-} m^2 s^{-1}	7.50×10^{-10}(25)	Krom and Berner (1980)
	5.74×10^{-10}(15)	(at infinite dilution)
	1.73×10^{-10}(25)	MacFarlane (1986)
	1.57×10^{-10}(15)[2]	
PO_4^{3-} m^2 s^{-1}	4.75×10^{-10}(15)	Li and Gregory (1974)
	-2.06×10^{-10}(15)[2]	(at infinite dilution)
HCl m^2 s^{-1}	2.30×10^{-9} (15)[2]	
H^+ m^2 s^{-1}	7.94×10^{-9} (15)[2]	
ACTIVITY COEFFICIENTS		
$H_2PO_4^-$	0.502(25)	Whitfield (1975)
HPO_4^{2-}	0.115(25)	
PO_4^{3-}	0.012(25)	

(1) The equilibrium reaction of phosphoric acid is

$$H_3PO_4 \underset{k_1}{\overset{k_1}{\rightleftharpoons}} H^+ + H_2PO_4^- \underset{k_3}{\overset{k_2}{\rightleftharpoons}} H^+ + HPO_4^{2-} \underset{k_5}{\overset{k_4}{\rightleftharpoons}} H^+ + PO_4^{3-}$$

where k_1 to k_6 represent the reaction rate constants and are very rapid, being only limited by the rate of diffusion in seawater.

(2) These diffusion coefficients were calculated by multiplying the diffusion coefficient (at 15 °C and 35 °/oo ionic strength) at infinite dilution (Li and Gregrory, 1974) by the activity factor (Whitfield, 1975). The calculated activity factors were; $H_2PO_4^-$ = 0.720, HPO_4^{2-} = 0.276, PO_4^{2-} = -0.435, H^+ = 1.018 and HCl = 0.891.

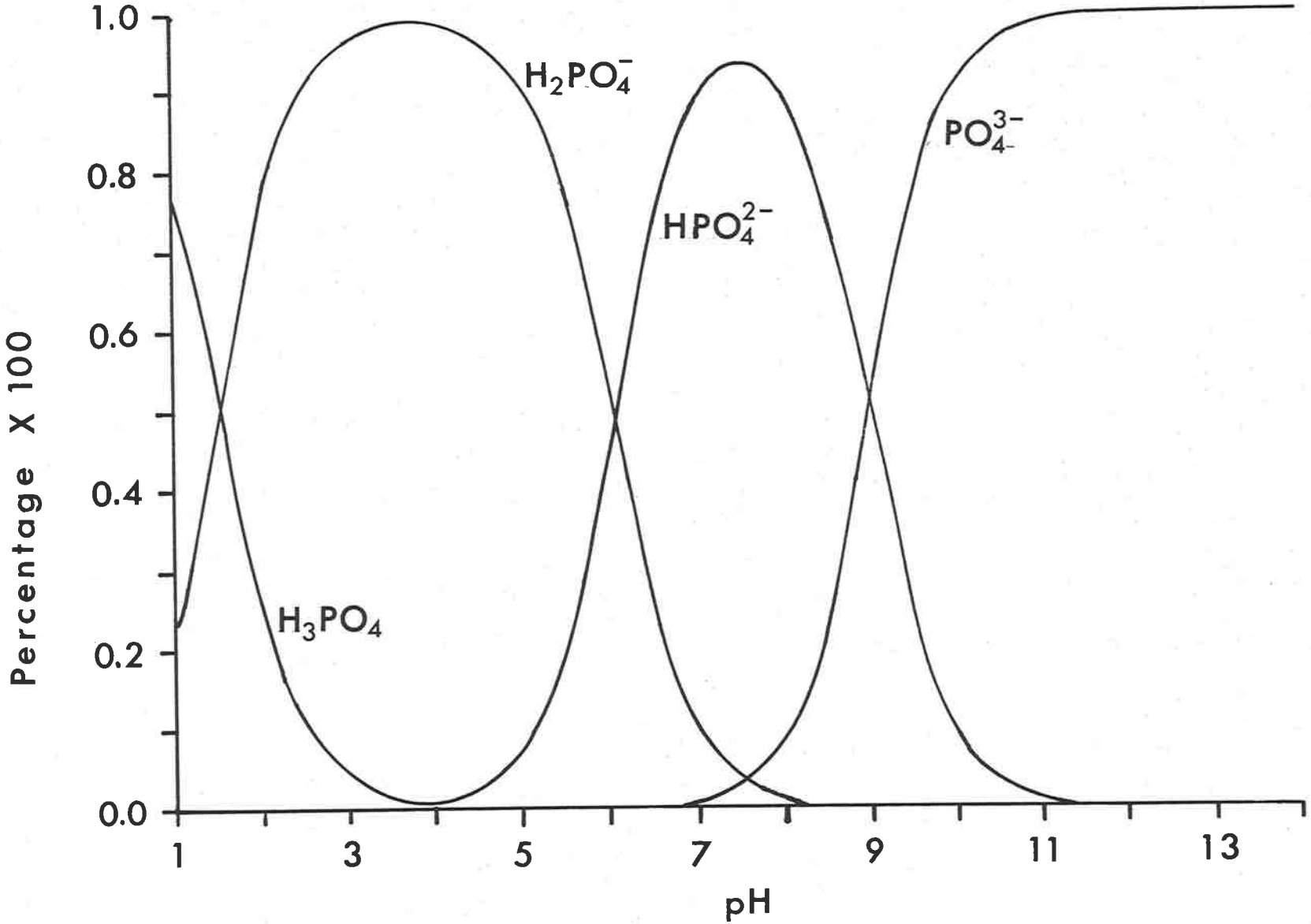

Figure 3.1. Changes in the percentage of the different phosphate species with increasing pH, calculated from the dissociation constants given in Table 3.1.

The evidence for active influx of phosphate via a membrane porter comes from Smith (1966) using *Nitella*, Blum (1966) using *Euglena*, Kylin (1966) using *Scenedesmus*, Raven (1974a,b) using *Hydrodictyon*, Falkner, Horner and Simonis,(1980) using *Anacystis*, Manley (1985) using *Macrocystis* and MacFarlane (1985) using *Ulva*. The kinetics of phosphate influx can be more complicated than that represented by a single porter. There is considerable evidence that two (Laties, 1969; Ullrich-Eberius, 1973; Vange, Holmern and Nissen, 1974; Lehman, Botkin and Likens, 1975; Beevers and Burns, 1980) or more (Nandi, Pant and Nissen, 1987) uptake systems are present, each exibiting varying values in Km and Vm. For marine plants the high affinity system is of the most ecological importance considering the lack of phosphate in marine waters. At extreme phosphate concentrations there is evidence that active influx is supplemented by diffusion (Schjorring and Jensen, 1984b). Efflux has been found to be negligible in comparisons between influx and net uptake when the external phosphate concentration is low (Perry, 1976; Schjorring and Jensen, 1984a). Schjorring and Jensen (1984a) found efflux increased when the internal concentration of phosphate increased.

It is generally assumed that influx includes co-transport, but the identity of the cotransport species is in doubt (excluding the possibilty of a uniport). Most evidence points to either H^+ (Bowling and Dunlop, 1978; Beevers and Burns, 1980; Ullrich-Eberius, Novacky, Fisher and Luttge, 1981;) for higher plants, or Na^+ (Kylin, 1964; Ullrich-Eberius and Simonis, 1970a,b; Raven and Smith, 1980) for algae, being co-transported.

A decreasing resistance to the diffusion boundary layer as manipulated by increasing water movement, has been shown to increase the uptake of a considerable range of nutrients (Table 3.2). The majority of this research has not related the data in any quantitative

TABLE 3.2. Previous research on the effect of water movement on nutrient uptake. (yes indicates an increase in nutrient uptake with increasing water movement)

Species	Nutrient	Does water velocity effect uptake	Reference
Ulva rigida	Phosphate	weak	MacFarlane 1985
Lolium perenne	Phosphate	yes	Breeze 1984
Synechoccus leopoliensis	Phosphate	yes	Mierle 1985
Oedogonium	Phosphate	yes	Schumacher et al. 1965
Eunotia	Phosphate	yes	Schumacher et al. 1965
Tribonenia	Phosphate	yes	Schumacher et al. 1965
Vaucheria	Phosphate	yes	Schumacher et al. 1965
Batrachospermum	Phosphate	yes	Schumacher et al. 1965
Andouinella	Phosphate	yes	Schumacher et al. 1965
Thermophilic algae	Phosphate	yes	Sperling et al. 1969
Oedogonium kurzii	Phosphate	yes	Whitford et al. 1964
Spirogyra	Phosphate	yes	Whitford et al. 1964
Oedogonium	Phosphate	yes	Whitford et al. 1982
Thalossiosira	Phosphate	yes	Canelli and Fuhs 1976
Macrocystitis pyrifera	NO_3^-	yes	Gerard, 1982
Ditylum brightwellii	NO_3^-	yes	Pasciak and Gavis 1975
Ditylum brightwellii	NO_2^-	yes	Pasciak and Gavis 1975
Mastigocladus laminosus	HCO_3^-	yes	Sperling and Hale 1973
Lemanea	HCO_3^-	yes	Thirb et al. 1982
Ulva	HCO_3^-	yes	Beer and Eshel 1983
Fontinalis	HCO_3	yes	James 1928
Fontinalis	CO_2	no	James 1928
Chlamydomonas reinhardtii	CO_2	no	Lehman 1978
Chlorella	CO_2	yes	Livansky 1982
Kelp	CO_2	yes	Wheeler 1976
Callitriche stagnalis	CO_2	yes	Madsen et al. 1983
Chara / Nitella	NH_4^{2+}	yes	Walker et al. 1979
Ulva lactuca	NH_4^{4+}	yes	Parker 1981
Gracilaria tikvahiae	NH_4^{4+}	yes	Parker 1982
Macrocystis pyrifera	NH_4	yes	Wheeler 1980
Ulva	O_2	yes	MacFarlane 1985
	Methylamine		

way to the variations in external boundary resistance. Only Wheeler (1980), MacFarlane (1985), MacFarlane and Raven (1985) and Mierle (1985) have attempted to relate the theory pertaining to diffusion boundary layer development to the observed results. The following section looks at short term phosphate influx to determine if there is the possibilty that the external boundary conditions can alter the influx to a sufficient degree to affect the alga's metabolism.

3.2 RESULTS AND DISCUSSION

3.2.1. THE EFFECT OF TIME ON PHOSPHATE TAKEN UP

Phosphate uptake was linear with time for the three phosphate concentrations used, as shown in Figure 3.2 ([Pi]b is the total phosphate concentration in the bulk solution). Using the cell dimensions (Table 2.1) it is possible to calculate an approximate determination of the increase in internal cell phosphate concentration as represented by the data in Figure 3.2. Table 3.3 shows that the internal phosphate concentration per cell increases with time to values well above [Pi]b. If this increase represents the change in phosphate concentration within the cytoplasm and it is assumed that the phosphate remains unmetabolized, then this would be in agreement with previous research showing an active uptake for phosphate against the negative electrochemical gradient which exists across the plasmalemma (Blum, 1966; Kylin, 1966; Smith, 1966; Raven, 1974a,b). However, the possibility of the formation of metabolized phosphate compounds, and the transport of phosphate into other compartments (e.g. vacuole) makes drawing such conclusions only speculative.

The linear relationship between uptake and time meant that the results for phosphate influx versus [Pi]b obtained over ten minutes are not obscured by declining influx as a result of increasing concentration of internal cell phosphate or phosphorus.

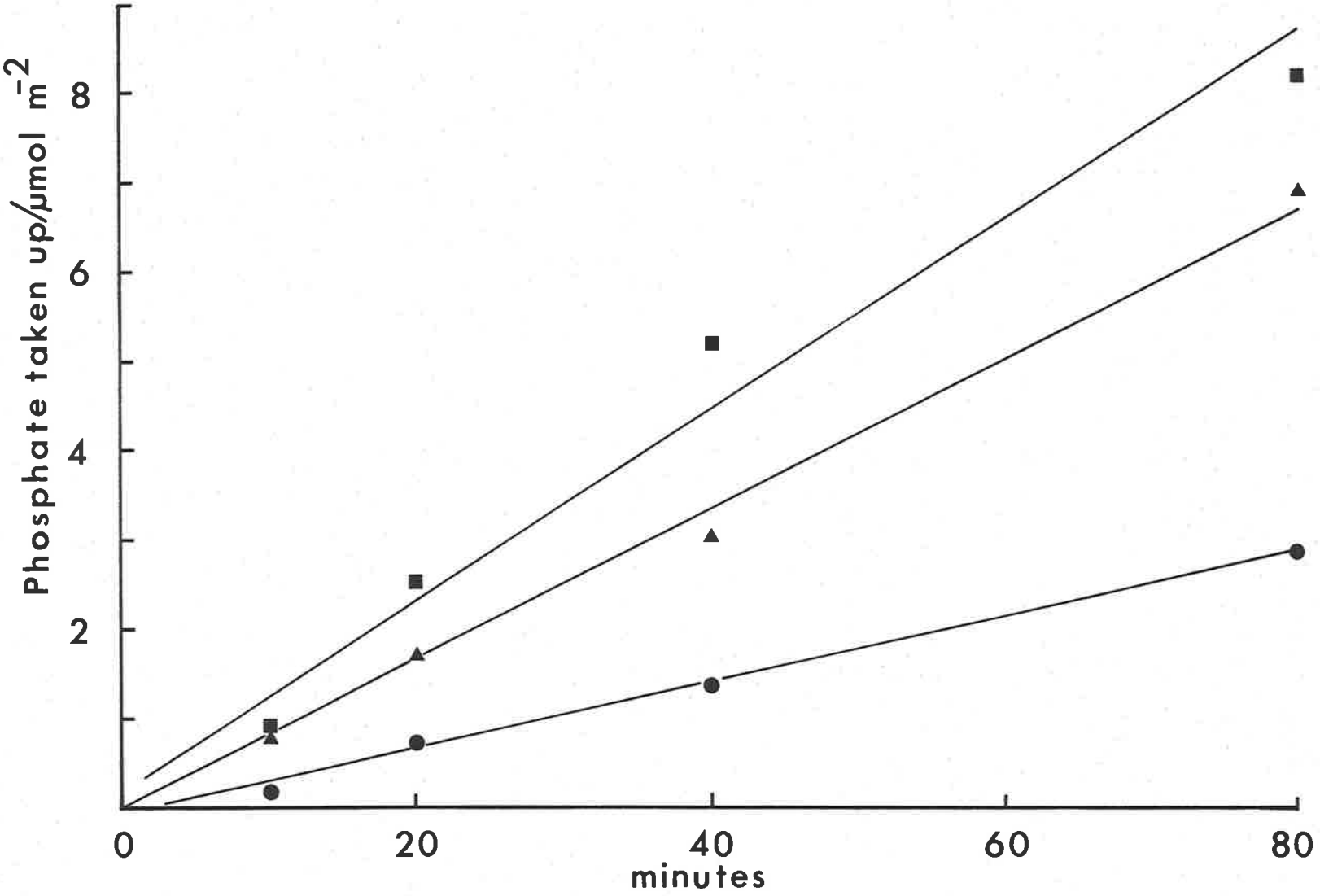

Figure 3.2. The relationship between phosphate taken up and time for [Pi]b = 0.25 ($\bullet$, r^2 = 0.99), 1.0 ($\blacktriangle$, r^2 = 0.99) and 10.0 mmol m^{-3} ($\blacksquare$, r^2 = 0.97).

TABLE 3.3. Increase in the concentration of phosphate within the cells of *Ulva australis*[a] (mmol m^{-3}).

Time (mins)	External Total Phosphate Concentration 0.25 mmol m^{-3}	1.0 mmol m^{-3}	10.0 mmol m^{-3}
10	6.31	28.07	36.60
20	26.72	61.39	90.14
40	49.17	108.34	185.26
80	101.93	24.576	291.43

(a) Assume cell approximately rectangular, dimensions from Table 2.1 are 28 x 10^{-6} m x 12.5 x 10^{-6} m x 12.5 x 10^{-6}, therefore volume is 4.41 x 10^{-15} m^3, number of cells per m^2 is 6.369 x 10^9 cells m^{-2} is 28.07 x 10^{-6} m^3 m^{-2}. Therefore phosphate taken up µmol m^{-2}/28.07 x 10^{-6} m^3 m^{-2} is the concentration of phosphate per m^3 of cells.

3.2.2. BRIGGS-HALDANE MODEL OF PHOSPHATE INFLUX

The results of four phosphate influx versus [Pi]b experiments, where water movement was varied in each, are presented in Figures 3.3 and 3.4. The results in each experiment, for the fastest water movement (Shaker-F) are typical of the rectangular hyperbola represented by the kinetics of a Briggs-Haldane type reaction. The variation in water movement (equivalent to varying Rt the mass transfer resistance) was sufficient to alter the Michaelis constant (Km) as predicted by the D.B.L. theory (Table 3.4). The value of Km for the smallest external resistance (Shaker-F) varied between 1-3 mmol m^{-3}, which agrees well with previously obtained results (Kautsky, 1982; Wallentinus, 1984; MacFarlane, 1985; Sentenac and Grignon, 1985). However the value for Vm was considerably lower when compared with other algae (Raven, 1974a; Gordon, Birch and McComb, 1981; Kautsky, 1982; Wallentinus, 1984; Manley, 1985; Mierle, 1985) and also for *Ulva* (MacFarlane, 1985).

The fitted curves in Figures 3.3 and 3.4 represent the Briggs-Haldane equation fitted using the calculated parameters from Table 3.4. The fitted curves show a good correlation with the results for both water movement treatments. However the increased error associated with the fitted Km for the slower water movement treatments (Shaker-S) represents the increased discrepancy between this fit and the true shape of the Briggs-Haldane equation. As previously explained (Section 1.3) this discrepency between Km for the two water movement treatments results when the flux through the D.B.L. limits the influx at the plasmalemma surface. Under these conditions the true Km is best approximated by the value determined for the Shaker-F treatment, and the Km determined for Shaker-S represents an apparent Km.

The variation in true Km (Shaker-F) is not constant between experiments. This cannot be correlated with the large variation which

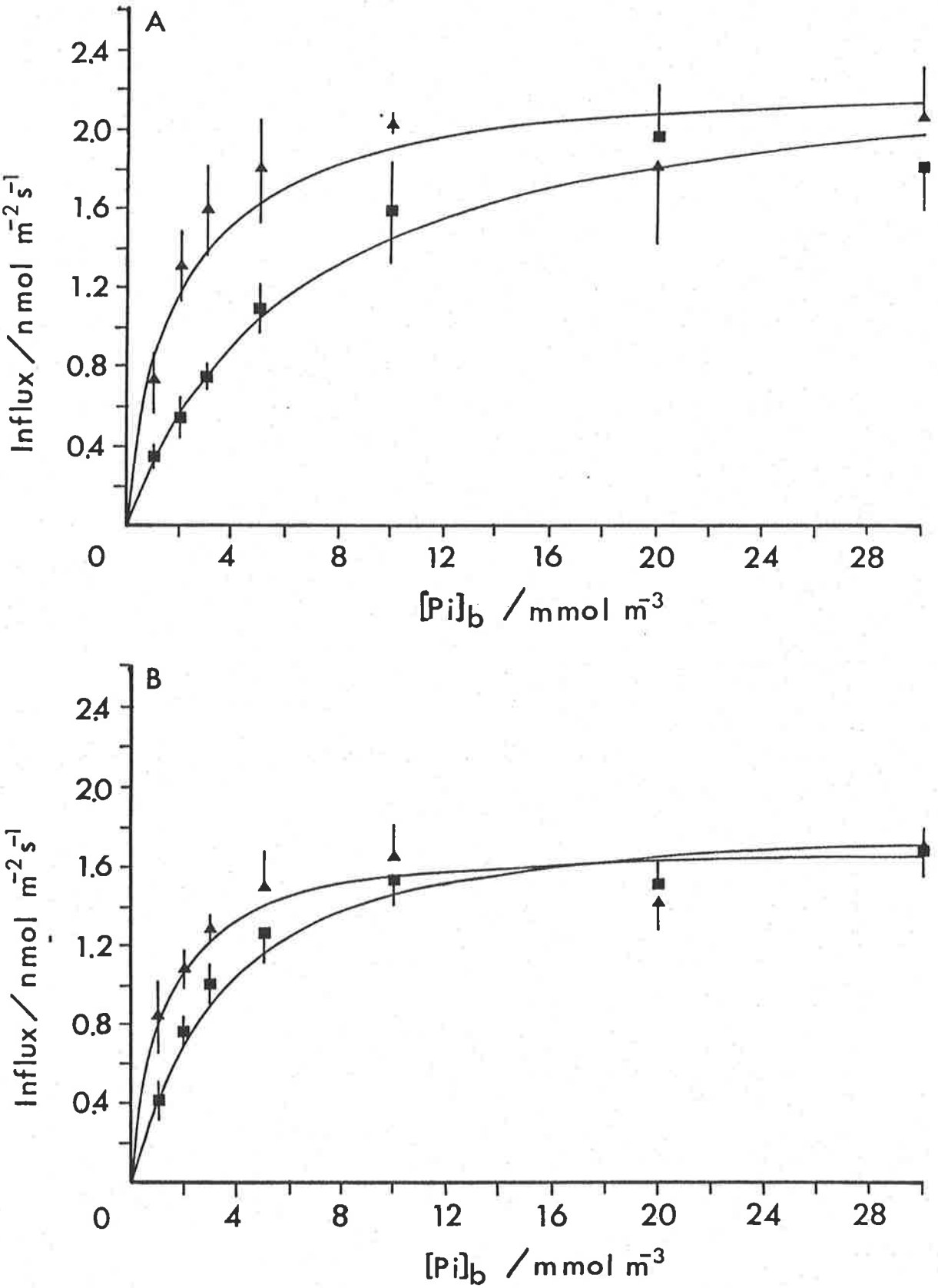

Figure 3.3. Phosphate influx versus [Pi]b for the Shaker-S (■) and Shaker-I (▲) treatments (n = 5, C.L.). The curves were fit using the Briggs-Haldane equation and the values of Km and Vm from Table 3.4. (A) Experiment 1 (B) Experiment 2.

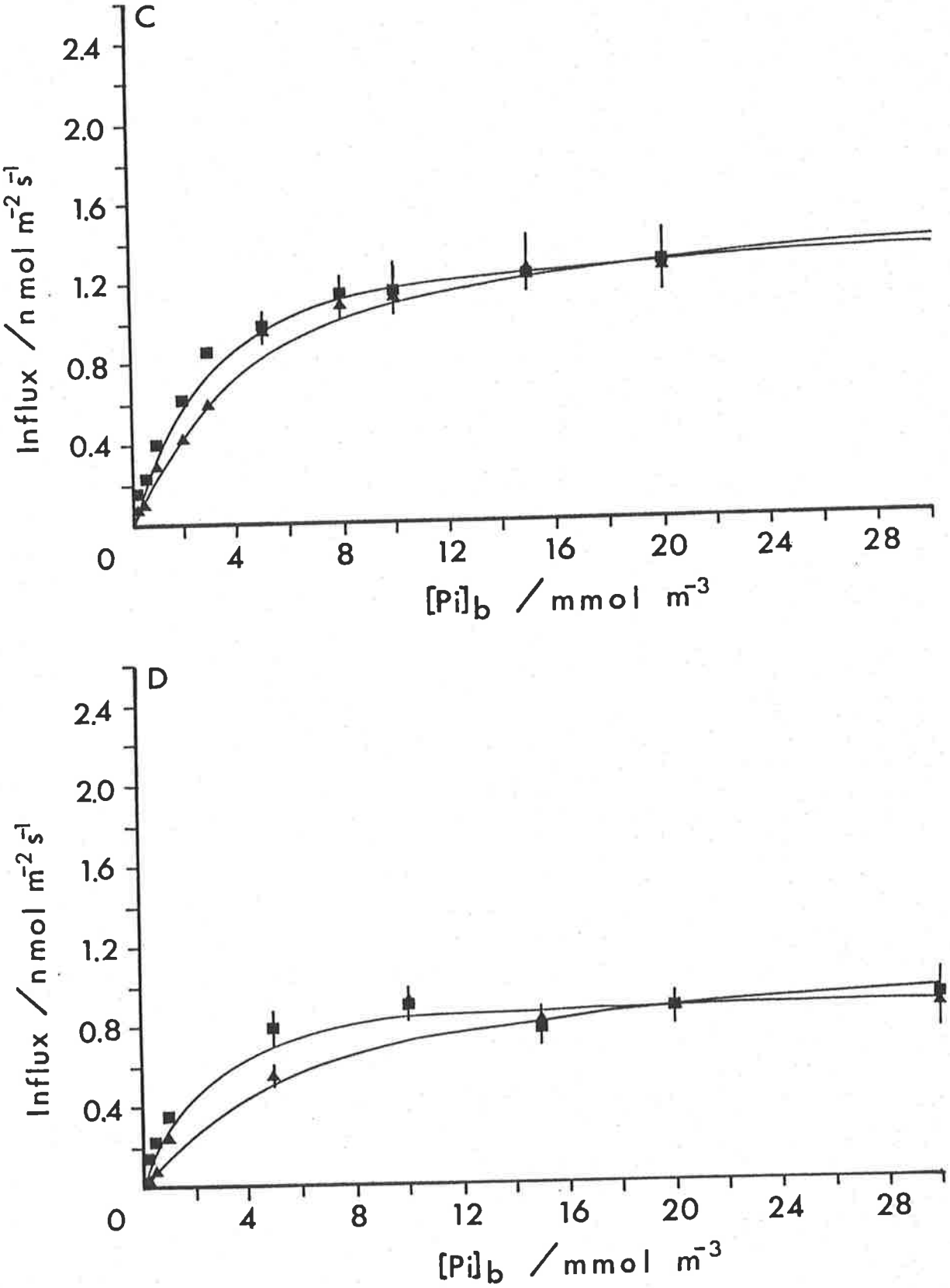

Figure 3.4. See Figure 3.3 for the explanation of the symbols and fitted curves, (C) Experiment 3 (D) Experiment 4.

TABLE 3.4. Michaelis parameters fitted using the program NONLIN.BAS [errors are standard errors (S.E.)].

	Shaker-F		Shaker-S	
	Vmax	Km	Vmax	Km
	nmol m^{-2} s^{-1}	mmol m^{-3}	nmol m^{-2} s^{-1}	mmol m^{-3}
Experiment 1	2.24 ± 0.16	1.76 ± 0.35	2.37 ± 0.16	6.14 ± 0.72
Experiment 2	1.70 ± 0.08	1.05 ± 0.18	1.98 ± 0.11	3.14 ± 0.42
Experiment 3	1.44 ± 0.05	2.42 ± 0.16	1.57 ± 0.09	4.31 ± 0.44
Experiment 4	0.94 ± 0.16	1.53 ± 0.13	1.15 ± 0.16	6.09 ± 1.42

also occurs between Vm for each experiment, and is probably a characteristic of the plant material used in each experiment. The significance of this is that it is not entirely possible to predict the magnitude of the metabolic response (e.g. growth rate) for any given water movement.

The results for Km (Table 3.4) are given as [Pi]b, however when they are calculated on the basis of $H_2PO_4^-$ influx, ($[H_2PO_4^-]b$ is 0.6% of [Pi]b at 15°C and pH 8.2; Figure 3.1), they still give the same curve fit to the data using the Briggs-Haldane equation(1). Consequently, the diffusion flux ($J = Kt([H_2PO_4^-]b - [H_2PO_4^-]s)$, Equation 1.19) through the D.B.L., which is proportional to the concentration of the diffusing nutrient, will be significantly slower (depending on the value of Kt) than the influx kinetics across the plasmalemma predicted by the Briggs-Haldane equation. Taken together, the discrepency between Km for the two treatments (i.e. the presence of an apparent Km) and the inequality between the external flux and the membrane influx, indicate that the D.B.L. resistance is significantly effecting the overall transport process. To determine the interaction between these two transport processes it is necessary to make use of the Briggs-Maskell equation (Section 1.3).

In the next section, an explanation of the coupling mechanism of the two transport processes is given followed by the use of this mechanism to explain the difference in $H_2PO_4^-$ influx between the different water movements.

---

(1) $V\text{-}(Pi) = Vm \times [Pi]b / (Km + [Pi]b)$

$V\text{-}(H_2PO_4^-) = Vm \times ([Pi]b \times 0.006) / ((Km \times 0.006) + ([Pi]b \times 0.006))$

$= Vm \times [Pi]b / (Km + [Pi]b)$

where V is the influx reaction velocity at the plant's surface

3.2.3. ELECTRICAL ANALOG DESCRIPTION OF THE TOTAL TRANSPORT PROCESS

The Briggs-Haldane model represents the kinetics associated with influx at the membrane surface. When a D.B.L. exists next to the membrane, then the possibility exits that the total transport kinetics can be altered by the resistance associated with the external diffusion flux (J). Under these conditions the two transport processes are in series, each with its own characteristic resistance to solute flux, and as such can be represented by an electrical type analog.

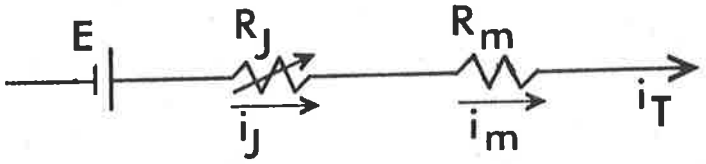

[Where R is the resistance of transport process j (equivalent to diffusion flux across the D.B.L., and Rj is the same as Rt by definition) or m (equivalent to the influx across the membrane), E the potential driving force, and i is the current of transport process j or m or the total transport process (T). By definition for resistances in series, $i_T = E/(Rj + Rm)$. The resistance (Rj) represented by the D.B.L. is shown as being variable to indicate that changes in water velocity can alter its value].

Using this analogy it is possible to determine the outcome of varying Rj or Rm on i_T. If the resistance of one transport process is far greater than the other, then that transport process will control the total transport, and vice versa. This is shown in the following two cases,

(1) $Rj >> Rm$ therefore $i_T \sim E/Rj \sim i_j$ Equ-3.1

(2) $Rm >> Rj$ therefore $i_T \sim E/Rm \sim i_m$ Equ-3.2

On the other hand when the resistances for each transport process are of similar magnitude, then the total transport process is equally controlled by the two processes. This is shown by the following case,

(3) Rj ∿ Rm therefore $i_T = E/(Rj + Rm)$ Equ-3.3

This analogy is not totally accurate in that it assumes that the driving force (E) is the same for each resistance when in fact the driving force across the D.B.L. (Ej) is the concentration gradient (Cb-Cs), and for the membrane (Em)[1] it is Cb2Km/Km+Cb.

For cases one and two the result still holds (where E is now Ej or Em), with the total transport being dependent on the transport process with the largest resistance. In the case when intermediate type kinetics exist (case 3), then the electrical analog breaks down. However the total transport can be determined for this case using the Briggs-Maskell equation, which equates the two transport processes assuming a steady state state between the processes. Though the electrical analog is inaccurate in determining the total transport flux, it does provide a good way pictorially to present the diffusion flux. It can also be used to determine the variable value of Rt under different models of phosphate diffusion. The calculated values of Rt can then be used in the Briggs-Maskell equation to calculate the total transport flux.

The phosphate values of Rt can be calculated using the results of the zinc calibration method (Section 2.7.2.). The logic for converting

---

(1) The driving force across the membrane can be determined by knowing that the membrane resistance (Rm) = 2Km/Vm (see Section 1.3) and therefore from i = E/R, V = Vm x Cb/2Km(1/2+Cb/2Km), consequently Em = Cb2Km/(Km+Cb). Note that the membrane transport and resistane for this model are not the same as the membrane transport in terms of a electrochemical potential difference.

the Kt and Rt values for zinc to phosphate is based on (laminar flow Equation 1.32) the ratio

$$\frac{\delta_p}{\delta_{HCl}} = \frac{3\ D_p^{0.33}\ U_b^{-0.5}\ \nu^{0.166}\ x^{0.5}}{3\ D_{HCl}^{0.33}\ U_b^{-0.5}\ \nu^{0.166}\ x^{0.5}} \qquad \text{Equ-3.4}$$

(where D_p and D_{Hcl} are the diffusion coefficients of phosphate and HCl respectively as given in Table 3.1, for 15 °C, and δ_p and δ_{HCl} are the D.B.L. thickness for phosphate and HCl respectively) consequently,

$$\delta_p = \delta_{HCl}\left(\frac{D_p}{D_{HCl}}\right)^{0.33} \qquad \text{Equ-3.5}$$

Similarily for turbulent flow (Equation 1.37),

$$\delta_p = \delta_{HCl}\left(\frac{D_p}{D_{HCl}}\right)^{0.25} \qquad \text{Equ-3.6}$$

by definition (Equation 1.19),

$$Kt = D/\delta \qquad (Rt = 1/Kt) \qquad \text{Equ-3.7}$$

therefore substituting 3.5 or 3.6 into 3.7,

Laminar
$$Kt^p = \left(\frac{D_p}{D_{HCl}}\right)^{0.66} Kt^{HCl} \qquad \text{Equ-3.8}$$

Turbulent
$$Kt^p = \left(\frac{D_p}{D_{HCl}}\right)^{0.75} Kt^{HCl} \qquad \text{Equ-3.9}$$

Where Kt^p is the mass transport coefficient for phosphate. The results are presented in Table 3.5.

Using the electrical analog model and the values of Rt it is now possible to determine what resistances within the D.B.L. are responsible for the divergence in Michaelis kinetic parameters (Section 3.2.2.)

TABLE 3.5. Rt for $H_2PO_4^-$ and HPO_4^{2-} converted from zinc calibration results.

Laminar Flow		Growth-1	Growth-2	Growth-3	Growth-4	Growth-5	Shaker-S	Shaker-F
$Rt^{(a)} \times 10^5$ s m^{-1}	$H_2PO_4^-$	7.26	3.35	2.08	1.84	1.10	7.43	0.80
	HPO_4^{2-}	15.20	7.00	4.36	3.85	2.31	15.55	1.67
$\delta = D/Kt^{(b)}$ µm	$H_2PO_4^-$	345	159	99	87	52	353	38
	HPO_4^{2-}	239	109	68	60	36	244	26
$\bar{\delta}_{lx}$ (d) µm	$H_2PO_4^-$	322(c)	130	94	85	81	322(c)	71
	HPO_4^{2-}	243(c)	90	65	59	56	243	49
Turbulent Flow								
$Rt^{(e)} \times 10^5$ s m^{-1}	$H_2PO_4^-$	8.28	3.82	2.38	2.10	1.27	8.47	0.91
	HPO_4^{2-}	19.01	8.76	5.45	4.81	2.89	19.46	2.09
$\delta = D/Kt$ µm	$H_2PO_4^-$	394	181	113	100	60	403	43
	HPO_4^{2-}	299	138	86	76	45	305	33
$\bar{\delta}_{tux}$ (f) µm	$H_2PO_4^-$	-	103	57	48	44	-	35
	HPO_4^{2-}	-	78	44	36	34	-	27

(a) The factor for laminar flow to convert Rt-zinc to Rt-$H_2PO_4^-$ or Rt-HPO_4^{2-} [using Rt-Pi = $(D^{HCl}/D^{Pi})^{0.66}$ Rt-HCl] is 2.86 and 5.99 respectively.

(b) Diffusion coefficient of $H_2PO_4^-$ or HPO_4^{2-} is 4.75 and 1.57 x 10^{-10} m^2 s^{-1} respectively (Table 3.1), at 15°C.

(c) Used Equation 1.43 where α = 92.13 cm^2 mol^{-1}.

(d) Used Equation 1.32, where $\bar{\delta}_{lx} = 0.5\ \delta_{l}$..

(e) The factors for turbulent flow, to convert Rt-$H_2PO_4^-$ or Rt-HPO_4^{2-} [using Rt-Pi = $(D^{HCl}/D^{Pi})^{0.75}$ Rt-HCl], is 3.26 and 7.49 respectively.

(f) Used Equation 1.37, where $\bar{\delta}_{tux} = 0.9\ \delta_{tu}$.

3.2.4. BRIGGS-MASKELL MODEL FOR $H_2PO_4^-$ OR HPO_4^{2-} INFLUX

Energetically the cheapest phosphate influx system would be that represented by the electrical analog for $H_2PO_4^-$ influx, Model A.

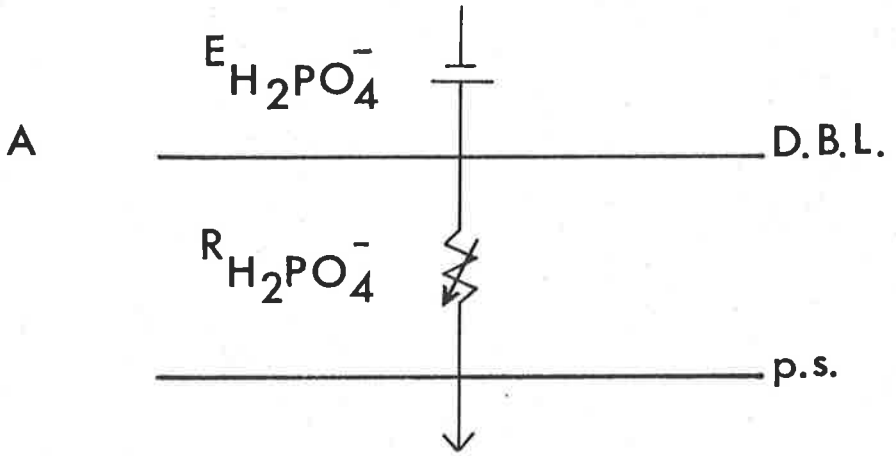

where $^{R}H_2PO_4^-$ equals Rt. [D.B.L. is the outer limit of the diffusion boundary layer, p.s. is the plasmalemma surface (the cell wall is ignored). In this analog the potential difference ($^{E}H_2PO_4^-$) represents the concentration gradient ($[H_2PO_4^-]b - [H_2PO_4^-]s$) . The resistance through the D.B.L. ($^{R}H_2PO_4^-$) is analogous to the mass transfer resistance (same units, s m^{-1}). The current to the p.s. is then an expression of the diffusive flux (J) as determined by Equation 1.19, $i_{H_2PO_4^-} = E_{H_2PO_4^-}/R_{H_2PO_4^-}]$.

When the experimental $H_2PO_4^-$ value for Rt (Table 3.5; using the laminar Rt for Shaker-S, and turbulent Rt for Shaker-F) is used to fit the Briggs-Maskell equation (Figure 3.5 and 3.6) there is a large under-estimation between the observed influx and the calculated influx. The Rt values estimated for $[H_2PO_4^-]b$, using the program FVKUP, show no relationship with the $^{Rt}H_2PO_4^-$ values from the zinc analysis (Table 3.6; FVKUP 0.13 or 0.038 ($x10^5$ s m^{-1}) for Shaker-S and Shaker-F respectively compared to for zinc 7.4 or 0.9 ($x10^5$ s m^{-1}) for Shaker-S and Shaker-F respectively). The most obvious explanation for this

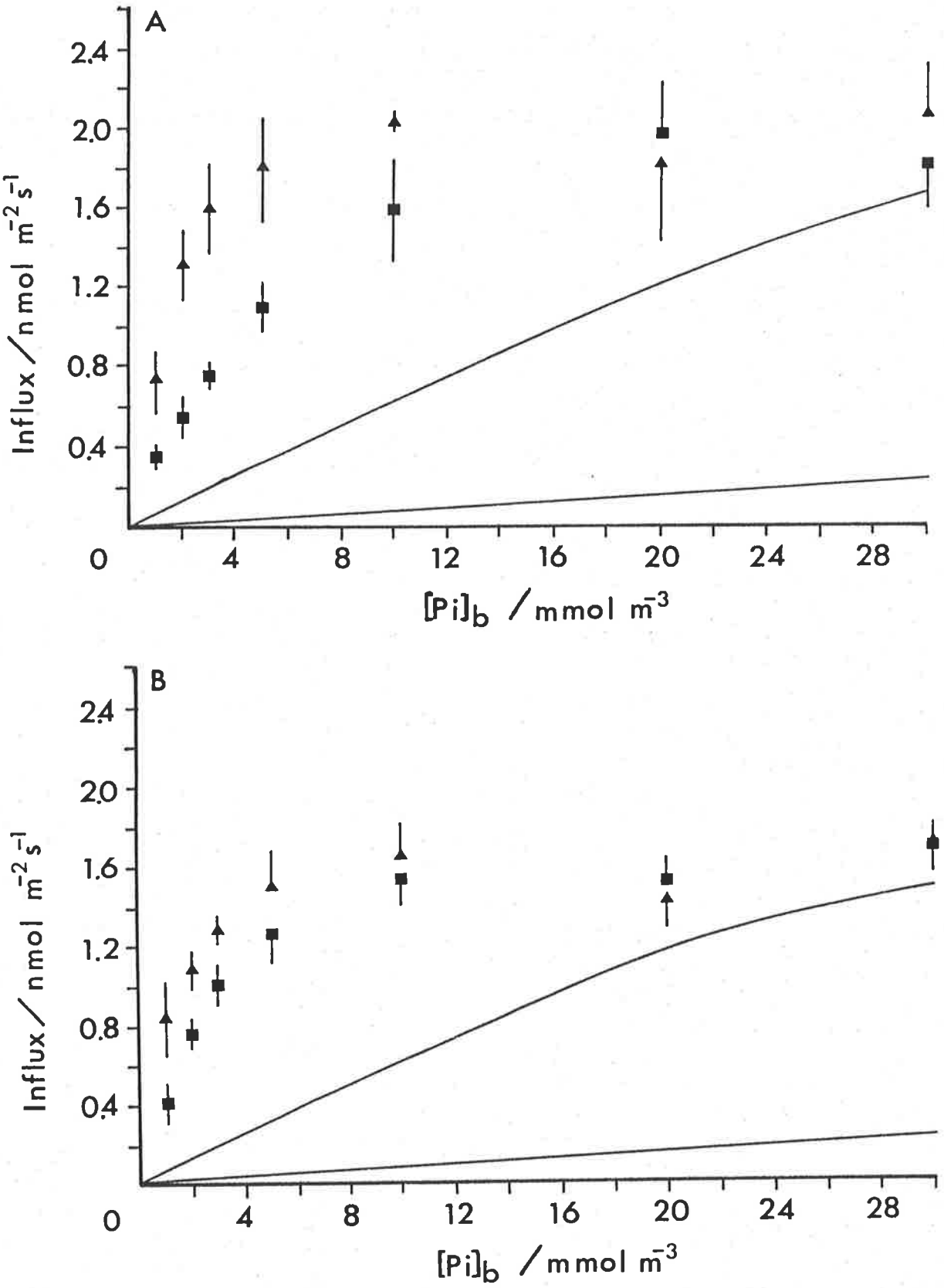

Figure 3.5. Phosphate influx versus [Pi]b for the Shaker-S (■) and Shaker-F (▲) treatments. The curves represent the predicted phosphate influx calculated using the Briggs-Maskell equation, the values of Rt for $H_2PO_4^-$ from Table 3.5 and the values of Km and Vm for the Shaker-F treatment assuming that these values represent the true kinetic constants. The Shaker-S and Shaker-F treatments are represented by the lower and upper curves respectively. (A) Experiment 1 (B) Experiment 2. (Model A)

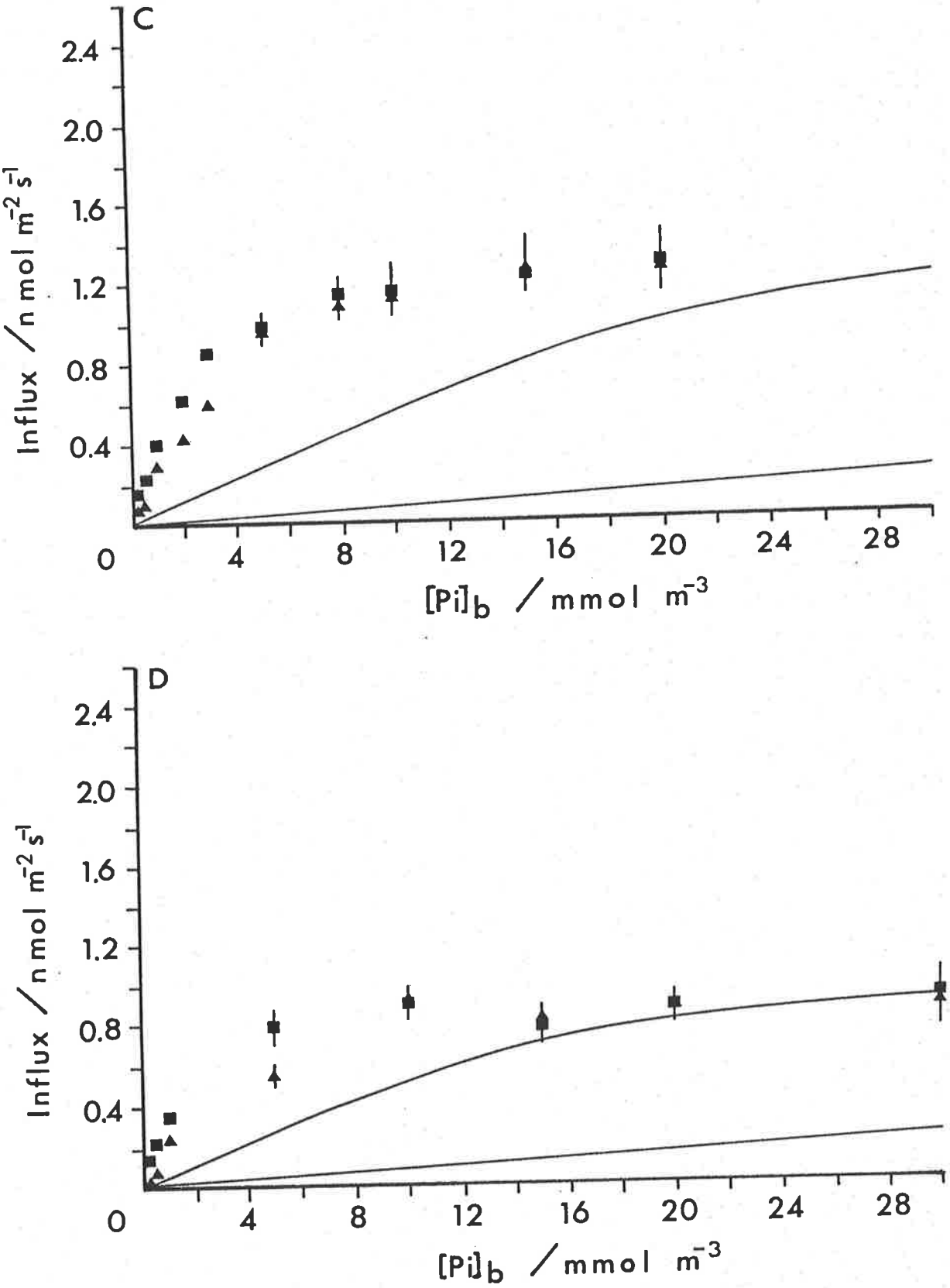

Figure 3.6. See Figure 3.5 for the explanation of the symbols and how the curves were calculated. (C) Experiment 3 (D) Experiment 4 (Model A).

difference, is that the low values of Rt predicted by the program FVKUP suggest that an alternative form of phosphate is diffusing in parallel to the $H_2PO_4^-$ flux, contributing to the total phosphate influx.

The most likely possibility is the influx of HPO_4^{2-}, though at an energetic cost to the plant's metabolism. The energy difference between using $H_2PO_4^-$ or HPO_4^{2-} can be calculated using the method of Raven (1980).

$$\Delta G = RT \ln [Pi]c/[Pi]b + zF \Psi ib \qquad \text{Equ-3.10}$$

(where ΔG is the free energy difference of phosphate between the two sides of the plasmalemma (kJ mol^{-1}), R is the universal gas constant (8.31 J $°K^{-1}$ $mole^{-1}$), T is the absolute temperature (288 °K), z is the charge (-1 or -2), F is the Faraday constant (9.65 x 10^4 coulombs $mole^{-1}$), Ψib is the electrical potential difference across the plasmalemma (-60 mVolts for *U. lactuca*, West and Pitman, 1967). For this example [Pi]b is taken as 1 mmol m^{-3}, therefore at pH 8.2 $[H_2PO_4^-]b$ = 0.006 mmol m^{-3} and $[HPO_4^{2-}]b$ = 0.861 mmol m^{-3}, and [Pi]c is the cytoplasmic phosphate concentration.) At a cytoplasmic pHc of 7.5 and a [Pi]c of 1 mol m^{-3} (Raven and Smith, 1980; Raven, 1980) then $[H_2PO_4^-]c$ and $[HPO_4^{2-}]c$ are 3.4% and 93.4% of [Pi]c respectively. The energy required for influx is then 26.7 kJ mol^{-1} or 28.3 kJ mol^{-1} for $H_2PO_4^-$ and HPO_4^{2-} respectively. The difference (1.6 kJ mol^{-1}) in energy, though making $H_2PO_4^-$ energetically more attractive for *Ulva*, is not that great that HPO_4^{2-} cannot be used at the expense of energy efficiency. Model B.

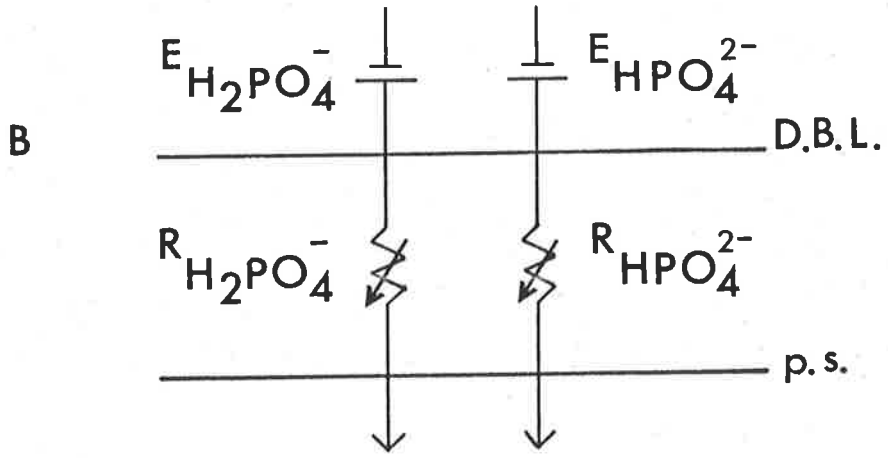

(where $^{R}HPO_4^{2-}$ is equal to Rt for HPO_4^{2-}, which assumes that the contributing diffusion flux of $H_2PO_4^-$ is negligible compared to that for HPO_4^{2-}.) Model B also assumes that no equilibrium between $H_2PO_4^-$ and HPO_4^{2-} exists in the D.B.L. (the symbols are the same as for Model A).

The Rt values for HPO_4^{2-} (Table 3.5) though larger than the equivalent value for $H_2PO_4^-$ (due to the smaller diffusion coefficient of HPO_4^{2-}) result in a far greater diffusion flux at the same [Pi]b (Figures, 3.7 and 3.8). The curves (Briggs-Maskell equation) give a good fit to the data, though there is some discrepancy especially for the slower velocity (Shaker-S) and most notably in Experiment 1. The values of Rt, for $[HPO_4^{2-}]$, calculated using the program FVKUP show a good fit with those determined from the zinc analysis (Table 3.7; FVKUP 18 or 2.5 (10^5 s m^{-1}) for Shaker-S and Shaker-F respectively, compared to those for zinc 15 or 2.1 (10^5 s m^{-1}) for Shaker-S and Shaker-F respectively). The values calculated for HPO_4^{2-} using FVKUP are, as would be expected, very similar to those calculated with the assumption that the total phosphate concentration is available for uptake (Table 3.8). The proposed model (B) of HPO_4^{2-} transport then adequately describes the observed influx of phosphate. The one complication to this model, is the possibilty that the phosphate equilibrium reaction within the D.B.L. is altering the actual concentrations of $H_2PO_4^-$ or HPO_4^{2-} at the plant's surface (MacFarlane, 1985).

3.2.5. MODIFICATION OF THE MASS TRANSFER RESISTANCE BY EQUILIBRIUM REACTION MAINTENANCE WITHIN THE D.B.L.

The existence of a concentration gradient within the D.B.L. can influence other solutes present, as the equilibrium concentration within the D.B.L. will vary from that existing in the bulk solution. The best cited example is the case of the apparent $[CO_2]$ being

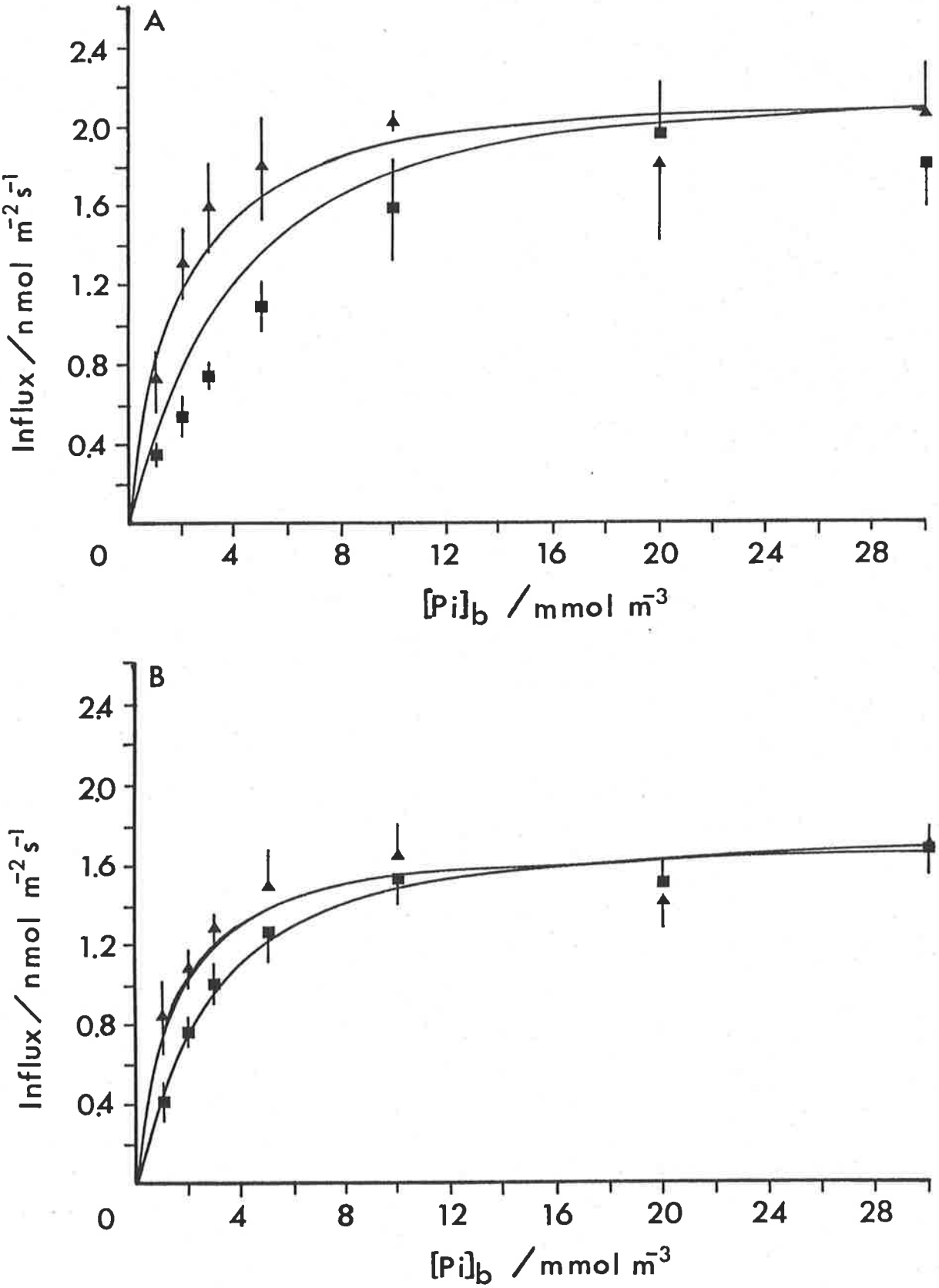

Figure 3.7. Phosphate influx versus [Pi]b for the Shaker-S (■) and Shaker-F (▲) treatments. Curves were determined by the same method described in Figure 3.5, except that the Rt values for HPO_4^{2-} were used (Model B, Table 3.5).
(A) Experiment 1 (B) Experiment 2

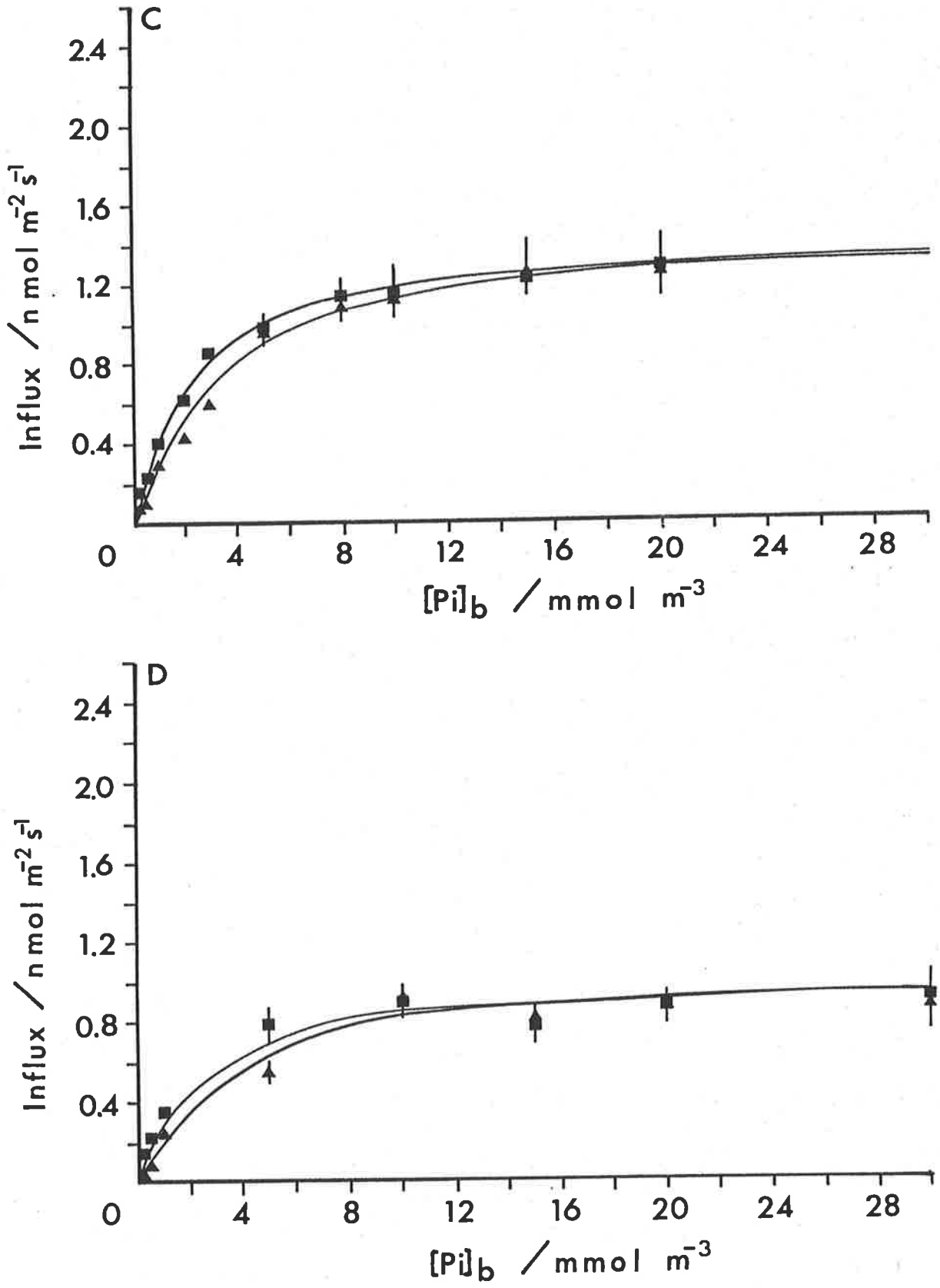

Figure 3.8. See Figure 3.7 for the explanation of the symbols and how the curves were calculated. (C) Experiment 3 (D) Experiment 4 (Model B).

TABLE 3.6. FVKUP for $H_2PO_4^-$ (0.6% of T.P.)

	Vm nmol m^{-2} s^{-1}		Km mmol m^{-3}		Rt x 10^5 s m^{-1}		Regression Coefficient (r^2)	
	Shaker-S	Shaker-F	Shaker-S	Shaker-F	Shaker-S	Shaker-F	Shaker-S	Shaker-F
Experiment 1	1.99	2.00	8.00	1.76	0.172	0.069	0.993	0.986
Experiment 2	1.68	1.65	5.62	3.61	0.097	0.036	0.995	0.938
Experiment 3	1.35	1.37	7.75	9.59	0.168	0.044	0.996	0.998
Experiment 4	1.00	1.00	16.00	10.60	0.078	0.003	0.984	0.983
Average ± S.E.					0.13 ± 0.02	0.038 ± 0.014		

TABLE 3.7. FVKUP for HPO_4^{2-} (86.1% of T.P.)

	Vm nmol m^{-2} s^{-1}		Km mmol m^{-3}		Rt x 10^5 s m^{-1}		Regression Coefficient (r^2)	
	Shaker-S	Shaker-F	Shaker-S	Shaker-F	Shaker-S	Shaker-F	Shaker-S	Shaker-F
Experiment 1	2.00	2.00	1.22	2.50	23.92	9.90	0.993	0.986
Experiment 2	1.68	1.69	0.82	0.85	13.74	0.041	0.995	0.934
Experiment 3	1.36	1.43	1.15	1.98	23.58	0.037	0.996	0.997
Experiment 4	1.00	1.00	2.28	1.54	11.49	0.097	0.984	0.983
Average ± S.E.					18.2 ± 3.2	2.52 ± 2.46		

TABLE 3.8 FVKUP for Total Phosphate (T.P.)

	Vm nmol m^{-2} s^{-1}		Km mmol m^{-3}		Rt x 10^5 s m^{-1}		Regression Coefficient (r^2)	
	Shaker-S	Shaker-F	Shaker-S	Shaker-F	Shaker-S	Shaker-F	Shaker-S	Shaker-F
Experiment 1	2.00	2.16	1.42	1.37	27.78	0.041	0.993	0.956
Experiment 2	1.68	1.69	0.95	0.97	15.90	0.050	0.995	0.934
Experiment 3	1.36	1.37	1.36	1.64	27.17	6.897	0.996	0.998
Experiment 4	1.00	1.00	2.65	1.79	13.32	0.119	0.984	0.983
Average ± S.E.					21.0 ± 3.8	1.78 ± 1.17		

supplemented within the D.B.L. by the dissociation of other carbon species to maintain equilibrium (Gutknecht and Tosteson, 1973; Walker, Smith and Cathers, 1980). The theory is that as the CO_2 is transported across the membrane the equilibrium between $[CO_2]$ and $[HCO_3^-]$ is unbalanced unless HCO_3^- dissociates into CO_2. The consequence is that the $[CO_2]_s$ is actually greater than that predicted by the D.B.L. theory. This is further complicated by the rates of the equilibrium reactions and the pH of the solution within the D.B.L..

A similar equilibrium exists within the bulk solution for phosphate, between its dissociation species (Table 3.1).

$$H_3PO_4 \rightleftharpoons H^+ + H_2PO_4^- \rightleftharpoons H^+ + HPO_4^{2-} \rightleftharpoons H + PO_4^{3-} \qquad \text{Equ-3.11}$$

Equilibrium between all the phosphate species is extremely fast (Mahan, 1975), therefore as $H_2PO_4^-$ is taken up its equilibrium concentration within the D.B.L. will be maintained. The consequence of the actual concentration of $H_2PO_4^-$ being augmented by an unbalanced equilibrium situation within the D.B.L. would be to increase the influx at the membrane above that predicted. This situation has already been developed for phosphate D.B.L. transport by MacFarlane (1985), who found that the equation for $H_2PO_4^-$ diffusion flux could be written in terms of the other phosphate species present[1],

$$J_{H_2PO_4^-} = \left[Kt_{H_2PO_4^-} + Kt_{HPO_4^{2-}} \frac{Ka_2}{[H^+]} \right] ([H_2PO_4^-]_b - [H_2PO_4^-]_s) \qquad \text{Equ-3.12}$$

where

$$\frac{1}{Rt} = \frac{1}{Rt_{H_2PO_4^-}} + \frac{Ka_2/[H^+]}{Rt_{HPO_4^{2-}}} \qquad \text{Equ-3.13}$$

This augmented $H_2PO_4^-$ diffusion flux can be depicted diagrammatically by,

Model C.

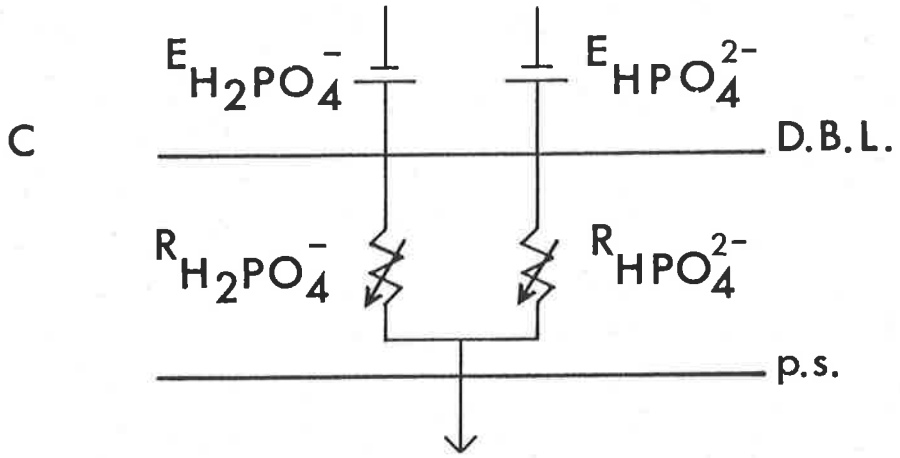

(Where the symbols are the same as Model A)

---

(1)
$$J_{H_2PO_4^-} = Kt_{H_2PO_4^-}([H_2PO_4^-]_b - [H_2PO_4^-]_s) + Kt_{HPO_4^{2-}}([HPO_4^{2-}]_b - [HPO_4^{2-}]_s) + Kt_{PO_4^{3-}}([PO_4^{3-}]_b - [PO_4^{3-}]_s)$$

The terms due to PO_4^{3-} can be ignored due to the slow rate of diffusion (Table 3.1). From,

$$[H^+][HPO_4^{2-}] = Ka_2[H_2PO_4^-]$$

the expression for the diffusion flux can be written in terms of $[H_2PO_4^-]$ (MacFarlane, 1985).

$$J_{H_2PO_4^-} = (Kt_{H_2PO_4^-} + Kt_{HPO_4^{2-}} \frac{Ka_2}{[H^+]})([H_2PO_4^-]_b - [H_2PO_4^-]_s)$$

The effect then of a parallel diffusion flux of $H_2PO_4^-$ and HPO_4^{2-} across the D.B.L. is to greatly reduce the mass transfer resistance. The Rt values predicted (Equation 3.13) are given in Table 3.9 for the combined phosphate transport (Total phosphate). When these values are used with the appropriate values of Vm and Km, the curves generated by the Briggs-Maskell equation are a good fit to most of the data (Figures 3.9 and 3.10). The average calculated Rt values for $H_2PO_4^-$, using the program FVKUP, are in good agreement with those determined using Formula 3.13 and the values from the zinc technique (Table 3.6; FVKUP, 0.13 or 0.038 (10^5 s m^{-1}) for Shaker-S and Shaker-F respectively, compared with the zinc calculations 0.12 or 0.016 (10^5 s m^{-1}) for Shaker-S and Shaker-F respectively). Mierle (1985) determined the phosphate value of Rt as 0.03 10^5 s m^{-1} for the alga *Synechococcus leopoliensis*, which is in good agreement with the FVKUP results for Shaker-F.

Most notably the variation between the fitted (for HPO_4^{2-} and total $H_2PO_4^-$, Figures 3.7-3.10) and the observed results occurred in Experiment 1. The conclusion is that an added external resistance is in some way complicating the expected results. Alternatively, the equilibrium time required for the D.B.L. to be established may be having a differential effect on the influx for the different water movement treatments. Equation 1.13 predicts that the time for equilibrium would be 100 to 1.5 s for Shaker-S and Shaker-F respectively (using the D.B.L. thickness for $H_2PO_4^-$ and the constant 0.38). However, the longer time required for equilibrium to be established for the Shaker-S treatment, should result experimentally in a smaller difference in influx between the treatments and not the larger difference observed in Experiment 1.

TABLE 3.9. Mass transport resistance for Model C and H^+ for both laminar and turbulent flow.

Laminar Flow		Growth-1	Growth-2	Growth-3	Growth-4	Growth-5	Shaker-S	Shaker-F
Rt x 10^5 s m^{-1}	Combined $H_2PO_4^-$ (a)	0.120	0.055	0.034	0.030	0.018	0.122	0.013
	H^+ (b)	1.11	0.51	0.32	0.28	0.17	1.14	0.12
$\delta^{H^+} = D^{H^+}/Kt$ (c)	µm	882	407	253	223	134	903	97
$\bar{\delta}_{lx}^{H^+}$ (d)	µm	800 (e)	332	240	217	208	800 (e)	182
Turbulent Flow								
Rt x 10^5 s m^{-1}	Combined $H_2PO_4^-$ (b)	0.148	0.068	0.043	0.038	0.023	0.152	0.016
	H^+ (b)	1.00	0.46	0.29	0.25	0.15	1.03	0.11
$\delta^{H^+} = D^{H^+}/Kt$	µm	795	367	228	201	121	814	87
$\bar{\delta}_{tux}^{H^+}$ (f)	µm	-	207	116	96	90	-	71

(a) Rt for combined $H_2PO_4^-$ diffusion flux (Rt^c) is calculated using $1/Rt^c = [^{Rt}_{H_2PO_4^-}]^{-1} + Fact[^{Rt}_{HPO_4^{2-}}]^{-1}$ where $Fact = Ka_2/[H^+]$, using the values for the appropriate laminar or turbulent flow (Table 3.5) and the constants in Table 3.1.

(b) The factor to convert Rt-Zinc to Rt-H^+ [using $Rt\text{-}H^+ = (D^{HCl}/D^{H})^{0.66 \text{ or } 0.75}\ Rt^{-HCl}$] is 2.28 and 2.53 for laminar and turbulent flow respectively.

(c) Diffusion coefficient of H^+ is 7.94×10^{-9} m^2 s^{-1} (Table 3.1), at 15°C.

(d) Used Equation 1.32, where $\bar{\delta}_{lx}^{H^+} = 0.3\ {}^{H^+}_{l}$.

(e) Used Equation 1.43 where $\alpha = 40$ cm^2 mol^{-1}.

(f) Used Equation 1.37, where $\bar{\delta}_{tux}^{H^+} = 0.9\ {}^{H^+}_{tu}$.

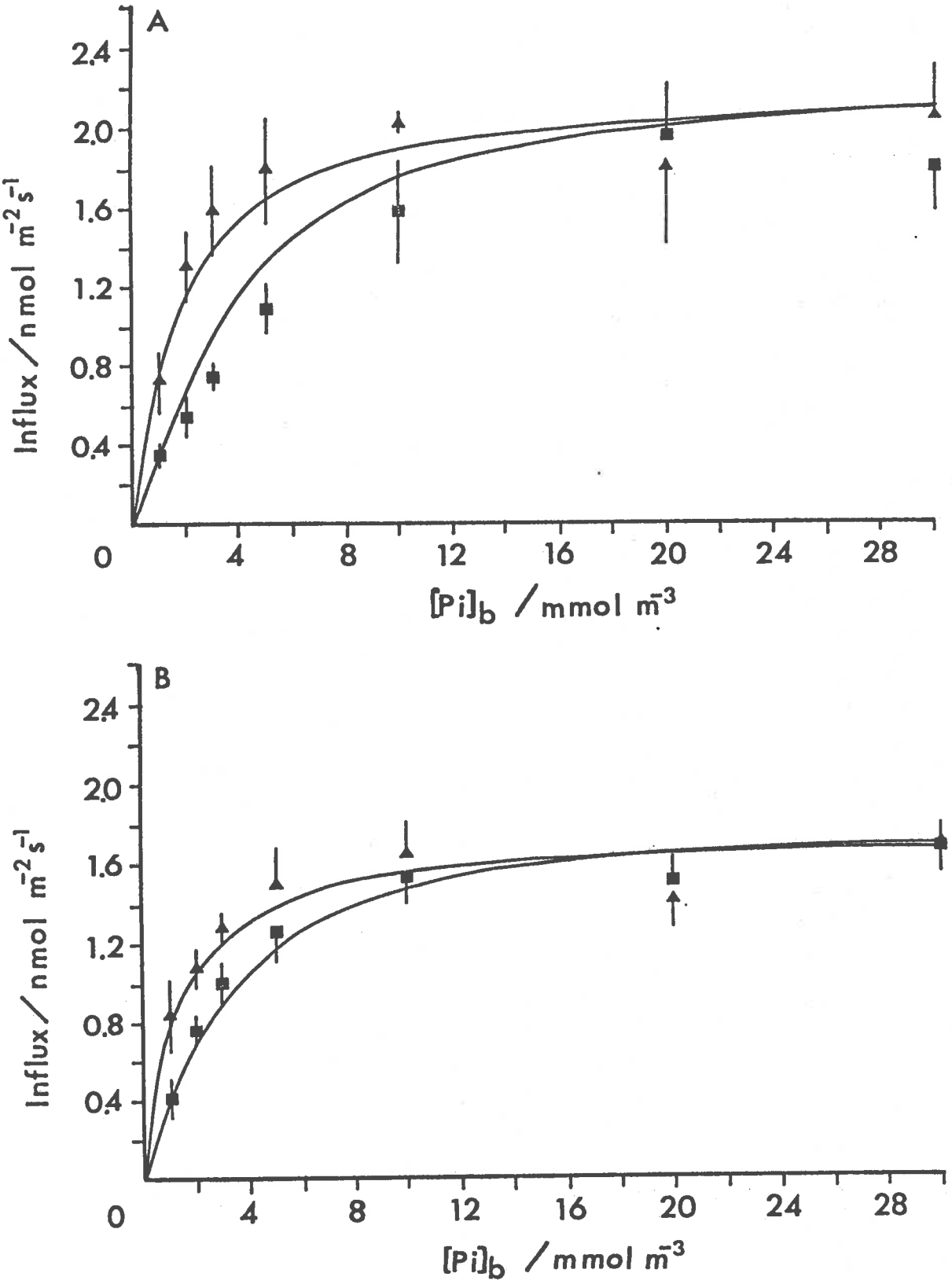

Figure 3.9. Phosphate influx versus [Pi]b for the Shaker-S (■) and Shaker-F (▲) treatments. Curves were determined by the same method described in Figure 3.5, except that the Rt values for the combined model of phosphate transport through the D.B.L. were used (Model C, Table 3.9). (A) Experiment 1 (B) Experiment 2

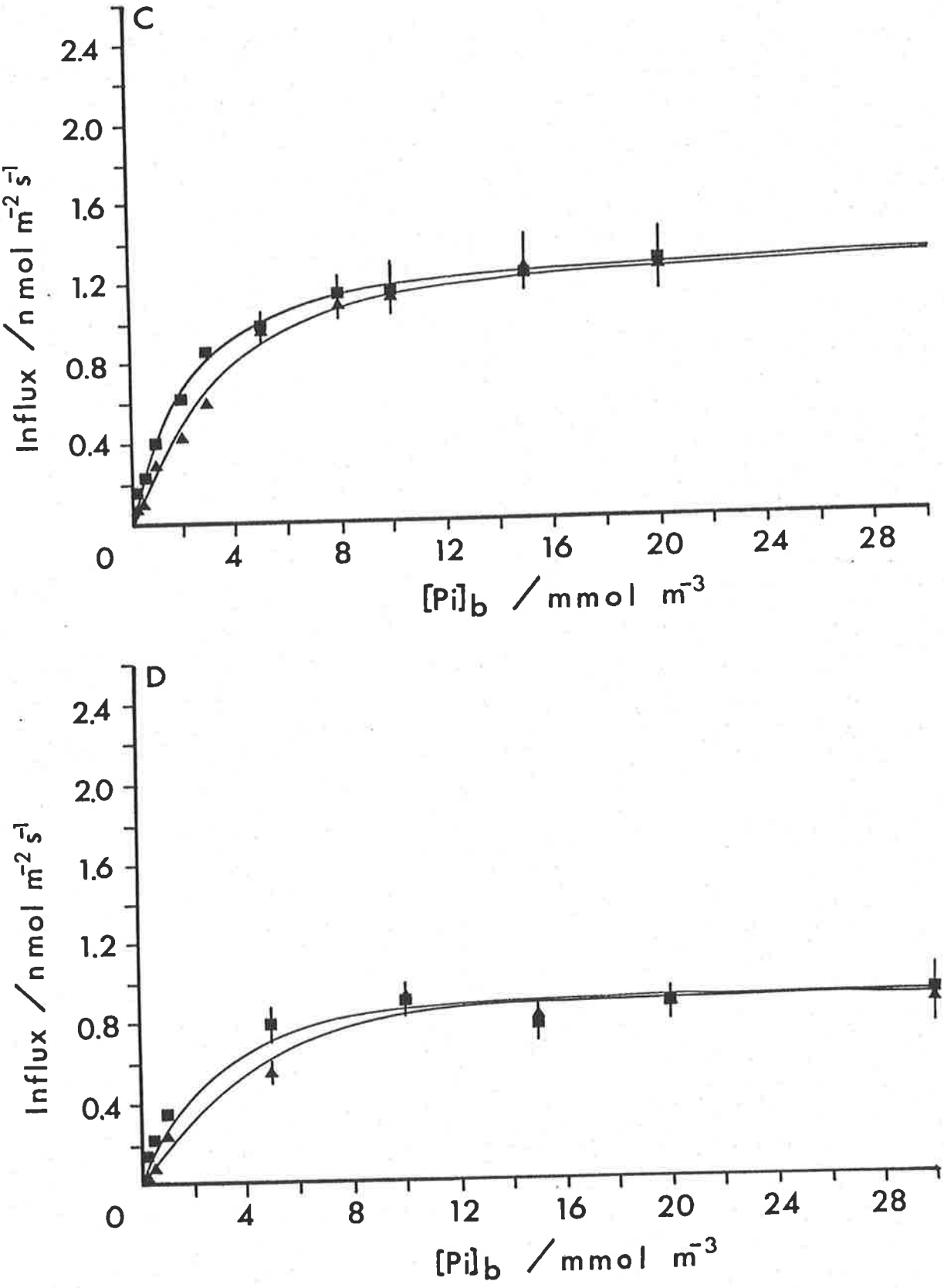

Figure 3.10. See Figure 3.9 for the explanation of the symbols and how the curves were calculated (Model C). (C) Experiment 3
(D) Experiment 4

3.2.6. MODIFICATION OF THE $H_2PO_4^-$ MASS TRANSPORT RESISTANCE BY THE EXTERNAL pH

Though the equilibrium conversion of HPO_4^{2-} to $H_2PO_4^-$ is fast the reaction does depend on the presence of sufficient protons to maintain equilibrium (Equation 3.11). The possibility for proton diffusional limitations within the D.B.L. has already been suggested by Walker, Smith and Cathers (1980) for *Chara* and Sentenac and Grignon (1987) for corn roots. In both these papers a theoretical acidification occurred next to the cell wall due to the rate limiting diffusional flux of protons into the bulk solution. If this was to occur for *U. australis* the increased percentage of $H_2PO_4^-$ would cause a response similar to that predicted by the combined $H_2PO_4^-$ and HPO_4^{2-} Model (C). The major problem with drawing this conclusion is that the physical systems for corn roots and *Chara* are quite dissimilar to that for *Ulva*. For corn roots the lack of a photosynthetic system, and for *Chara* the possibilty of acid-alkaline banding, due to the size of the cells, means that the transport processes can be quite different. The critical point is whether there is net acidification or alkalization outside the cell. This will depend on the form of nutrition.

Table 3.10 is an attempt to determine the possible net direction of protons across the cell membrane, using data drawn from the literature as specified. The net direction of protons depends greatly on the form of carbon crossing the membrane for photosynthesis. Table 3.10 shows that the magnitude and direction of proton flux across the cell membrane ranges from an influx of 1054 μmol m^{-2} s^{-1} (HCO_3^-), to an efflux of 214 μmol m^{-2} s^{-1} (CO_2). The conclusion of Beer and Eshel (1983) and MacFarlane (1985) is that for *Ulva* the transport of HCO_3^- from the bulk solution is necessary to account for the rates of photosynthesis achieved. Cummins, Strand and Vaughan (1969) found that with the onset of photosynthesis in *Ulva* there was a net influx of

TABLE 3.10. Minimum and maximum proton flux based on cell nutrient composition.

	Content	Net influx[(a)] nmol m^{-2} s^{-1}		Minimum charge balance nmol m^{-2} s^{-1}			Maximum charge balance nmol m^{-2} s^{-2}		
Element	mmol g^{-1} (D.W.)	Low	High	Ion	Low	High	Ion	Low	High
C	25	461	1010	HCO_3^-	-461	-1010	CO_2	0	0
N	1.07 - 3.20	20	129	NO_3^-	-20	-129	NH_4^+	20	129
P	0.026 - 0.12	0.83	4.80	$H_2PO_4^-$	-0.83	-4.80	$H_2PO_4^-$	-0.83	-4.80
K	1.40	25.80	56.50	K^+	25.80	56.50	K^+	25.80	56.50
Na	0.112	2.97	4.52	Na^+	2.07	4.52	Na^+	2.07	4.52
Ca[(b)]	0.23	4.23	9.26	Ca^{2+}	8.46	18.52	Ca^{2+}	8.46	18.52
Mg[(b)]	0.29	5.39	11.78	Mg^{2+}	10.78	23.56	Mg^{2+}	10.78	23.56
Cl[(c)]	0.32	5.87	12.83	Cl^-	-5.87	-12.83			
H^+ total[(d)]					441	1054		-60	-214
H^+ (-N)[(e)]					421	925		-40	-85

(a) Net influx during growth is calculated using the absolute growth rate (A.G.R.), which ranged from 2.3 to 15.4 x 10^{-9} gm s^{-1} (D.W.) The influx was then computed using Influx = content x A.G.R./area.

(b) Rosell and Srivastava (1984) for the brown alga *Macrocystis integrifolia* assume that these values

(c) Ritchie and Larkum (1984) for the green alga *Enteromorpha intestinalis* would be similar for *Ulva* [equivalent to 105 to 21 µmol cm^{-2} s^{-1}].

(d) The range in H^+ movement is 1054 influx - 214 efflux (nmol m^{-2} s^{-1})

(e) These calculated values represent the proton balance when nitrogen is not present in the growth solution, as is the case when A.S.W. is used.

protons which was coupled with the influx of HCO_3^-. The calculated charge imbalance found using HCO_3^- (0.4-1 μmol m^{-2} s^{-1}, Table 3.10) would then require a net positive influx of protons to balance the charge. A further point is whether the media contains nutrients for growth (as is the case in seawater or not as for A.S.W.) and the form of nitrogen (NH_4^+ versus NO_3^-; Table 3.10), as this will modify the magnitude of the proton flux across the cell membrane.

If we take the worst case scenario with the following boundary conditions,

$[H^+], [H_2PO_4^-], [HPO_4^{2-}], [PO_4^{3-}]$ = constant at y > D.B.L. thickness

$[H^+]$ = 0 at y = 0 (cell surface)

$[H_2PO_4^-], [HPO_4^{2-}], [PO_4^{3-}]$ = value satisfying the Briggs-Maskell equation for variable Rt at y = 0 then it is possible to determine the relationship which defines the value of Rt. The simplest model for proton diffusion being rate limiting is when all the species are transported in parallel across the D.B.L.

Model D.

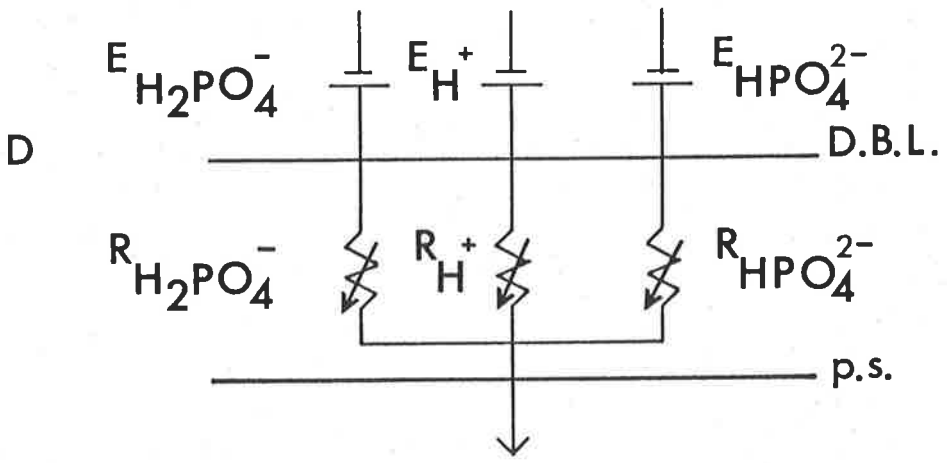

(where the symbols are the same as used in Model A)

Using the same logic as used to determine Rt for Model C. the total resistance for the D.B.L. can be determined from (Table 3.9),

$$i_{H_2PO_4^-} = E_{H_2PO_4^-} \quad \frac{1}{R_{H_2PO_4^-}} + \frac{Ka_2/[H^+]}{R_{HPO_4^{2-}}} + \frac{Ka_2/[HPO_4^{2-}]}{R_{H^+}}$$

Equ-3.14

where,

$$\frac{1}{Rt} = \frac{1}{R_{H_2PO_4^-}} + \frac{Ka_2/[H^+]}{R_{HPO_4^{2-}}} \text{ or } \frac{Ka_2/[HPO_4^{2-}]}{R_{H^+}}$$

Equ-3.15

The resultant values of Rt (for Experiment 1) are given in Table 3.11, and are variable with increasing total phosphate concentration. At low [Pi]b the values of Rt are less than the corresponding values for Model C, however as the [Pi]b increases the Rt values for Models C and D converge so that there is no apparent change in the diffusional flux as fitted using the two models. The problem with the logic of Model D is that it assumes that the equilibrium reaction is in parallel with the proton diffusion flux, when a more accurate representation would have the equilibrium dependent on the rate limiting step. If Model D is altered so that the diffusion flux of protons and HPO_4^{2-} are in series then this mistakenly assumes that the driving force for both diffusion fluxes is the same.

To overcome this a better electrical analog of the total resistance would have the diffusion fluxes due to protons and HPO_4^{2-} in a either/else situation as would be depicted by switch. That is when the diffusion flux due to protons is less than that due to HPO_4^{2-} then the resistance of the equilibrium reaction would depend on the proton diffusion flux equated to $H_2PO_4^-$, and vice versa.

Model E.

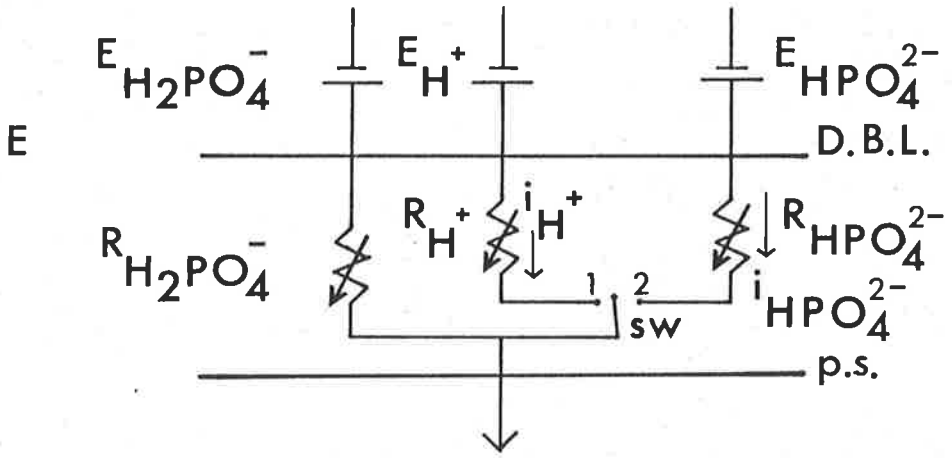

$$\frac{1}{Rt} = \frac{1}{R_{H_2PO_4^-}} + \left[\frac{\frac{Ka_2}{[H^+]}}{R_{H_2PO_4^-}} \text{ or } \frac{\frac{Ka_2}{[HPO_4^{2-}]}}{R_{H^+}} \right]$$

Equ-3.16

(where Sw represents the either/else switch,

if $i_{H^+} < i_{HPO_4^{2-}}$ then Sw points to position 1

or $i_{H^+} > i_{HPO_4^{2-}}$ then Sw points to position 2,

i represents the current (diffusion flux).)

The values of Rt (for Experiment 1) for Model E are larger and far more variable than those of Model D, as a consequence of being more dependent on the diffusion flux of protons (Figure 3.11; Table 3.11). Because the value of Rt for Model E depends on the concentration of HPO_4^{2-} there is a decrease in Rt with decreasing phosphate concentration. However the value of Rt at zero concentration has a lower limit equivalent to the Rt value for $H_2PO_4^-$. A plot of the expected total influx, using the Briggs-Maskell, versus [Pi]b shows that the curves, especially in the case of Shaker-F, are rate limited as they approach the diffusion flux (Figure 3.12). The poor agreement between the observed data for Experiment 1 and the calculated flux using Model E, indicates that the proton diffusion flux is not rate

TABLE 3.11. Predicted mass transport resistance (Rt) for Experiment 1, calculated using Models C, D and E.

	Mass transport resistance (x 10^5 s m^{-1})					
[Pi]b	Model C		Model D		Model E	
mmol m^{-3}	Shaker-S	Shaker-F	Shaker-S	Shaker-F	Shaker-S	Shaker-F
0.25	0.121	0.016	0.087	0.011	0.295	0.029
0.50	0.121	0.016	0.101	0.013	0.569	0.060
0.75	0.121	0.016	0.107	0.014	0.822	0.081
1.00	0.121	0.016	0.110	0.014	1.050	0.105
5.00	0.121	0.016	0.119	0.016	3.360	0.359
10.00	0.121	0.016	0.120	0.016	4.630	0.515
15.00	0.121	0.016	0.120	0.016	5.300	0.602
20.00	0.121	0.016	0.120	0.016	5.710	0.657
30.00	0.121	0.016	0.120	0.016	6.180	0.724

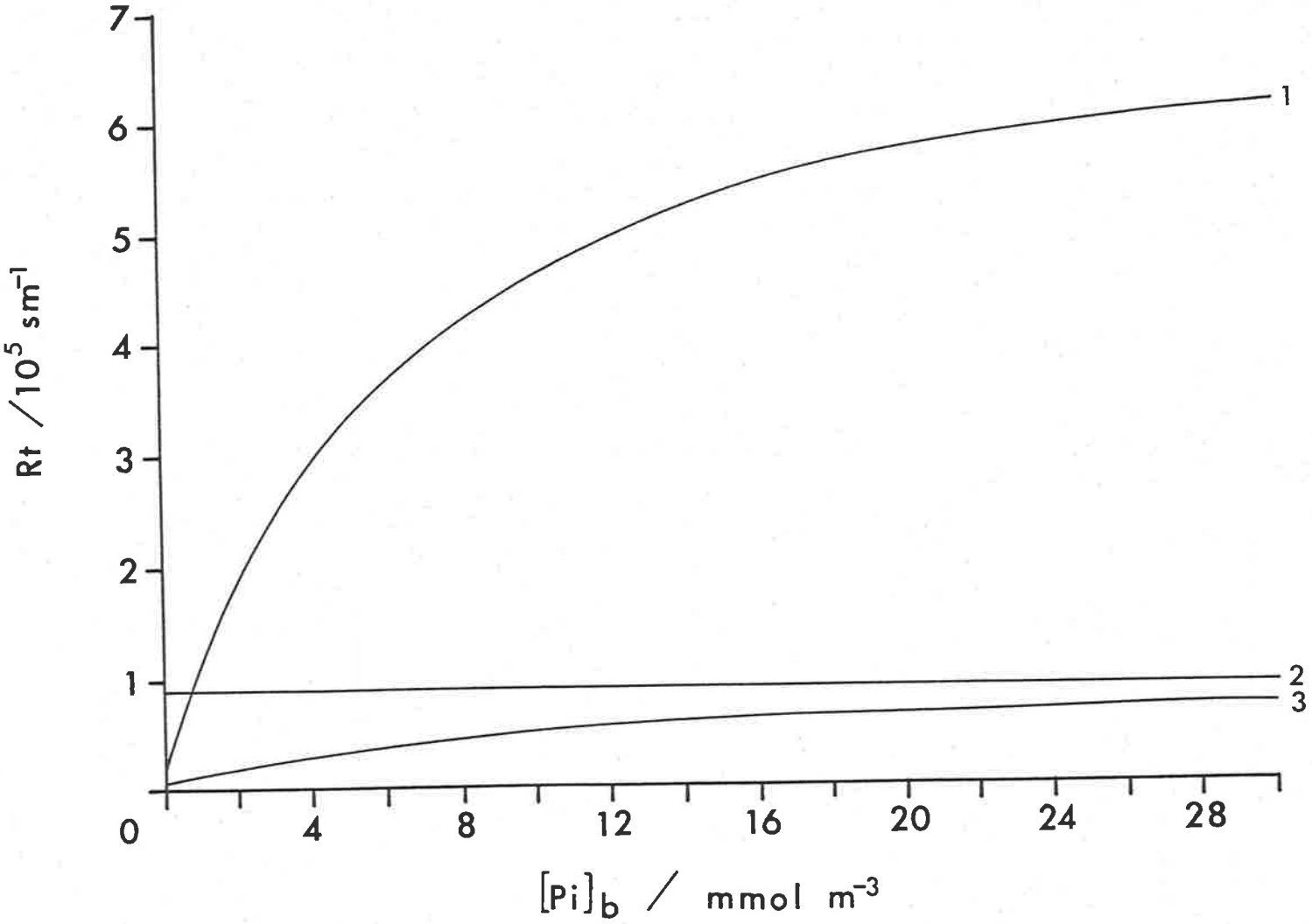

Figure 3.11. Relationship between Rt and [Pi]b for data from Experiment 1, where curve (1) is Model E for Shaker-F, line (2) is Model A Shaker-F and curve (3) is Model E for Shaker-S.

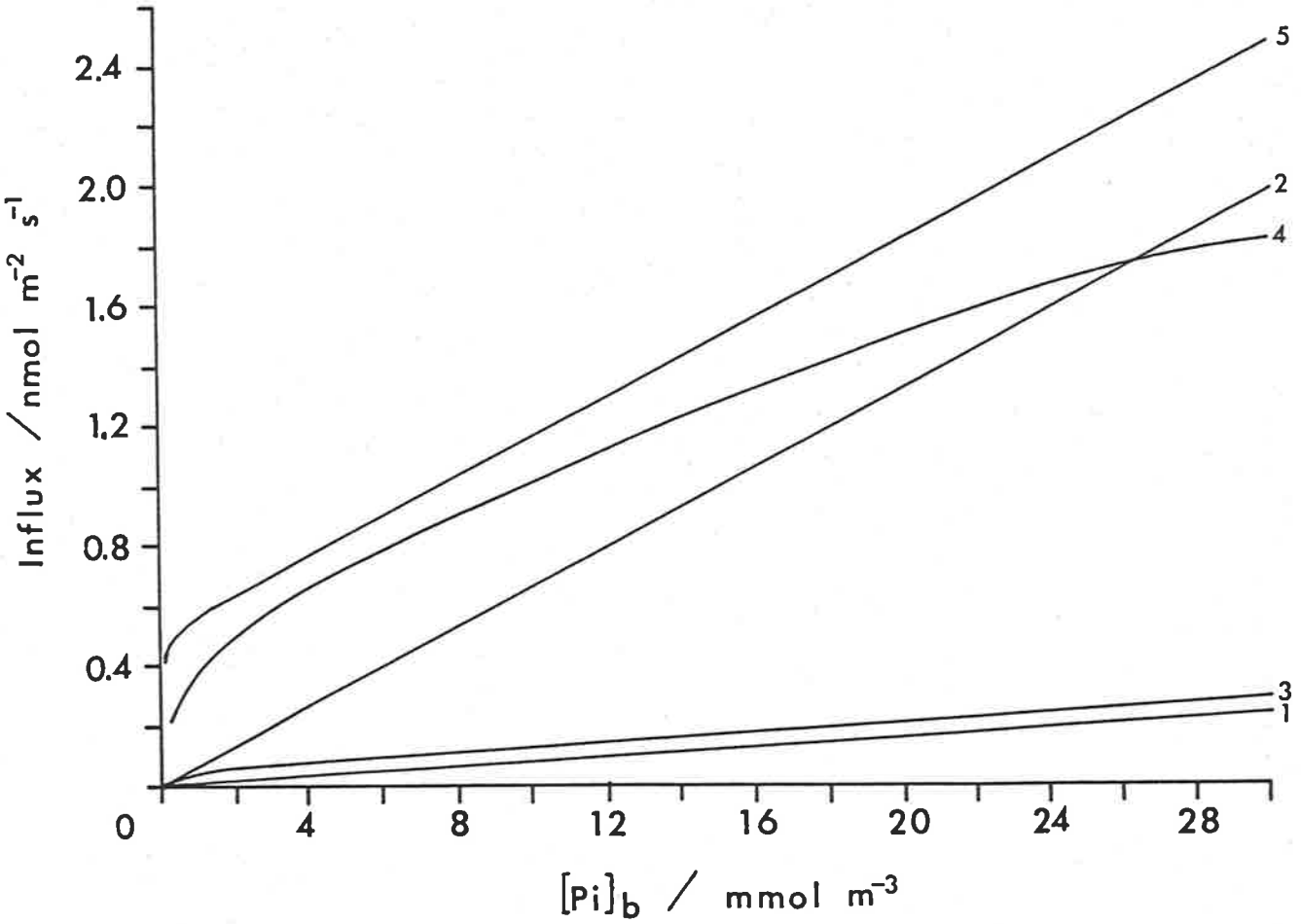

Figure 3.12. Relationship between predicted phosphate influx and [Pi]b for data from Experiment 1. (1) Model A diffusion flux for Shaker-S, (2) Model A diffusion flux for Shaker-F, (3) Model E diffusion flux and Briggs-Maskell influx for Shaker-S, (4) Model E Briggs-Maskell influx for Shaker-F and (5) Model E diffusion flux for Shaker-F.

limiting to the degree expected based on the initial assumptions for Model D. The assumption that the pH at the surface is zero, based on the charge balance (Table 3.10), clearly needs to be modified to account for the presence of protons.

The buffering index of seawater was 25 x 10^{-6} (Butler, 1964), which considering the volume of the D.B.L. surrounding the plant's surface and the large influx of protons is clearly inadequate to maintain the pH. Buffering in seawater is due mostly to carbon (Pytkowicz, 1967), which is at a far greater concentration than phosphate (2 mol m^{-3}), so the pH at the surface is probably dependent on the diffusion flux of carbon and its slower equilibrium reactions.

Another possibility is the proton attraction within the Donnan Layer maintaining the pH. Evidence against this comes from the results of Sentenac and Grignon (1985), who found that the concentration of $H_2PO_4^-$ was reduced within the cell walls as a consequence of binding with Ca^{2+}) even though there was an acidifying of the cell wall. Caution must be taken with these results as they apply to corn roots. Hanisak (1987) has indicated that within the marine situation calcium can bind to phosphate and therefore reduce its apparent concentration available for influx.

Smith (1984) has suggested the presence of a proton pump to maintain cytoplasmic pH in *Chara corallina*, which could also maintain the external pH if protons are cotransported with $H_2PO_4^-$. However as already mentioned for marine algae the most likely cation cotransported with $H_2PO_4^-$ is Na^+.

More work needs to be done in regard to surface pH measurements and the reactions that maintain the pH for small celled algae which cannot have acid banding on their surface.

3.3. CONCLUSIONS

The observed variation in the parameters Vm and Km between experiments and the variation between experimments to the within experiment response to water movement shows two things: (1) Cells of *U. australis* have different phosphate influx requirements, which could possibly be correlated with their age, internal phosphate concentration and their habitat (culture) history, (2) The variation in Km and Vm interacts with the D.B.L. effects. Taken together, the results indicate the plant's metabolism will be influenced to varying degrees by changes in the thickness in the D.B.L.. The implication is that sweeping conclusions attributed to the effect of increasing water movement will not always be correct without knowing the response of individual plants to water movement. It is also important not to generalize for all nutrients the effect of transport limitations through the D.B.L. for one nutrient.

Equations 3.1 and 3.2 can be written in terms of the resistances appropriate to chemical transport as:

(1) Rt >> 2Km/Vm therefore V = ([Pi]b - [Pi]s)/Rt Equ-3.17

(2) Rt << 2Km/Vm therefore V = Vm [Pi]s/(Km + [Pi]s) Equ-3.18

Therefore as Vm decreases the total transport process becomes more dependent on the resistance associated with the membrane. This depends on Km staying constant, and the conclusion in comparing the results of MacFarlane (1985) for *Ulva rigida* (Km $\sim$ 1.5 mmol m^{-3}, Vm $\sim$ 15 nmol m^{-2} s^{-1}) and those in Table 3.4 is that Km is relatively constant under these conditions. The variation observed in Vm then can have some influence on the dependency of the total transport process on the resistance associated with the D.B.L..

The evidence from the models presented for different phosphate species influx, points to a parallel diffusion flux of $H_2PO_4^-$ and HPO_4^{2-} across the D.B.L.. However the results did not necessarily show that HPO_4^{2-} could not be the ion transported across the plasmalemma. The Briggs-Maskell equation adequately describes the observed effect of the D.B.L. when either the combined $H_2PO_4^-$ and HPO_4^{2-} model (C) or the HPO_4^{2-} model (B) of influx are used. Complications associated with the simultaneous influx of other ions and the role of protons in rate limiting the equilibrium reaction can still only be conjectured. This applies to situations where multiple diffusion fluxes are modeled, and the false assumption that the thickness of the D.B.L. is constant for all solutes (Walker, Smith and Cathers, 1980). Tables 3.5 and 3.9 show that the calculated and measured D.B.L. thicknesses for the different ions vary considerably for a particular water movement.

Most of the discussion so far has dealt with the physical and chemical processes external to the membrane transport processes. The possibilty exists though for the cell to manipulate the rate and direction of flux and the solute species at the membrane in response to internal and external signals. This possibility has already been contemplated by Walker, Smith and Cathers (1980) with regard to the plant's manipulation of the rate of the proton flux, with the possibility of acidification within the D.B.L. and therefore stimulating CO_2 influx. A similar situation could occur for *Ulva*, as a means of controlling the influx of phosphate under cbnditions when phosphate is limiting the plant's metabolism, and the extra energy expenditure is offset against gains in metabolism.

The values of the D.B.L. thickness calculated from the results of the zinc method (Tables 3.5 and 3.9) and those estimated using the D.B.L. theory are in good agreement when the formula are applied to single ion diffusion fluxes. Disagreement occurs for the case of $H_2PO_4^-$

influx, when these values are fitted to the observed results. The calculation of an effective D.B.L. thickness for the model of combined $H_2PO_4^-$ influx is not possible using the D.B.L. theory. The values of Rt that fit the data for the combined model suggest that the D.B.L. thickness is very small. As a consequence of this it needs to be pointed out that applying the theory of D.B.L. with out knowing the true chemical situation within the D.B.L. can lead to incorrect assumptions as to its importance for metabolism.

This leads to the question of whether the observed difference in influx with varying resistance is enough to result in a significant variation in growth rate. Gavis (1976) has noted that when diffusion limits the uptake of nutrients (not applicable for CO_2) it results in a "smaller change in growth rate than it does in uptake rate". The small variation in phosphate influx (Figures 3.3 and 3.4) observed then might not be great enough to cause any variations in growth rate even at the greatest resistance used (Growth-1). This question will be tested in the next chapter.

CHAPTER 4. THE EFFECT OF WATER MOVEMENT ON THE GROWTH RATE OF *Ulva australis*: EXPERIMENTAL LIMITATIONS.

4.1 INTRODUCTION

The question of whether the decrease in influx caused by decreasing water movement should influence the rate of growth in long term experiments, depends on the relationship that exists between the influx and the growth rate. The Monod (1942) equation for growth relates the relative growth rate (R.G.R.) to the external nutrient concentration (Cs),

$$\mu = \frac{\mu m \; Cs}{Ks + Cs} \qquad \text{Equ-4.1}$$

where μ is the R.G.R., μm is the maximum R.G.R. (Weight Weight^{-1} Time^{-1}), and Ks is the half saturation for growth (mol m^{-3}), and both μm and Ks are based on the external nutrient concentration. The constant Ks is quantitatively and empirically different to the Michaelis constant Km for influx. Droop (1973) found that Ks was approximately five percent of the value of Km, and a similar result was found by Gotham and Rhee. However the results determined for the macroalga *Chordaria flagelliformis* show that Km was only approximately twice that of Ks (Probyn and Chapman, 1983). This equation has been experimentally verified for marine macroalgae by Chapman, Markham and Luning (1978), DeBoer, Guigli, Israel and D'Elia (1978), Gordon, Birch and McComb (1981) and Probyn and Chapman (1983) for both batch and continuous flow through experiments. Plotting μ against Cs provides a curve with the same general shape as the Briggs-Haldane equation.

In the same way in which the Briggs-Maskell equation was derived for influx, so too can an equation for growth rate, incorporating the effect of the D.B.L. resistance. This was done

by equating Equations 1.19 and 1.46 (assume steady state),

$$Kt(Cb-Cs) = \frac{Vm\ Cs}{Km + Cs}$$

and solving for Cs to give the quadratic equation

$$Cs^2 + Cs(Vm/Kt + Km - Cb) - KmCb = 0 \qquad \text{Equ-4.2}$$

simplifying

$$Cs = 0.5[Cb-Km-Vm/Kt + \sqrt{(Vm/Kt+Km-Cb)^2+4KmCb}] \qquad \text{Equ-4.3}$$

Note the negative sign has been dropped as this would imply a negative concentration (Cs) at the plant's membrane surface. The units for Cs, Cb, and Km were mol m^{-3}, for Kt, m s^{-1}, and for Vm, mol m^{-2} s^{-1}. Pasciak and Gavis (1974) came to the same solution, except they divided through by the constant Km, producing a dimensionless version of Equation 4.3. This created a term equivalent to Vm/KtKm (dimensionless) which they called 1/P. They arbitrarily chose that when P was less than 0.56, the overall transport process was limited by the D.B.L. resistance. This is the same term derived in Equation 1.50 (Kt << Vm/2Km equal to KtKm/Vm << 0.5) for the same condition. As shown in Section 3.2.3., the term 2Km/Vm (s m^{-1}) is equivalent to the resistance of the Briggs-Haldane reaction and the inverse of Kt is the resistance of the D.B.L. (Rt, s m^{-1}). This can be used to predict the conditions under which the D.B.L. resistance significantly affects the growth rate.

Substituting the solution for Cs (Equation 4.3) into Equation 4.1 creates an expression which describes the relationship between the growth rate and the external physical and nutrient conditions.

$$\mu = \mu m/(Ks/(0.5[Cb-Km-Vm/Kt+\sqrt{(Vm/Kt+Km-Cb)^2+4KmCb}])+1) \qquad \text{Equ-4.4}$$

Figure 4.1a shows a plot of R.G.R. versus [Pi]b. The values of Vm and Km were taken from Chapter 3 (2.0 nmol m^{-2} s^{-1} and 1.5 mmol m^{-3} respectively), the values of Kt are the inverse of Rt determined for the combined model of $H_2PO_4^-$ and HPO_4^{2-} influx (Table 3.9) and Ks is calculated using Ks = μmKqKm/Vm where Kq was the minimum internal

concentration of the limiting nutrient (Kq = 20 μmol g^{-1}, therefore Ks = 0.868 mmol m^{-3}, Droop 1973). Kq is approximated from the minimum Q determined from numerous experiments. Figure 4.1b shows a plot of influx (Briggs-Maskell equation) versus [Pi]b using the values of Vm, Km and Kt as described above for Figure 4.1a. As shown in Figures 4.1a and 4.1b, the D.B.L. resistance has the same qualitative effect on growth rate as it did on influx. There is a 2 to 7% decrease in the magnitude of the effect when compared with the response for influx (graphically this is hard to display). This decrease was predicted by Gavis (1976) using a similar expression to Equation 4.2, but no empirical application of this type of formula has been done. The consequence of Equation 4.2 is that for low values of Cb the rate of growth will be reduced for plants growing in slow water movement compared to faster water movement environments.

The experimental evidence for the limitation of growth rate due to an external D.B.L. resistance has been restricted to very few studies, involving both field and laboratory measurements (Jones, 1959; Matsumoto, 1959; Whitford and Kim, 1966; Doty, 1971a,b; Gerard and Mann, 1979; Lapointe and Ryther, 1979; Andrake, 1980; Cousens, 1981, 1982; Parker, 1981, 1982; Kain, 1982; Fujita and Goldman, 1985). The reason for this probably lies in the incorrect assumption that the results obtained for reduced influx can be directly applied to growth rate. The general result, where growth rate was plotted against water velocity, was that growth rate saturates with increasing water velocity. Parker (1981, 1982) found that the growth rate of *Ulva lactuca* and *Gracilaria tikvahiae* was maximized at the lowest water velocity tested (7.5 cm s^{-1}). The predicted saturation water velocity from Equation 4.4 is equivalent to the Kt for Growth-2.

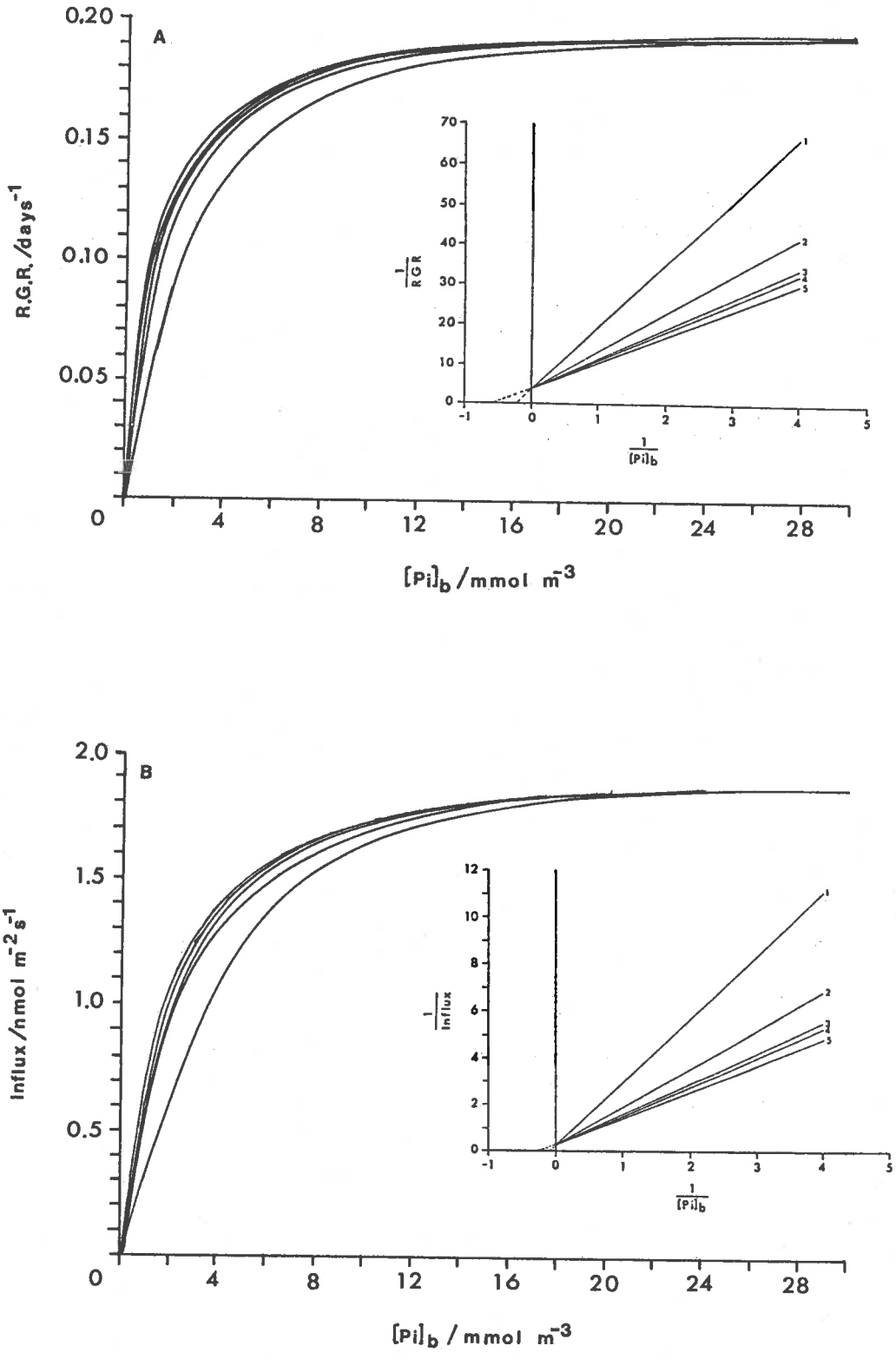

Figure 4.1. (A) Predicted R.G.R. (μ) versus [Pi]b calculated using Equation 4.4. The curves from bottom to top represent the increase in water movement for the Growth-1 to Growth-5 treatments (μm = 0.2 day^{-1}, Ks = 0.87 mmol m^{-3}, Vm = 2.0 nmol m^{-2} s^{-1}, Km = 1.5 mmol m^{-3}, and Kt values from the reciprocal values of Rt (Table 3.9)). Inset, reciprocal plot (numbers correlate to the five growth treatments).
(B) Predicted phosphate influx versus [Pi]b calculated using the Briggs-Maskell equation and the data from Chapter 3 for the combined model of phosphate diffusion (Model C). The curves from bottom to top are in the same sequence as in (A) above. Inset, reciprocal plot.

The conditions required to elucidate any variation in growth rate due to the influence of the D.B.L. resistance should be such that all other factors that can influence the growth rate were optimal. It was obvious that for suboptimal light conditions for instance, that the two factors will compete in their effect on the growth rate making it difficult to distiguish the magnitude of each factor separately. Also because the variation in water velocity predicts only a small difference in growth rate, any attempt to quantify this reponse will require accurate measurement of the growth rate. This may not be good enough as the variation naturally inherent in any population may be large enough to obscure the effect of the D.B.L. resistance.

4.2. RESULTS AND DISCUSSION

For the results presented, the method of growth rate determination was the one cut method (see Section 2.5.3.1.). The medium was filtered seawater and Hoagland's solution as described in Sections 2.2.2. and 2.2.4.. The three experimental water movement conditions chosen were Growth-1, Growth-2, and Growth-4 (see Tables 2.2 and 3.9). The concentration of phosphate in the seawater was 0.59 $\pm$ 0.08 mmol m^{-3} (n=21, standard error), and the pH was 8.22 $\pm$ 0.01 (n=41, standard error). The pH varied by 0.008 $\pm$ 0.005 (n=41, standard error) between the fresh and old seawater, replaced daily.

4.2.1. THE EFFECT OF Rt ON GROWTH RATE

Figure 4.2a shows that there was no significant difference in the increase in surface area over time between the different water velocities. A similar response was shown for changes in dry weight with time (Figure 4.3a). The slopes of inset Figures 4.2b and 4.3b represent

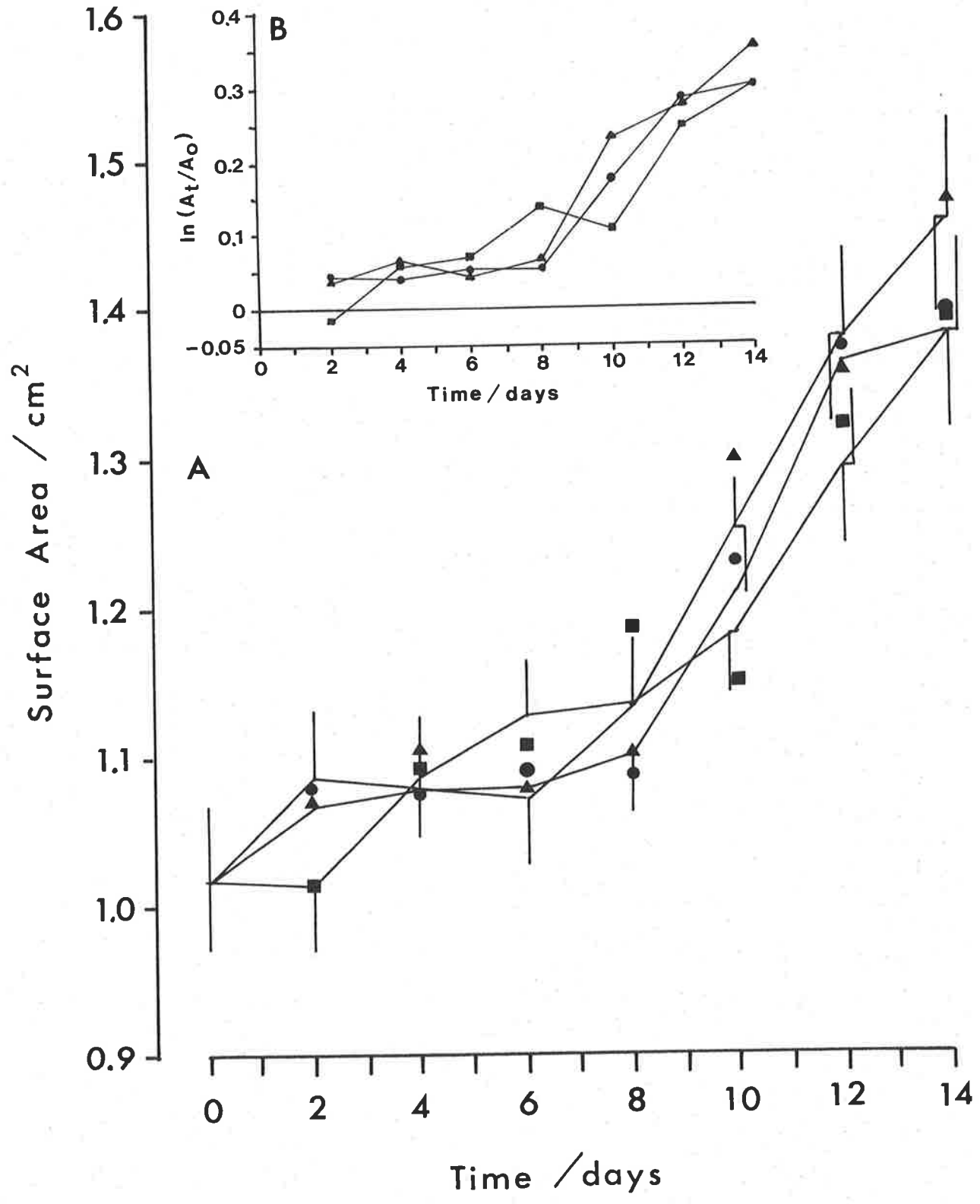

Figure 4.2. (A) Disk surface area versus time for the Growth-1 (■), Growth-2 (●) and Growth-5 (▲) treatments. The symbols are positioned at the average value for the raw data. The lines and 95% confidence limits (C.L.) were calculated using the Hunt program which explains the discrepancy between the position of the symbols and the position of the C.L. (n = 15).
(B) The natural logarithm of the surface area at successive experimental time periods (A_t) divided by the surface area at time zero (A_o) versus time. The slopes represent approximately the R.G.R. for each growth treatment (symbols are the same as in (A) above.

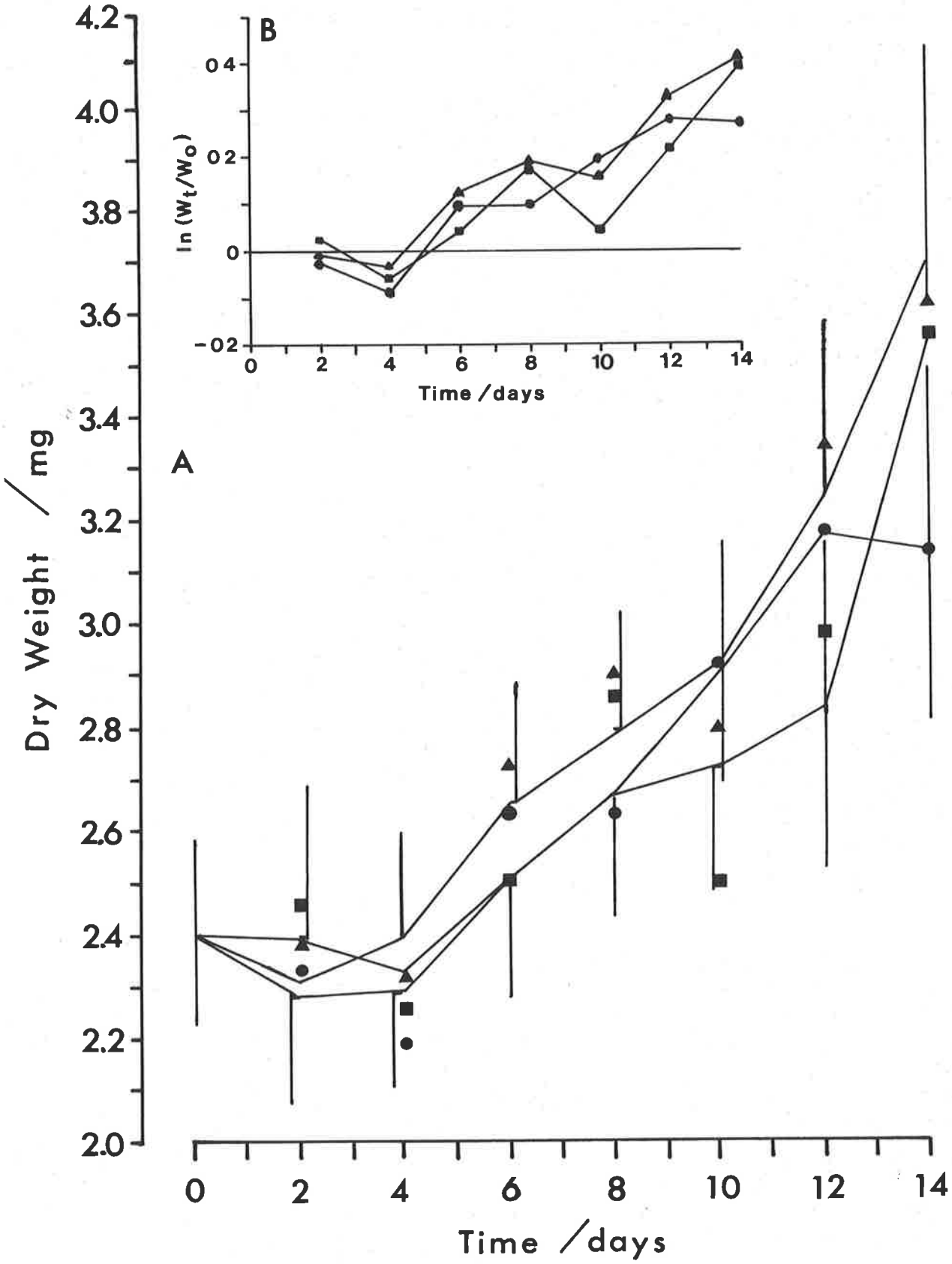

Figure 4.3. (A) Disk dry weight versus time (Hunt program, n = 10, C.L.). The symbols are the same as Figure 4.2.
(B) Wt is the dry weight at successive time periods and Wo is the dry weight at time zero. The line slopes represent the average R.G.R.

the change in growth rate with time, indicating that a considerable time lag (4 days) exists between the start of the experiment and the point at which the disks begin to grow. The calculated relative growth rates using both the Hunt program and raw data, are shown in Table 4.1. The values calculated by the Hunt program smooth out the discontinuities present in the raw data values, and indicate that the R.G.R. was not constant for any of the treatments. Also a large variance was associated with every rate which obscured the detection of any difference between treatments, and time periods.

For comparison, maximum values of R.G.R. from previous research for *Ulva* are shown in Table 4.2. The values from Table 4.2 for R.G.R., based on dry weight, are two to five times larger than the maximum values in Table 4.1. This might indicate that the growth conditions were not maximizing the growth potential, and would help to explain the inability to distinguish a response to the D.B.L. resistance.

It was possible to fit Equation 4.4 to the raw data in Figure 4.3a, by using the expression

$$W2 = W1\ e^{(\mu t)} \qquad \text{Equ-4.5}$$

where W1 and W2 are the dry weights at the initial and final time periods and are t time apart, and μ is the R.G.R. calculated from Equation 4.4. (Hunt, 1982). When this was done using the dry weight at time zero (2.4 mg) there was no relationship with the raw data. The reason for this was that Equation 4.4 results in a constant R.G.R. for all time periods, which meant that no account of the initial lag phase was taken into account. To overcome this Equation 4.5 was fitted to the raw data by using the dry weight at day 4 as the starting point (W1). Figure 4.4 shows that the curve generated by Equation 4.5 for Growth-1 was a reasonable fit to the raw data, for all treatments. The curves generated for Growth-2 and Growth-4 indicate that the growth for these

TABLE 4.1. Relative growth rate calculated using Hunt program and raw data averages (day^{-1}).

Time (days)	Average R.G.R. (Raw Data) Growth-1	Growth-2	Growth-4	Hunt program (C) Growth-1	Growth-2	Growth-4
2	0.012 A	-0.004	-0.013	-0.085 ± 0.021	-0.069 ± 0.021	-0.081 ± 0.019
4	-0.042 B	-0.013	-0.031	0.034 ± 0.030	0.069 ± 0.021	0.052 ± 0.025
	-0.015 A	-0.008 A	-0.022 A			
6	0.050 B	0.080 B	0.091 B	0.034 ± 0.023	0.035 ± 0.031	0.035 ± 0.019
	0.007 A	0.021 A	0.016 A			
8	0.067 B	0.032 B	0 B	0.020 ± 0.023	0.021 ± 0.021	0.031 ± 0.019
	0.022 A	0.024 A	0.012 A			
10	-0.067 B	-0.018 B	0.05 B	0.005 ± 0.030	0.032 ± 0.028	0.030 ± 0.025
	0.004 A	0.015 A	0.020 A			
12	0.088 B	0.088 B	0.043 B	0.052 ± 0.023	0.076 ± 0.022	0.030 ± 0.020
	0.018 A	0.028 A	0.023 A			
14	0.089 B	0.040 B	-0.005 B	0.0182 ± 0.094	0.153 ± 0.090	-0.048 ± 0.081
	0.028 A	0.029 A	0.019 A			

(A) $\mu = \ln (Wt/Wo) / (Tt - To)$
Where Wo is the initial dry weight at To = 0, and Wt is the dry weight at successive time periods.

(B) $\mu = \ln (W2/W1) / t$
Where W2 and W1 are the dry weights at successive time periods. (where t = 2 days)

(C) Hunt program use 1 knot (n = 10, C.L.)

TABLE 4.2. Observed maximum relative growth rates (R.G.R.) for *Ulva* sp. (The R.G.R. values cited are maximum for the experiments or field observations but not all the experiments were designed to determine the maximum R.G.R. possible).

R.G.R. day^{-1}	Parameter measured		*Ulva* species	Reference
0.125	dry weight	(a)	*U. fasciata*	Rice 1984
0.250	dry weight	(b)	*U. lactuca*	DeBusk et. al. 1986
0.257	fresh weight	(c)	*U. rigida*	Kelly 1980
0.243	fresh weight	(d)	*U. fasciata*	Lapointe and Tenore 1981
0.078	fresh weight	(a)	*U. curvata* or *rigida*	Rosenburg and Ramus 1981
0.053	fresh weight	(a)	*U. curvata* or *rigida*	Rosenburg and Ramus 1982a
0.086	fresh weight	(a)	*U. curvata* or *rigida*	Rosenburg and Ramus 1982b
0.093	fresh weight	(a)	*U. lactuca*	Fujita 1985
0.083	area	(c)	*U. lactuca*	Steffensen 1976
0.094	area	(c)	*U. fasciata*	Oza and Rao 1977
0.23	area	(a)	*U. lactuca*	Fortes and Lüning 1980
0.209	area	(d)	*U. lactuca*	Vermaat et. al. 1987
0.255	disk diameter	(e)	*U. lactuca*	Parker 1981

(a) Converted to R.G.R from 100 x R.G.R. (sometimes called specific growth rate).
(b) Converted to R.G.R. from yield and density values.
(c) Converted to R.G.R. from percentage increases over a known time period.
(d) Converted to R.G.R. from doublings per day.
(e) Converted to R.G.R. from compound interest percentage rates.

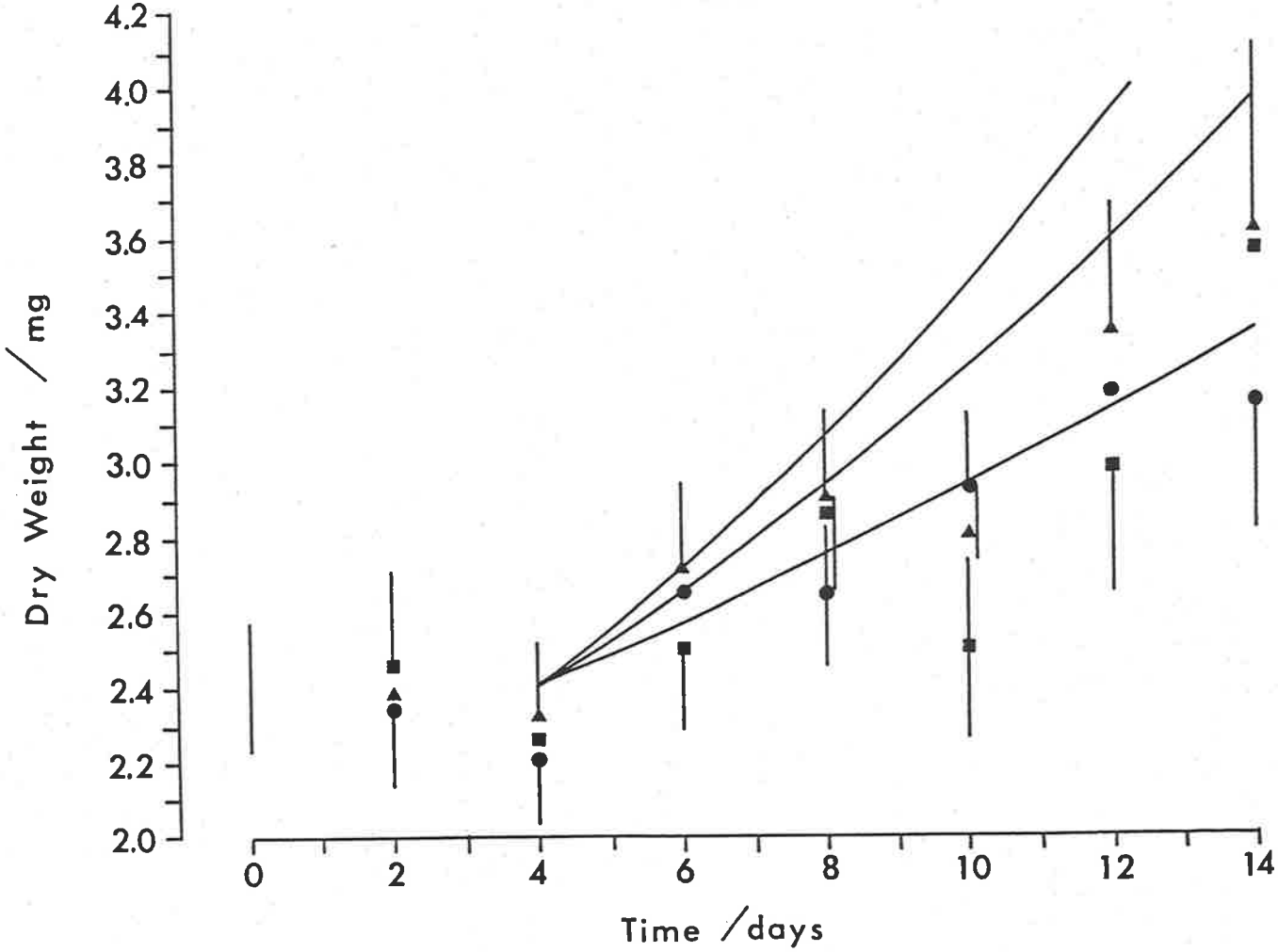

Figure 4.4. The symbols represent the average raw data values shown in Figure 4.3 (Growth-1 (■), Growth-2 (●) and Growth-5 (▲)). The lines were generated using Equations 4.4 and 4.5 and data for phosphate influx from Chapter 3. ($\mu m = 0.2\ day^{-1}$, $[Pi]b = 0.59\ mmol\ m^{-3}$, $Ks = 0.87\ mmol\ m^{-3}$, $Vm = 2.0\ nmol\ m^{-2}\ s^{-1}$, $Km = 1.5\ mmol\ m^{-3}$, Kt values from the reciprocal values of Rt (Table 3.9) and W1 = 2.4 mg)

treatments was inhibited by some other factor apart from the D.B.L.. This assumes that the assumptions of Equation 4.5 apply to the experimental conditions used. The assumptions, that the experimental conditions result in the growth being at a steady state (constant R.G.R.) and dependent on the external nutrient conditions obviously did not hold. These problems will be further expanded in Section 4.2.4..

4.2.2. THE EFFECT OF Rt ON THE PHOSPHATE UPTAKE OF GROWING DISKS

The inabilty to find a significant difference in growth rate between water velocities might be caused by similar uptake rates. Note that uptake was measured over long time periods and therefore takes into account both influx and efflux, and in this context refers to the net increase or decrease in total phosphate. The general trend in Figure 4.5a was that for Growth-2 and Growth-4 there was no net change in total phosphate per disk implying that no uptake of phosphate occurred for the duration of the experiment. This was confirmed by the decrease in total phosphate when expressed per g dry weight (internal concentration), which takes in to account the growth of the disks with time (Figure 4.5b). The response exhibited by the Growth-1 treatment was slightly different from the other two. Figure 4.5a shows an initial negative change in the net total phosphate per disk for Growth-1, and a consequent decline in the internal total phosphate concentration, which was partly obscured by the large variation around the mean. The general response from the initial to the final measurement was similar to the other two treatments on a per disk and per g dry weight basis.

As mentioned in Chapter 3, previous research has found that efflux was negligible compared to influx at low values of [Pi]b (Perry, 1976; Schjorring and Jensen, 1984a). The possibility exists that in response to cutting the integrity of the remaining cell membranes was reduced.

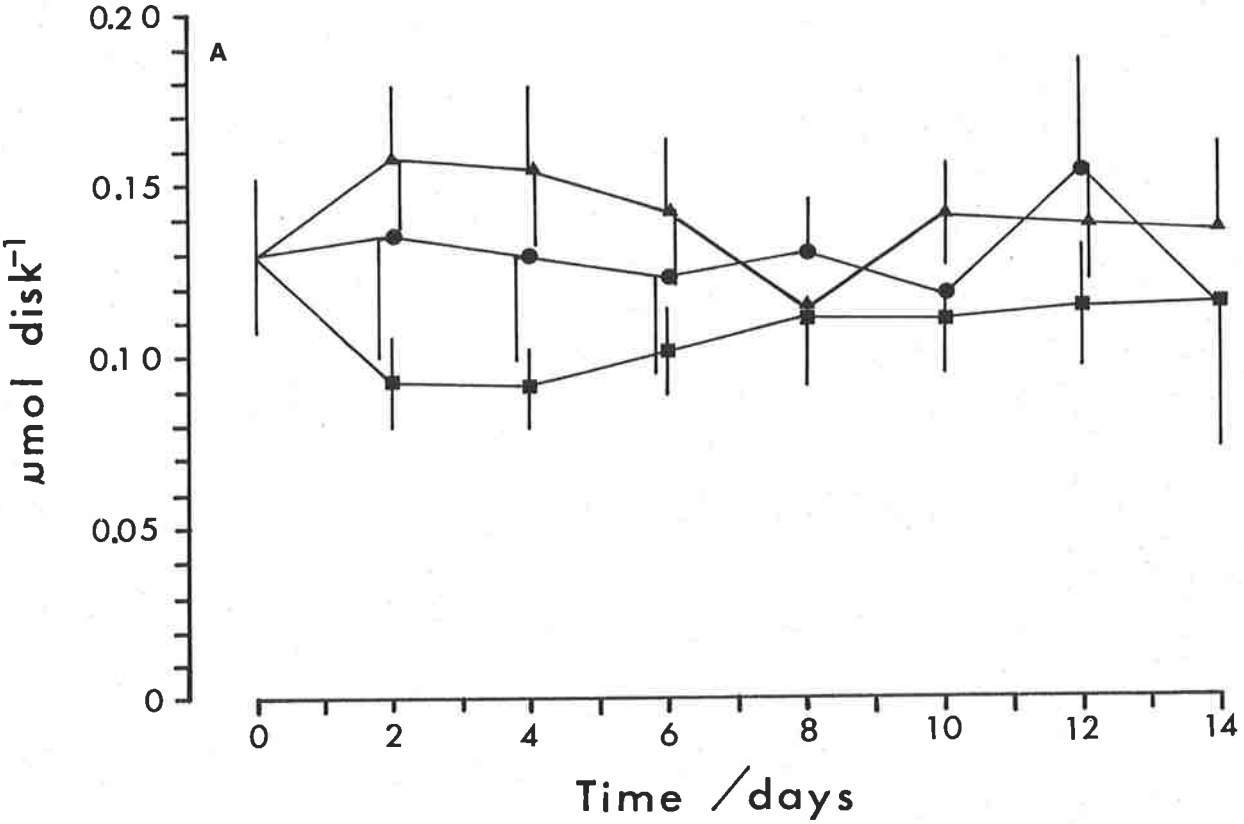

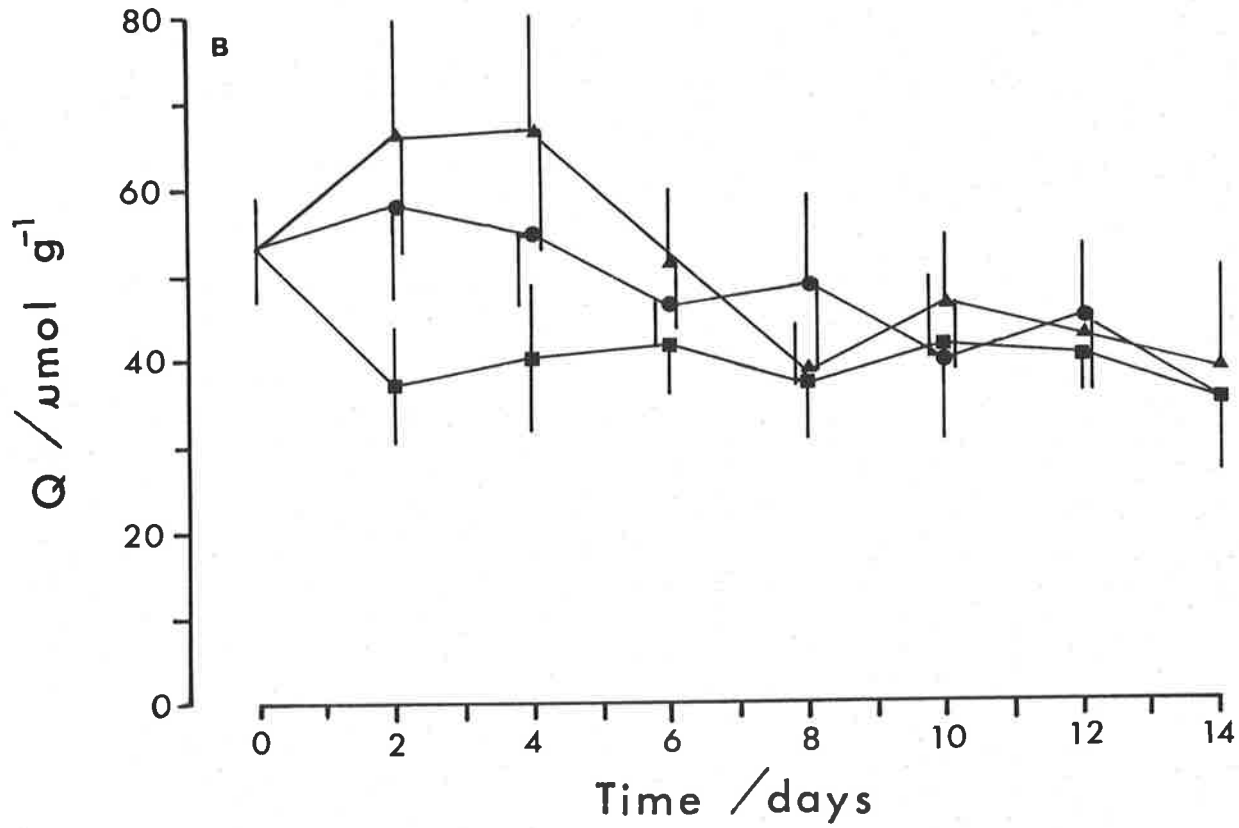

Figure 4.5. (A) Total phosphate per disk versus time (n = 10, C.L.). The symbols are the same as Figure 4.2a.
(B) Cellular total phosphate concentration (Q, D.W.) versus time (n = 10, C.L.). The symbols are the same as Figure 4.2a.

The ratio of dry weight to fresh weight for all treatments remained approximately constant for the experimental duration indicating that any changes in cell total phosphate concentration were not being influenced by changing cell volume (Figure 4.6).

4.2.3. THE EFFECT OF Rt ON THE GROWTH CAPACITY (STATUS)

Figure 4.7a shows that total chlorophyll per disk remained relatively constant for the experimental duration, except for the Growth-4 treatment in the last six days. This indicates that no more pigment complexes were being synthesised which was reflected in the decline of total chlorophyll per mg fresh weight (Figure 4.7b). What must have occurred, was a redistribution over time between the cells of the initial pigment complexes indicating that either some nutrient was limiting pigment synthesis or that the cells conserved their metabolic energy by decreasing the amount of energy used for pigment synthesis. For the fastest water movement treatment (Growth-4) the general response was similar until day eight when a sudden increase in the synthesis of pigments occurred. The increase was great enough that the concentration of pigment on a fresh weight basis increased (Figure 4.7b). A possible explanation for this might be obtained from the nitrogen data (Table 4.3).

TABLE 4.3. Nitrogen data from C.H.N. analysis for the initial and final time measurement periods (errors were 95% confidence limits).

	Nitrogen [%N g^{-1} (dry weight)]
Initial (t = 0)	2.21 $\pm$ 0.21 (n = 8)
Growth-1 (t = 14 days)	2.45 $\pm$ 0.44 (n = 8)
Growth-2 (t = 14 days)	2.89 $\pm$ 0.18 (n = 9)
Growth-4 (t = 14 days)	3.56 $\pm$ 0.21 (n = 10)

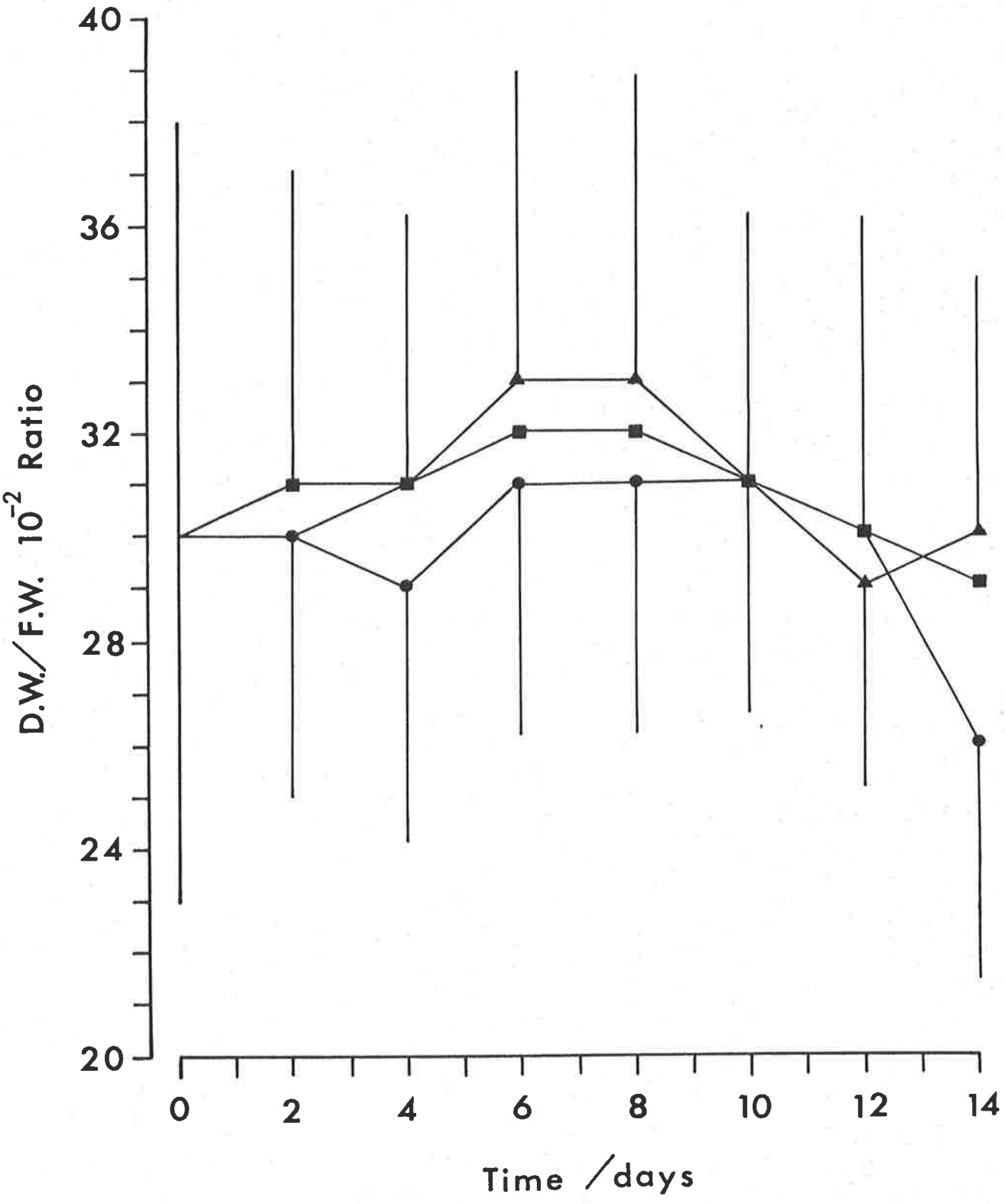

Figure 4.6. Dry weight to fresh weight ratio versus time (n = 10, C.L.). The symbols are the same as Figure 4.2a.

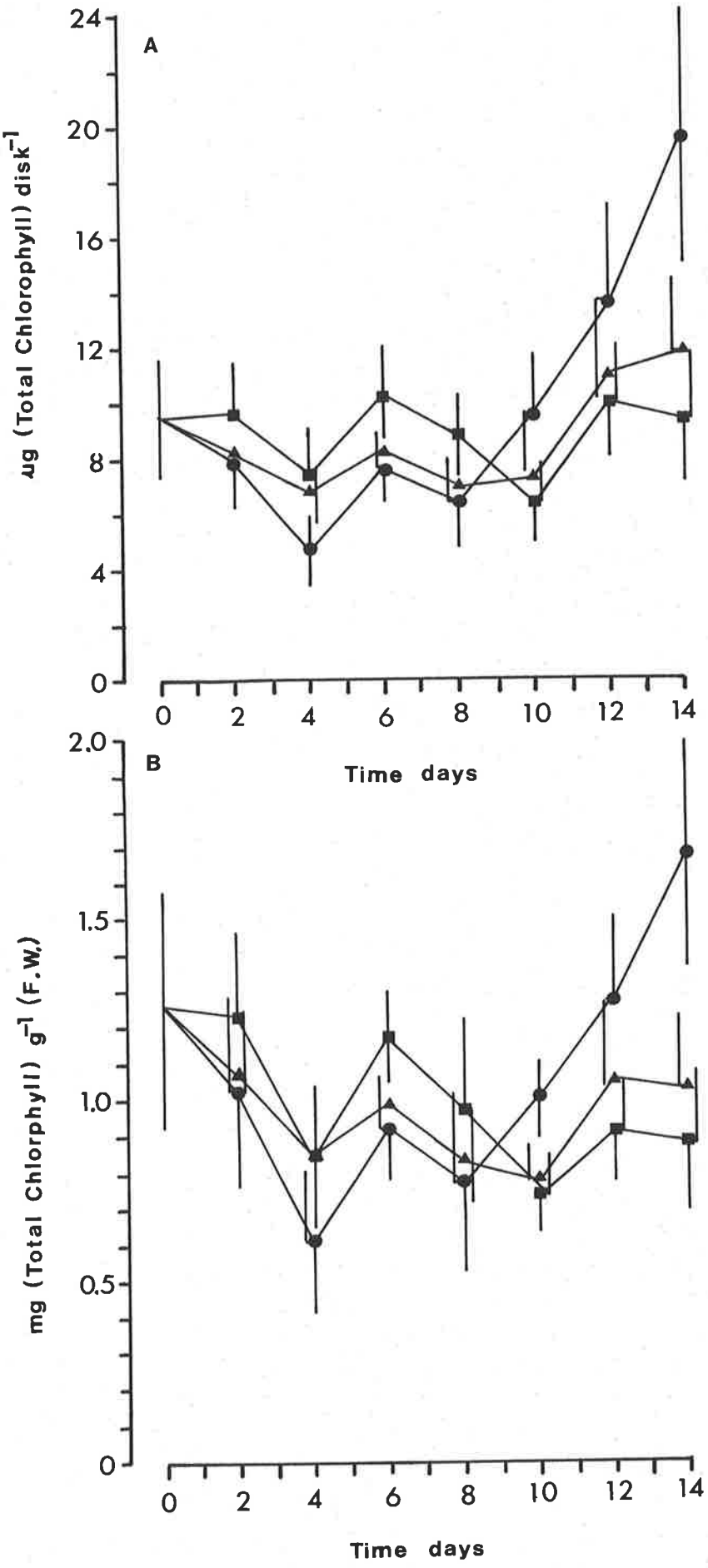

Figure 4.7. (A) Disk total chlorophyll versus time (n = 5, C.L.). The symbols are the same as Figure 4.2a.
(B) Total chlorophyll concentration (F.W.) versus time (n = 5, C.L.). The symbols are the same as Figure 4.2a.

This shows that the fastest water movement treatment had an appreciable increase in nitrogen compared to the other treatments. Previous research has shown that under growth limiting conditions marine macroalgae have the capability to store surplus accumulated nitrogen as pigments (Gantt, 1981; Gordon, Birch and McComb, 1981; Lapointe, 1981; Ryther, Corwin, Debusk and Williams, 1981; Bird, Habig and DeBusk, 1982; Rosenberg and Ramus, 1982a; Ramus, 1983; Dawes, Chen, Jewett-Smith, Marsh and Watts, 1984; Shivji, 1985). This fits in with the observation that disks in the Growth-4 treatment were appreciably greener in colour, and Ramus (1983) has pointed out that colour can indicate the nitrogen status of macraoalgae. The ability to utilize the stored nitrogen in the increased pigmentation for future growth differs for different macroalgae (Shivji, 1985). The increased pigment content in *Ulva* has been shown to reflect an increased growth capacity (Lapointe and Tenore, 1981; Ramus, Beale and Mauzerall, 1976). Therefore, the results suggest that the experimental plants had the capacity for an increased growth rate but were being limited by some other factor.

4.2.4. EXPERIMENTAL LIMITATIONS

By combining different experiments done under the same conditions it would be possible to determine more accurately the growth rate response to the different treatments. However, experiments done under the same conditions while producing the same general response have large differences in growth rates which makes comparison impossible. An attempt to compare experiments was done by assuming that the total chlorophyll concentration reflected the initial growth capabilities, and using it as the covarient in an analysis of covariance (Sokal and Rohlf, 1981). However the data did not comply with the assumptions of such analysis, because the total chlorophyll concentration did not adequately reflect the growth capacity. This means that other measures of the

initial growth capacity status are needed before such an analysis can be done. Before this can be done a more complete understanding is needed of the internal factors that influence growth.

The use of the Hunt program to smooth and fit confidence limits to the raw data results in a subjective influence in determining the position of any change in R.G.R. by selecting the program knot positions. The method for positioning the knots was to examine the raw data for any large changes in growth rate, and the knots were positioned accordingly. For the present work a single knot was determined for the inflection of the data at the end of the initial lag phase in growth. A further problem with the Hunt program was an increased variance at the ends of the experimental time period. This makes it difficult to achieve a significant difference between treatments for the final time period, and leads to the rejection of a significant difference in the data when the converse was true (a Type 2 error, Sokal and Rohlf, 1981). Poorter and Lewis (1986) have pointed out that this thickening of the confidence limits at the beginning and end of the fitted curve lacks any biological meaning. To overcome this a subjective decision was made to ignore the final values where nonsignificance occurred if the previous time periods were significantly different.

The single nutrient limiting theory predicts that the growth rate will be directly related to that nutrient which was in the least supply (Droop, 1973). Kunikane, Kaneko and Maehara (1984) concluded that the single nutrient limiting theory only applies when the concentration of the other nutrients were large compared to the limiting nutrient, and optimal for the plant's maximum R.G.R. Conversely, the "multiplicative effect is a principle that the growth is dependent on the concentration of all suboptimal nutrients which might be exerting influence simultaneously" (Kunikane, Kaneko and Maehara, 1984). To determine the relationship between [Pi]b and the D.B.L. the experimental design used

attempted to create the situation whereby the limiting nutrient theory applies. It was thought that this was more likely to show the relationship under study and was simpler to model. If the multiplicative effect was affecting the growth response then it was difficult to determine the quantitative relationship between the experimentally limited nutrient and the growth rate. That was because the other suboptimal nutrients were having an unknown effect on this relationship. The results indicate that the possibility exists that this situation was occurring in this experiment making it difficult to achieve a significant difference between water movement treatments. The pre-conditioning conditions were suitable for maintaining healthy plants but the rate of growth was lower than in other studies (Table 4.2). The filtered seawater contained no added nutrients so that all nutrients were reduced internally. Even when added nutrients were used for the experiment, in the beginning the plants would be responding according to the multiplicative effect.

Alternatively, the preconditioning process might have been inadequate to achieve a growth state whereby the plants were dependent on the external phosphate as the limiting nutrient. The aim of the preconditioning was to reduce the internal phosphate concentration levels within the cells so that growth was dependent on the rate of the limiting nutrient taken up through the D.B.L. and membrane. The preconditioning conditions maintained the health of the plants but did not produce conditions suitable for growth, and therefore the plants would be maintaining their internal concentrations. Steffensen (1976) has pointed out that two weeks of preconditioned growth of *Ulva lactuca* in low nutrients was insufficient to reduce the internal concentrations of phosphorus and nitrogen. Equation 4.1 depends on the internal and external concentration of the limiting nutrient being in steady state. Because uptake can exceed the rate of growth usage, a surplus internal

nutrient concentration can be achieved (luxury consumption, Gerloff and Krombholz, 1966). It would then be possible for the plant to maintain its growth rate without being dependent on the limiting effect of the D.B.L.

Ulva australis disks grow by diffuse cell expansion (Rosenberg and Ramus, 1981) so all cells should be responding to the D.B.L. and not just the peripheral cells. This was important because the use of zinc disks to derive the values of Kt assumed that the acid reaction was constant over the surface. Therefore the values of Kt should apply as well for growth as they did for influx. Previous research on the use of disks for experimental purposes gives contradictory evidence on their validity when compared to whole plants. Wheeler (1979) found that methylamine influx was reduced by up to eighty percent when using tissue segments of *Macrocystis pyrifera* compared with whole plants. King and Schramm (1976) concluded that disks did not accurately represent the normal situation, with regard to photosynthetic rates, for whole plants of *Fucus vesiculosus* and *Laminaria digitata*. In contrast Drew (1983) showed that disks of *Laminaria* were a realistic way to measure their physiology. Hatcher (1977) found that respiration of freshly cut tissue segments of *Laminaria longicruris* was 23 to 48% higher than segments that had been allowed time to recover from the cutting process. After 10 to 16 hours the recovery response had saturated with no further decrease in respiration. Hatcher (1979) also showed that while short term respiration measurements were affected by using disks long term measurements of net photosynthetic rates were not. The general conclusion appears to be that if disks were used immediately then they would not represent the response achieved for whole plants, as they require time to recover from the injury. Also, the longer the experimental duration is the more accurately will disks reflect the whole plants. The significance for the methodology used here for *U. australis* was that disks should be an accurate reflection of how

whole plants would respond both quantitatively and qualititatively. Also attributed to the use of disks, by Hatcher, (1979), was a significant increase in the variability of metabolic measurements. This was attributed to the non-uniform nature of the tissue between different disks. The results presented for *U. australis* also show a large variance around the mean which could be reduced by selecting more uniform tissue. This was the rationale behind the two cut method (see Section 2.5.3.2) that, by selecting only disks that had grown to specific criterion would reduce this variabilty.

4.3. CONCLUSIONS

The important experimental finding was that to achieve a reliance of growth on the external phosphate concentration, and thereby showing the effect of the D.B.L. resistance, it was necessary to use a more defined preconditioning process. The experimentally measured large variance and lag in growth rate for each water movement treatment resulted in no signficant difference between treatments for growth. If the experimentally determined lag was not an experimental artifact *U. australis* plants growing in the field under low water movement and growth conditions (e.g. calm turbid low nutrient seawater), would have a considerable lag phase before they could utilize any change in conditions. This lag response appears to be controlled by the low growth rate and low growth capacity of the plants. The importance to the plant of their previous water movement history, in determining their effect to increasing water movement will be tested in the next chapter.

The application of Equation 4.1 was found to be incorrect in this experimental context as the formula does not take into account the variable growth associated with the declining internal phosphate concentration. This needs to be incorporated into the relationships describing the effect for the D.B.L. on growth rate.

CHAPTER 5. THE RELATIONSHIP BETWEEN UPTAKE, INTERNAL PHOSPHATE CONCENTRATION AND WATER MOVEMENT, AND THEIR EFFECT ON THE GROWTH RATE OF *U. australis*

5.1 INTRODUCTION

When the growth rate is at steady state, the rate of limiting nutrient taken up is equal to the amount used in growth. Under this condition

$$V = \mu Q \qquad \text{Equ-5.1}$$

where Q was equivalent to the internal nutrient concentration (mol g^{-1}). For the terminology used by researchers working on phytoplankton Q is the cell quota. Equation 5.1 predicts that for a constant uptake both μ and Q will be constant, and their magnitudes will depend on the relationship between μ and Q. For the very limiting conditions under which Equation 5.1 applies then Equation 4.1 can be used to predict the effect of water movement. Fuhs (1969), Muller (1970) and Droop (1973) have empirically derived an expression for the relationship between Q and μ, hence

$$\mu = \mu mq(Q - qo)/(Kq + (Q - qo)) \qquad \text{Equ-5.2}$$

where μmq is the theoretical asymptotic growth rate as Q becomes infinite, qo is the minimum internal concentration at which the growth rate is zero (subsistence quota), and Kq is the internal nutrient half saturation constant for growth. The value of μmq is not equivalent to μm and the difference is related by the expression,

$$1/\mu mq = 1/\mu m - Kq/Vm \qquad \text{Equ-5.3}$$

therefore μmq is larger than μm (Droop, 1973; Gavis, 1976). In affect μmq is a mathematical abstraction as μ can not exceed the value of μm, and arises from the lack of conditional limitations on the maximum value of Q. The internal concentration in reality should be finite and reach a maximum value (qm). Previous research on *Cladophora* has found that for inorganic nitrogen Q saturation did occur, and for phosphate only partial saturation was found (Gordon, Birch and McComb, 1981).

The concept qc is useful in determining when the nutrient is limiting to growth, and is defined as the internal concentration at which $\mu/\mu mq = 0.9$. In affect it is a threshold limit below which growth will be increasingly limited, and defines the internal nutrient condition when the external D.B.L. resistance can inhibit growth rate.

Equation 5.2 by implication only applies when the nutrient is limiting to growth, and therefore does not need to account for these high internal valus of Q. Also Kq is mathematically equivalent to Q + qo when $\mu = \mu mq/2$ and therefore is not a true, (in the mathematical sense) half saturation constant.

Droop (1973) and Rhee (1973) experimentally determined that Kq = qo, therefore Equation 5.2 can be simplified to a hyperbolic curve,

$$\mu = \mu mq(1 - (qo/Q)) \qquad \text{Equ-5.4}$$

hence if Q = 2qo then $\mu = \mu mq/2$. The shape of Equation 5.4 is similar to that for the Briggs-Haldane equation, and the initial slope is dependent on the magnitude of the shift for qo from zero concentration (Figure 5.1a). Previous research has shown that the rate of saturation differs depending on the species of the limiting nutrient. Both phytoplankton and macroalgae saturate their growth rate over a small range of inorganic nitrogen (Droop, 1973; Gordon, Birch and McComb, 1981; Probyn and Chapman, 1983). However, for phosphate the rate at which μ increases to its asymptote was comparatively slower for phytoplankton, though there were marked species differences (Fuhs, 1969; Tilman and Kilham, 1976; Brown and Button, 1979; Gotham and Rhee, 1981). Gordon, Birch and McComb found that for the macroalga *Cladophora*, the ratio qc/qo was 2 and 6 for inorganic nitrogen and phosphate respectively. The curve in Figure 5.1a is generated using $\mu mq = 0.2\ day^{-1}$ and $qo = 20\ \mu mol\ g^{-1}$, and shows that μ reaches its asymptote at high internal concentrations. The relationship between μQ (nutrient consumed by growth) and Q is linear, and can be used to predict the magnitudes of Q and μ for steady state growth at different values of V (Figure 5.1b), also the slope is μmq and the line intercepts

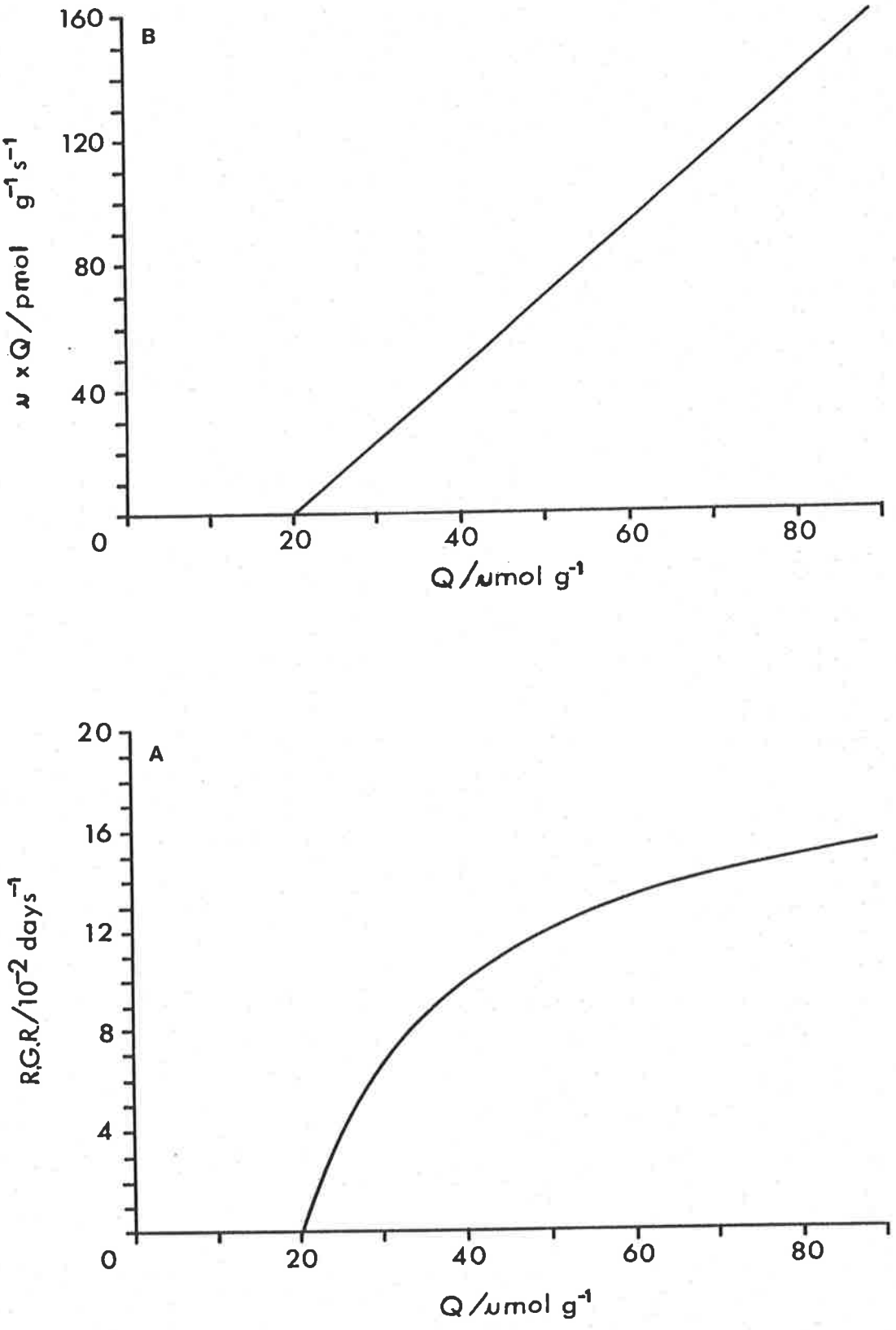

Figure 5.1. (A) The relationship between growth rate (μ) and internal nutrient concentration (Q) predicted by Equation 5.4 (q_o = 20 μmol g^{-1} (D.W.), μ_{mq} = 0.2 day^{-1}).
(B) Plot of μQ versus Q, data same as in (A) above.

the X-axis at qo. Further, because Equation 5.4 relates μ to Q and not Cs, the use of this equation does not predict the possible influence of water movement on growth rate. For example plants with the same value of Q growing in different water movement environments would according to Equation 5.4 have the same growth rate.

Regulation of growth rate by Q was intuitively not difficult to comprehend considering the ability of algae to continue to grow on stored nutrients when the external concentration was limiting. Luxury consumption was defined by Droop (1973), and formulated by Brown and Button (1979), as the ratio of Q when it was not limiting, to that when it was limiting, Q/qo (where Q > qc). Previous research has found that for the majority of marine macroalgae luxury consumption occurs for both inorganic nitrogen and phosphate, and was important in determining their seasonal productivity and persistence within their habitat (Chapman and Craigie, 1977; Buggeln , 1978; Chapman, Markham and Lüning, 1978; D'Elia and DeBoer, 1978; Gordon, Birch and McComb, 1981; Morgan and Simpson, 1981; Ryther, Corwin, DeBusk and Williams, 1981; Bird, Habig and DeBusk, 1982; Rosenberg and Ramus, 1982; Dawes, Chen, Jewett-Smith and Watts, 1984; Rosenberg, Probyn and Mann, 1984; Rosell and Srivastava, 1984; Wallentinus, 1984; Lapointe, 1985; Shivji, 1985).

To determine the effect of water movement on growth, if any, we need a relationship for non-steady state growth incorporating the relationship between Q and μ (Equation 5.4) and the variation of Q with time. This model requires two differential equations

$$(1/W)\,dW/dt = \mu mq(1 - qo/Q) = \mu \qquad \text{Equ-5.5}$$

$$dQ/dt = (1/W)\,dCb/dt - \mu Q \qquad \text{Equ-5.6}$$

where W is the dry weight, (1/W)dCb/dt is the rate of uptake (V) and can

be substituted by the Briggs-Maskell equation [1]. Equation 5.5 approximates the instantaneous growth rate to Equation 5.4. Equation 5.6 describes the rate of change in Q with time as a result of the balance between uptake and growth requirements. By incorporating the Briggs-Maskell equation for uptake, Equation 5.6 will take into account variations in uptake as a result of variations in water movement. Note that it is not necessary to displace the value of Q by qo in the expression μQ (Equation 5.6) as this displacement is incorporated into the relationship between μ and Q. It is possible to determine an approximate solution for Q at a time interval Δt

$$Q2 = Q1 + (\Delta t)dQ/dt \qquad \text{Equ-5.7}$$

where Q2 and Q1 are the internal nutrient concentrations time Δt apart. Equations 5.5 and 5.6 are conditional on the inequalities,

$$Vm > V > 0 \qquad \text{Equ-5.8}$$

$$\mu mq > \mu > 0 \qquad \text{Equ-5.9}$$

$$qc > Q > qo \qquad \text{Equ-5.10}$$

where Equation 5.10 depicts the situation for the nutrient to be limiting to growth, and limits the maximum flux for growth to μmq.qc.

There are three possible outcomes from the mass balance Equation 5.6; firstly V > μQ results in a positive change in Q with time. There are two possible reasons for this; (1) If the measured nutrient being taken up is non-limiting to growth, even when Q is within the range specified by Equation 5.10, Equation 5.6 cannot be used. The predicted outcome would be for luxury consumption of the measured nutrient until the growth conditions altered, (2) If the measured nutrient (Q) was

---

(1) The Briggs-Maskell equation cannot be used in this context because its units are incompatible with the units of dQ/dt (mass mass^{-1} time^{-1}). Therefore, the Briggs-Maskell equation was multiplied by the ratio of surface area to dry weight (m^2 g^{-1}) to convert V to the same units as dQ/dt. Note, the surface area was doubled as phosphate was taken up on both sides of the disks.

limiting growth and an increase in the external nutrient concentration occurred, the increased uptake would result in an increase in Q which would consequently result in an increased growth rate. With time, μQ would increase relative to uptake until dQ/dt was zero (steady state). Clearly changes in the D.B.L. resistance will result in this equilibrium being established at different magnitudes of Q and theoretically as a result affecting the growth rate. Figure 5.2 depicts this situation given the initial (t = 0) condition that Q = qo therefore μ = 0, the result was an asymptotic decrease and increase in dQ/dt and uQ respectively. Interestingly the time required for equilibrium to be established was greater than expected given that the value of [Pi]b was ecologically relevant for growth limiting conditions. Experimentally this will result in non-steady state growth conditions for the experimental duration. Figures 5.3a and 5.3b show that both Q and growth rate will increase over time at different rates for different values of Rt, and reach different asymptotes.

Secondly, if V = μQ then by definition the system would be at steady state, consequently dQ/dt would be zero resulting in a constant internal concentration with time. This is the situation required for Equation 4.1 to be applicable and can occur at various values of Q. However, realistically the value of Q must be such that it is significantly growth limiting compared with the other growth nutrients. Graphically it is possible to determine when this outcome occurs as a plot of V versus μQ should be a straight line with a slope of one.

Finally, if μQ > V the rate of uptake is inadequate to supply the nutrient at the rate of usage for growth, therefore, the internal nutrient concentration decreases with time until it reaches a steady state, at which time μQ = V. In the case when the rate of uptake was essentially zero (e.g. the plant growth was dependent on its internal nutrient

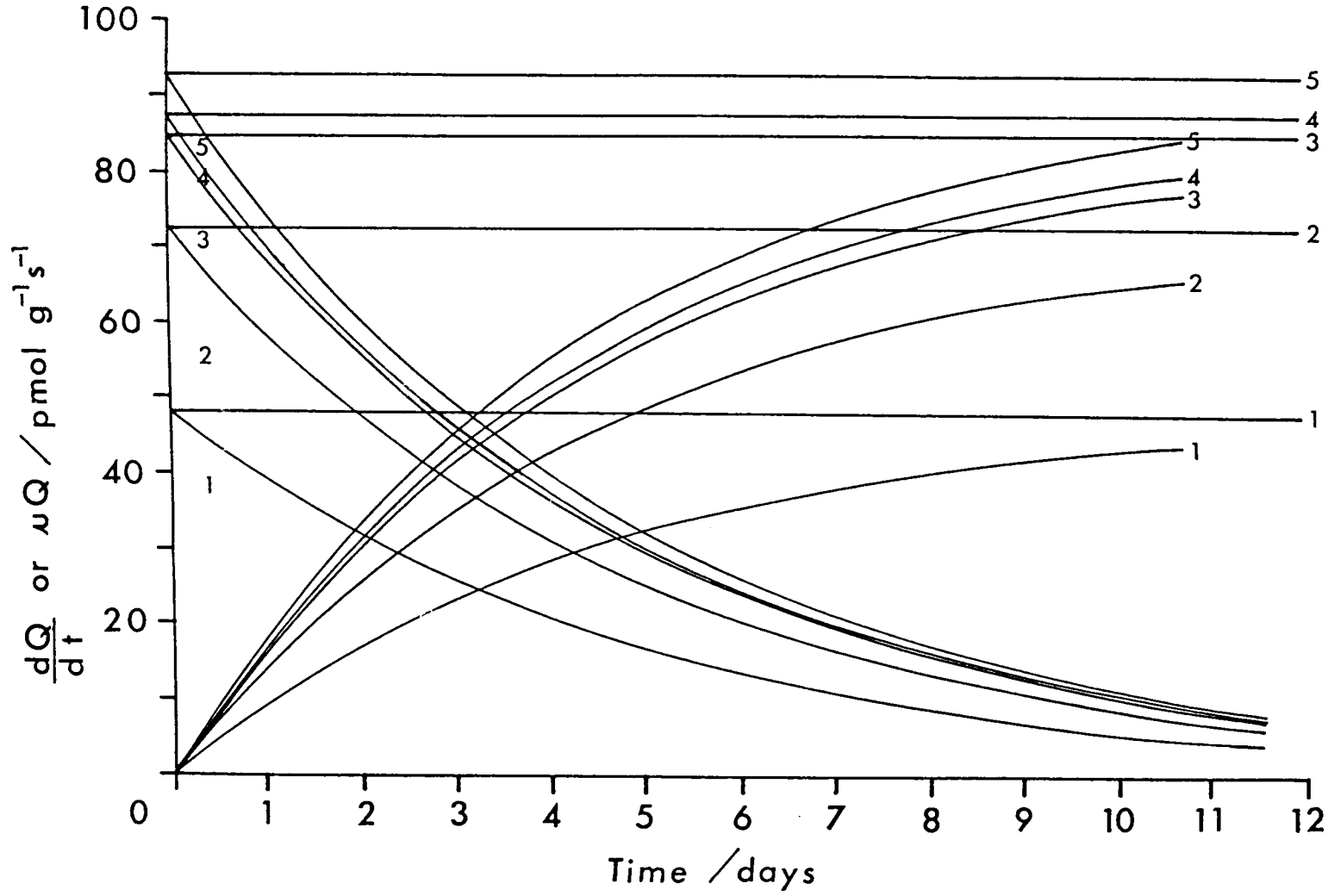

Figure 5.2. The horizontal lines represent phosphate influx calculated using the Briggs-Maskell equation ($[Pi]b = 0.67$ mmol m^{-3}). The curves decreasing with time represent dQ/dt, and μQ is represented by the curves increasing with time. dQ/dt and μQ were calculated using Equations 5.5, 5.6 and 5.7 (q_o and μ_{mq} are the same as for Figure 5.1). The numbers 1 to 5 represent the five growth treatments (Growth-1, Growth-2 etc.).

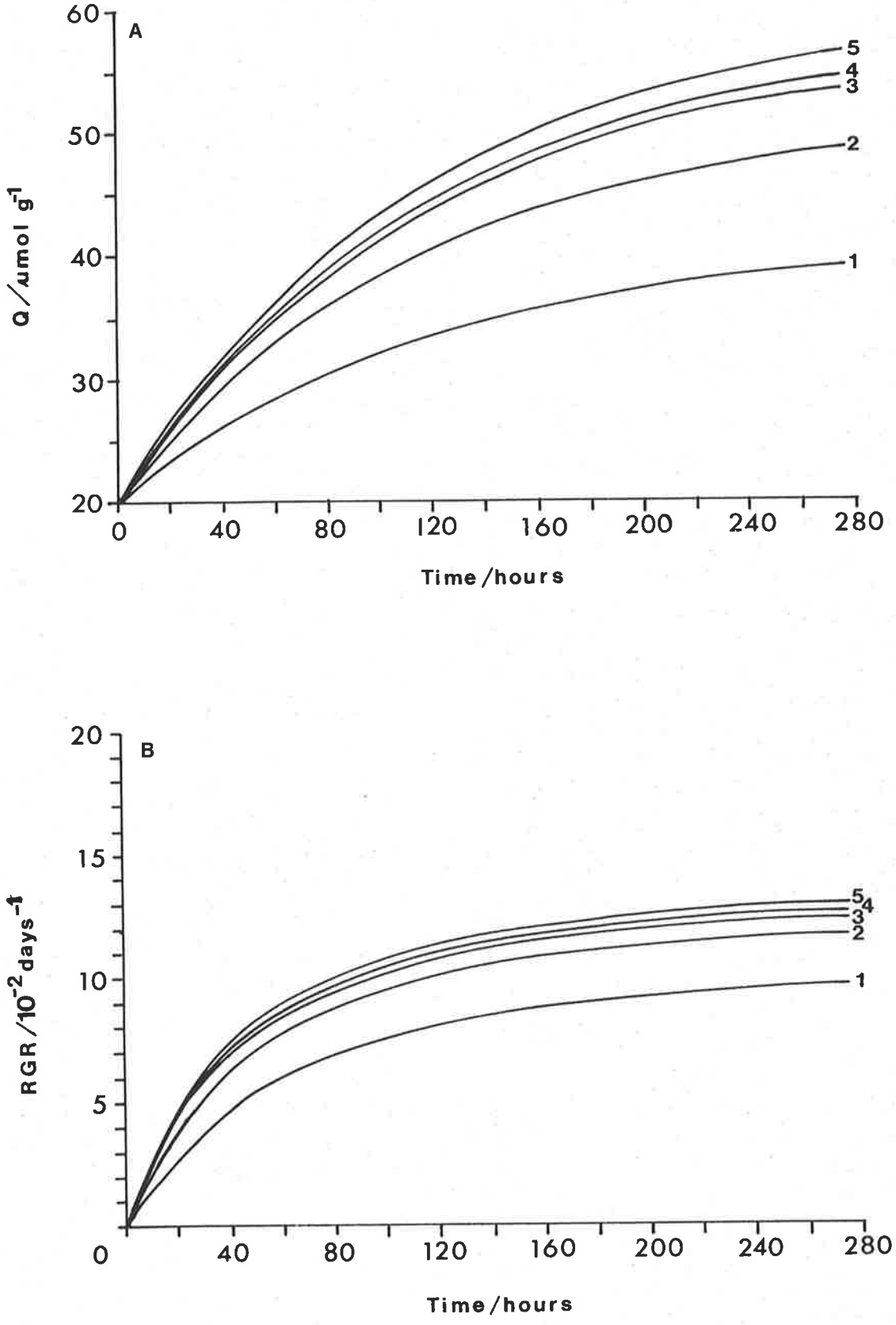

Figure 5.3. The numbers 1 - 5 represent the five growth treatments.
(A) Theoretical curves relating changes in Q for each growth treatment to time.
(B) Theoretical curves relating changes in R.G.R. to time.
Both (A) and (B) were calculated from Equations 5.5, 5.6 and 5.7, and data from Figures 5.1 and 5.2.

concentration), the plant's growth rate will decline to zero (Q = qo). The time required for the sytem to reach steady state will be dependent on the inital magnitude of Q, and the response would be the reverse of that shown in Figure 5.2.

If Equation 5.6 was rearranged to make growth rate a function of specific nutrient uptake and the specific rate of internal nutrient change,

$$\mu = V/Q - (1/Q)dQ/dt \qquad \text{Equ-5.11}$$

therefore at steady state dQ/dt is zero and the growth rate can be calculated from the specific nutrient uptake rate. At non-steady state conditions (1/Q)dQ/dt can be approximated by,

$$(1/Q)dQ/dt = \ln(Q2/Q1)/t2 - t1 \qquad \text{Equ-5.12}$$

where Q2 and Q1 are the internal nutrient concentrations at t1 and t2 respectively. However, this approximation can only be applied with any degree of accuracy to the situation when the difference between Q1 and Q2 is small (a small time period).

The aim of the following experiments was to vary the initial magnitude of Q, the dependence of growth on the measured nutrient (phosphate) and water movement to determine the validity of Equations 5.5 and 5.6.

5.2. THE EFFECT OF WATER MOVEMENT ON GROWTH RATE WHEN ALL NUTRIENTS WERE AT SUBOPTIMAL CONCENTRATIONS

5.2.1. RESULTS

The experimental method is as detailed for the two cut method in Section 2.5.3.1. The experimental and preconditioning medium was filtered seawater, which had a fresh phosphate concentration of 0.98 ± 0.10 mmol m^{-3}, and final concentration of 0.62 ± 0.14 mmol m^{-3} (n = 18, standard errors). The pH was 8.15 ± 0.01, and prior to seawater replacement, the

pH was 8.15 ± 0.03 (n = 18, standard errors). Growth-1 and Growth-5 were used for the experimental water movement treatments, to maximize the difference in D.B.L. resistance. The R.G.R. (μ) of the disks at the end of the preconditioning period was 0.095 ± 0.008 day^{-1} (Standard error). For phosphate, dQ/dt declined at -18.7 pmol g^{-1} s^{-1} during preconditioning indicating that the rate uQ was greater than V (16.9 pmol g^{-1} s^{-1} at final time period) and as a consequence Q for phosphate declined to a point where it was limiting to growth. Using Equation 5.11, μ was calculated as 0.093 (final Q for total phosphate was 32.9 μmol g^{-1}) confirming the validity of the mass balance equation, and adding additional evidence that phosphate was controlling the growth rate during preconditioning.

5.2.1.1. GROWTH RATE

Figures 5.4, 5.5 and 5.6 show that there was a significant difference in growth rate between the two water movement treatments. This difference was more marked for the change in surface area compared to the changes in either dry weight or fresh weight. There was a lag of between 6 and 9 days in the time it took for the significant difference in growth between water movement treatments to occur (Figure 5.4). The dry weight/fresh weight ratio declined with time for both treatments (Figure 5.7). Average R.G.R. in the slowest water movement treatment showed a relatively constant decline over time (Table 5.1). The average R.G.R. was calculated by taking the natural logarithm of the division of the average dry weight (for each successive time period) by the initial average dry weight, and dividing by the elapsed time in days. The Hunt program analysis for this treatment shows that growth rate peaked between days six and nine and thereafter declined to zero growth. However the growth-5 treatment had a similar growth rate (average value) for the first six days as the Growth-1 treatment, but after that its growth rate increased

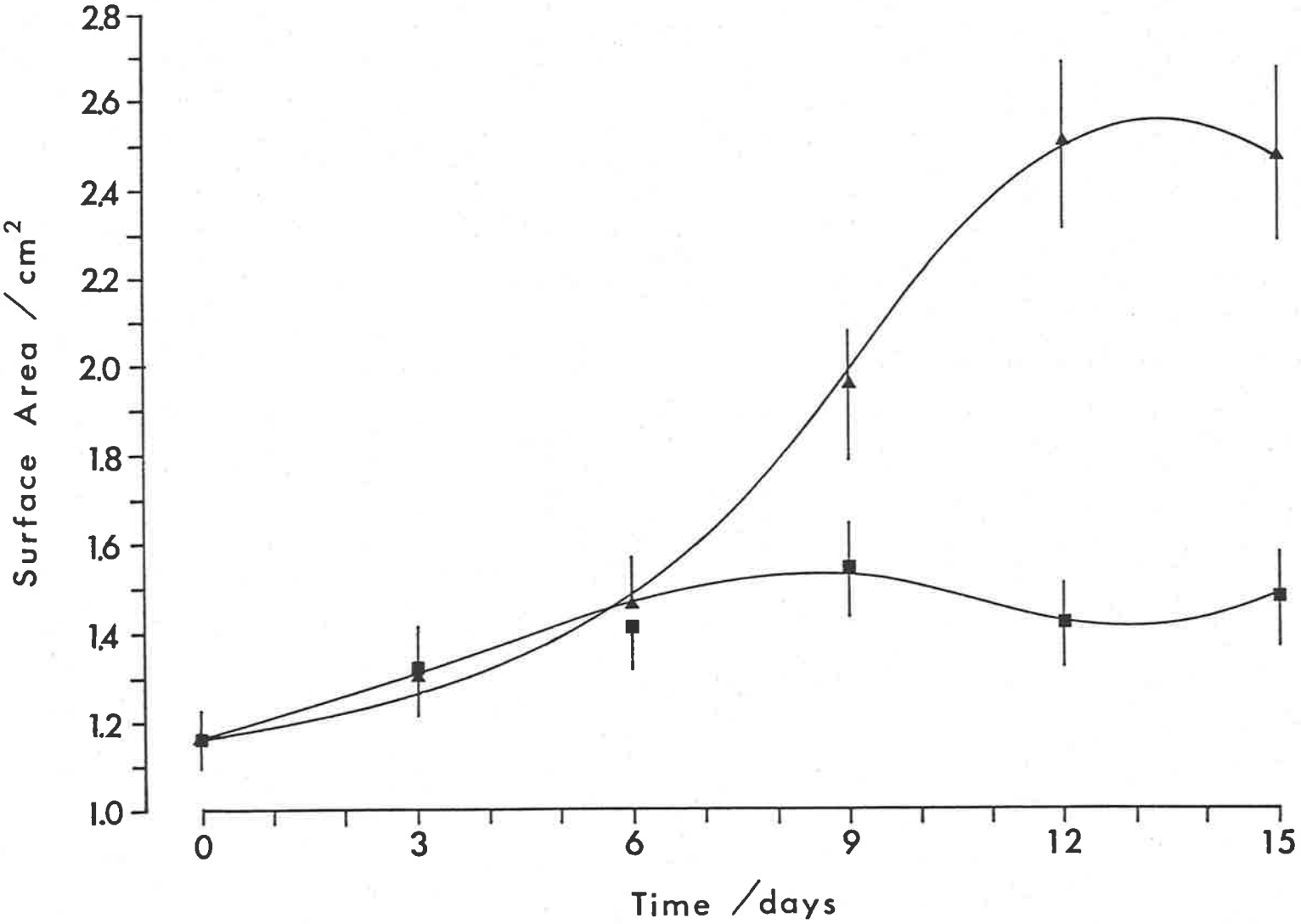

Figure 5.4. Changes in disk surface area for the Growth-1 (■) and Growth-5 (▲) treatments. Curves fitted using the Hunt program, with 1 knot (n = 15, C.L.). Note the symbols are positioned at the average raw data value and differ in some cases from the average value calculated using the Hunt program.

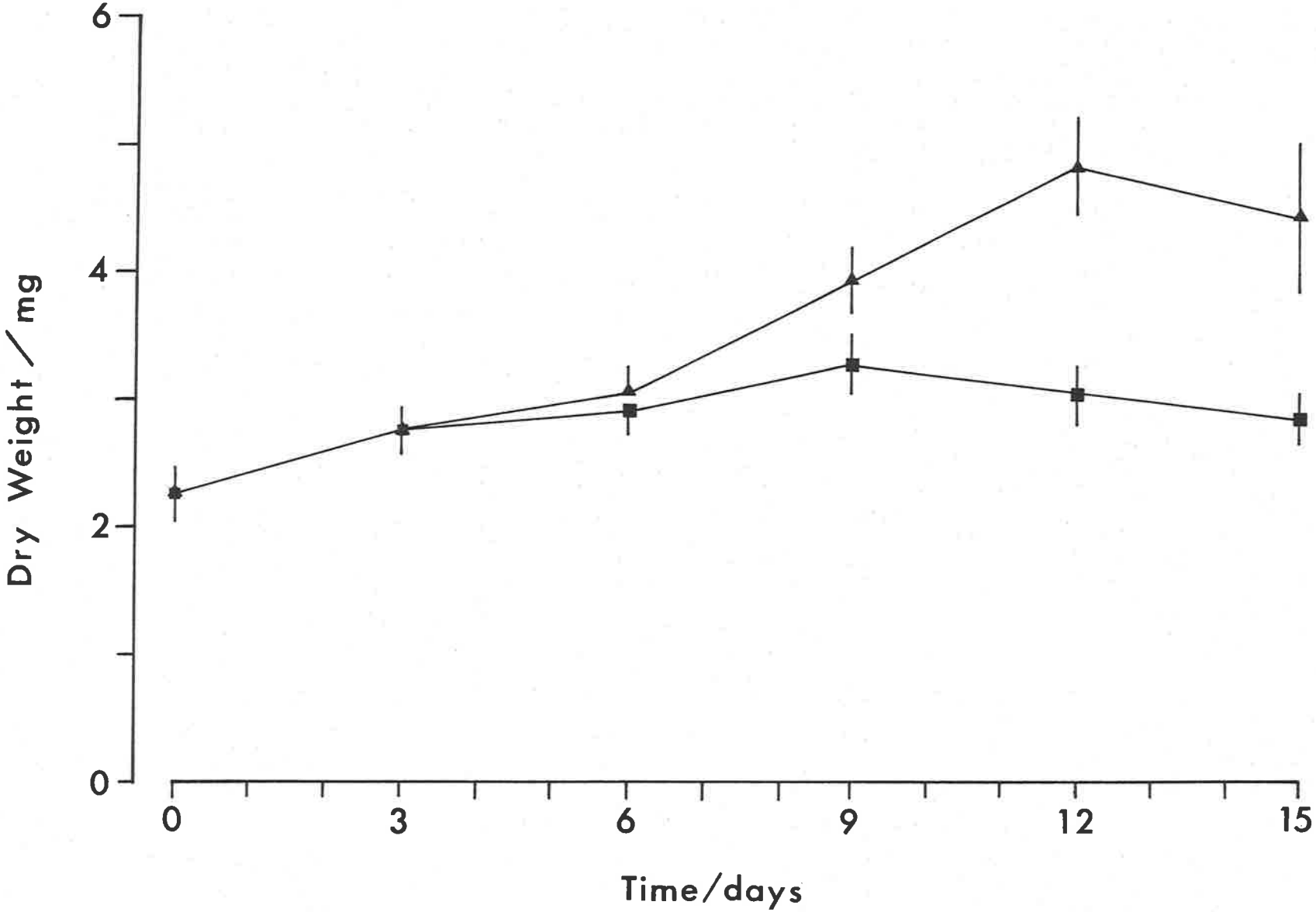

Figure 5.5. Changes in disk dry weight versus time. The symbols are the same as Figure 5.4 (Hunt program, n = 10, C.L.).

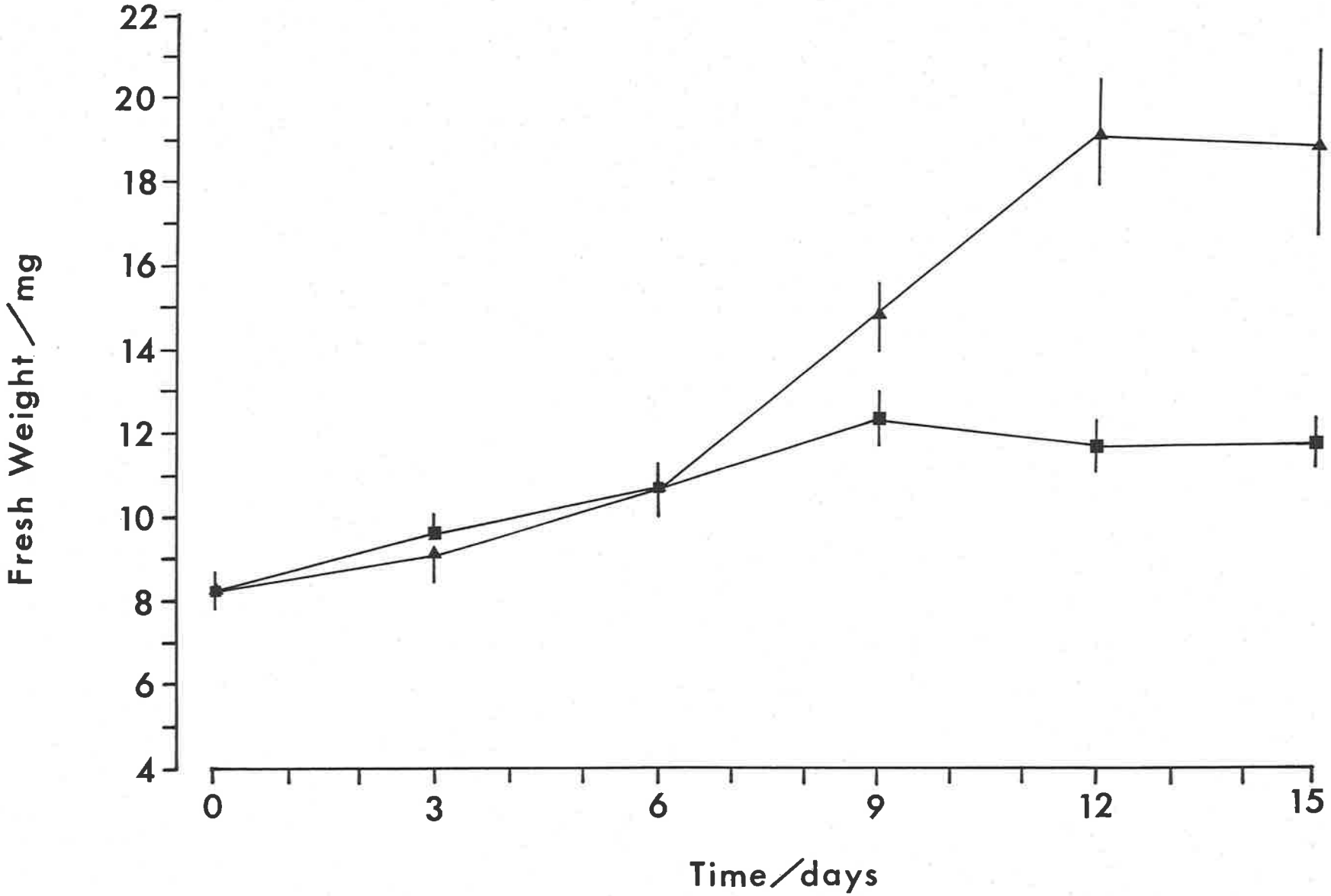

Figure 5.6. Changes in disk fresh weight versus time. The symbols are the same as Figure 5.4 (Hunt program, n = 15, C.L.).

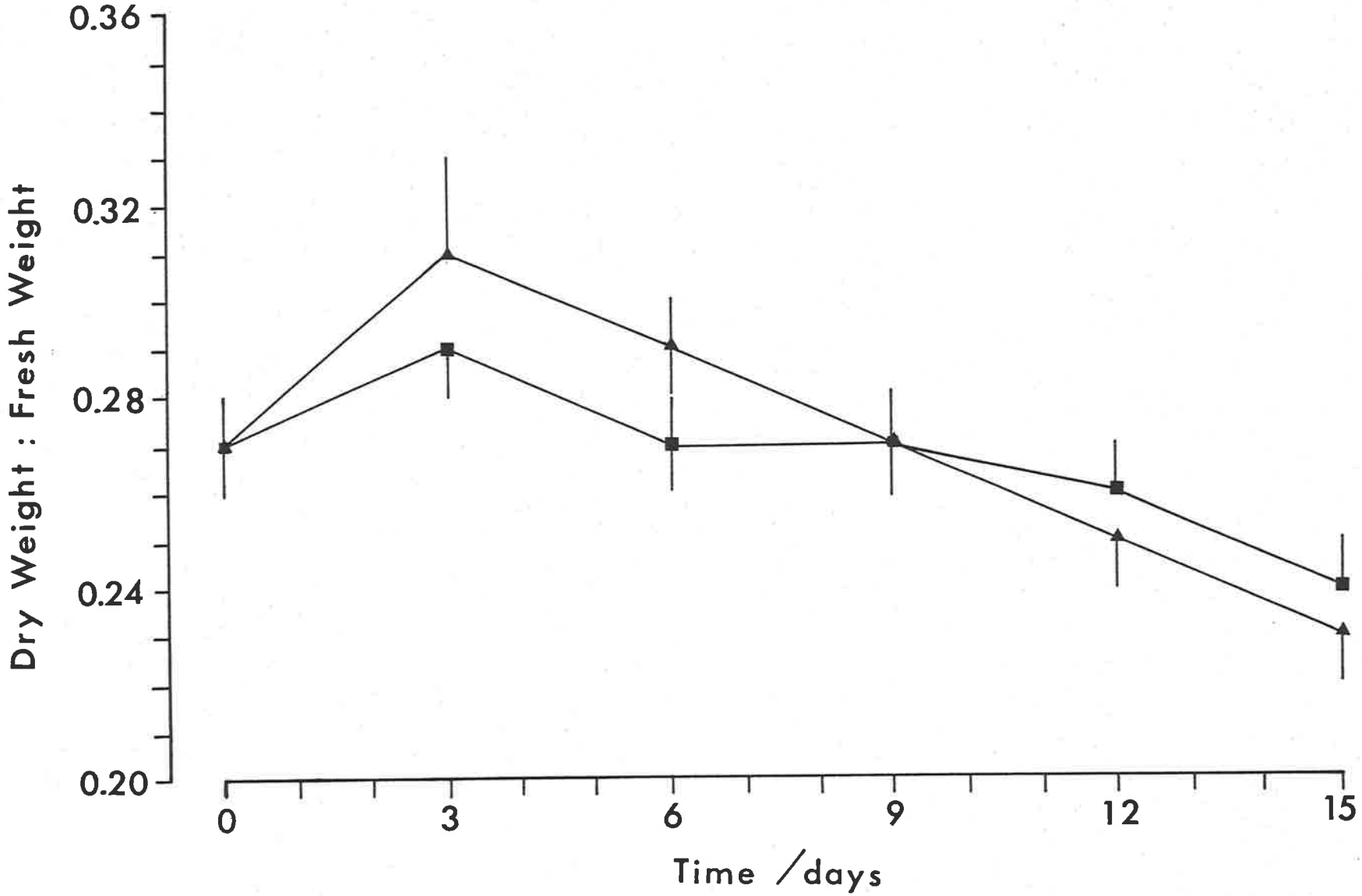

Figure 5.7. Dry weight to fresh weight ratio versus time. The symbols are the same as Figure 5.4 (Hunt program, n = 10, C.L.).

with a slight decline at the end of the experiment (Table 5.1). The instantaneous values of growth rate fitted using the Hunt program show a more variable picture, with growth rate peaking at day nine and then declining (Table 5.1).

TABLE 5.1. R.G.R. (day^{-1}) calculated using Hunt program and average values using raw data.

	Hunt Program (n =10)		Raw Data Averages	
Time days	Growth-1	Growth-5	Growth-1	Growth-5
3	0.019 ± 0.041	0.027 ± 0.044	0.050	0.050
6	0.039 ± 0.026	0.065 ± 0.024	0.038	0.041
9	0.015 ± 0.026	0.091 ± 0.025	0.036	0.056
12	-0.048 ± 0.043	0.032 ± 0.045	0.020	0.059
15	0.034 ± 0.121	-0.101 ± 0.155	0.011	0.041

(Raw data averages calculated using = $\ln(Wt/Wo)/\Delta t$, where Wt was the average dry weight at succesive time periods and Wo was the initial average dry weight at time zero)

Significantly, the results were as predicted with increasing water movement enhancing the growth rate. Also the results agree with the limited previous research on the effect of water movement on the growth rate of macroalgae (Matsumoto, 1959; Boalch, 1961; Conover, 1968; Sperling and Grunewald, 1969; Santelices, 1977; Lapointe and Ryther, 1979; Parker, 1981, 1982; Thirb and Benson-Evans, 1982; Fujita and Goldman, 1985). It has been suggested that the reponse may vary depending on the species (Conover, 1968), light intensity (Santelices, 1977; Parker, 1981, 1982) and nutrient concentration (Lapointe and Ryther, 1979; Parker, 1981, 1982; Fujita and Goldman, 1985). The results for *U. australis* indicate that when the other environmental and physical conditions were not limiting growth then the external nutrient concentration, in particular the single most limiting nutrient, will interact with the increased water movement to stimulate growth.

Figures 5.8a,b show that the predicted response of μ to Q, as shown in Figures 5.1a,b, was not observed. With a slight increase in Q for the Growth-1 treatment, μ declined, when an increase in μ would have been predicted (Figure 5.8a). A similar response occurred for the Growth-5 treatment with a greater increase in Q. Apparently for these experimental conditions growth was not related to internal phosphate concentration, but to some other limiting nutrient. Previous research has shown that for marine algae that inorganic nitrogen was most likely to limit growth when phosphate was non-limiting (Chapman and Craigie, 1977; Jackson, 1977; DeBoer, Guigli, Israel and D'Elia, 1978; Gerard, 1982a,b; Dean and Jacobsen, 1984; Smith, 1984; Fujita, 1985; Howarth and Cole, 1985). The results from the C.H.N. analysis (Table 5.2) show that the percent nitrogen per dry weight at the end of the preconditioning period was low and comparable to nitrogen limiting values measured by Fujita (range of nitrogen 1 to 3.59% dry weight for starved and non-starved *Ulva lactuca* plants respectively, 1985). DeBusk, Blakeslee and Ryther (1986) found that *Ulva lactuca* had a saturation internal concentration of nitrogen of approximately 3.5% D.W. when plants were grown in seawater with added NH_4^+. Fujita (1985) found that *Ulva lactuca* was nitrogen growth limited for C:N ratio between 13.5 and 25.

TABLE 5.2. C.H.N data for final preconditioning and experimental time period. Results expressed as % D.W.

Treatment	Carbon	Hydrogen	Nitrogen	C/N
Final preconditioning (S.E. n = 16)	32.6 ± 0.2	4.60 ± 0.16	1.82 ± 0.03	17.9
Growth-1 (S.E. n = 8)	31.4 ± 0.9	4.34 ± 0.22	1.87 ± 0.09	16.8
Growth-5 (S.E. n = 6)	31.7 ± 0.3	4.44 ± 0.10	2.90 ± 0.07	10.9

The results for the Growth-1 treatment show that the nitrogen

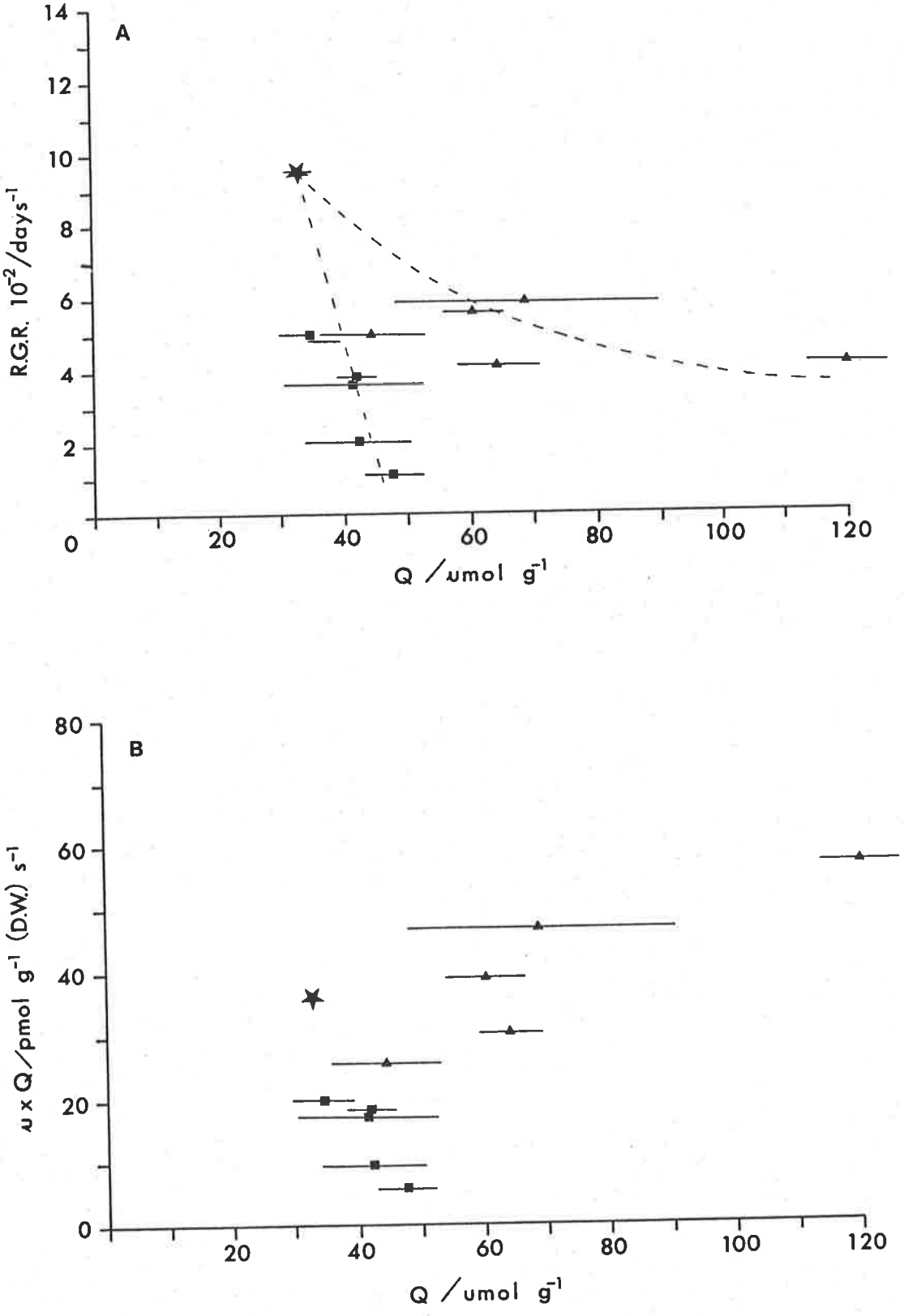

Figure 5.8. (A) Average R.G.R. (D.W.) versus Q (internal total phosphate concentration, D.W.), lines fitted by eye.
(B) Average R.G.R. times by Q (equivalent to the rate of phosphate consumption by growth) versus Q.
The symbols are the same as Figure 5.4, except ★ represents the value at time zero (n = 10, C.L.).

concentration was constant, and remains within the range at which it can limit growth (Table 5.2). The C.H.N. results for the Growth-1 treatment indicate that at the start of the experiment nitrogen was potentially growth limiting, and for the experimental duration dQ/dt for nitrogen was approximately zero; therefore with respect to nitrogen the growth was at steady state (Table 5.2). The increased water movement associated with the Growth-5 treatment results in an increase in nitrogen quota with time as would be predicted from the D.B.L. theory (Table 5.2), however initially the Growth-5 treatment would be growth limited by nitrogen. Collectively the results from the final preconditioning period, and the experimental growth (Table 5.1) and C.H.N. data (Table 5.2) indicate that under these growth conditions both inorganic nitrogen and phosphate were growth limiting. Therefore the growth rate in each treatment will respond as predicted by the multiplicative theory of growth (Kunikane, Kaneko and Maehara, 1984).

Table 5.3 shows that for the Growth-1 treatment the R.G.R. calculated using the steady state Equation 5.1 (for phosphate), was in agreement with average R.G.R, apart from the value at day 3. Also, the Growth-5 treatment attains steady state at day 12, and the two alternative measures of R.G.R. were in agreement.

TABLE 5.3. A comparison of the predicted R.G.R. using the relationship for growth at steady state ($\mu = V/Q$) versus measured R.G.R. ($days^{-1}$).

	V/Q		Raw Data Average	
Time days	Growth-1	Growth-5	Growth-1	Growth-5
3	0.009	0.099	0.050	0.050
6	0.040	0.094	0.038	0.041
9	0.030	0.072	0.036	0.056
12	0.021	0.054	0.020	0.059
15	0.021	0.058	0.011	0.041

MacFarlane (1985) found that for *Ulva rigida*, the limitations of the presence of a D.B.L. resistance on methylamine influx (analogue of ammonia) were more pronounced than for phosphate. Therefore because both inorganic nitrogen and phosphate were limiting growth in both treatments, the observed response was a combination of both the inorganic nitrogen and phosphate diffusion limitation which results in greater response to water movement than that predicted for phosphate alone.

5.2.1.2. UPTAKE

Figure 5.9 shows a significant difference in internal phosphate concentration (Q) between the two water movement treatments over time. There was a significant increase in Q for the final time period (Figure 5.9) which correlates with an increased uptake for this time period (Figure 5.10). Uptake was calculated by dividing the difference in phosphate from the initial time period by the period of growth and relating it to the surface area or dry weight at the final time period. This method assumes that uptake was constant over the 24 hour light/dark period. However previous research has shown that phosphate uptake was decreased in the dark for algae (Raven, 1974a,b; Gordon, Birch and McComb, 1981; Manley, 1985). In the dark, Raven (1974b) found that the ATP required for uptake was supplied by oxidative phosphorylation which from the research of Gordon, Birch and McComb (1981) and Manley (1985) results in a 10 to 20 percent reduction in phosphate uptake for macroalgae. This method of uptake calculation results in an average value for both the light and dark periods. Assuming that there was not a differential response to phosphate uptake in the dark between the growth treatments, this method should measure the effect of the D.B.L. resistance to phosphate uptake. However the results are difficult to compare with short term phosphate influx measurements which do not incorporate the effect of darkness on phosphate uptake.

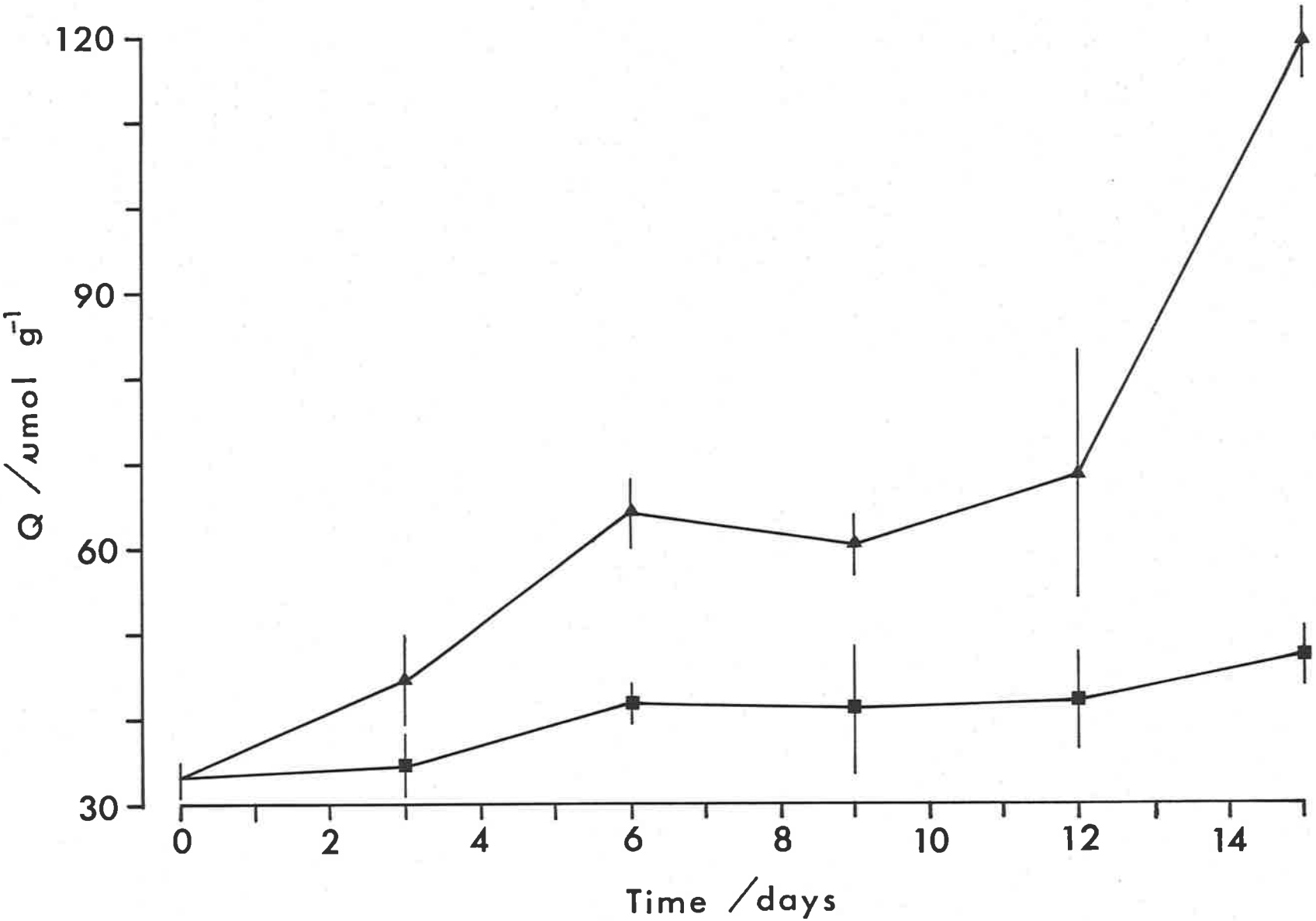

Figure 5.9. The relationship between Q (cellular total phosphate concentration, D.W.) and time. The symbols are the same as Figure 5.4 (n = 10, C.L.).

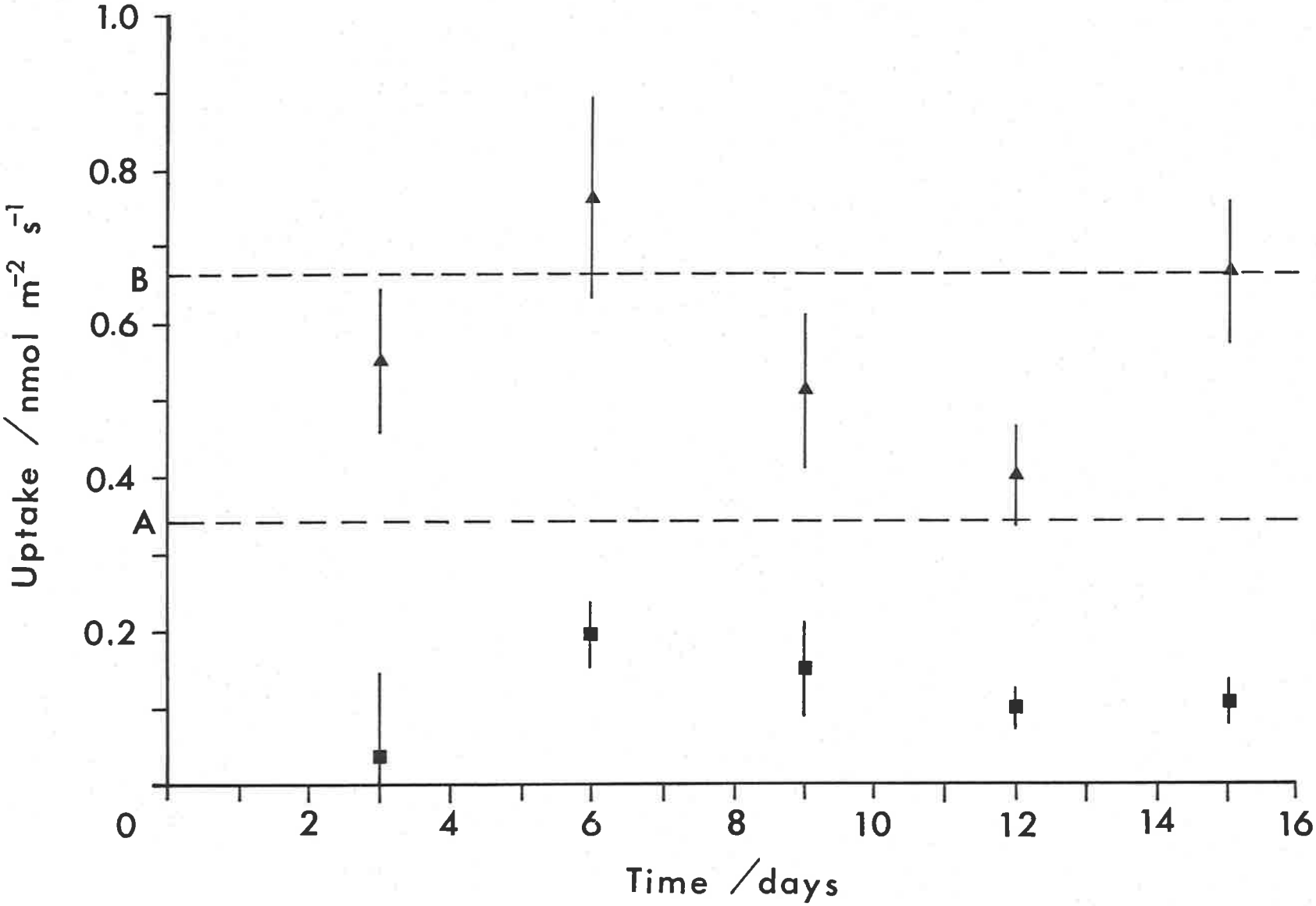

Figure 5.10. Phosphate uptake versus time (n = 10, C.L.). The parallel lines A and B represent the predicted phosphate influx calculated using the Briggs-Maskell equation for the Growth-1 and Growth-5 treatments respectively. The symbols are the same as Figure 5.4.

Figure 5.10 shows that there was a significant difference in uptake (per unit area) between the two treatments. The uptake in the Growth-1 treament was relatively constant with time, however uptake in the Growth-5 treatment varied with time, though generally showing a consistency when averaged over time. The expected uptake based on the Briggs-Maskell equation is shown in Figure 5.10, using the kinetic parameters determined from the short term experiments in Chapter 3. As predicted earlier in the previous discussion on the effects of darkness on phosphate uptake, short term influx measurements gave an overestimate of the actual uptake in the Growth-1 treatment (Figure 5.10). This effect was not so pronounced in the Growth-5 treatment. The percentage difference in uptake between the two treatments was only comparable to the predicted difference from the Briggs-Maskell equation for days nine and twelve.

5.2.2. CONCLUSION

Collectively the results show that, plants growing in seawater can be significantly influenced by variations in water movement. However, when more than one nutrient can limit growth the stimulation of growth depends on the response of individual nutrients to water movement. The magnitude of this response varies for each nutrient depending on the external transport processes.

The two cut method reduced the measurement errors of all parameters as a percentage of the mean compared to the parameter measurements in Chapter 4. This resulted from a more uniform growth material at the start of the experiment and the use of greater replication. However, the lag in growth observed in Chapter 4 was also observed for the Growth-5 treatment (Figure 5.4), indicating that this lag affect probably can be attributed to the physical damage and trauma caused to the peripheral cells of the disk when cut. Therefore the lag time constitutes the time required to

overcome the initial wounds on being cut. This lag response was not apparent in the Growth-1 treatment, most likely because its growth rate was being influenced to an equivalent or greater extent by nutrient limitation.

The next section examines the effect of water movement on growth when only one nutrient (phosphate) limits growth.

5.3. THE EFFECT OF WATER MOVEMENT ON GROWTH RATE : PLANTS PRECONDITIONED IN A.S.W. AT OPTIMAL NUTRIENT CONCENTRATIONS MINUS PHOSPHATE

5.3.1 RESULTS

The experimental method used was the two cut method.The two water movement treatments were Growth-1 and Growth-5. The disks were preconditioned in the Growth-5 water movement chamber. A.S.W. was used for both the preconditioning and experimental periods. During preconditioning Hoagland's solution minus phosphate was added as described in Section 2.2.4.. The experimental medium was the same as used for preconditioning except that phosphate was added to give a final concentration of 1 mmol m^{-3}. This concentration was chosen as previous experiments had shown that significant growth occurred while phosphate was still growth limiting. The pH was 8.20 initially and 8.28 ± 0.03 (S.E.) prior to replacement. The reasoning behind using A.S.W. for the experiment was that it allowed for a more controlled experimental medium and therefore all nutrient concentrations were controlled.

The average R.G.R. for the preconditioning period was 0.107 day^{-1}. Phosphate concentration declined at a rate (dQ/dt) of -31.9 pmol g^{-1} s^{-1}, and the final value of Q for phosphate was 29.68 µmol g^{-1} (D.W.).

5.3.2. GROWTH

Figures 5.11 and 5.12 show a significant difference in growth between the two treatments. The growth response to increased water movement was more pronounced when measured on a surface area basis (Figure 5.11) than compared to the dry weight results (Figure 5.12). The average R.G.R was approximately constant in the Growth-5 treatment, but the Growth-1 treatment showed an initial lag in growth rate and a decline for the last time period (Table 5.4). The Hunt program shows a similar trend in R.G.R. for the two treatments. One of the problems associated with the Hunt program was that for short duration experiments with few time intervals and variable growth rate discontinuities could not be smoothed out without predicting a large error. The reason for this was that the program was not subjective in its response to the variable growth rate and attempts to fit as few changes in growth rate as possible to the data.

TABLE 5.4. R.G.R. (day^{-1}) calculated using the Hunt program or average method based on initial time period dry weight.

	Hunt Program (n = 10)		R.G.R. Raw Data Averages	
Time (d)	Growth-1	Growth-5	Growth-1	Growth-5
2	0.020 ± 0.047	0.084 ± 0.046	0.006	0.055
4	0.038 ± 0.046	0.066 ± 0.029	0.023	0.069
6	0.047 ± 0.137	0.037 ± 0.045	0.032	0.062
8	-0.145 ± 0.380	0.088 ± 0.135	0.017	0.061

Results from the C.H.N. analysis are summarized in Table 5.5. These indicate that for the experimental duration nitrogen was within the range previously predicted where growth rate is not limited. This is based on the C/N ratios. The measured nitrogen values for the Growth-1 treatment were less than those for the Growth-5 treatment for all but one of the time periods (day 4). Thus the response to water movement variation in

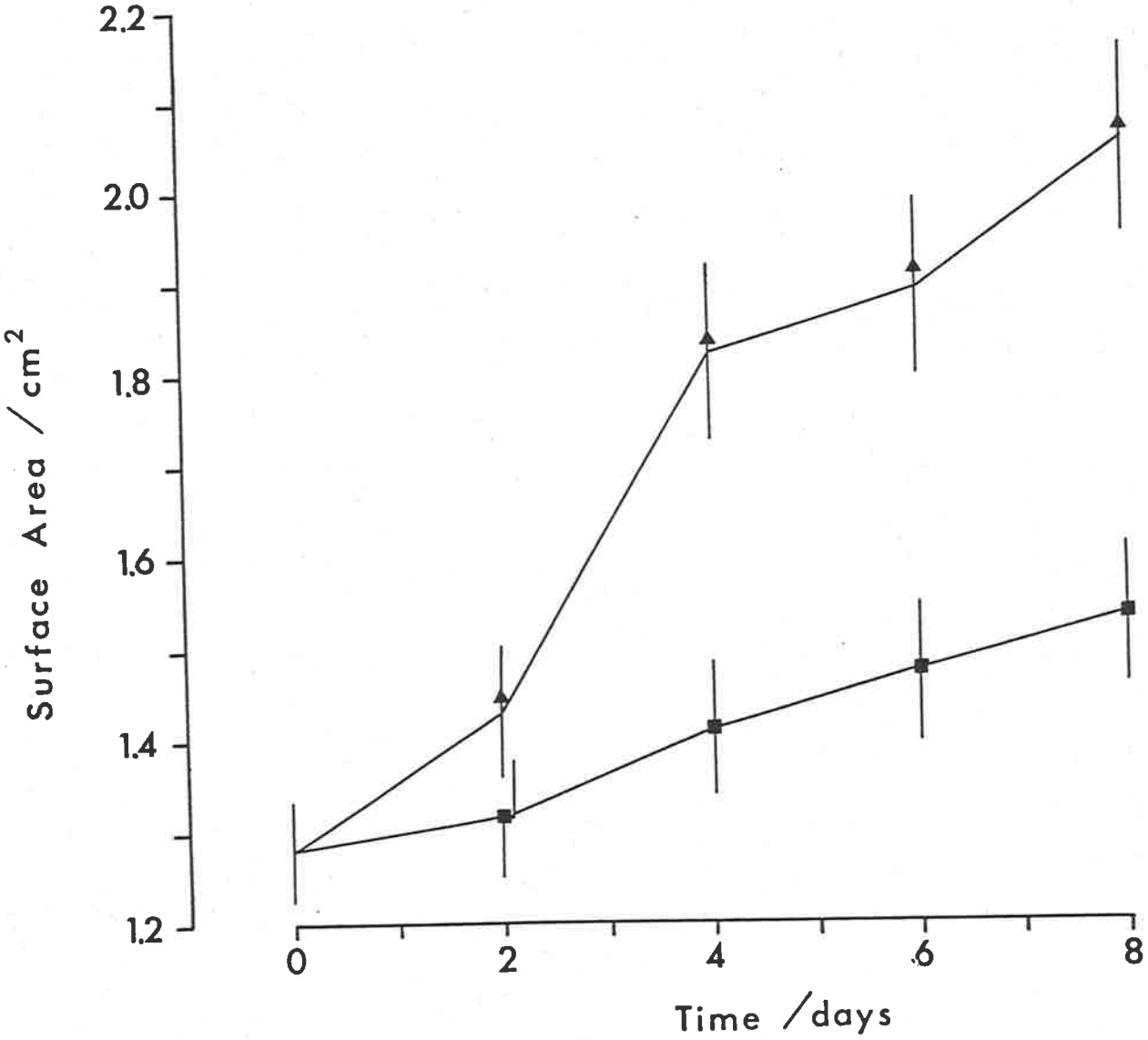

Figure 5.11. The relationship between disk surface area and time for the Growth-1 (■) and Growth-5 (▲) treatments (Hunt program, n = 15, C.L.).

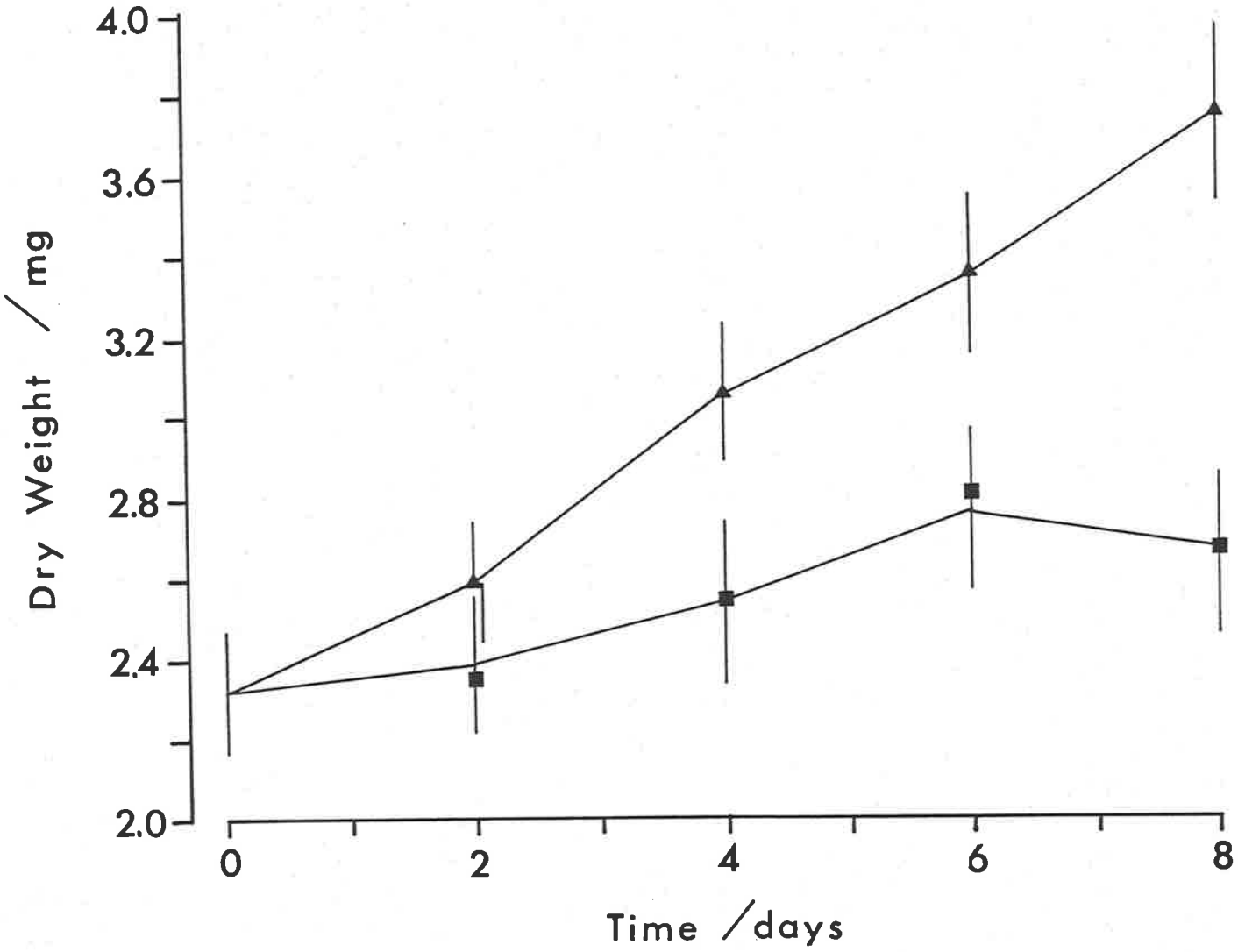

Figure 5.12. Changes in disk dry weight versus time. The symbols are the same as Figure 5.11. (Hunt program, n = 10, C.L.).

TABLE 5.5. C.H.N. data, results expressed as % D.W. (Standard errors, n = 5).

Treatment	Time (d)	Carbon	Hydrogen	Nitrogen	C/N
Final Precondition	0	32.2 ± 0.9	4.47 ± 0.07	2.98 ± 0.12	10.8
Growth-1	2	32.7 ± 0.3	4.76 ± 0.05	3.05 ± 0.04	10.7
Growth-5	2	32.9 ± 0.3	4.73 ± 0.04	3.74 ± 0.08	8.8
Growth-1	4	32.7 ± 0.5	5.19 ± 0.19	3.58 ± 0.14	9.1
Growth-5	4	31.8 ± 1.0	4.64 ± 0.08	3.58 ± 0.07	8.9
Growth-1	6	31.5 ± 0.3	4.68 ± 0.06	3.34 ± 0.04	9.4
Growth-5	6	32.5 ± 1.1	4.29 ± 0.13	4.28 ± 0.18	7.6
Growth-1	8	31.8 ± 0.5	4.64 ± 0.05	3.76 ± 0.10	8.5
Growth-5	8	32.6 ± 0.3	4.76 ± 0.04	4.11 ± 0.07	7.9

the two treatments resulted in a differential ability to take up nitrogen even when it was not predicted to be growth limiting. This was in agreement with the response predicted by the D.B.L. theory. The ecological implication was that when nitrogen does become limiting to growth the increased nitrogen accumulation attributed to the faster water movement treatment will delay for a longer period any growth reductions.

Figure 5.13a shows that the total chlorophyll per disk doubles within the Growth-5 treatment, however on a concentration basis it was relatively constant (Figure 5.13b). The Growth-1 treatment results show a decline in total chlorophyll on both a per disk basis and per gram fresh weight (Figures 5.13a,b). Collectively the C.H.N. and total chlorophyll results indicate no correlation between increasing nitrogen and chlorophyll. For example the large increase in total chlorophyll (per disk and per g fresh weight) between days two and four for the Growth-5 treatment was associated with a decline in the nitrogen concentration (Table 5.5, Figure 5.13a,b). This contradicts the previous assertion made in Chapter 4 that nitrogen can be stored as pigments.

The experimental results presented in this section indicate, given the low phosphate concentration at the start of the experiment, that the growth rate was being controlled by a single limiting nutrient, namely phosphate. This was confirmed by plotting R.G.R versus Q for phosphate (Figure 5.14a). This conforms to the predicted shape of the Droop model of internal nutrient control of growth for a single limiting nutrient (Equation 5.4). A plot of R.G.R. Q (μQ) versus Q also shows a straight line with the slope, equivalent to μmq, equal to 0.139 day^{-1}, and intercepts the X-axis (qo) at 32.7 $\mu mol\ g^{-1}$ (r^2 = 0.90, Figure 5.14b). Figure 5.14a also shows the fit of Equation 5.4 using the values of μmq and qo derived from Figure 5.14b. At the lower values of Q there was a greater discrepancy between the fit which was associated with the values measured from the Growth-1 treatment, in comparison the Growth-5 results were a comparatively good fit to the predicted response.

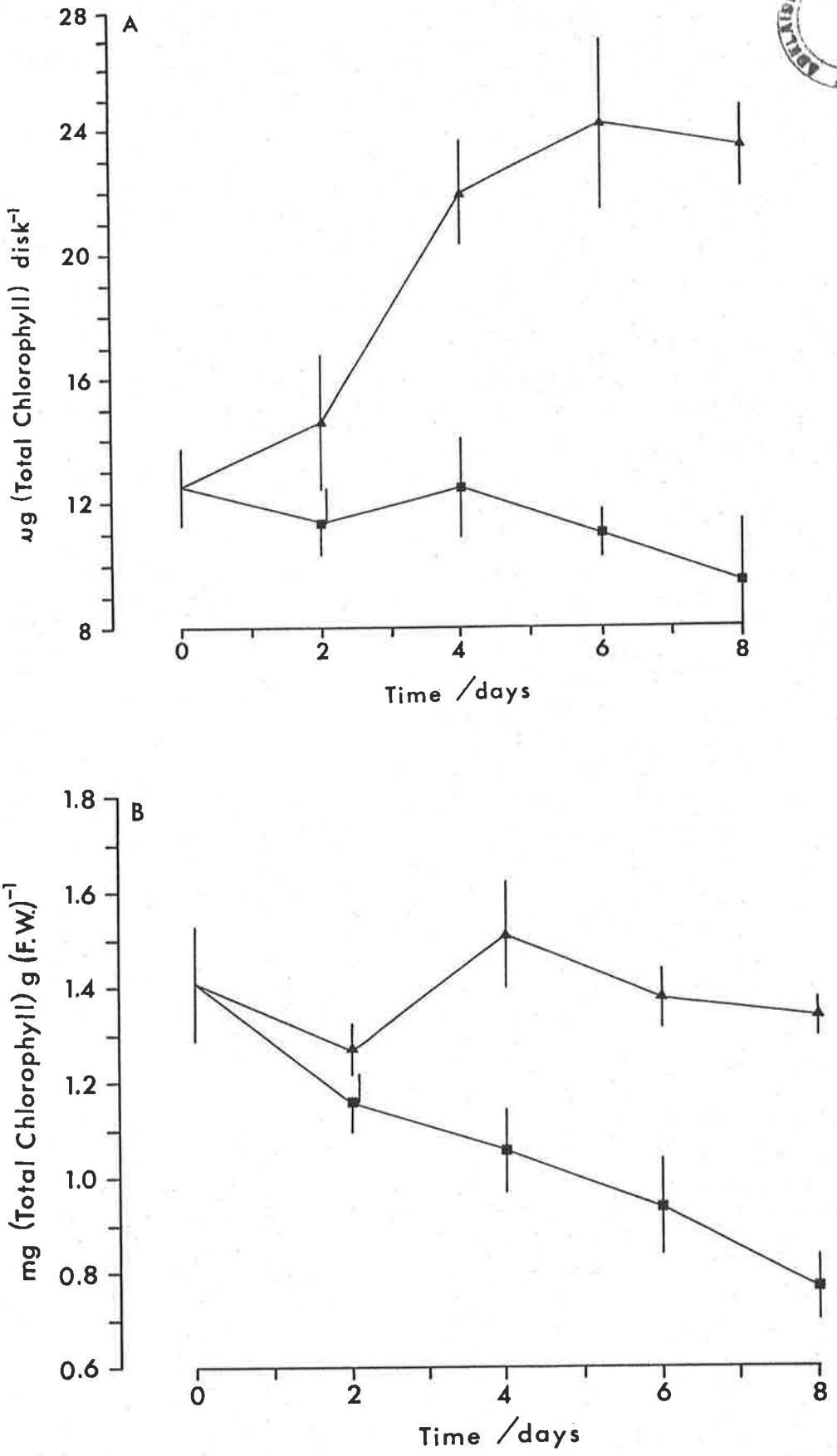

Figure 5.13. (A) Changes in total chlorophyll per disk with time.
(B) Total chlorophyll concentration versus time.
The symbols are the same as Figure 5.11 (n = 5, C.L.).

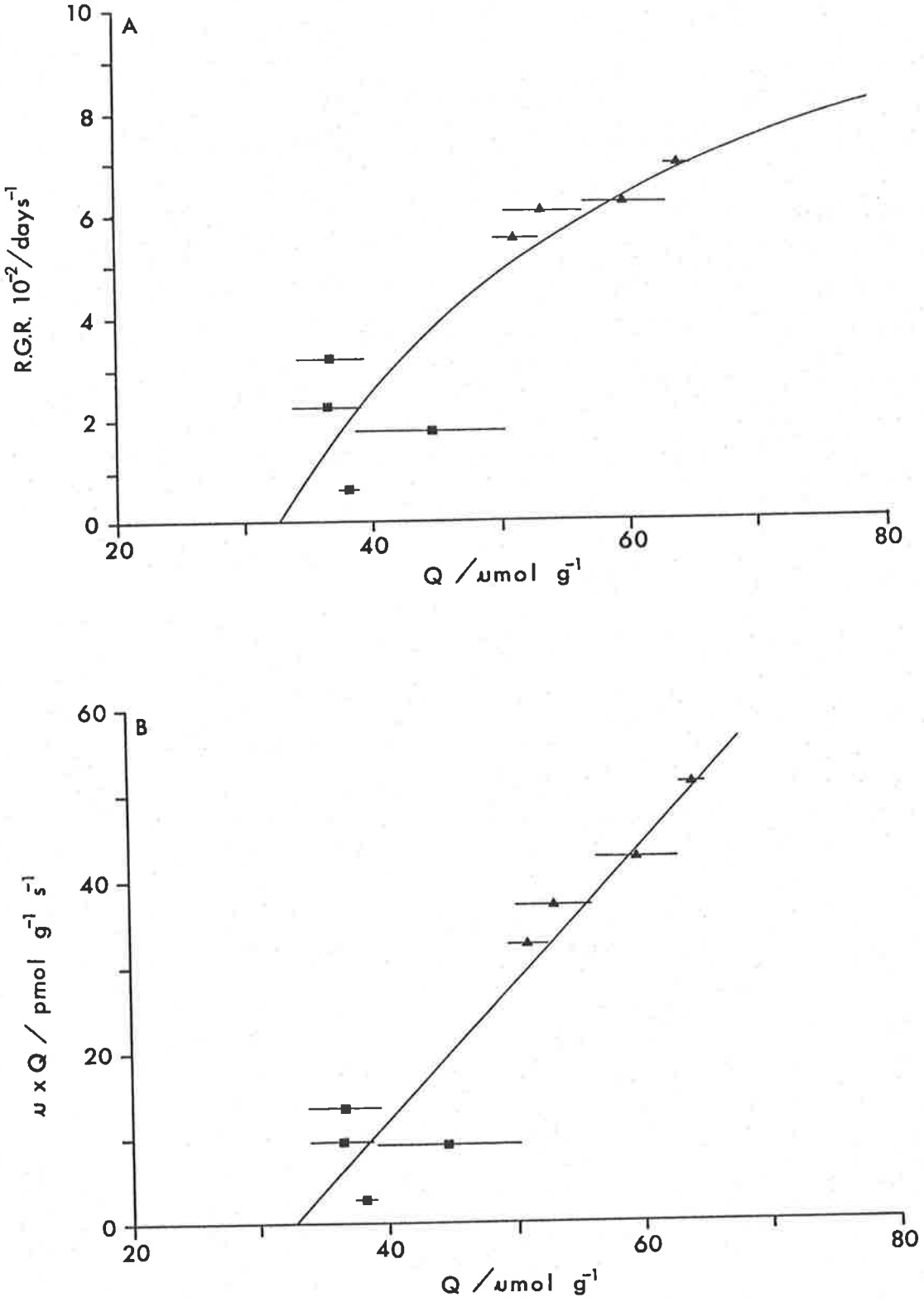

Figure 5.14. (A) The relationship between average R.G.R. (D.W.) and Q (internal total phosphate concentration, D.W.). Curve fitted using Equation 5.4 (Droop growth equation) and the parameters calculated in (B) below.
(B) R.G.R.xQ versus Q. Fitted line calculated by linear regression (slope (µmq) = 0.139 day^{-1} and the X-axis intercept (qo) = 32.7 µmol g^{-1} D.W.)

Using Equations 5.5, 5.6 and 5.7 it was possible to predict the response to water movement for the two treatments. Figure 5.15 shows that the predicted change in dry weight with time was an approximate fit for both treatments. Because the initial experimental value of Q was lower than the calculated qo this situation equates with the outcome predicted from Equation 5.6 for $V > \mu Q$. Initially the growth rate is zero according to the model and as dQ/dt increases in relation to V, the growth rate progressively increases until equilibrium is established between μQ and V. At this time according to Equation 5.11, $V/Q = \mu$ and the system is at steady state. The model predicts that this time period is reached asymptotically and occurs approximately after 15 days. Table 5.6 shows that the system did not reach steady state (μ does not equal V/Q). The model predicts the constant decline in V/Q, which will reach equilibrium with μ when the μ was approximately 0.057 and 0.080 day^{-1} for the Growth-1 and Growth-5 treatments respectively.

TABLE 5.6. Comparison of μ calculated from the changes in dry weight and from the measured uptake and quota.

	V/Q		R.G.R. Raw Data Averages	
Time (d)	Growth-1	Growth-5	Growth-1	Growth-5
2	0.134	0.257	0.006	0.055
4	0.063	0.166	0.023	0.069
6	0.059	0.111	0.032	0.062
8	0.057	0.084	0.017	0.061

5.3.3. UPTAKE

Figure 5.16 shows that there was a significant difference in Q for phosphate between treatments with time, but the difference was decreased at the final time period. The rate dQ/dt (slope) was initially constant, for the Growth-5 treatment peaks at day four and thereafter a negative

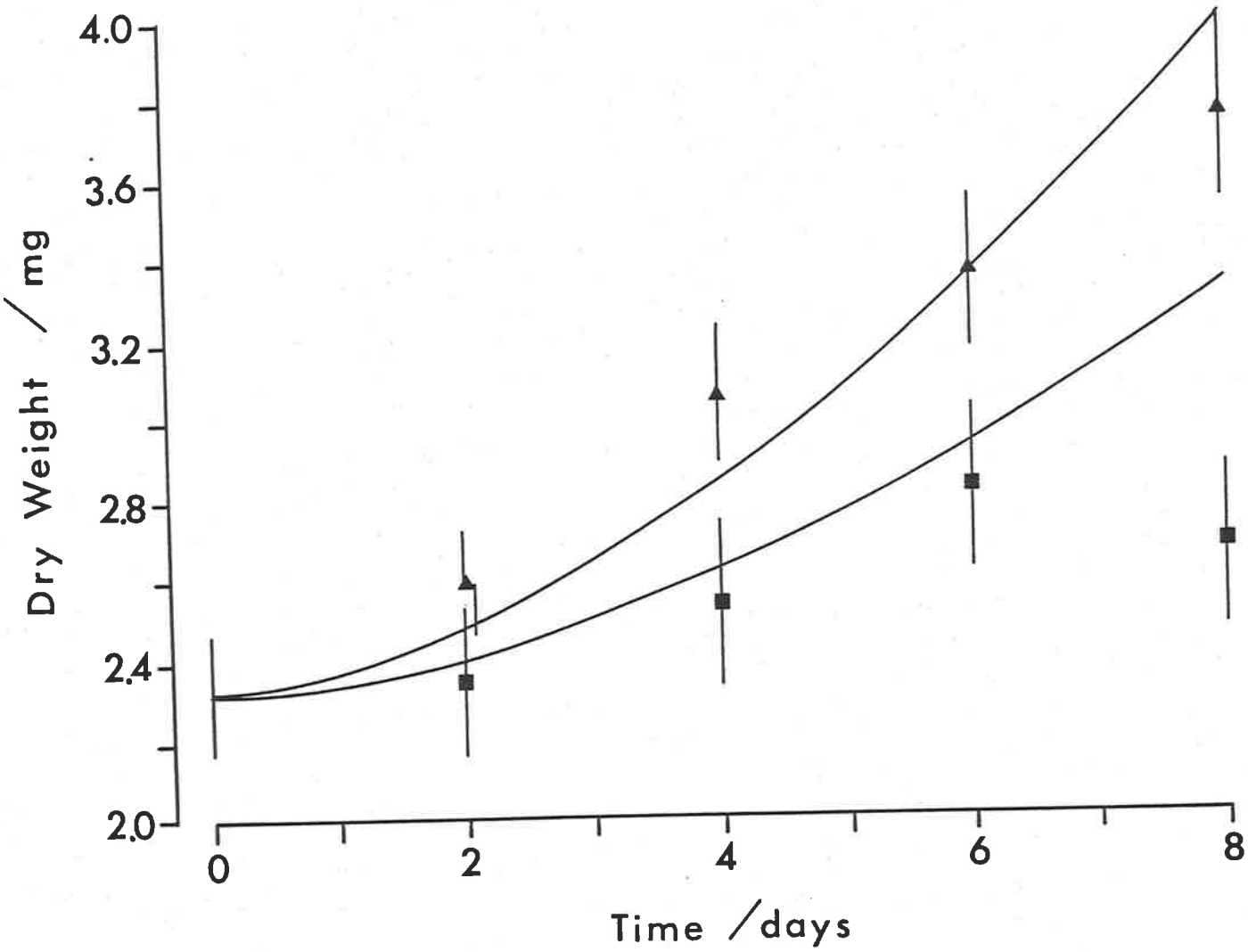

Figure 5.15. The relationship between the raw data averages (n = 10, C.L. from Figure 5.12) and the predicted changes in dry weight calculated using Equations 5.5, 5.6 and 5.7 (Top curve is the Growth-5 treatment and the bottom curve is the Growth-1 treatment). The symbols are the same as Figure 5.11.

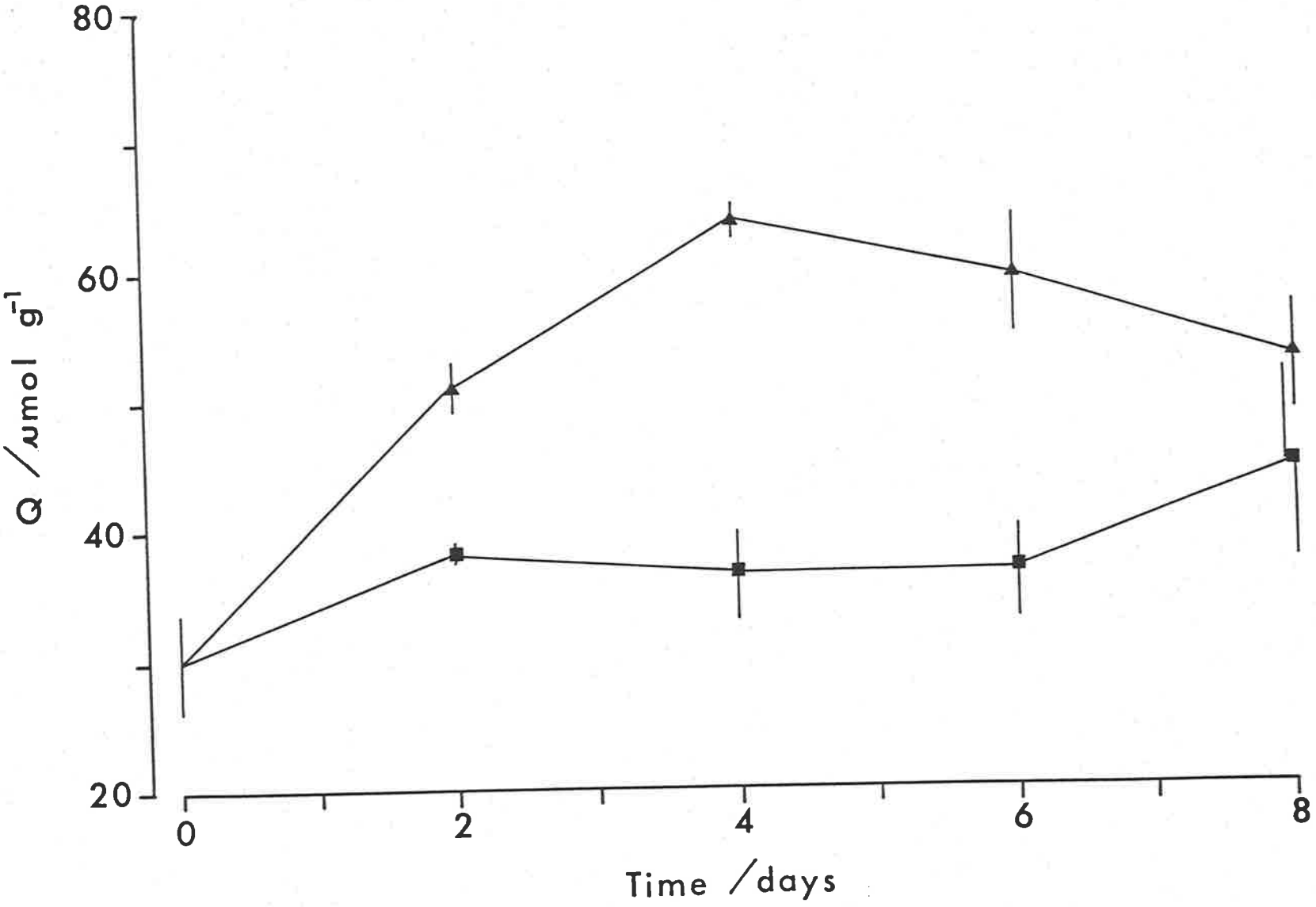

Figure 5.16. Internal total phosphate concentration (Q, D.W.) versus time (n = 10, C.L.). The symbols are the same as Figure 5.11.

rate was observed (Figure 5.16). The rationale for this response was that initially uptake (V) was greater than the rate of phosphate usage by growth (μQ), which after day four was reversed. The model for dQ/dt, from Equation 5.6, predicts the decline in dQ/dt with time. However, the lower asymptote value according to the model would be zero when equilibrium was established, and this was contrary to the observed results (Figure 5.16) of treatment Growth-5. A possible explanation for this decline comes from the calculated uptake rate for each treatment with time. Figure 5.17 shows that in both treatments there was a decline in uptake with time, although this was less pronounced in the Growth-1 treatment, being restricted to the first time period only. Considering the constant external concentration of phosphate this suggests that the increasing internal phosphate concentration was in some way having a negative feedback effect on phosphate uptake.

Figure 5.18 shows that uptake calculated on a dry weight basis, has no significant trend with Q. There was a general trend for an increase in uptake with increasing Q. This however ignores the previous internal phosphate concentration, as uptake was averaged over the time period and Q represents the concentration of phosphate at the end of each time period. This was better represented by Table 5.7, which shows that the high uptake correlates with the initial low Q at the end of the preconditioning period. For the Growth-5 treatment, where the most dramatic uptake response occurred, the uptake declined by one third with time as Q increased.

The influx predicted from the Briggs-Maskell equation for [Pi]b equal to 1 mmol m^{-3}, was 38 pmol g^{-1} s^{-1} and 74 pmol g^{-1} s^{-1} for Growth-1 and Growth-5 respectively (Vm = 220 pmol g^{-1} s^{-1}, Km = 1.5 mmol m^{-3} data from Chapter 3). Table 5.7 shows that the maximum uptake for the Growth-5 treatment was twice that predicted from the influx experiments. Also, Growth-1 showed a similar large maxima compared to the influx results.

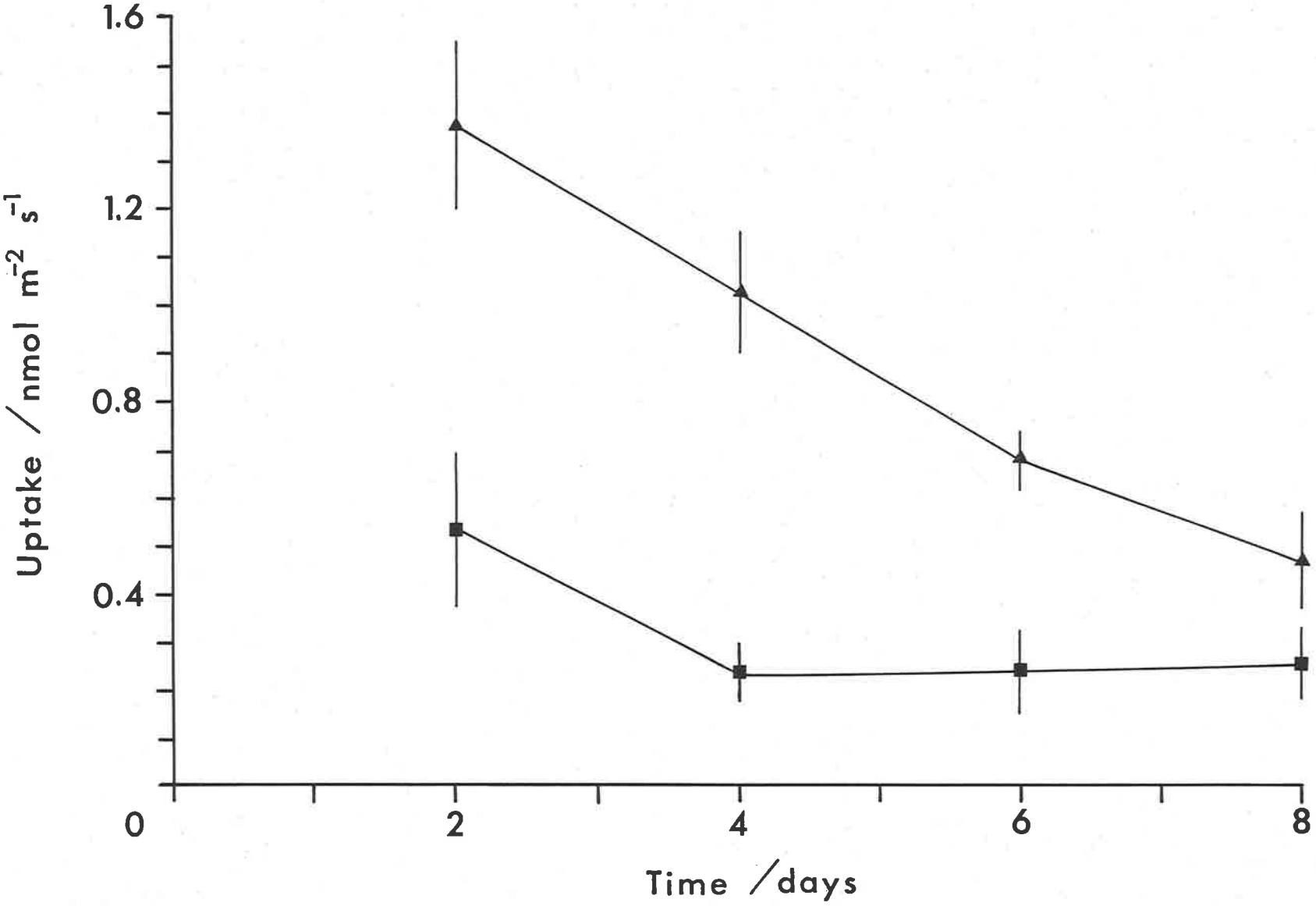

Figure 5.17. Phosphate uptake versus time (n = 10, C.L.). The symbols are the same as Figure 5.11.

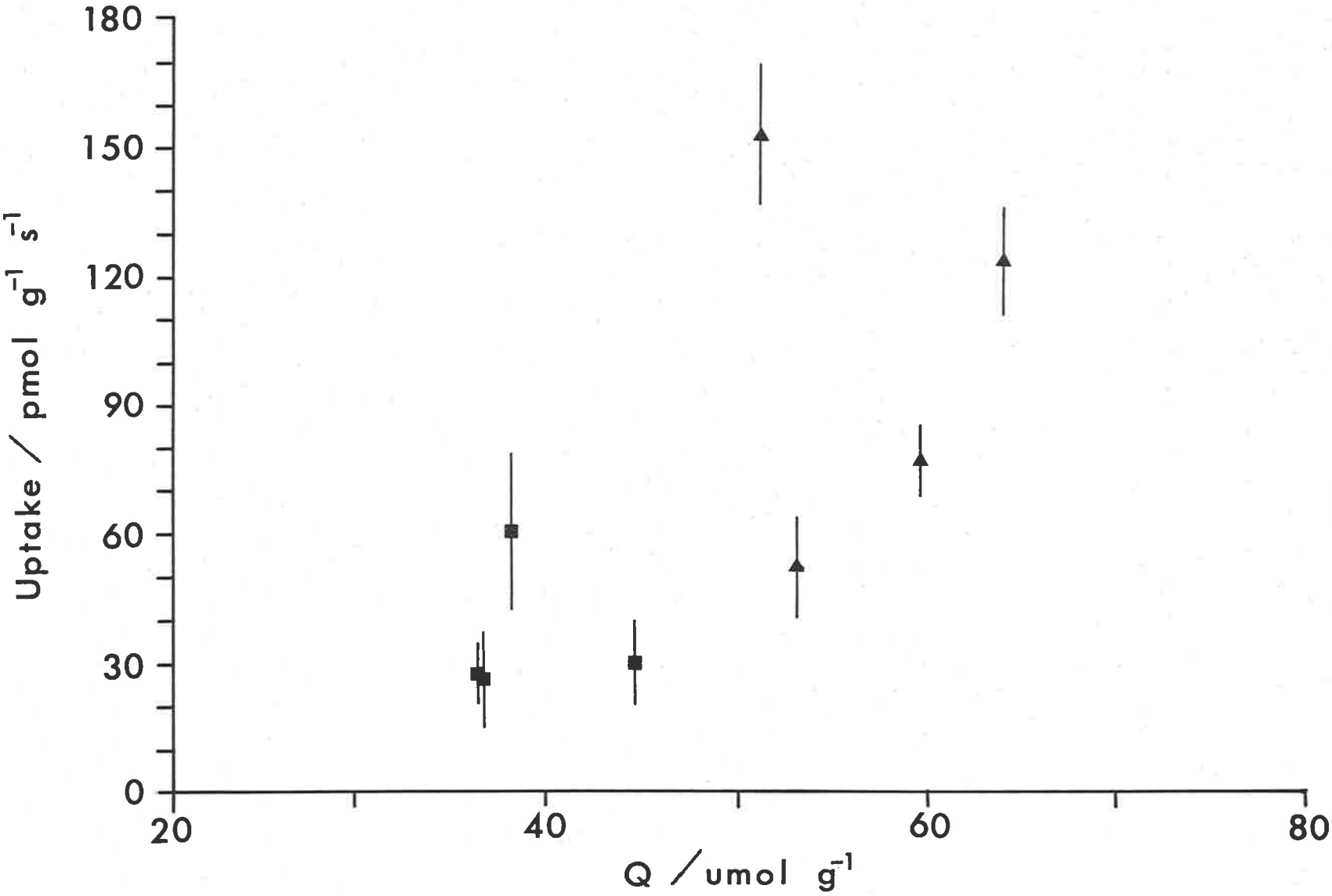

Figure 5.18. The relationship between phosphate uptake (calculated on a D.W. basis) and internal total phosphate concentration (Q, D.W.). The symbols are the same as Figure 5.11 (n = 10, C.L.).

TABLE 5.7 Comparison of phosphate uptake measured per unit area and per unit weight, and internal phosphate concentration (Q, errors are 95% confidence limits).

Treatment	Time (d)	Uptake (area) nmol m^{-2} s^{-1}	Uptake (D.W.) pmol g^{-1} s^{-1}	Q µmol g^{-1}
Final Precondition	0	negligible uptake, [Pi]b = 0		29.68 ± 2.6
Growth-1	2	0.54 ± 0.16	59.57 ± 19.0	38.16 ± 0.3
Growth-5	2	1.37 ± 0.18	152.12 ± 17.7	51.07 ± 1.4
Growth-1	4	0.24 ± 0.07	26.50 ± 7.5	36.49 ± 2.5
Growth-5	4	1.03 ± 0.13	122.88 ± 12.6	63.87 ± 0.8
Growth-1	6	0.24 ± 0.10	25.24 ± 11.2	36.49 ± 2.8
Growth-5	6	0.68 ± 0.09	76.49 ± 8.8	59.55 ± 3.1
Growth-1	8	0.26 ± 0.08	29.40 ± 9.6	44.65 ± 5.3
Growth-5	8	0.47 ± 0.11	51.60 ± 11.8	53.10 ± 2.9

Table 5.7 also shows that the uptake declined to a value below that predicted by the Briggs-Maskell equation.

This explains the variation observed in the fit of the model for Equations 5.5, 5.6 and 5.7 as shown in Figure 5.15. The model assumed that the influx results of Chapter 3 could be used to predict the rate of uptake with growth. The initial high growth rate in the Growth-5 treatment (Figure 5.15) correlates with the higher than predicted phosphate uptake. Previous research has shown that algae starved of nitrogen or phosphate display an increased short term affinity for the limiting nutrient (Rhee, 1973; Chen, 1974; D'Elia and DeBoer, 1978; Gotham and Rhee, 1981; Ryther, Corwin, DeBusk and Williams, 1981; Probyn and Chapman, 1982; Parslow, Harrison and Thompson, 1984a,b, 1985; Fujita, 1985; Thomas and Harrison, 1985). This increased affinity for phosphate when the plants were starved of phosphate interacts with the model proposed for the equilibrium between the D.B.L. uptake and growth.

5.3.4. CONCLUSION

The main point made was that the growth of phosphate starved plants could be modelled using the Droop equation (Equation 5.4). A model between the interaction of the D.B.L., uptake, internal concentration and growth gave an approximate fit to the observed results. However, this model needed to be modified to take into account the interaction between the internal limiting nutrient concentration and the variation in uptake kinetics. A further point was that it was difficult to model the interaction of the physical and metabolic factors without a complete understanding of how they interact.

Logistically, the use of A.S.W. for growth experiments was difficult because of the large volume required (approximately 300 litres), therefore it was restricted in its use to only a limited number of growth experiments. Nevertheless, the results have shown that by manipulating the nutrients it was possible to make phosphate the single limiting nutrient. This can also be achieved using seawater.

The next section examines the possibility of growth limitation by carbon.

5.4. THE EFFECT OF WATER MOVEMENT ON GROWTH RATE: PLANTS PHOSPHATE STARVED AND BUBBLED WITH CO_2

5.4.1. RESULTS

Disks were preconditioned in seawater with Hoagland's minus phosphate. Four growth chambers and two water movements (Growth-1 and Growth-5) were used for the experiment, and disks were also grown in Growth-5 for pretreatment. For each water movement chamber one was bubbled with air as usual while the other was bubbled with air plus a 1% CO_2 air mixture. Total inorganic carbon in the CO_2 unenriched medium was 2.2 ± 0.04 mol m^{-3}, and in the CO_2 bubbled medium it was 2.5 ± 0.2

mol m^{-3} (S.E., see Section 2.2.6. for methods). Additional buffer was added to each treatment using 10 mol m^{-3} TAPS (Zwitterionic buffer, pKa 8.4 at 25°C) to compensate for the acidifying effect of the additional CO_2. Initially pH was 8.24 ± 0.07 and [Pi]b was 0.37 ± 0.09 mmol m^{-3}, prior to seawater replacement the pH was 8.30 ± 0.11 and [Pi]b was 0.17 ± 0.12 mmol m^{-3} (S.E.). Essentially the experiment and preconditioning conditions were set up to make phosphate the single growth limiting nutrient.

5.4.2. CO_2 EFFECT ON GROWTH STIMULATED BY WATER MOVEMENT

Figure 5.19 shows that there was a significant difference in growth between the water movement treatments for the final two time periods. It also shows that the addition of CO_2 did not stimulate the growth rate for each water movement treatment. A similar response was observed for growth measured as dry weight increases Figure 5.20, although the response was not as significant as that observed in Figure 5.19. The initial internal concentration of phosphate was 30.1 ± 2.3 µmol g^{-1} (D.W.) and by day eight had reduced to 15.2 ± 0.8 and 20.4 ± 1.2 µmol g^{-1} (S.E.) for the Growth-1 and Growth-5 treatments respectively (the non-enriched and CO_2 enriched treatments have been combined for each water movement). Significantly the results indicate that CO_2 was nonlimiting to growth for conditions when phosphate was depleted internally.

DeBusk and Ryther (1984) found that for batch growth conditions (no water flow or replacement) the pH increased to 9.5 which was associated with low yields of *Gracilaria*. When additional CO_2 or HCl was added yields increased five fold. Previous research has found that aeration increases productivity in *Ulva lactuca* (DeBusk, Blakeslee, and Ryther, 1986) and *Gracilaria* (Ryther, 1983; Guerin and Bird, 1987). The general point from these studies was that high productivity could be maintained

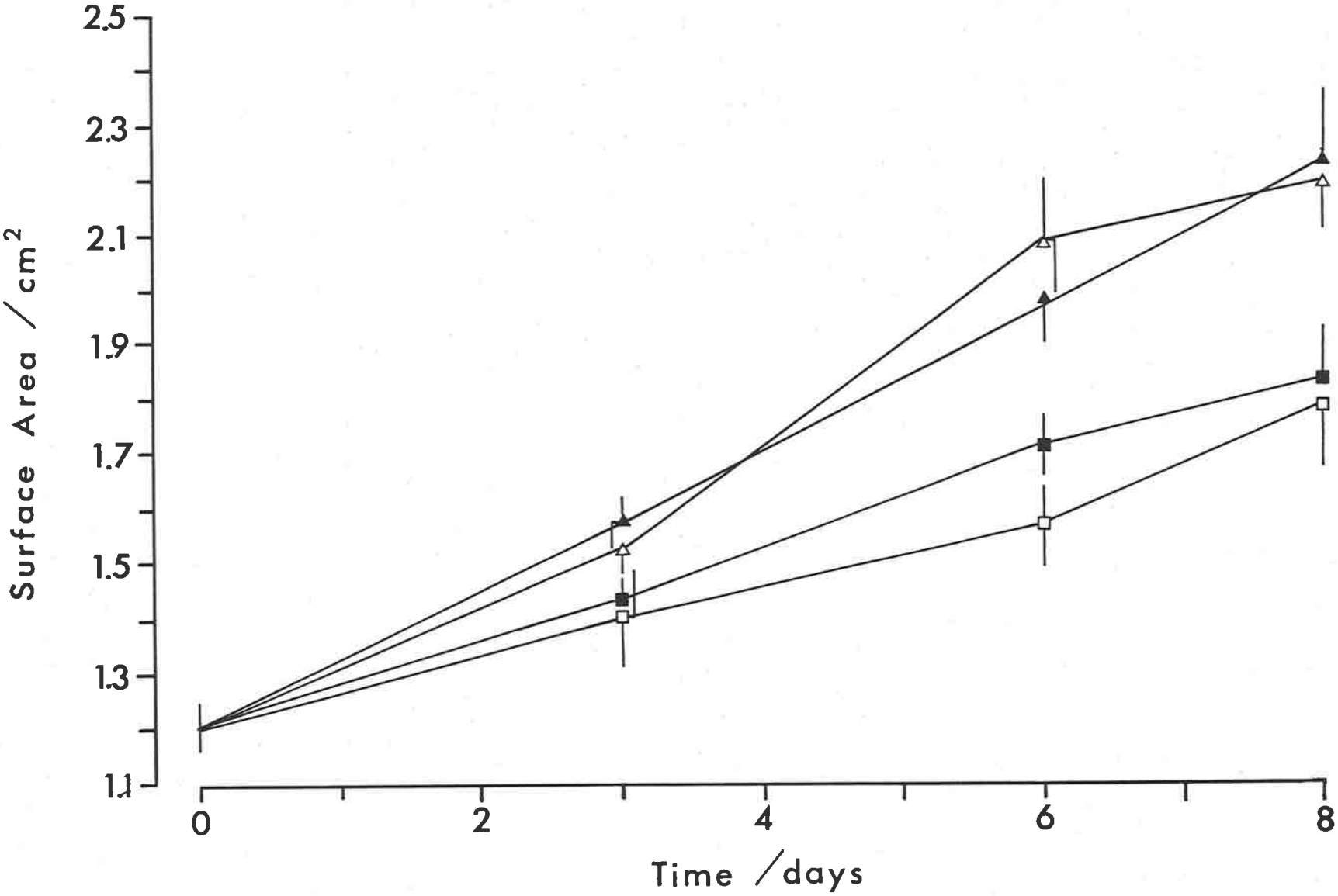

Figure 5.19. Disk surface area versus time for the Growth-1 (□) and Growth-5 (△) treatments with added CO_2, and the Growth-1 (■) and Growth-5 (▲) treatments with no added CO_2 (n = 15, C.L.).

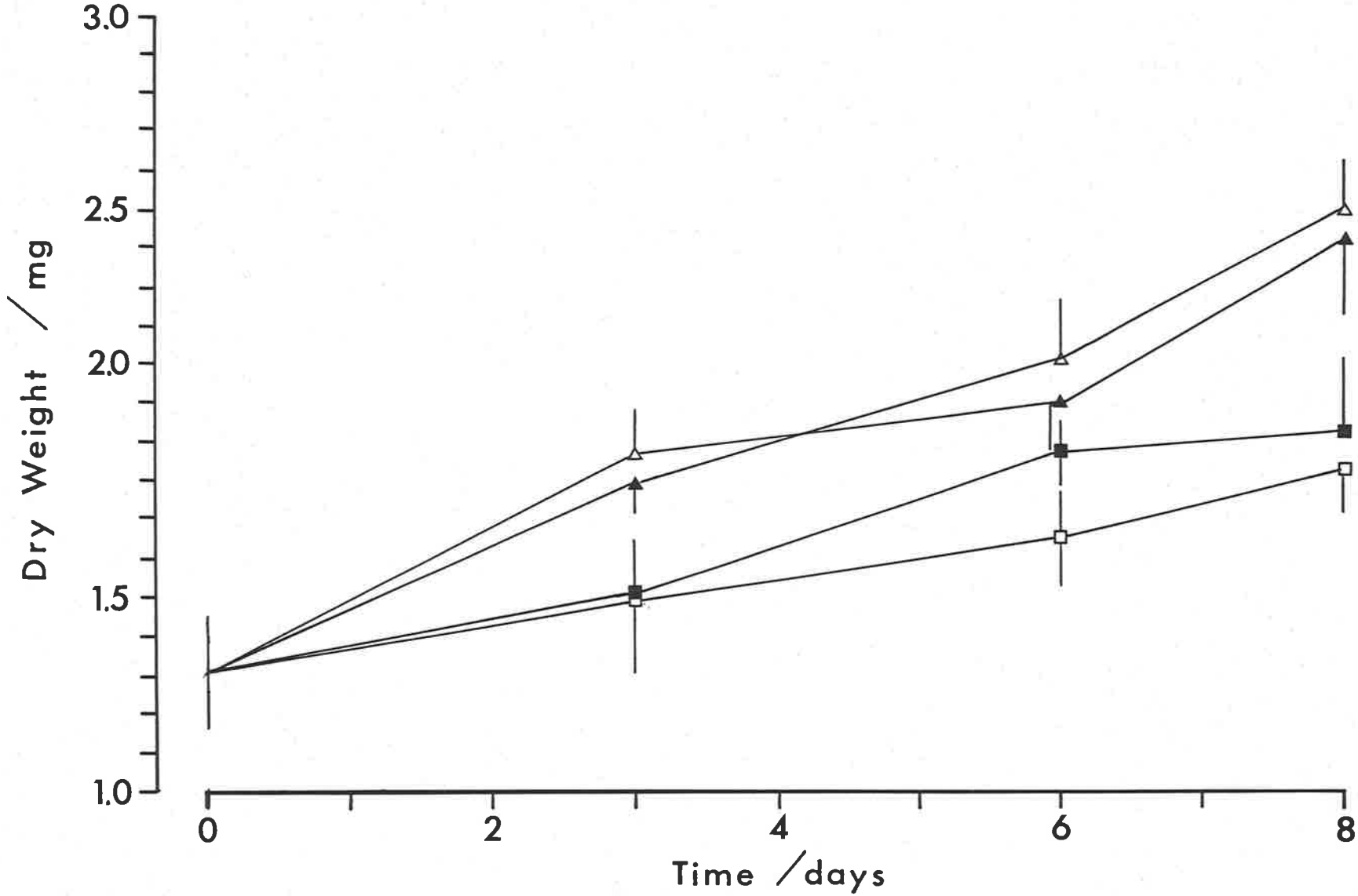

Figure 5.20. Disk dry weight versus time (n = 10, C.L.). The symbols are the same as Figure 5.19.

with aeration periods of less than 24 hours (Guerin and Bird, 1987) or even with 15 minute pulses for a total of only six hours per day (Ryther, 1983). MacFarlane (1985) found that at the pH of seawater (8.0 - 8.2) the effect of the D.B.L. on CO_2 uptake for *Ulva rigida* was slight due to the enhancement of HCO_3^- uptake. These results are in agreement with the present results, indicating that the large volume of seawater compared to the small biomass of *U. australis* in each growth chamber, and the daily replacement of medium was sufficient to minimize the effects of pH or carbon limitation on growth.

5.4.3. CONCLUSION

The main conclusion to be drawn from this experiment was that the experimental conditions overcame any potential limitations of pH or carbon limitation on growth. Nevertheless, more work needs to be done on carbon nutrition, pH and aeration with the greater application of aquaculture techniques for production of algae. This is also important considering the high costs involved in maintaining the optimum nutrient and flow conditions (Huguenin, 1976).

The next section examines the effect of preconditioning plants at different water velocities and the effect on their growth rate. Short term changes in influx with increased phosphate starvation is also examined.

5.5. THE EFFECT OF WATER MOVEMENT ON GROWTH AND INFLUX: PLANTS PRECONDITIONED AT DIFFERENT WATER VELOCITIES

5.5.1 RESULTS

Seawater with Hoagland's minus phosphate was used for both the preconditioning and experimental period. The seawater had an initial phosphate concentration of 0.41 ± 0.07 mmol m^{-3} (S.E.) and a final

concentration prior to replacement of 0.18 ± 0.11 mmol m^{-3} (S.E.). The pH initially was 8.18 ± 0.02, and finally 8.27 ± 0.01 (S.E.). The two cut method was used, and the water movement treatments were Growth-1 and Growth-5. The disks were preconditioned in either the Growth-1 or Growth-5 water movement chambers and then re-cut. Half the disks from each initial pretreatment velocity were placed in alternate experimental water movement treatments. For example disks pretreated in the Growth-5 treatment were subsequently grown in either the Growth-5 or Growth-1 treatments. The consequence of having different pretreatment regimes was that the disks were not uniform in weight, phosphate concentration or surface area at the start of the experiment.

The variation in surface area for re-cut disks between pretreatments is difficult to explain considering that disks were all re-cut at the same time with the same cork borer. The most obvious explanation is that disks grown in the slower water movement had a tendency to curl up making cutting them more difficult. The final average R.G.R. was 0.12 and 0.17 day^{-1} for the Growth-1 and Growth-5 pretreatments respectively. The large growth rate was attributed to the high initial internal phosphate concentration (103.4 ± 5.0 µmol g^{-1} dry weight, S.E.). The final internal phosphate concentration was 45.8 ± 0.2 and 48.4 ± 0.4 µmol g^{-1} (D.W., S.E.) for the Growth-1 and Growth-5 pretreatments respectively. The initial experimental internal phosphate concentrations differed from the final pretreatment results as a result of the cutting process. For the initial experimental time period the values of Q were 45.1 ± 1.3 and 46.1 ± 1.6 µmol g^{-1} (D.W., S.E.). for the Growth-1 and Growth-5 treatments respectively. These initial values of Q were greater than the previously determined value of qo (32.7 µmol g^{-1}), indicating that the plants were not completely starved of phosphate in both initial pretreatments. The average uptake for the preconditioning period was 0.03 and 0.30 nmol m^{-2} s^{-1} for the Growth-1 and Growth-5 pretreatments.

The C.H.N. results showed that the plants had a surplus of internal nitrogen for growth (3.78 ± 0.19 and 3.55 ± 0.18 % D.W. for the Growth-1 and Growth-5 pretreatments respectively).

The initial pretreatment total chlorophyll concentration was 2.33 ± 0.17 mg (total chlorophyll) g^{-1} (F.W.), and the final concentration was 2.28 ± 0.13 and 2.41 ± 0.15 mg (total chlorophyll) g^{-1} (F.W.) for the Growth-1 and Growth-5 pretreatments respectively.

5.5.2. THE EFFECT OF PAST WATER MOVEMENT HISTORY ON GROWTH RATE

Figure 5.21 (see Table 5.8 for explanation of terminology for each treatment) shows, that as previously found, water movement has a significant effect on growth. This effect was not as significant when measured on a fresh or dry weight basis (Figures 5.22, 5.23), although the same growth trend was apparent. However Figures 5.21, 5.22 and 5.23, show that the past water movement history of the plants has a differential effect in their response to water movement. The disks grown in the Growth-1-1 treatment compared to those in the Growth-5-1 treatment have a significant difference in growth rate measured on an area basis (Figure 5.21). No such lag in growth was observed in comparison between the Growth-1-5 and Growth-5-5, although there was a slight insignificant lag between the two.

TABLE 5.8 Terminology for experimental treatments

Abbreviation	Pretreatment	Experiment
Growth-1-1	Growth-1	Growth-1
Growth-1-5	Growth-1	Growth-5
Growth-5-1	Growth-5	Growth-1
Growth-5-5	Growth-5	Growth-5

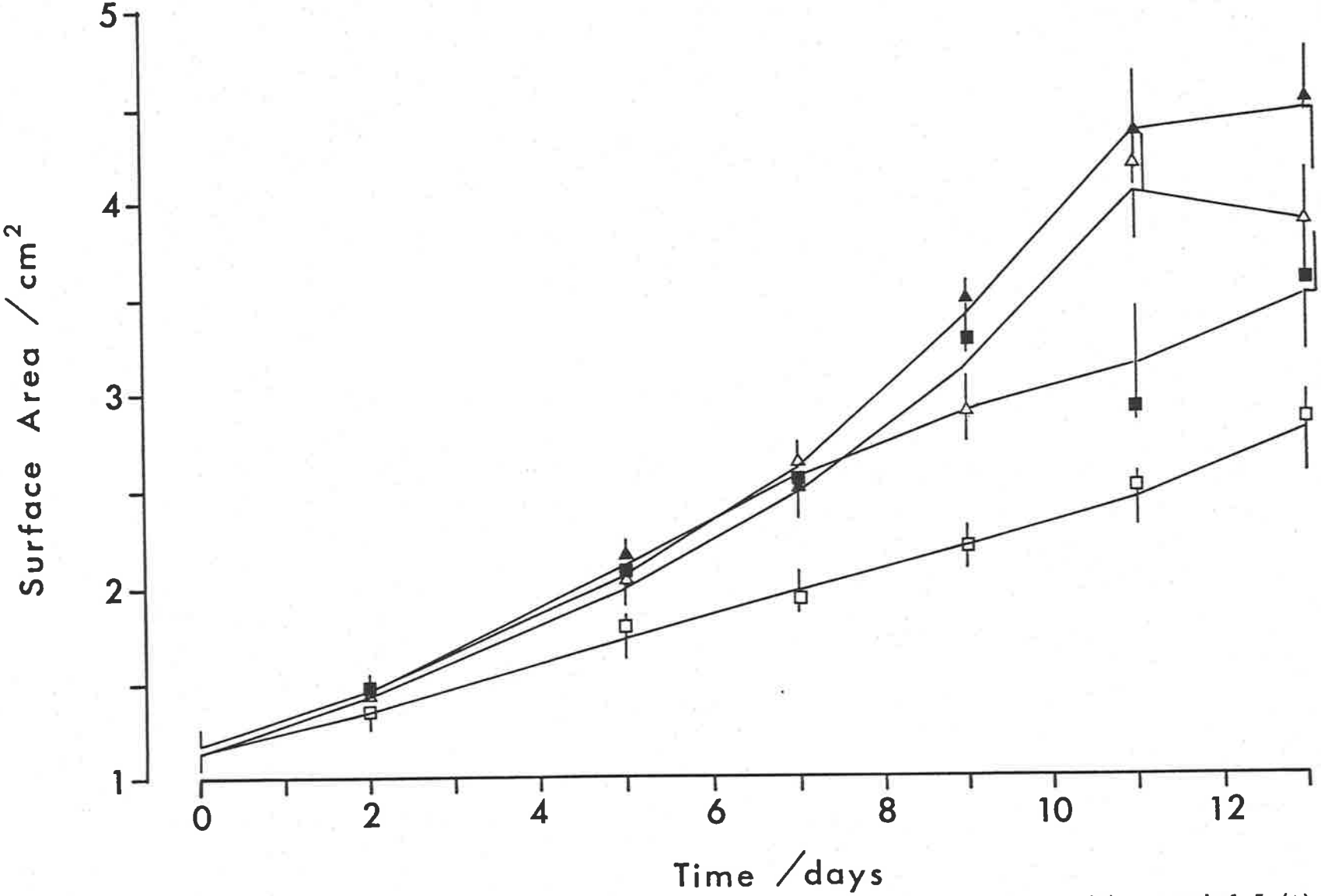

Figure 5.21. Disk surface area versus time for the Growth-1-1 (□), Growth-5-1 (■), Growth-1-5 (△) and Growth-5-5 (▲) treatments (Hunt program, n = 15, C.L.).

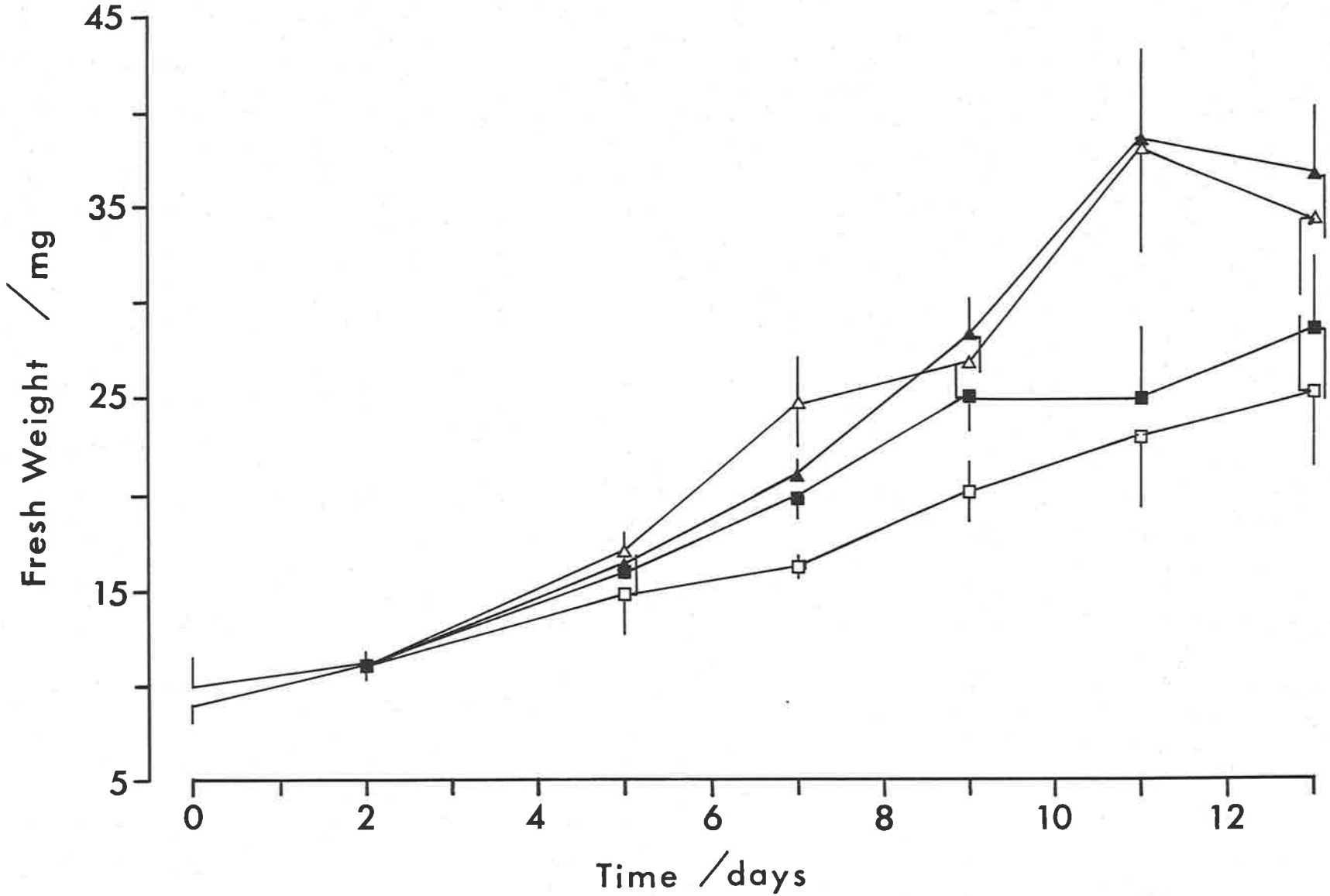

Figure 5.22. Disk fresh weight versus time. The symbols are the same as Figure 5.21 (Hunt program n = 15, C.L.).

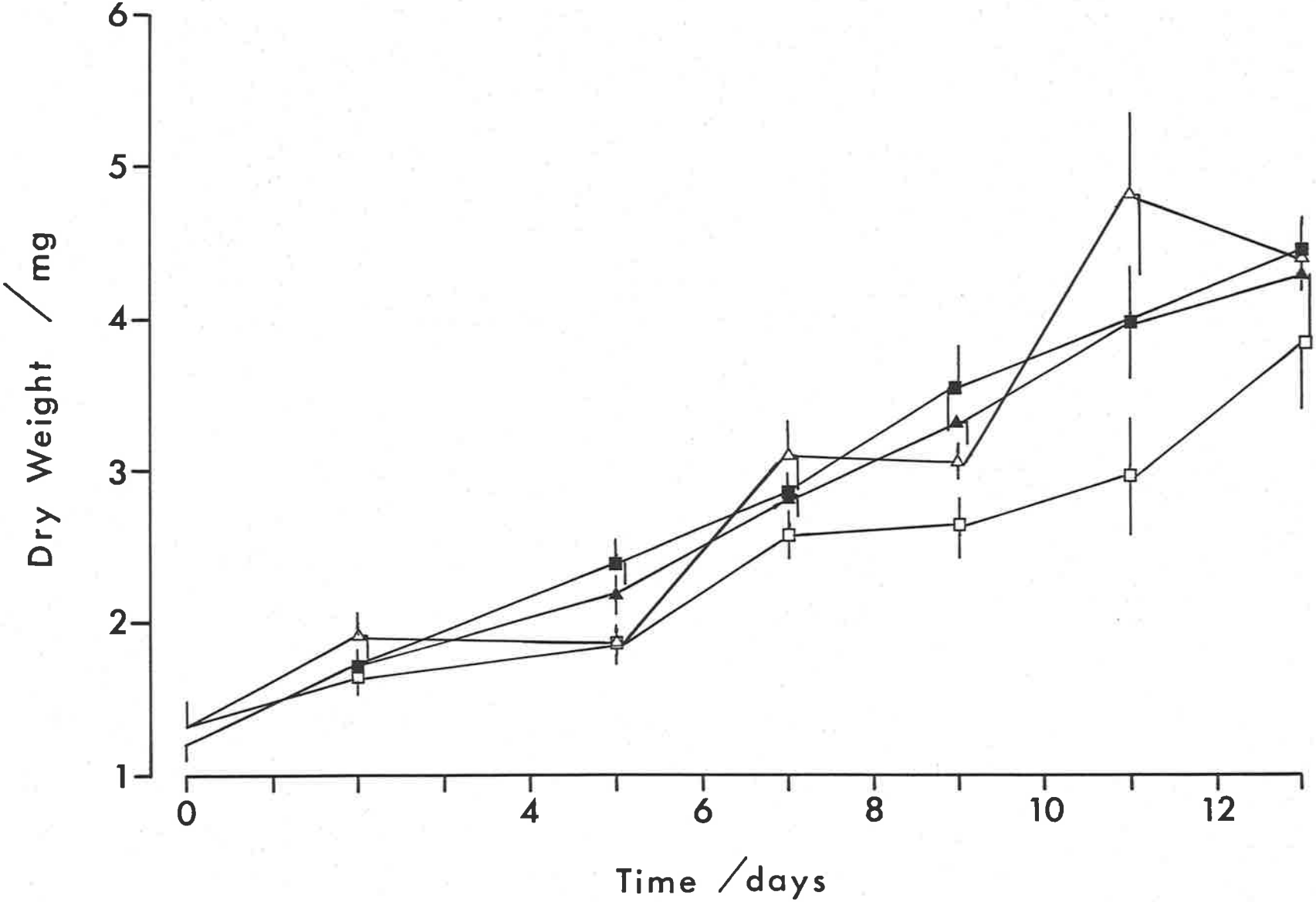

Figure 5.23. Disk dry weight versus time. The symbols are the same as Figure 5.21 (Hunt program n = 10, C.L.).

TABLE 5.9. Average R.G.R [g g^{-1} day^{-1} (D.W.)] and instantaneous R.G.R. [m^2 m^{-2} day^{-1} (surface area)] calculated using the Hunt program.

	Treatments							
Time (d)	Growth-1-1		Growth-1-5		Growth-5-1		Growth-5-5	
	D.W.	Area	D.W.	Area	D.W.	Area	D.W.	Area
2	0.129	0.087	0.184	0.114	0.120	0.119	0.172	0.113
5	0.067	0.073	0.067	0.111	0.134	0.119	0.117	0.119
7	0.095	0.056	0.120	0.114	0.122	0.081	0.119	0.126
9	0.075	0.052	0.092	0.122	0.118	0.044	0.111	0.136
11	0.073	0.060	0.117	0.129	0.108	0.041	0.124	0.092
13	0.082	0.081	0.092	-0.287	0.099	0.073	0.096	-0.089

The average R.G.R. (Table 5.9) was higher initially in all treatments than previously observed, and can be attributed to the high average R.G.R. measured in the pretreatments. Table 5.9 also shows that the instantaneous R.G.R. calculated on an area basis, declined in the Growth-1-1 and Growth-5-1 treatments while remaining approximately constant in the Growth-1-1 and Growth-5-1 treatments The last day values should be ignored for the Hunt analysis as the program has difficulties determining the curve fit at the end of the time sequence (Poorter and Lewis, 1986).

The high initial instantaneous R.G.R. for the Growth-5-1 treatment compared to the Growth-1-1 treatment declines at approximately day seven (Table 5.9). This decline was not associated with a marked difference in Q between these two treatments during the first two time periods (Table 5.10). Both the Growth-1-1 and Growth-5-1 treatments have a similar rate of change in Q (dQ/dt), as do the Growth-1-5 and Growth-5-5 treatments (Table 5.10). Therefore the dQ/dt response to the change in D.B.L. resistance was similar for each treatment with the same water movement.

TABLE 5.10. Internal phosphate concentration (Q, µmol/g (D.W.), S.E. n = 7).

	Treatments			
Time (d)	Growth-1-1	Growth-1-5	Growth-5-1	Growth-5-5
0	45.1 ± 1.3	45.1 ± 1.3	46.1 ± 1.6	46.1 ± 1.6
2	45.7 ± 1.0	55.4 ± 0.8	47.7 ± 1.4	59.8 ± 1.1
5	34.4 ± 1.4	51.8 ± 2.2	37.4 ± 1.0	53.8 ± 1.6
7	31.6 ± 0.7	50.0 ± 0.8	34.9 ± 0.7	54.4 ± 0.7
9	30.1 ± 0.5	41.1 ± 0.7	28.6 ± 1.0	42.2 ± 1.0
11	28.0 ± 0.5	36.0 ± 0.6	23.4 ± 0.5	35.5 ± 0.8
13	22.9 ± 0.9	32.5 ± 1.2	21.6 ± 0.6	35.2 ± 0.6

Figure 5.24a shows a divergence from the relationship between µ and

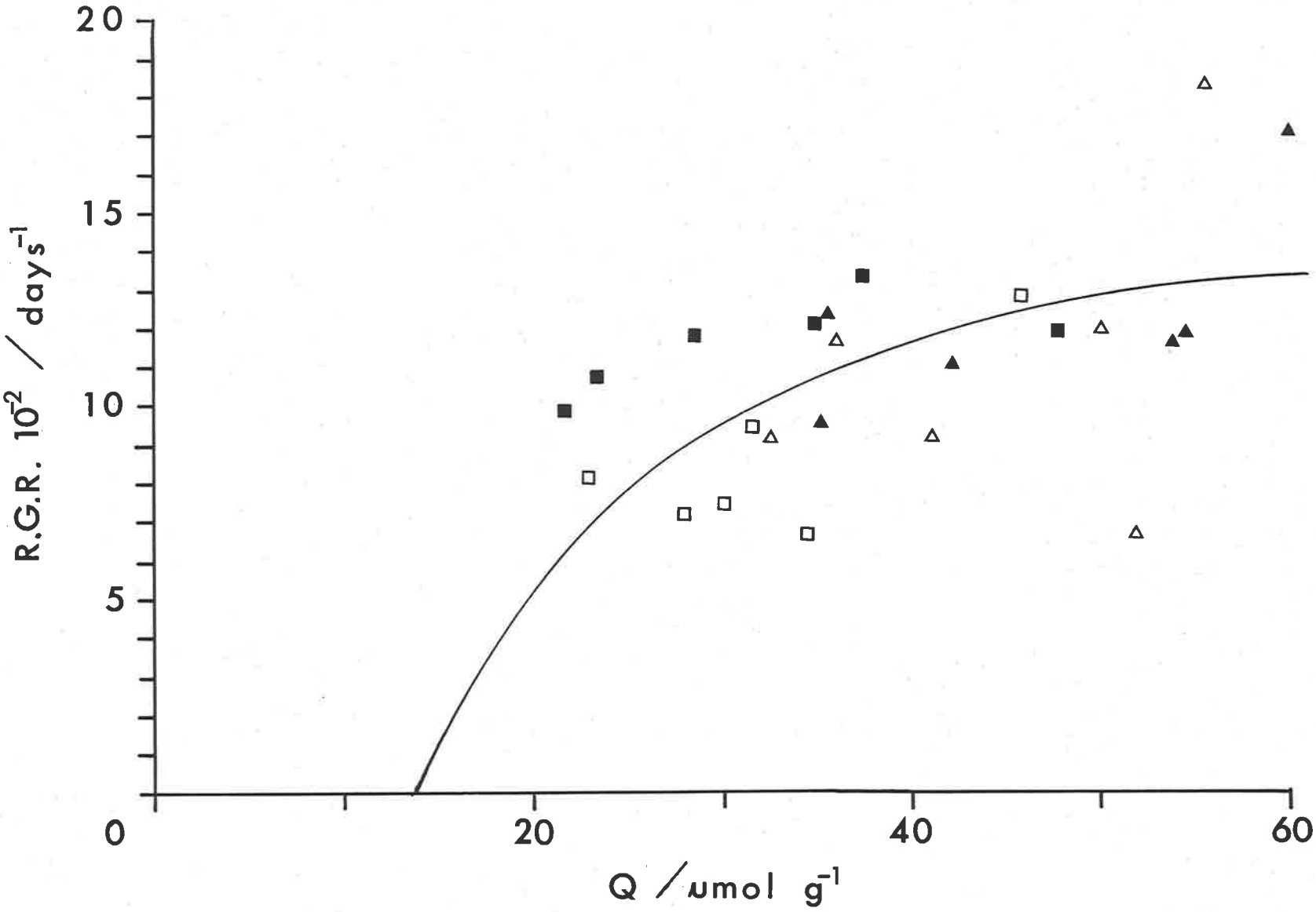

Figure 5.24a. Average R.G.R. (D.W.) versus internal total phosphate concentration (Q, D.W.). The symbols are the same as Figure 5.21. The curve was fitted using the Droop growth equation.

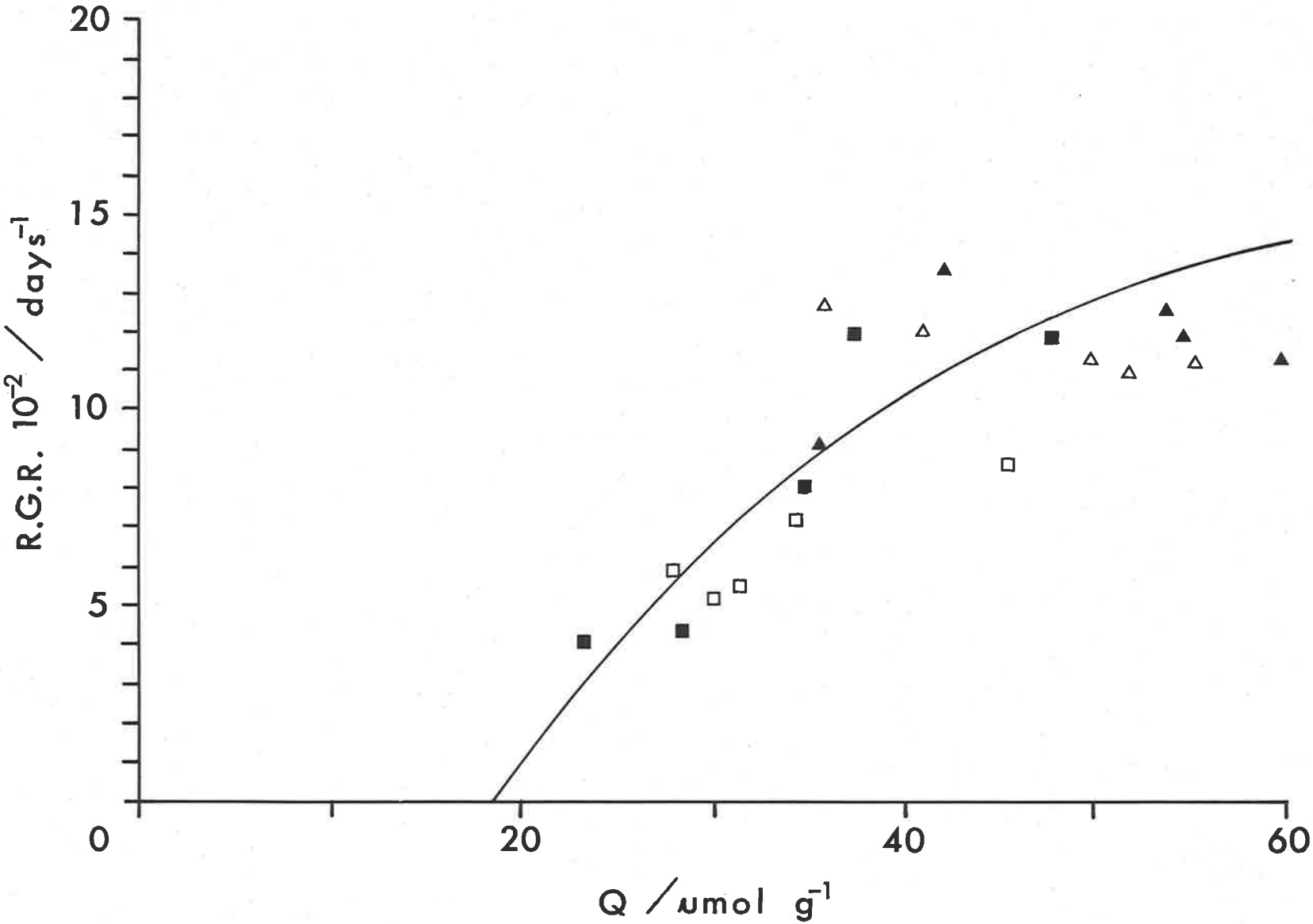

Figure 5.24b. Instantaneous R.G.R. (surface area) versus internal total phosphate concentration (Q, D.W.). The symbols are the same as Figure 5.21. The curve was fitted using the Droop growth equation.

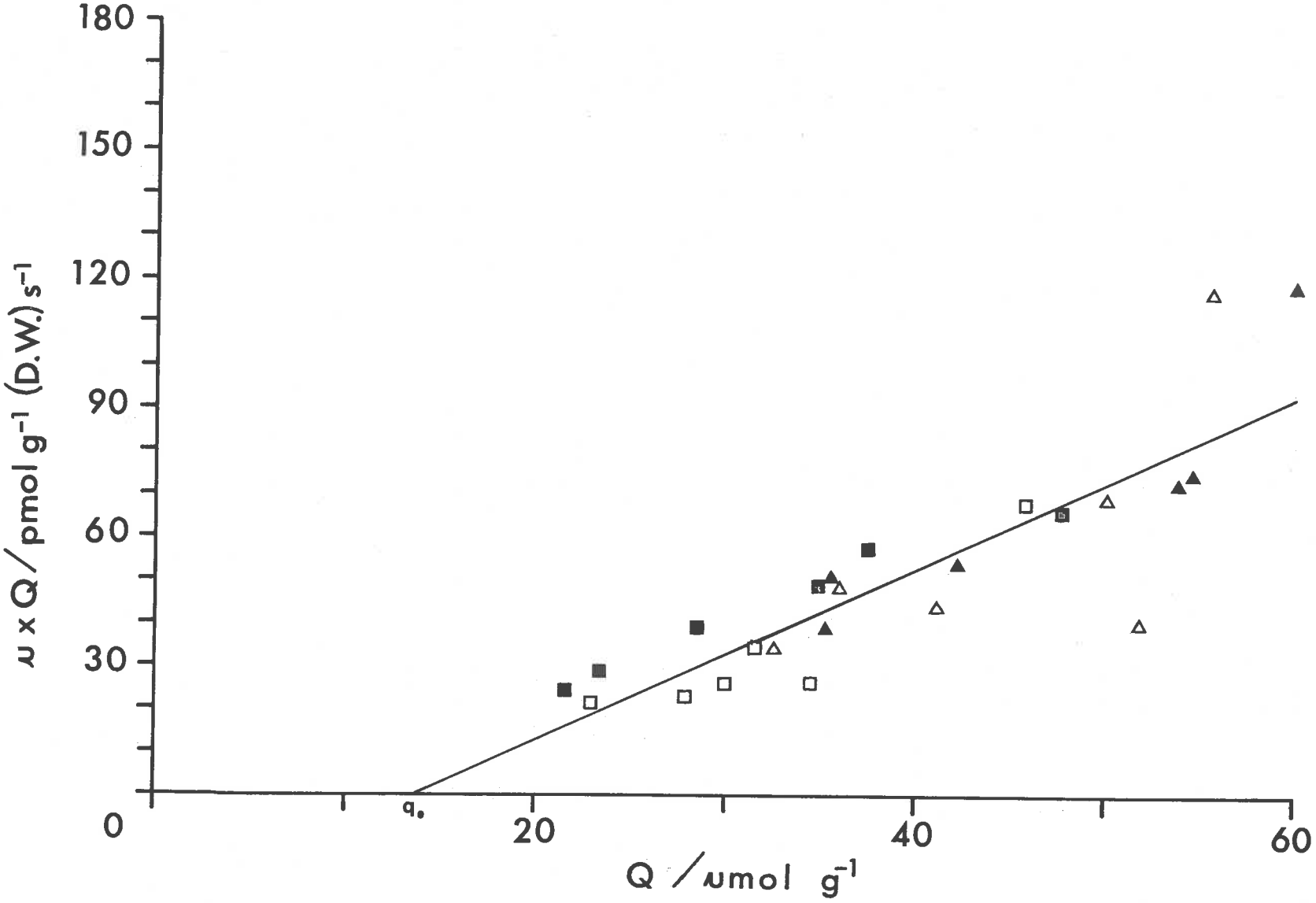

Figure 5.25a. Average R.G.R. (μ, D.W.) multiplied by Q (internal total phosphate concentration, D.W.) versus Q. The straight line was fitted using a linear regression, X-axis intercept = qo = 13.6 μmol g^{-1}, and the slope = μmq = 0.174 day^{-1} (r^2 = 0.73). The symbols are the same as Figure 5.21.

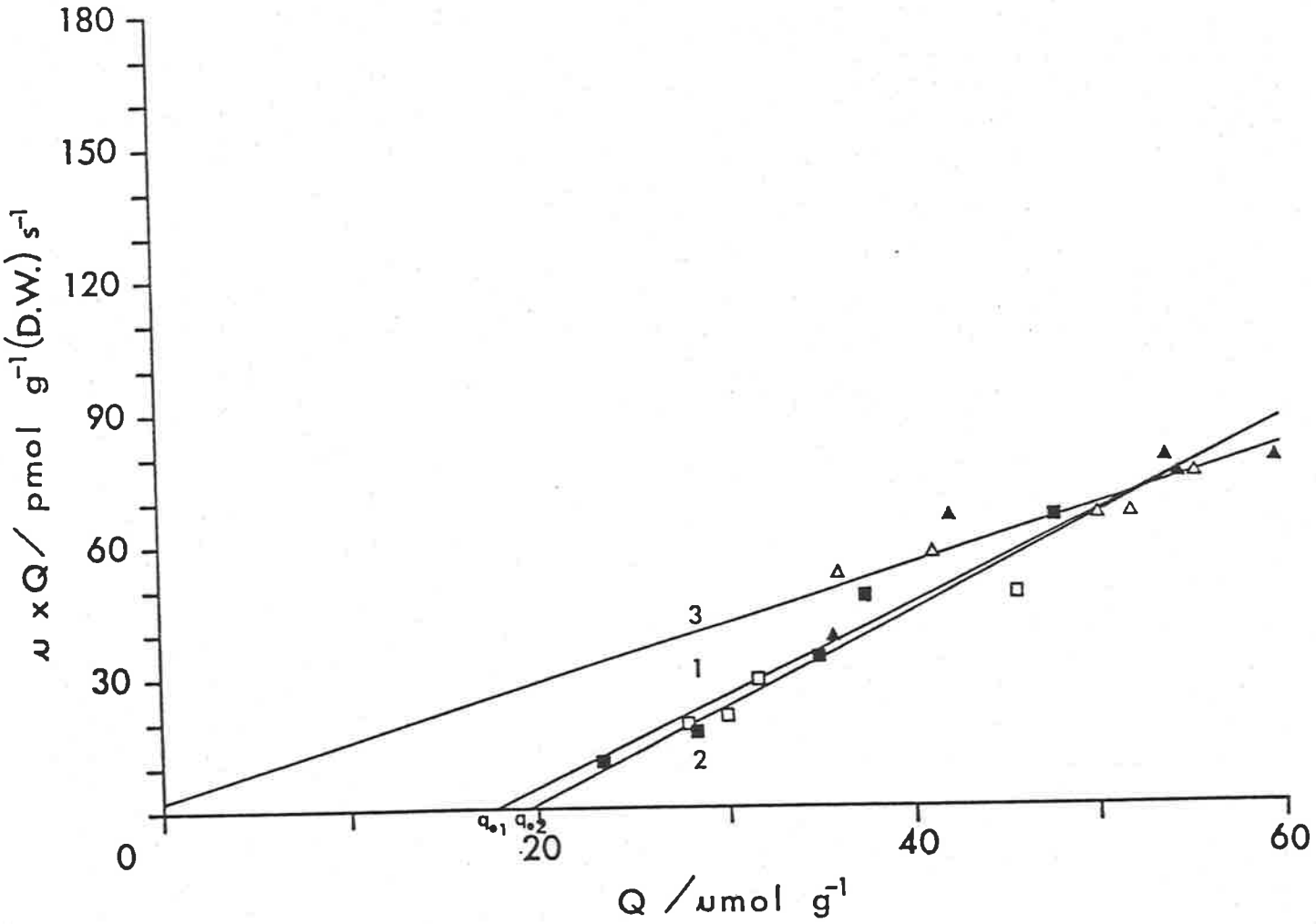

Figure 5.25b. Instantaneous R.G.R. (μ) multiplied by Q (internal total phosphate concentration, D.W.) versus Q. (1) Linear regression for all treatments combined, X-axis intercept = qo = 17.7 μmol g^{-1}, and the slope = μmq = 0.177 day^{-1} (r^2 = 0.88). (2) Linear regression for the Growth-1-1 and Growth-5-1 treatments, qo = 19.95 μmol g^{-1} and μmq = 0.188 day^{-1} (r^2 = 0.86). (3) Linear regression for the Growth-1-5 and Growth-5-5 treatments, qo = -1.5 μmol g^{-1} and μmq = 0.114 day^{-1} (r^2 = 0.81). The symbols are the same as Figure 5.21.

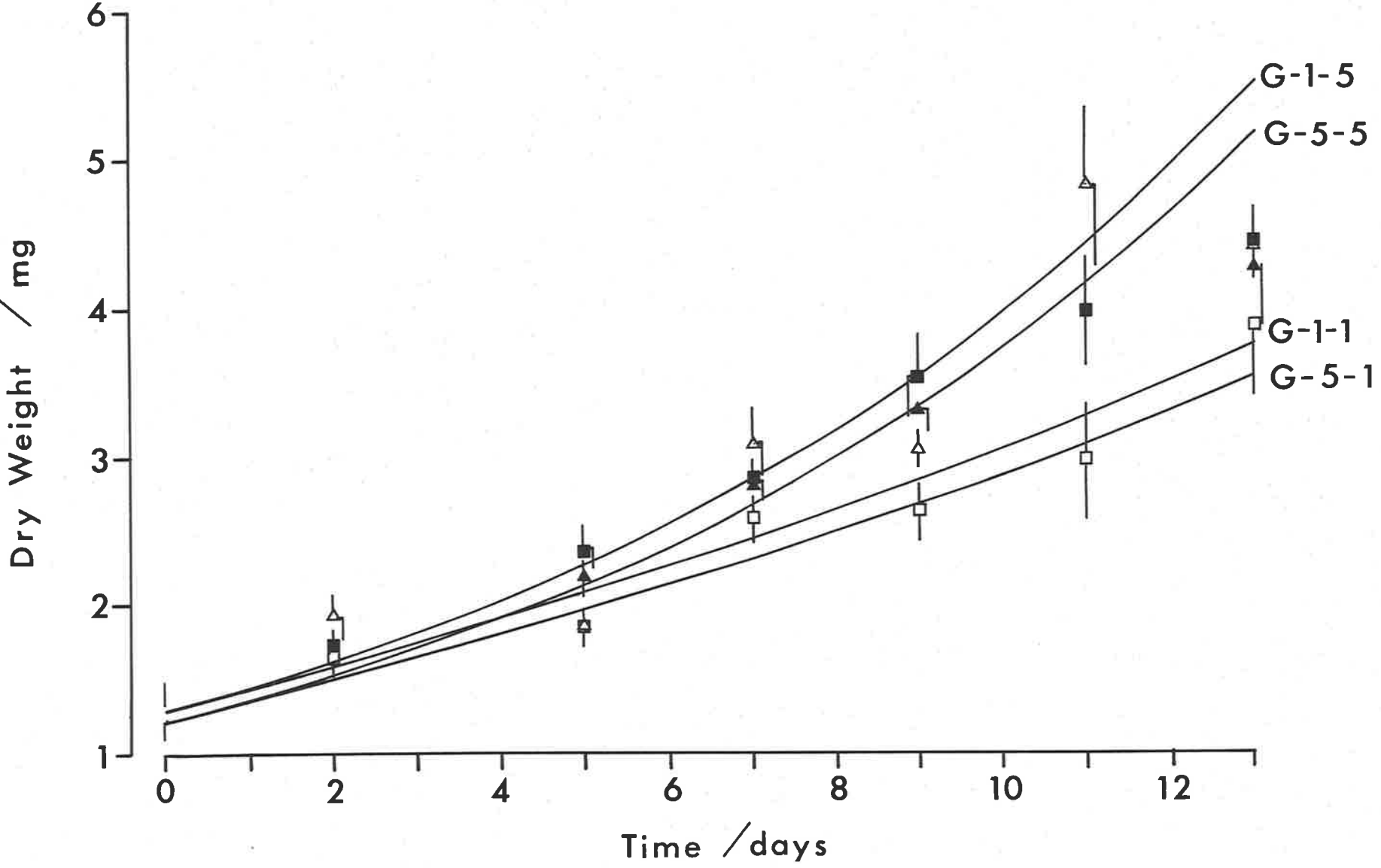

Figure 5.26. Curves were fitted to the raw data average dry weights for each of the four growth treatments using Equations 5.5, 5.6 and 5.7. The symbols are the same as Figure 5.21 (n = 10, C.L.).

Q for all the treatments. The fit in Figure 5.24a was obtained from a linear regression of Figure 5.25a, with μmq = 0.174 g g^{-1} day^{-1} and qo = 13.6 μmol g^{-1} (r2 = 0.73). The difference in growth rate between the Growth-1-1 and Growth-5-1 treatments was more clearly depicted when the instantaneous R.G.R. was plotted against Q. Figure 5.24b shows that qc occurs at aproximately 35 μmol g^{-1} which correlates with the decline in growth for both the Growth-1-1 and Growth-5-1 treatments at approximately days 2 and 7 respectively (Table 5.9). It also correlates with the decline in instantaneous R.G.R. for the Growth-1-5 and Growth-5-5 at approximately day 11 (see Figure 5.21 and Tables 5.9 and 5.10). Therefore the decline in Q explains the decreasing growth rate in all treatments, but it does not explain the difference in growth rate between the two slower water movement treatments.

Application of Equations 5.5, 5.6 and 5.7, to predict the change in dry weight with time for all treatments, shows that the growth model was an approximate fit to the raw data (Figure 5.26). However the model underestimates the growth in the Growth-5-1 treatment, and does not predict the decrease in growth when Q declines below qc. The next section examines the relationship between the change in uptake and these discrepancies.

Figure 5.24b shows that the instantaneous R.G.R. are a better fit to Q than the average R.G.R., shown in Figure 5.24a (linear regression μmq = 0.177 m^2 m^{-2} day^{-1}, qo = 17.68 μmol g^{-1}, r^2 = 0.88). There was also an apparent difference between the two water movement treatments when they are regressed separately Figure 5.25b (slow water movement treatment μmq = 0.188 m^2 m^{-2} day^{-1} qo = 19.95 μmol g^{-1} r2 = 0.86, faster water movement treatment μmq = 0.114 m^2 m^{-2} day^{-1} qo = -1.50 μmol g^{-1} r^2 = 0.81). Significantly, parameters μmq and qo do not appear to be constant as they vary between experiments and possibly between water movement treatments. This to some extent might explain the initial difference in growth

between the Growth-1-1 and Growth-5-1 treatments, as plants transferred to a slower water movement treatment would experience a lag time during which the kinetic parameters for plant growth adapted. This also could explain the slight growth lag between the Growth-1-5 and Growth-5-5 treatments (Figures 5.21, 5.22 and 5.23). Cunningham and Maas (1978) suggested that a possible reason for the lag in growth, observed for *Chlamydomonas reinhardii* transferred to and from environments of different growth potential was due to a partial uncoupling between growth and the systems controlling cell division. The plant's growth system could become partially uncoupled from its dependence on Q as the kinetic parameters change. However, there was no metabolic explanation for what these parameters refer to, as the growth process is dependent on a number of enzyme reactions.

Fujita (1985) found that for *Enteromorpha* sp. and *Gracilaria tikvahiae* the qo determined for plants grown at high inorganic nitrogen and then starved was approximately half that of plants starved after being grown at low inorganic nitrogen. This would then explain the difference in qo between the results in this section and those presented in Section 5.3. The initial pretreatment Q (phosphate) for the experiment in Section 5.3 was 55 µmol g^{-1} with a calculated value of qo = 32.7 µmol g^{-1} compared to 103.4 and 17.68 µmol g^{-1} for Q and qo respectively. The implication was that plants growing at low internal quotas regulate their reliance on Q to increase their safety factor. Safety factor is used to describe the concept whereby plants allocate margins of environmental tolerance (similar to engineers in designing building). For example a plant growing in a nutrient rich environment does not require a storage capacity, however a plant growing in a nutrient variable environment requires a larger qo to survive during large time periods between nutrient pulses.

5.5.3. COMPARISON OF PHOSPHATE UPTAKE, GROWTH AND SHORT TERM INFLUX

Figure 5.27 shows that uptake on an area basis declines with time, although there was a significant difference between the two water movement treatments. The decline in uptake coincides with the decline in Q (Table 5.10) and R.G.R. and contradicts the previous assertion (Section 5.3.3) that uptake increases with declining Q. The initial significant difference in uptake between the Growth-1-1 and Growth-5-1 treatments relates to their initial differences in R.G.R. (Table 5.9) and Q (Table 5.10). Therefore apart from the physical difference in uptake resulting from the D.B.L. between water movements, there was also a metabolic difference which influenced the uptake kinetics. Further, there appears to be a causal link between the increased growth rate and the increase in uptake. However there was no evidence as to the nature of the mechanism which creates or signals the metabolic difference.

Table 5.11 and Figure 5.27 show that concurrent with this change in the metabolism associated with water movement was a change in the surface area to dry weight ratio. The implication was that the increased uptake capacity of the disks growing in the faster water movement was due to both the decreased D.B.L. thickness and an increased surface area to volume ratio. Rosenberg and Ramus (1984) have shown that the rate of uptake of different shaped algae was related to their surface area to volume ratio. This was consistent with the functional-form model proposed by Littler and Littler (1980). The morphological plasticity of *U. australis* can therefore not only allow it to exist in high water movement environments (reduced drag, Gerard and Mann 1979; Gerard 1987) but also change its morphology to increase its growth rate.

The fitted curves in Figure 5.26 depended on a constant surface area to dry weight ratio (used the ratios for the initial time period) for the conversion of units in the Briggs-Maskell equation. Figure 5.28 shows the fit between Equations 5.5, 5.6 and 5.7, but the surface area to dry

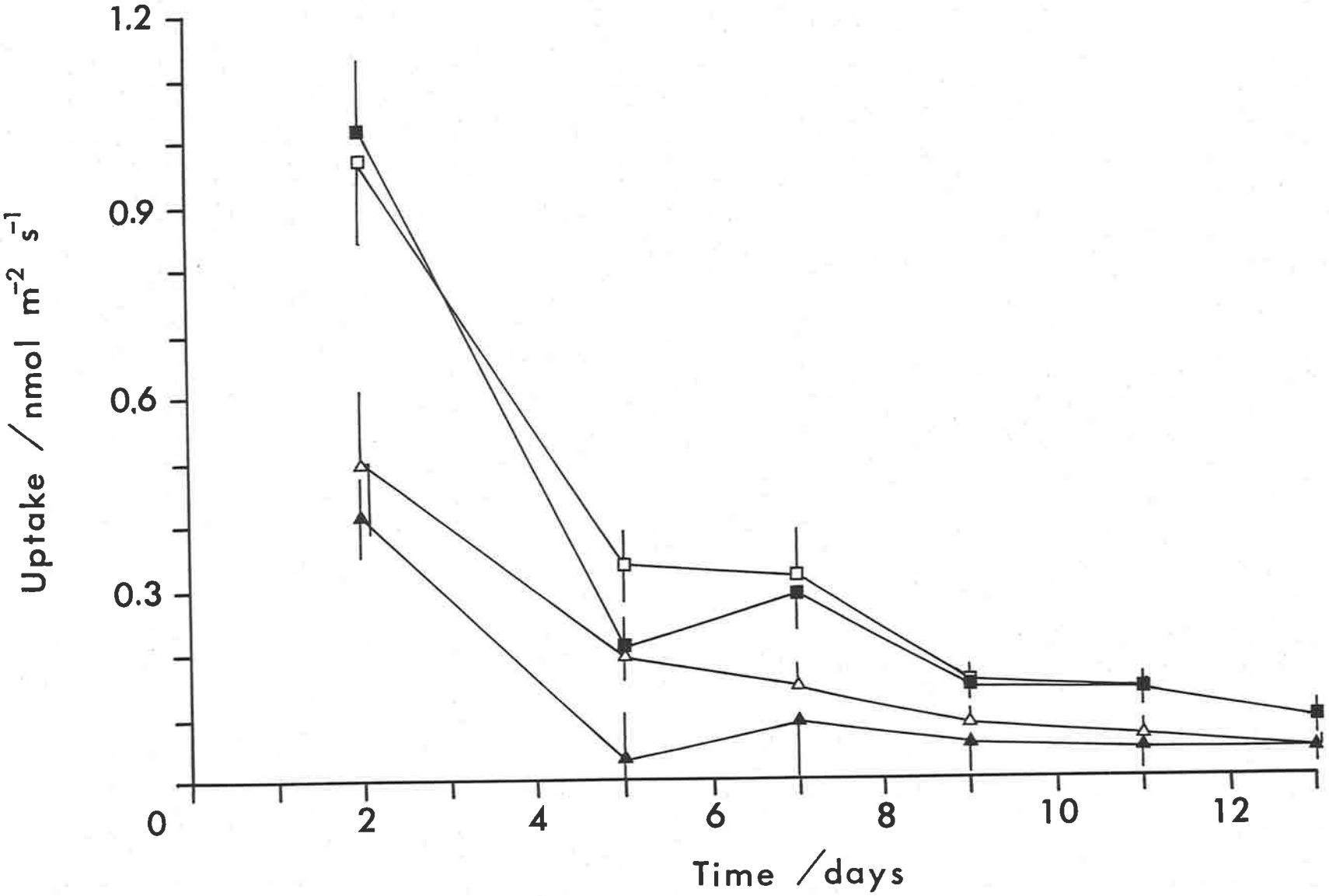

Figure 5.27. Phosphate uptake versus time (n = 10, C.L). The symbols are the same as Figure 5.21.

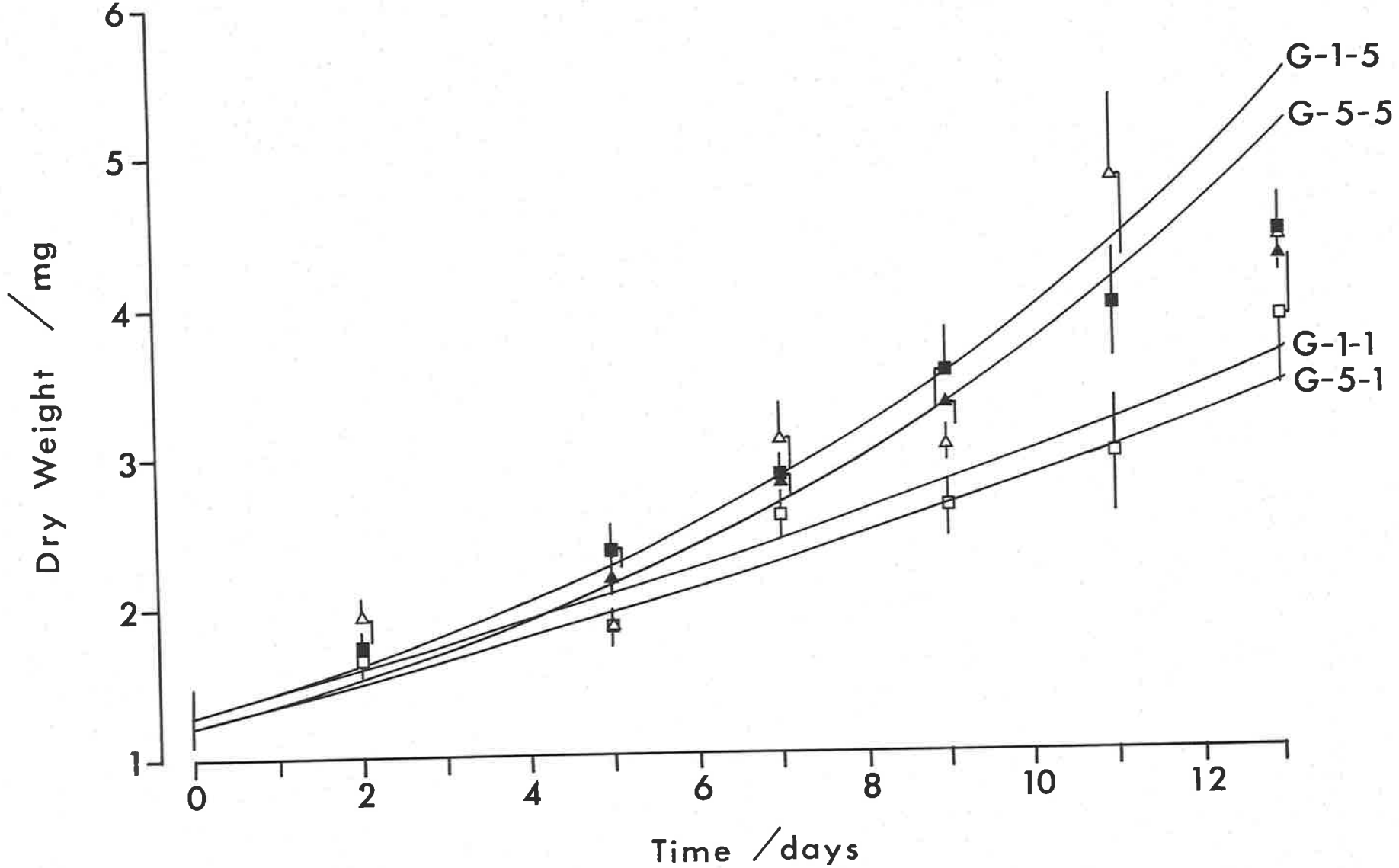

Figure 5.28. Curves were fitted to the raw data average dry weights for each of the four growth treatments using Equations 5.5, 5.6 and 5.7. Further, the changes in surface area to dry weight ratio with time for each treatment were compensated for within the three equations. The symbols are the same as Figure 5.21 (n = 10, C.L.).

TABLE 5.11. Surface area to dry weight ratio (m^2 : g).

	Treatments			
Time (d)	Growth-1-1	Growth-1-5	Growth-5-1	Growth-5-5
0	0.084	0.084	0.101	0.101
2	0.078	0.070	0.088	0.083
5	0.095	0.109	0.087	0.098
7	0.074	0.086	0.086	0.090
9	0.083	0.094	0.093	0.105
11	0.083	0.087	0.073	0.091
13	0.074	0.089	0.081	0.106

weight ratio was varied according to the values in Table 5.11 for each treatment. The observed fit between the predicted curves and the raw data (Figure 5.28) was similar to that observed in Figure 5.26. The main effect of applying the results of Table 5.11 to the growth model was to increase (slightly) the predicted difference in growth rate between the two water velocities. Therefore the use of the growth model predicts only a slight enhancement of the growth rate due to changes in the surface area to dry weight ratio. Nevertheless this enhancement in growth would increase the competitiveness of these plants in the field.

Previous research has shown that at steady state there is a linear relationship between uptake and Q as predicted from Equation 5.1 (Droop 1973). Figure 5.29 shows that although the system was not at steady state (Q decreasing) there was still an approximately linear relationship between V and Q. The linear relationship was a result of the simultaneous decrease in Q and V with time. It also shows that the line curves upwards at higher values of Q, which was similar to the response found by Brown and Button (1979) for a plot of μQ versus Q, at steady state. They concluded that this inflection was due to their measuring Q on a per cell

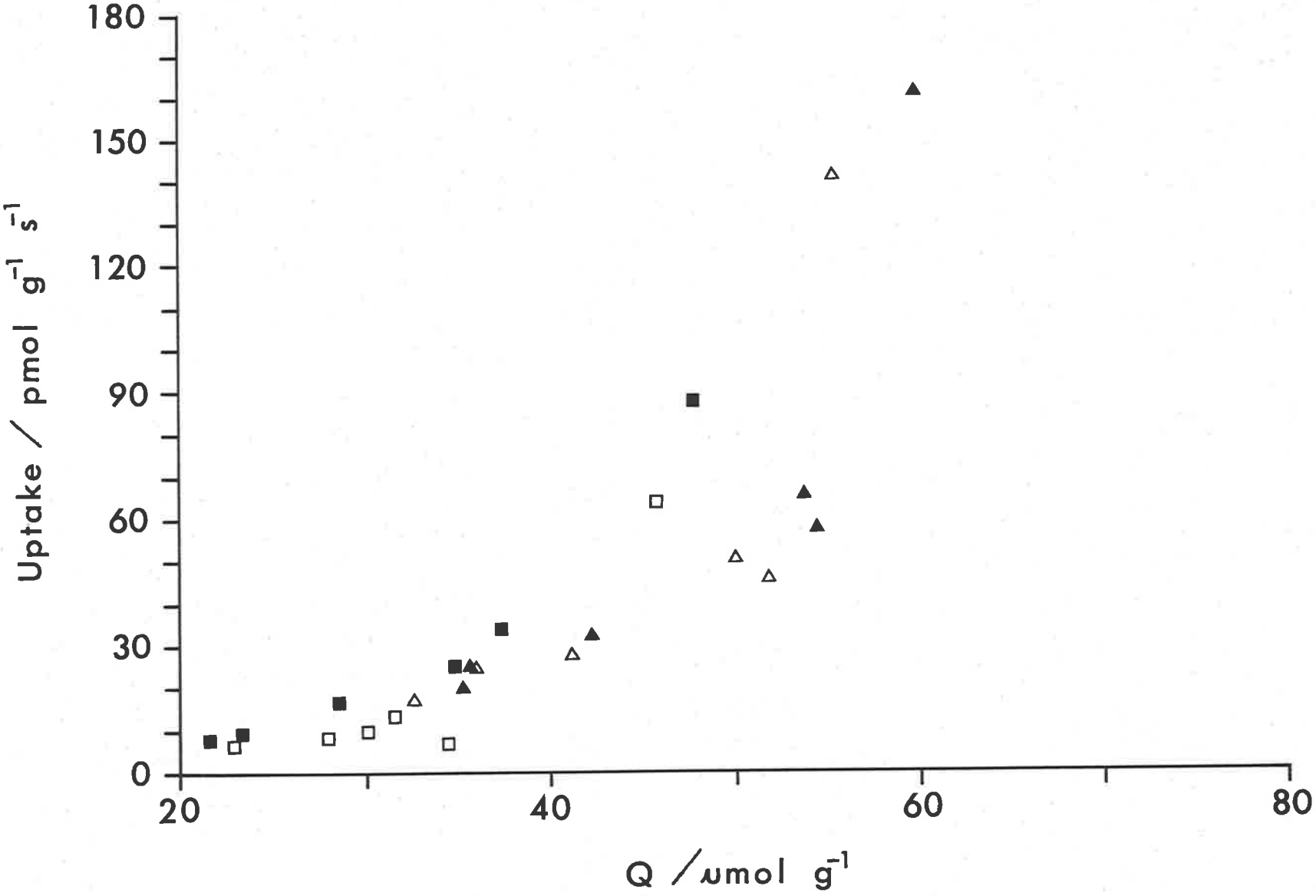

Figure 5.29. Phosphate uptake (D.W.) versus Q (D.W.). The symbols are the same as Figure 5.21.

basis rather than per unit mass. However, if this was the case the curve should bend downwards because as μQ reaches its maxima (μmq.qc) Q should continue to increase (luxury consumption) due to the imbalance between V and μQ (see Equation 5.6). The slight curving probably reflects that the system was not at steady state. The comparison of μ and V/Q shows that initially the mass balance equation was not at steady state ($dQ/dt \neq 0$) due to the high uptake and low growth rate, but by day 5 the situation was reversed (Table 5.12). Therefore equilibrium between uptake and growth was not established for the experimental duration.

TABLE 5.12. Comparison of the average R.G.R (u) and V/Q g g^{-1} day^{-1} (D.W.)

	Treatments							
Time (d)	Growth-1-1		Growth-1-5		Growth-5-1		Growth-5-5	
	μ	V/Q	μ	V/Q	μ	V/Q	μ	V/Q
2	0.129	0.120	0.184	0.220	0.120	0.156	0.172	0.232
5	0.067	0.016	0.067	0.076	0.134	0.079	0.117	0.105
7	0.095	0.037	0.120	0.087	0.122	0.063	0.119	0.092
9	0.075	0.027	0.092	0.058	0.118	0.049	0.111	0.067
11	0.073	0.025	0.117	0.060	0.108	0.035	0.124	0.061
13	0.082	0.024	0.092	0.045	0.099	0.032	0.096	0.048

Interestingly there was a good fit (r^2 = 0.91) between μQ and V (linear regression slope, = 0.618, Y-intercept = 26.9 pmol g^{-1} s^{-1}, Figure 5.30). The positive Y-intercept indicates that at zero uptake the plants were consuming their internal phosphate storage pool. At steady state the slope should be one. The slope at low uptake indicates the use of internal stores and the flattening of the slope at higher uptake rates reflects luxury consumption of phosphate.

Short term (10 minutes) phosphate influx was measured using the technique described in Section 2.8.1.1.6., except that influx was only measured at one [Pi]b (1 mmol m^{-3}) for seven disks from each treatment.

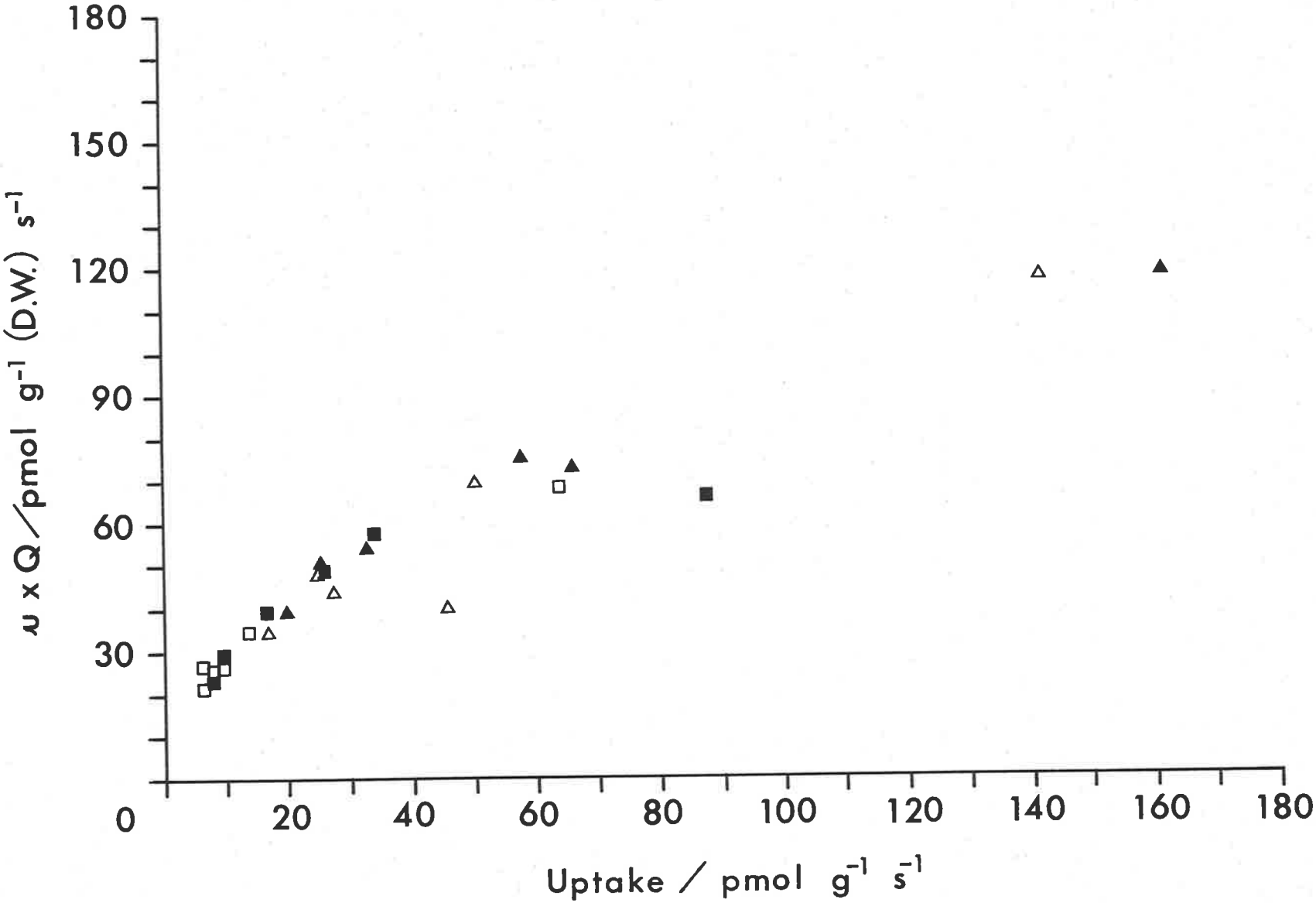

Figure 5.30. Predicted phosphate consumption by growth (R.G.R. x Q) versus phosphate uptake (D.W.). The symbols are the same as Figure 5.21.

The results showed a decline in influx with time, however the decrease in influx was greatest for the faster water movement treatments (Growth-1-5 and Growth-5-5, Table 5.13). The faster decrease in influx for the Growth-1-5 and Growth-5-5 treatments correlates with the larger value of Q in comparison to the other two treatments.

TABLE 5.13. Short term phosphate influx at 1 mmol m^{-3} [Pi]b, using approximate method described in Section 2.8.1.1.6. n =7 and standard errors used.

	Treatments			
Time (d)	Growth-1-1	Growth-1-5	Growth-5-1	Growth-5-5
0	4.85 ± 0.19	6.28 ± 0.32	4.85 ± 0.19	6.28 ± 0.32
2	6.35 ± 0.37	6.01 ± 0.19	6.62 ± 0.24	6.49 ± 0.13
5	7.10 ± 0.12	6.49 ± 0.08	6.24 ± 0.31	6.60 ± 0.18
7	6.28 ± 0.10	5.34 ± 0.09	5.02 ± 0.07	5.33 ± 0.07
9	5.77 ± 0.11	4.59 ± 0.13	5.12 ± 0.14	4.49 ± 0.12
11	5.79 ± 0.25	5.53 ± 0.11	3.91 ± 0.16	4.16 ± 0.14
13	5.61 ± 0.26	4.81 ± 0.07	4.21 ± 0.18	4.32 ± 0.25

The next chapter will examine the short term changes in influx in more detail with a view to relating the change to an interaction with Q.

5.5.4. GROWTH STORAGE CAPACITY

As Vogel (1981) has observed, water movement was a source of mechanical energy which if used by the plant could reduce its metabolic costs. Section 1.4 described the previous research which had shown that algae benefitted from water movement through various metabolic, reproductive and physical advantages. To determine if the presence of a D.B.L. could adversly effect the productivity of *U. australis* it was necessary to know the storage capacity. Storage capacity was defined as the time the algae can continue to grow without any external nutrient

uptake relying on the internal pool of stored nutrients (Fujita 1985). The importance of this in relation to the D.B.L. was that if the plant can continue to grow between periods of disturbance when seawater nutrient levels are above optimum for growth (luxury consumption occurs) then the plant's reliance on overcoming the D.B.L. is reduced. By implication under this condition the D.B.L. limitation on growth will have a reduced emphasis on the ecology of the plant, and other physical factors will be of more importance (e.g. light, temperature etc). Therefore the timing of environmental nutrient pulses in relation to the plant's storage capacity will determine the effect on growth of the D.B.L.. However, this assumes that during the nutrient pulses the concentrations are optimum and their duration was long enough for luxury consumption to take place. Therefore if the pulse of nutrient was for a small duration then the combination of increased uptake (as a result of being starved) and water movement would increase the plant's survival and productivity.

For the situation where the plant was entirely dependent on its internal storage capacity for growth (no uptake), then according to Equation 5.6 dQ/dt is negative as Q approaches qo, until at time Tf it will be zero. Because this expression was asymptotic, Q will theoretically never reach qo therefore as an approximation we can take Tf as occurring when qo/Q is 0.95.

Table 5.14 The time Tf for Q to reach 0.95% of qo, comparing different experimental values of qo, μmq and Q (where Wo was the initial weight, Tf calculated using Equations 5.5, 5.6 and 5.7, and phosphate was assumed to be growth limiting).

qo μmol g^{-1}	μmq g g^{-1} day^{-1}	Wo mg	Q μmol g^{-1}	Tf days	T50 days
17.68	0.177	2.0	100	23	10
32.7	0.139	2.0	100	23	9
17.69	0.177	2.0	50	18	7
32.7	0.139	2.0	50	14	4

Table 5.14 shows that the storage capacity was equivalent for the two different growth kinetic systems at the highest Q achieved in culture. However, with a 50% decrease in Q there was a difference in the storage capacity for the two systems. Fujita (1985) calculated the storage capacity of *Ulva lactuca* to be 9 and 6 days for plants grown at high nitrogen or starved, respectively. The large discrepancy between the results in Table 14 and Fujita's results was that Fujita calculated the storage capacity assuming constant growth rate (used $Tf = \mu^{-1} \ln(Wf/Wo)$, where Wf was the final weight, this equation is Equation 4.5 rearranged) which underestimates Tf, Ryther, Corwin, DeBusk and Williams (1981) found that N-starved *Gracilaria* plants soaked in complete nutrient media for 6 hours and returned to unenriched seawater, will grow at non-limiting rates for as long as 2 weeks. Similarly, Morgan and Simpson (1981) found that *Palmaria* could take up enough nitrate to grow for one week. The values of Tf indicate that growth will continue for up to 18 days when the quota was low, however the results for T50 (50% reduction in initial μ) show that for most of this time μ would be less than 50% of its initial value. Therefore for the plants to maintain their growth rate the uptake restrictions of the D.B.L. play an integral part in the plant's growth rate.

5.5.5. CONCLUSION

The main conclusion is that the water movement history of *U. australis* can influence its growth rate. The mechanics of the difference observed for the different water movement pretreatment involve changes in the growth kinetic parameters and also morphology. The reason for the variation in uptake with time and between treatments is still unclear and will be examined in the next chapter.

Previous research on the comparison of the Droop and Monod models of growth have shown that they predict the variation of growth observed with

changes in the limiting nutrient (Fuhs 1969; Tilman and Kilham 1976; Tilman 1977; Brown and Button 1979; Probyn and Chapman 1982). Most of these studies have been concerned with growth at steady state which for field grown algae is a very limited condition. The mass balance equation predicts the observed differences in growth rate for non-steady state growth, although it does not explain the observed variation in uptake. No previous study has attempted to relate water movement, uptake, internal limiting nutrient concentration and growth rate. The present study has shown that water movement can modify the predicted growth rate and uptake, and therefore it needs to be taken into account when determining the growth potential of plants in the field.

CHAPTER 6. THE EFFECT OF PHOSPHATE STARVATION ON SHORT TERM PHOSPHATE INFLUX.

6.1 INTRODUCTION

The observation of an increase in phosphate influx when plants were grown under phosphate starved conditions has been observed for most plant types and similar effects have been found with other various nutrients (Table 6.1). Previous research on macroalgae is limited to an observed influx enhancement of phosphate by *Gracilaria tikvahiae* (Lapointe, 1985) and *Macrocystis* (Manley, 1985), and inorganic nitrogen by *Porphyra perforata* (Thomas and Harrison, 1985), *Gracilaria tikvahiae* (D'Elia and DeBoer, 1978; Fujita, 1985), *Chordaria* (Probyn and Chapman, 1982), *Entermorpha* and *Ulva* (Fujita, 1985)

Table 6.1 shows that most of the previous research postulates the control of nutrient influx by either an allosteric mechanism or the filling or depletion of an internal nutrient pool. To explain the correlation between internal nutrient concentration and uptake many different models of uptake have been proposed. The variation in these models has occurred because of the different response of the Km for different nutrients to starvation conditions. Table 6.1 shows that Vm increases in response to starvation, but the variation in the response of Km to enhanced uptake indicates that different plants have adapted kinetically to nutrient starvation in different ways.

Glass (1976) has proposed an allosteric model of potassium regulation by barley roots to account for the observed changes in K+ influx with starvation. To account for this, Siddiqi and Glass (1982) formulated an empirical model based on the exponential relationship between influx and the root potassium concentration,

$$V(i) = (MaxVm.e^{-bi}.Cs)(MinKm.e^{di} + Cs)^{-1} \qquad \text{Equ-6.1}$$

where V(i) is the influx at a given internal concentration (i), MaxVm is the maximum Vm when i is hypothetically zero, MinKm is the minimum Km when i is hypothetically zero, b and d are the slopes of Vm and Km

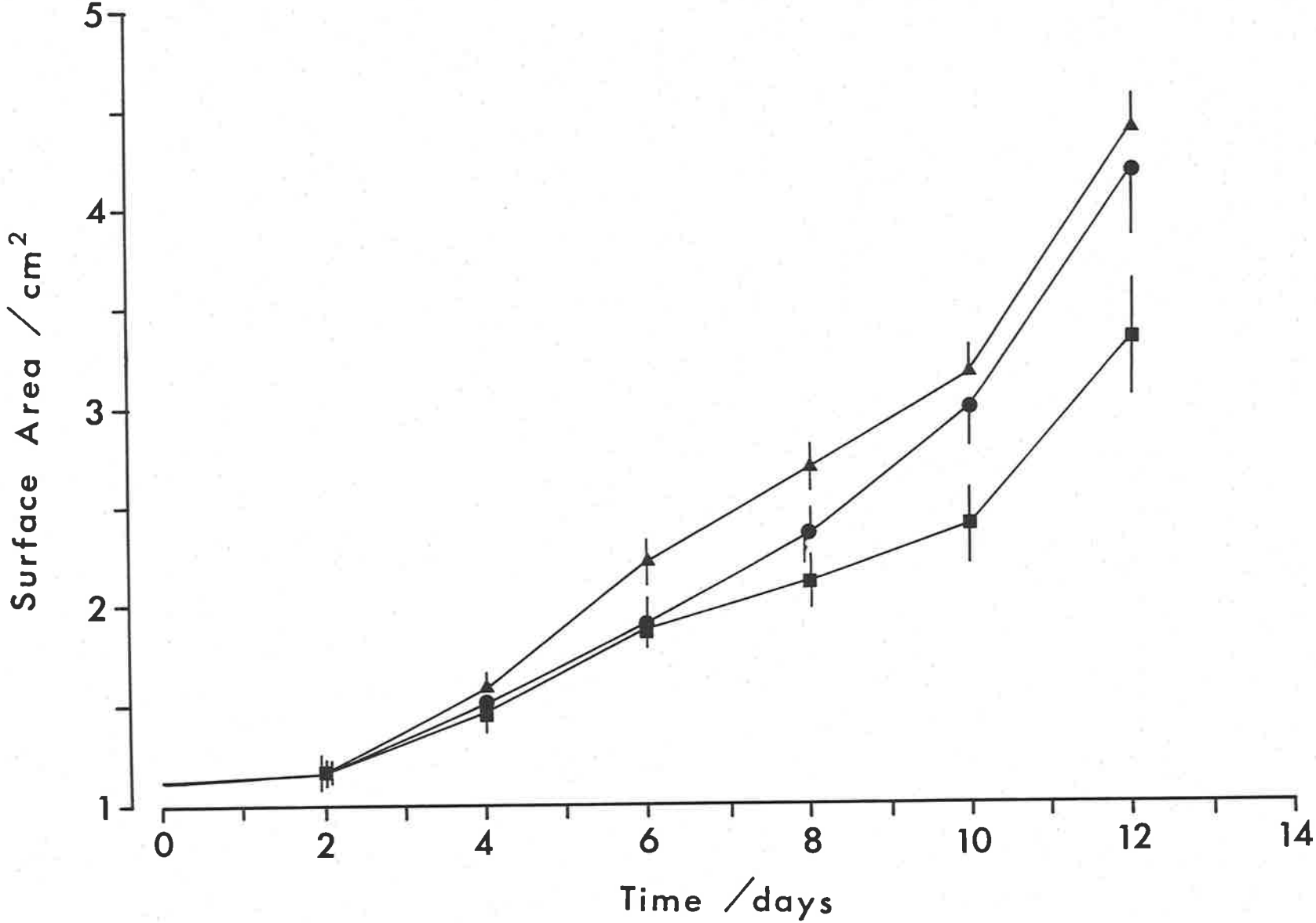

Figure 6.1. Disk surface area versus time (Hunt program, n = 15, C.L.), for the growth treatments Growth-1 (■), Growth-3 (●) and Growth-5 (▲).

versus i. Both MaxVm and MinKm are the theoretical values of Vm and Km respectively, when the allosteric inhibition of influx is zero. Also because Vm increases while Km decreases with decreasing i, the slopes of their relationship with s have opposite signs. Therefore this model accounts for the decline in influx with increasing i by direct blocking internally of the binding sites for the carrier protein. This does not account for the changes in Km observed. Glass (1976) overcame this anomaly by suggesting the repression of carrier synthesis with increasing i, but no link was established between i and carrier synthesis.

TABLE 6.1. Previous research on enhanced nutrient uptake when the plant was starved of that nutrient. I, C, or D indicate that the kinetic parameters (Km or Vm) increase, remain constant or decrease respectively with enhanced uptake.The following symbols equate to the theory or model used to explain the enhanced influx; A = allosteric, nc = non-competitive model, e = exponential model, P = internal pool.

Plant species	Limiting Nutrient	Km	Vm	Model	Reference
Macroalgae					
Gracilaria	Pi				Lapointe 1985
Macrocystis	Pi			A	Manley 1985
Gracilaria	NH_4^+			P	D'Elia and DeBoer 1978
Chordaria	NH_4^+	I	I	P	Probyn and Chapman 1982
Enteromorpha	NH_4^+	D	I	P	Fujita 1985
Gracilaria	NH_4^+	C	I	P	
Ulva	NH_4^+	D	I	P	
Porphyra	NH_4^+			P	Thomas and Harrison 1985
Microalgae, Bacteria, Diatoms					
Scenedesmus	Pi	C	I	A, nc	Rhee 1973
Bacteria	Pi	D	I	P	Chen 1974
Thalassiosira	Pi	C	I	P	Perry 1976
Anacystis	Pi	D	I	P	Falkner et al. 1980
Phytoplankton	Pi	C	I	P	Gotham and Rhee 1981
Phytoplankton	Pi			P	Falkner et al. 1984
Thalassiosira	NH_4^+			P	Parslow et al. 1984a,b
Terrestrial Angiosperms					
Wheat	Pi			A	Szabo-Nagy et al. 1980
Barley	Pi, Cl^-	D	I	P	Lee 1982
Barley	SO_4^{2-}	C	I	P	
Barley	Pi			A	Lefebvre and Glass 1982
Barley	Pi			P	Schjorring and Jensen 1984
Buckwheat	Pi			P	
Rape	Pi			P	
Barley	K^+	D	I	A, e	Siddiqi and Glass 1982
Freshwater Angiosperms					
Spirodela	Pi	C	I	A	McPharlin and Bieleski 1987
Lemna	Pi	C	I	A	

The use of enzyme inhibition mechanics has been used in two ways to account for the observed enhancement of influx. Firstly, Rhee (1973) proposed that the relationship between Vm and Km with varying i resembled the non-competitive type of enzyme inhibition,

$$V(i) = Vm[(1 + Km/Cs)(1 + i/Ki)]^{-1} \qquad \text{Equ-6.2}$$

where i is the inhibitor concentration and Ki is the inhibitor constant. This model accounted for the observed relationship between phosphate influx and Cs (constant Km) for the microalga *Scenedesmus*. Rhee (1973) proposed that the internal polyphosphate pool acted as the inhibitor (i), but also suggested that other compounds seem to work as inhibitors because of the equilibria between the internal phosphorus compounds.

Secondly, Chen (1974) and Rhee (1973) used a mixed type inhibition kinetic model to predict the relationship between phosphate influx and s for the bacteria, *Corynebacterium bovis*,

$$V(i) = Vm.Cs[Km(1 + Cs/Km + i/Ki]^{-1} \qquad \text{Equ-6.3}$$

Chen (1974) found that Vm increased and Km decreased with decreasing internal phosphate, which is what would be predicted for a mixed type inhibition model.

This chapter addresses itself to the relationship between the enhanced phosphate influx with varying levels of internal phosphate starvation, and seeks to establish which model can be adequately used to describe the observed changes in kinetic parameters. The influence of water movement on the observed enhancement of phosphate influx was also measured. Results of the previous chapters show that there are interactions between growth and phosphate influx. Accordingly the data for growth are presented and discussed in detail.

6.2. ENHANCED PHOSPHATE INFLUX IN RESPONSE TO PHOSPHATE STARVATION OF *U. australis*: THE INTERACTIVE EFFECTS OF WATER MOVEMENT AND GROWTH.

6.2.1. RESULTS

Disks of *U. australis* were preconditioned in A.S.W. with Hoagland's solution minus phosphate. The aim of preconditioning was to decrease the internal phosphate concentration, resulting in growth being dependent on phosphate as the single most limiting nutrient. The water movement used for preconditioning was Growth-5. Growth-1, Growth-3 and Growth-5 were used for the experimental period. The experimental medium was seawater which had been stored for over three months and then refiltered (Section 2.2.2.). This had the effect of reducing the concentration of phosphate within the seawater (Watts and Nduku, 1981). Hoagland's minus phosphate was also added to the seawater. The seawater had a phosphate concentration prior to use of 0.11 ± 0.09 mmol m^{-3} and a final concentration of 0.08 ± 0.07 mmol m^{-3} (n = 32, S.E). After disks were removed for measurement and the seawater replaced on day 10, 20 mmol m^{-3} KH_2PO_4 was added to supplement the addition of Hoagland's. The experimental pH varied daily by ± 0.08 from the initial value of 8.19 ± 0.03.

The growth rate at the end of the preconditioning period was 0.02 day^{-1}, which was slow compared to the previously observed growth rates, indicating that the disk growth rate was being inhibited by the internal nutrient content as predicted.

Phosphate influx was measured using the technique described in Section 2.8.1.1.6. By measuring the phosphate influx at constant water velocity, using the Shaker-F treatment water velocity, the kinetic constants should be equivalent to the true values at zero D.B.L. resistance. This experimental assumption was based on the results from Chapter 3, which showed that the kinetic constants measured in the

Shaker-F treatment were approximately equivalent to the kinetic values which would occur when no D.B.L. was present. Therefore variations in the phosphate influx between growth treatments and time periods would result from the influence of the plants previous growth history. The initial Vm and Km at the start of the experimental period was 0.82 ± 0.03 nmol m^{-2} s^{-1} and 1.43 ± 0.14 mmol m^{-3} (n = 16, S.E.) respectively.

6.2.2. GROWTH

Figures 6.1 and 6.2 show that the growth rate, as previously found, was stimulated in the faster water movement treatments. There was, however, no significant difference in growth rate between the two faster water movement treatments (Growth-3 and Growth-5).

Nitrogen concentration (C/N = 17.9) was initially low in the disks but by day two the C/N ratio was less than 12 in all treatments, indicating that nitrogen was not limiting to growth after this period. Figure 6.3 shows that nitrogen was increasingly accumulated with time in all treatments. It also showed that the faster water treatment significantly increased its nitrogen concentration compared to the other two treatments. Two different mechanisms are most likely controlling the difference in uptake rates for nitrogen between the treatments. First, as previously mentioned (Chapter 5) the D.B.L. has a strong influence on nitrogen influx in comparison to its influence on phosphate (MacFarlane, 1985). Thus, a greater enhancement in nitrogen influx with decreasing D.B.L. resistance could be predicted. Second, the decrease in phosphate with time (Table 6.2) could lead to a decrease in the nitrogen influx as a result of a decrease in the metabolism of the plant. Clearly as a result of phosphate starvation the plant's energetic capacity must be reduced because of the importance of phosphate to energy transfer and membrane integrity, two important factors controlling nitrogen influx. Thus, nitrogen influx would also be affected because of its dependence

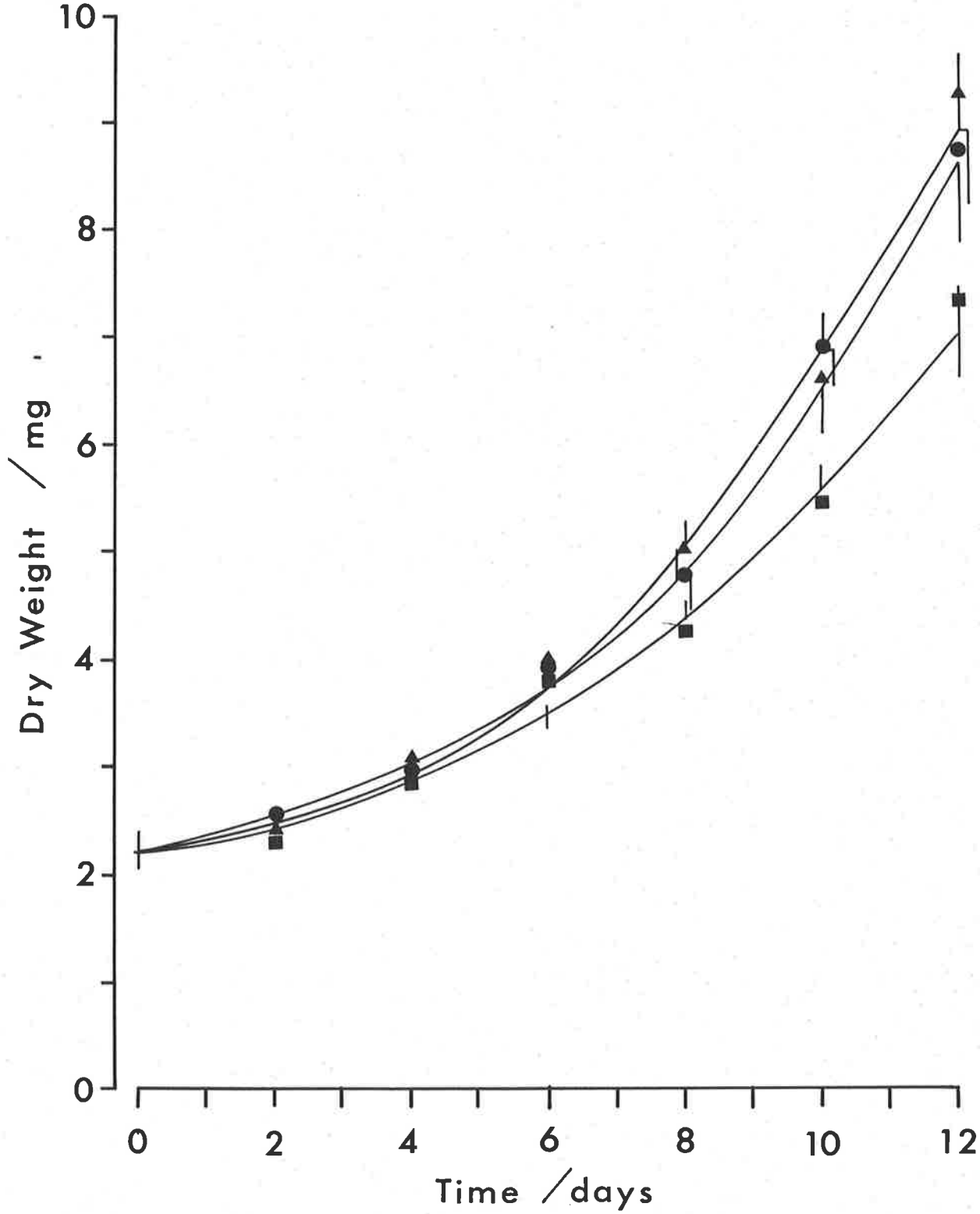

Figure 6.2. Disk dry weight versus time for the three water movement treatments (Hunt program, n = 16, C.L.). The symbols are the same as Figure 6.1.

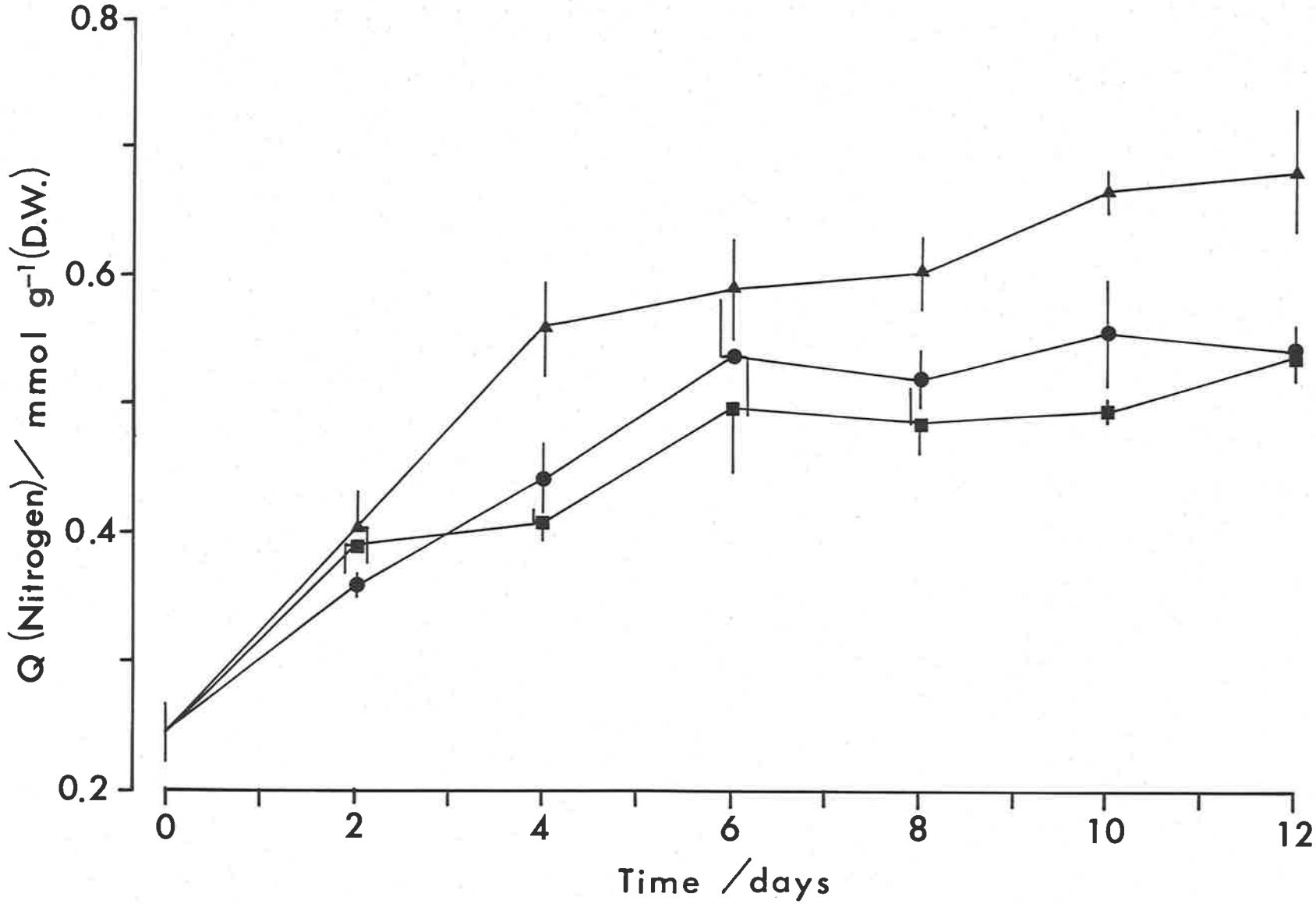

Figure 6.3. Cellular nitrogen concentration for the three growth treatments determined from the C.H.N. analysis method. The symbols are the same as Figure 6.1.

on the phosphate status of the plant. Therefore, a dual limitation of nitrogen influx ocurs when both phosphate limitation and water movement control growth and uptake.

TABLE 6.2. Internal phosphate concentration (Q), μmol g^{-1} (D.W.) (S.E., n = 16). Q for day 12 reflects the increased external phosphate concentration (20 mmol m^{-3}).

Time (d)	Growth-1	Growth-3	Growth-5
0	55.1 ± 8.1	55.1 ± 8.1	55.1 ± 8.1
2	48.3 ± 8.0	57.6 ± 6.3	65.4 ± 7.1
4	49.3 ± 6.1	60.4 ± 7.1	60.1 ± 7.8
6	39.0 ± 5.2	40.0 ± 3.1	57.2 ± 4.7
8	30.6 ± 3.1	28.8 ± 3.6	34.9 ± 4.4
10	21.4 ± 1.9	20.0 ± 1.6	26.3 ± 2.8
Phosphate spike			
12	84.8 ± 6.4	93.4 ± 6.6	117.8 ± 9.8

Table 6.2 shows that the decrease in Q (phosphate), was related to the water movement, with the slowest water movement treatment showing the fastest decline in Q. It also showed a rapid increase in Q with the addition of phosphate after day 10, and this increase in Q was related to the water movement. One would predict the value of Q to reach a maximum (qm) in each treatment, but this value could be affected by the different water movement in each treatment in a manner similar to qo was in Chapter 5. This conclusion depended on whether the magnitude of Q at day 12 represented the maximum internal phosphate concentration.

TABLE 6.3. Average growth rate based on dry weight (day^{-1})

Time (d)	Growth-1	Growth-3	Growth-5
2	0.022	0.066	0.020
4	0.065	0.074	0.075
6	0.091	0.095	0.097
8	0.082	0.097	0.101
10	0.091	0.114	0.109
Phosphate spike			
12	0.101	0.115	0.119

An anomaly occurred in relating R.G.R. to Q (Tables 6.2 and 6.3), because the predicted result (Equation 5.4, Droop) would be that as Q declined there would be a correlated decline in R.G.R. In two out of the three times that this type of growth-influx experiment was done R.G.R. and Q declined in synchrony, but as previously shown a lag can occur between growth and Q. Interestingly in this experiment R.G.R. continued to increase as Q declined to a magnitude in all treatments approximately equivalent to the minimum qo observed in prior experiments. This uncoupling of growth rate from the internal limiting nutrient concentration has been previously found to occur during experimental transients (Cunningham and Mass, 1978; Parslow, Harrison and Thompson, 1984a,b). Thus when plants grown in one set of environmental conditions are transferred to another set of conditions, initially the plant's metabolism (including growth rate) continues to perform at the same rate irrespective of the new environmental conditions (Cunningham and Mass, 1978). This lag time varies depending on the characteristics of the metabolic function, and for growth rate the results presented indicate that the lag can exist for as long as 10 days.

Droop's (1973) Equation 5.4 can be modified to make growth rate a function of time,

$$\mu = \mu mq(1 - qo/Qt) \qquad \text{Equ-6.4}$$

where Qt is the internal limiting nutrient concentration t hours or days before the actual calculation of μ. Cunningham and Maas (1978) found that t was approximately 10 hours for nitrogen limited growth of *Chlamydomonas reinhardtii*. The results for *U. australis* indicate that the lag time varies from one to ten days. Furthermore the lag for this type of experimental methodology is a combination of both wound (as previously mentioned) and transient responses. The variation in magnitude of the combined lag response reflects both the variation in response to wounding and the variation between the alternative set of environmental conditions. To empirically quantify the conditions to enable the lag response to be predicted is extremely difficult without a complete understanding of the plant's growth response to all combinations of factors that influence it. For this experiment, where the largest lag response was observed, the only experimental difference in comparison with the experiment presented in Section 5.3 was the change from A.S.W. to seawater in experimental medium. Predicting the growth lag magnitude requires further extensive research, especially considering the transient nature of the environment in reality. For *Ulva*, a plant that has adapted to environments characterized by a high degree of disturbance (Littler and Littler, 1980; Raven, 1981), its ability to minimize the effect of changes in environmental conditions would allow it to compete successfully for persistence (space) within the environment. It is therefore not surprising that *Ulva* can continue to grow at a high rate in conditions unfavourable for growth and this would increase its adaptive advantage.

6.2.3. THE EFFECT OF PHOSPHATE STARVATION ON SHORT TERM PHOSPHATE INFLUX.

Short term phosphate influx increased with time for all treatments when calculated on an area or fresh weight basis (Figures 6.4a,b,c and 6.5a,b,c). The initial influx was comparable with the observed results for Chapter 3. As predicted, the increase in influx correlated with the decline in Q with time (Figures 6.4a,b,c and 6.5a,b,c, Table 6.2). Figure 6.6 shows that phosphate influx at [Pi]b equal to 20 mmol m^{-3} increased with time, and for each treatment the influx plateaued at day 6 except for a sharp peak for the Growth-3 treatment at day 10. The rate of short term phosphate influx at day 10 meant that the change in Q over the final time period would occur in 7.9, 4.1 and 7.2 hours for the Growth-1, Growth-3 and Growth-5 treatments respectively. The rapid decline in influx when 20 mmol m^{-3} phosphate (Figure 6.6) was added after day 10 means that these times underestimate the time taken to reach the measured values of Q at day 12. Nevertheless, the enhanced phosphate influx rates provide a mechanism for rapid phosphate storage during spikes in the external phosphate concentration.

As a consequence of the increase in Vm the difference in D.B.L. resistance results in a more pronounced difference in phosphate influx between each treatment (Thomson and Dietschy, 1977). Therefore, a greater difference in growth rate between treatments would be predicted as Vm increases.

A hysteresis type phenomenon was observed for Vm and Km in comparing their initial values and those of day 12. Initially Vm = 0.82 ± 0.03 nmol m^{-2} s^{-1} and Km = 1.43 ± 0.14 mmol m^{-3}. By comparison the values for day 12 presented in Table 6.4 show that both Vm and Km were approximately five times or double respectively the initial values. The magnitude of the hysteresis, for the kinetic parameters, was related to

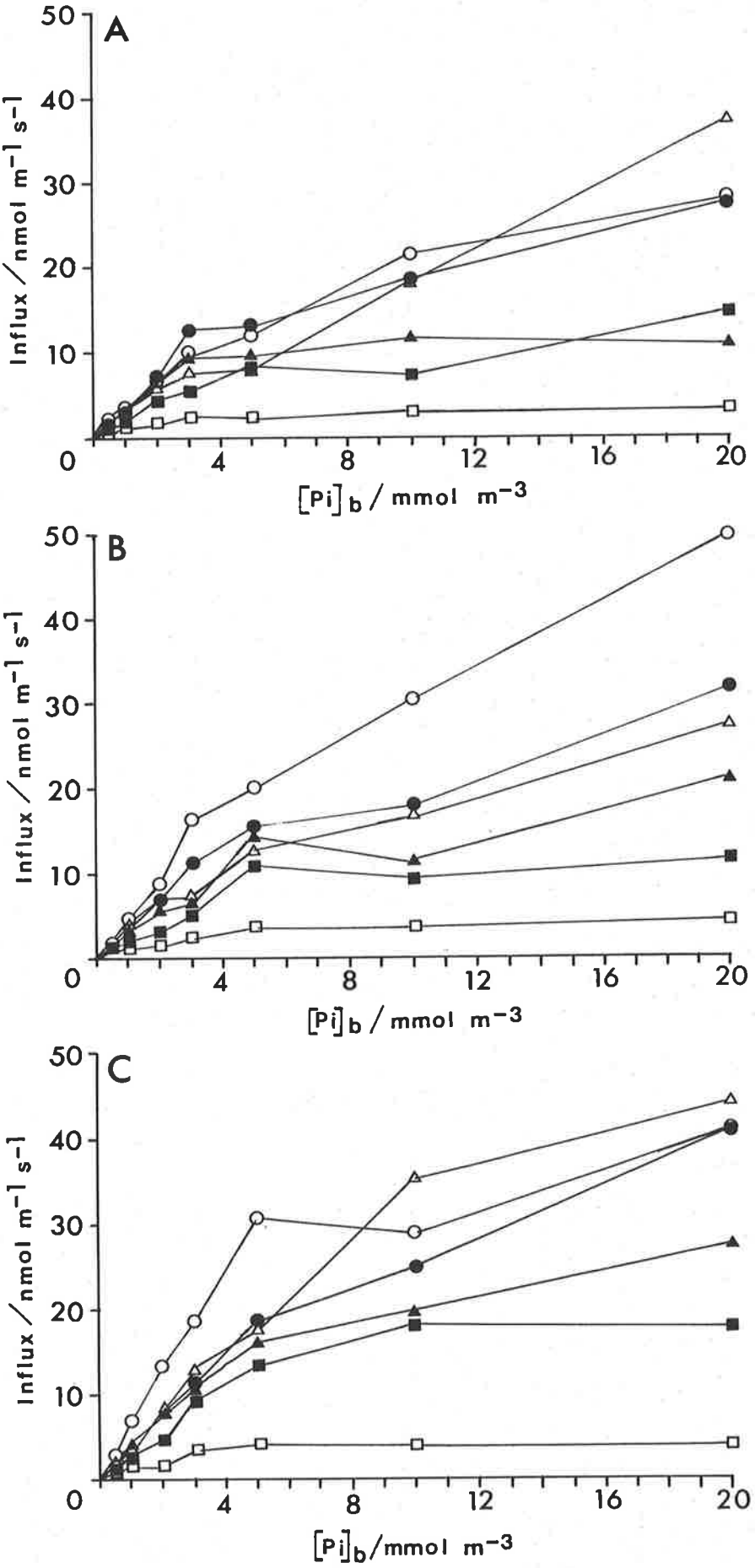

Figure 6.4. Phosphate influx (area) versus [Pi]b for days 2 (■), 4 (▲), 6 (△), 8 (●), 10 (○) and 12 (□). (A) Growth-1, (B) Growth-3, (C) Growth-5 (n = 2).

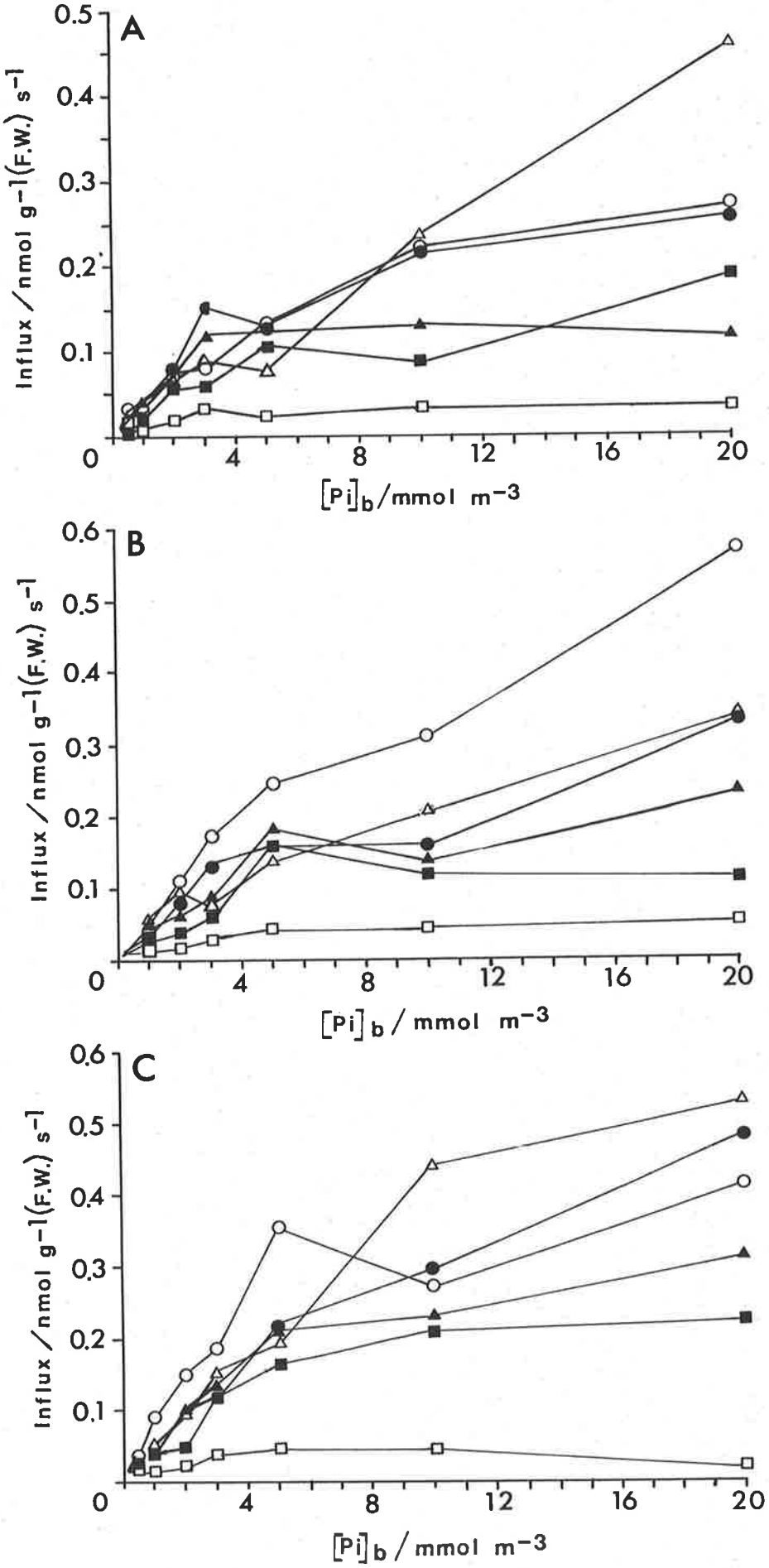

Figure 6.5 Phosphate influx (F.W.) versus [Pi]b. The symbols are the same as Figure 6.4. (A) Growth-1, (B) Growth-3, (C) Growth-5 (n = 2).

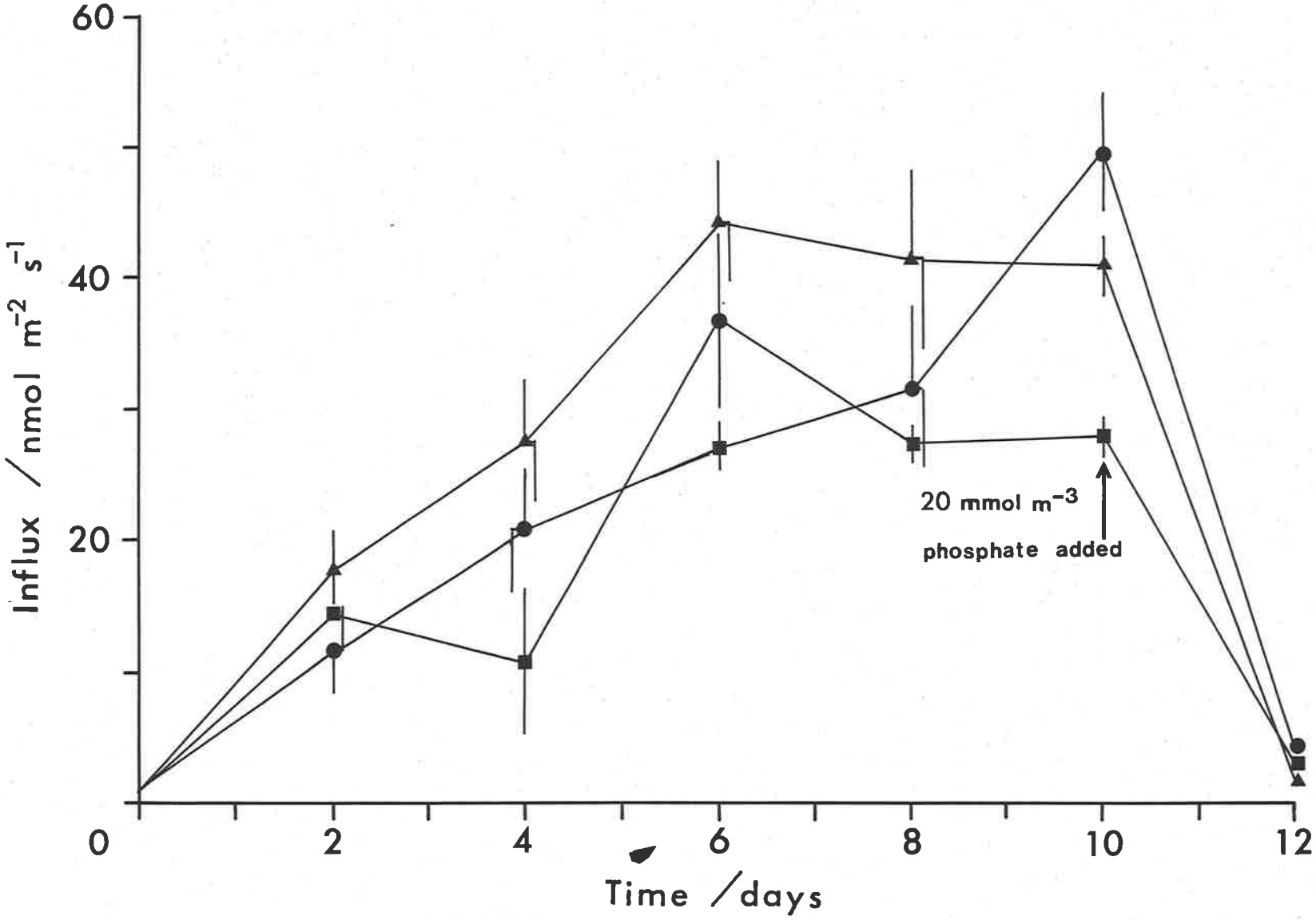

Figure 6.6. Short term phosphate influx at [Pi]b = 20 mmol m^{-3}, where the arrow indicates the addition of 20 mmol m^{-3} KH_2PO_4 at the end of day 10 (n = 2, C.L.). The symbols are the same as Figure 6.1.

the water movement of each treatment. Therefore the influence of the internal phosphate concentration in regulating the influx rate can be modified by the external water movement stimulus, and correlates with the increased growth rate for the final time period in comparison with the initial growth rate.

TABLE 6.4. Vm and Km for day 12 calculated using the program NONLIN (n = 16, S.E)

Kinetic Paramater	Experimental Treatment		
	Growth-1	Growth-3	Growth-5
Vm (nmol m^{-2} s^{-1})	3.72 ± 0.06	4.94 ± 0.14	5.00 ± 0.17
Km (mmol m^{-3})	2.84 ± 0.08	2.96 ± 0.14	2.56 ± 0.15

Specfic phosphate influx was calculated by dividing the short term influx (pmol g^{-1} (D.W.) s^{-1}) by Q (µmol g^{-1} (D.W.)), and is equivalent empirically to V/Q. Figures 6.7a,b,c show the specific influx saturating with [Pi]b in a similar fashion to influx. Equation 5.11 predicted that as growth reached steady state then the growth rate (µ) would equal V/Q, however the observed results predict a µmq sixty times the largest µmq measured. Nevertheless this is misleading as a more accurate comparison is between the specific influx and R.G.R. at [Pi]b. Table 6.5 shows that at time zero both V/Q and R.G.R. are approximately the same, indicating that growth was nearly at steady state. For the Growth-1 treatment, V/Q was approximately double the R.G.R during the experimental period. For the other two treatments V/Q initially parallels the increases in R.G.R., but as Q declined further the enhanced influx rate resulted in V/Q increasing to more than double the R.G.R..

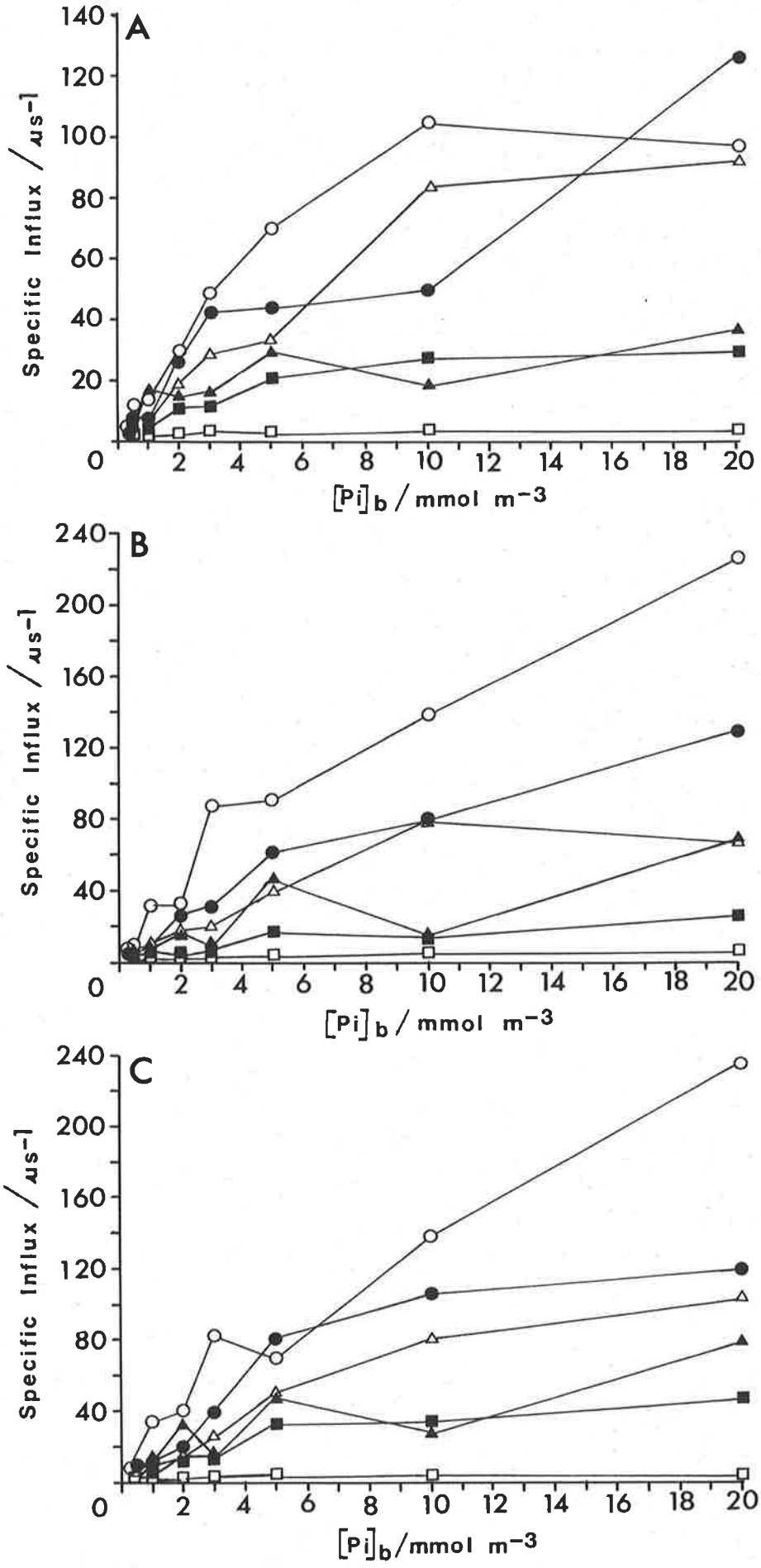

Figure 6.7. Specific phosphate influx versus [Pi]b for days 2 (■), 4 (▲), 6 (△), 8 (●), 10 (○) and 12 (□). (A) Growth-1, (B) Growth-3, (C) Growth-5 (n = 2).

Interestingly there was a good linear relationship between Km and Vm measured at constant water velocity (Figure 6.8, $r^2 = 0.95$, n = 19). The slope of this line was positive, indicating that Km increased as Vm increased. This contradicts most of the previous research on

TABLE 6.5. Comparison of average growth rate based on dry weight (day^{-1}) and specific phosphate influx (day^{-1}) at 0.11 mmol m^{-3} [Pi]b, data from Figures 6.7a,b,c.

Time	Growth-1		Growth-3		Growth-5	
(d)	R.G.R.	V/Q	R.G.R.	V/Q	R.G.R.	V/Q
0	0.020	0.021	0.020	0.021	0.020	0.021
2	0.022	0.081	0.066	0.086	0.020	0.048
4	0.065	0.115	0.074	0.082	0.075	0.061
6	0.091	0.120	0.095	0.097	0.097	0.114
8	0.082	0.143	0.097	0.133	0.101	0.291
10	0.091	0.194	0.114	0.292	0.109	0.289
Phosphate spike						
12	0.101	0.012	0.115	0.015	0.119	0.021

phosphate which had found that Km either decreased or remained constant with increasing Vm (Table 6.1). However the result is similar to that found by Probyn and Chapman (1982) for nitrogen influx into the brown alga *Chordaria flagelliformis*.

The enhancement in phosphate influx and its correlation with Q agree with an allosteric control of influx by the internal phosphate pool. However, the increase in Km cannot be explained by this allosteric effect. The change in Km with declining Q could be related to the

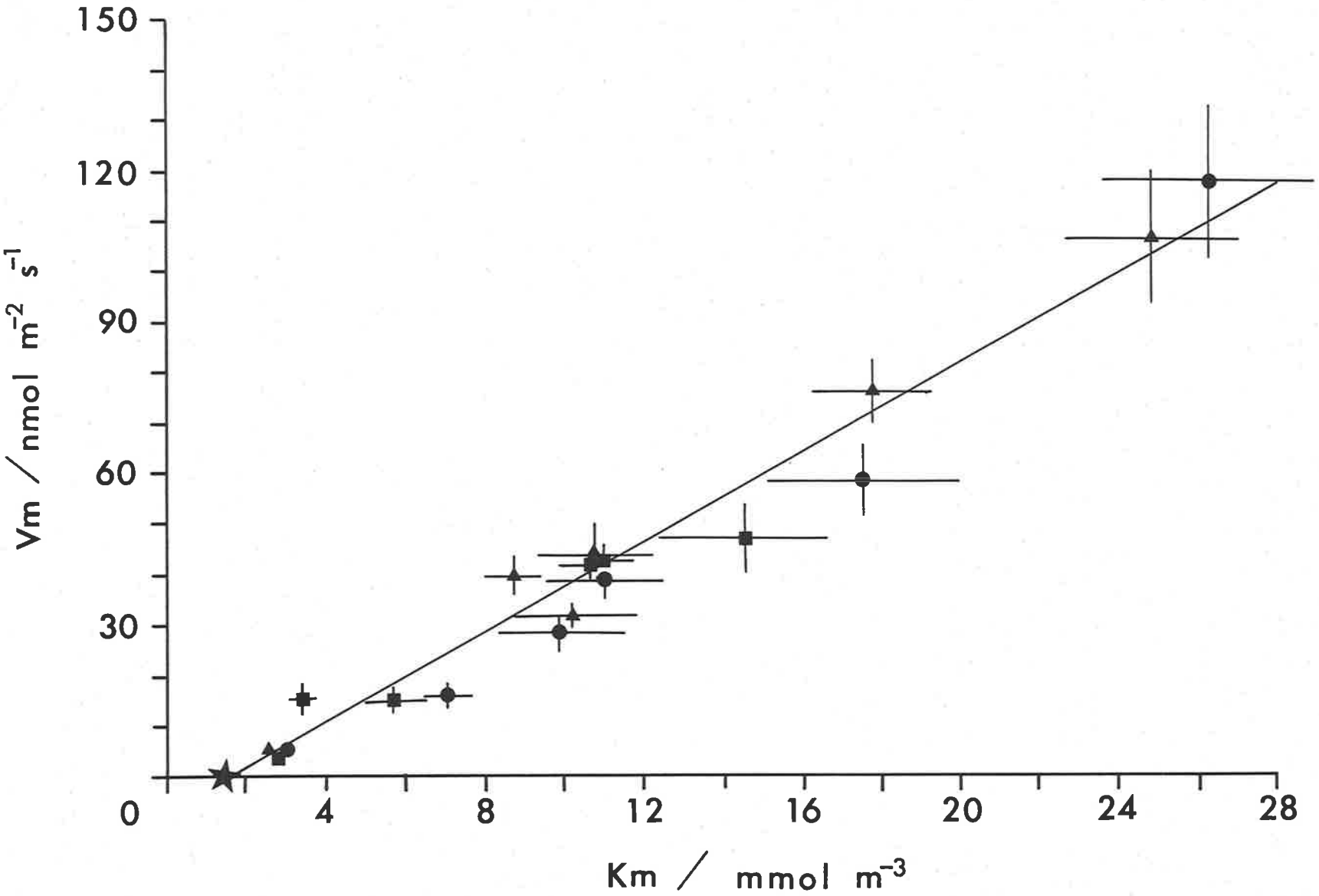

Figure 6.8. The relationship between Vm and Km, which were calculated using the program NONLIN. The fitted line was calculated by linear regression. The symbols are the same as Figure 6.1.

degradation of the carrier as a result of a decline in metabolic energy similar to the affect postulated for variation in nitrogen influx. The internal scenario would be that as Q declines, less metabolic energy would be available to maintain the carrier, therefore its affinity for phosphate would decrease resulting in a larger Km.

This concept could also explain the anomalous result that occurs in comparing influx with the uptake results measured over time (Table 6.6). In the Growth-1 treatment short term influx was greater than uptake for the experimental period, and in the other two treatments uptake declined continuously with time while influx increased initially and saturates at a relatively constant rate (Table 6.6). The initial values of uptake were larger than the influx values in the Growth-3 and Growth-5 treatments because uptake represents the total phosphate taken up over the two day period while influx represented the final uptake capability at the end of each two day period. Theoretically the uptake results should be related to the short term influx results averaged over time. The difference between uptake and influx indicates that efflux was an important component of the uptake observed with time. Previously it had been asserted that phosphate efflux was negligible compared to influx, nevertheless when Q declined the membrane integrity could be decreased which would allow phosphate to diffuse from the disks. Both Bieleski (1973) using *Nitella* and Schjorring and Jensen (1984a) using barley, buckwheat and rape seedlings have concluded that the balance between phosphate influx and efflux is important to plant growth. Schjorring and Jensen (1984a) also suggested that the control of phosphate efflux could be critical in maintaining adequate phosphate for growth. This argument precludes the difference in uptake that would occur during the dark period as this would not result in the large differences that were observed between influx and uptake. It also ignores the minor daily decrease in phoshate concentration within the medium.

The uptake rates for day 12 shown in Table 6.6, represent the time averaged enhanced influx rates, and as such should be larger than the final influx rate for each treatment.

TABLE 6.6. Phosphate uptake with growth calculated from difference in phosphate disk content with time (n = 16, S.E.). By comparison influx at 0.11 mmol m^{-3} (determined from Figures 6.4a,b,c) and for final time period at 20 mmol m^{-3} (units of uptake and influx were nmol m^{-2} s^{-1}).

Time	Growth-1		Growth-3		Growth-5	
(d)	Uptake	Influx	Uptake	Influx	Uptake	Influx
2	-0.305 ± 0.038	0.28	0.513 ± 0.064	0.25	0.736 ± 0.091	0.34
4	0.247 ± 0.028	0.47	0.556 ± 0.043	0.32	0.520 ± 0.066	0.50
6	0.152 ± 0.019	0.35	0.151 ± 0.014	0.39	0.494 ± 0.062	0.48
8	0.057 ± 0.008	0.42	0.073 ± 0.011	0.36	0.154 ± 0.024	0.47
10	0.009 ± 0.002	0.42	0.038 ± 0.004	0.49	0.064 ± 0.008	0.45
Phosphate spike						
12	4.365 ± 0.425	3.15	4.970 ± 0.286	4.52	6.295 ± 0.393	4.19

Healey (1980) has shown that the initial influx slope is a better measure of the ability of an alga to compete for nutrient resources than the use of its affinity constant (Km). As an approximation Healey calculated the initial slope as Vm/Km. Table 6.7 shows that Vm/Km rapidly increased within the first two days for all treatments and then stablized at between 3 and 4 µm s^{-1}. With the addition of the phosphate spike, Vm/Km decreased to approximately half its value at the previous time period. The increase in Vm/Km correlated with the decline in Q with time, indicating that although Km increased the *U. australis* disks had a greater capability to remove phosphate from

the external medium. The linear relationship between Vm and Km shown in Figure 6.8 correlates with the relatively constant ratio of Vm/Km between days 2 to 10 for all treatments. However, as shown in Table 6.6 this did not result in a greater uptake rate at the concentration of phosphate in the medium used for the experiment. Nevertheless, the enhanced influx rate resulted in a rapid increase in Q (Table 6.2) when the medium was spiked with additional phosphate. Therefore, the enhancement of phosphate influx enables the plant to utilize short term surges in the external phosphate concentration, but does not influence uptake during periods of stable low phosphate concentration.

TABLE 6.7. Initial slope (Vm/Km $\mu m\ s^{-1}$) of the influx versus [Pi]b (Vm/Km at time zero = 0.57 $\mu m\ s^{-1}$). Vm and Km were calculated using the program NONLIN.

Time (d)	Growth-1	Growth-3	Growth-5
2	2.60	2.31	3.10
4	4.36	2.84	4.55
6	3.23	3.54	4.37
8	3.87	3.31	4.27
10	3.89	4.46	4.05
Phosphate spike			
12	1.31	1.67	1.95

The existence of small scale nutrient patches within the water column has been used by researchers working with phytoplankton (McCarthy and Goldman, 1979; Lehman and Scavia, 1982) to account for both the diversity of the assemblages and the existence of enhanced uptake capacity. Parslow, Harrison and Thompson (1984b) have discredited this theory claiming that the duration of these patches is very short due to

their rapid dispersal by diffusion. They claim that the enhanced influx rates are an important adaptation for growth of phytoplankton during long periods of low uniform concentrations. As shown for *U. australis* during periods of low uniform concentrations of phosphate the uptake rate declines irrespective of the enhanced influx rates. This is not surprising considering the difference in scale between micro and macroalgae, and the importance scale has in determining the selection criteria for plant adaptation. The environmental conditions at Saint Kilda where the *U. australis* plants were collected, are generally benign with periodic disturbances and surges in the external nutrient concentration. The larger scale of both the plants and the nutrient patches would fit with the ability of *U. australis* plants to rapidly take advantage of any sudden increases in phosphate concentration.

Lapointe (1985) has shown that pulses of phosphate are important in the growth strategy of *Gracilaria tikvahiae*, and further that phosphate was equally as important if not more so than nitrogen in conditions where the plant relied on pulses of higher nutrient concentration for growth. This has considerable implications for aquaculture management, because by pulsing the nutrient supply at the appropriate duration the managed plant can utilize the increased nutrient supply therefore reducing the nutrients available for economically damaging epiphyte growth. Thus the plant can be nutrient loaded for considerable periods without affecting its growth rate. Further, nutrient costs would be reduced because losses to epiphytes would be considerably reduced.

The nature of the inhibitor which signals the changes in influx has not been identified (Rhee, 1973). However, because of the rapid equilibrium between the different forms of internal phosphorus any one type can be correlated with the magnitude of the inhibitor signal (Chen, 1974). It is not surprising then that the total phosphate concentration

internally correlates with the changes in influx.

The use of multiphasic, dual uptake isotherms or slip models (Borstlap, 1981, 1983; Sanders, 1986) are inappropriate for explaining the relationship between enhanced influx and changes in the internal concentration. Therefore any attempt to model the allosteric influence of phosphate requires postulating only one transport system. Because the enhancement of phosphate occurred relatively quickly over the first two days, the models do not need to account for a lag in the initiation of the phosphate enhancement. The next two sections derive two models of influx which can account for the observed changes in influx, Q and changes in the kinetic constants.

6.2.3.1. EXPONENTIAL MODEL OF PHOSPHATE INFLUX

Figures 6.9a,b show an exponential relationship between Vm or Km with Q (Km and Vm were calculated using the program NONLIN). For Vm, this is similar to the relationship observed by Siddiqi and Glass (1982). However, they found the opposite exponential relationship between Km and Q (as mentioned in Section 6.1). Linear regressions of the natural logarithms of Vm or Km versus Q show a good correlation except for lnKm versus Q (Table 6.8).

An empirical expression, relating influx (V(i)), Q and the external phosphate concentration, similar to that derived by Siddiqi and Glass (1982) can be formulated from the expression for the relationship between ln of Vm or Km versus Q. This expression has the form,

$$Vm(i) = MaxVm.e^{ki} \qquad \text{Equ-6.5}$$

or

$$Km(i) = MaxKm.e^{k'i} \qquad \text{Equ-6.6}$$

where Vm(i) and Km(i) represent the kinetic parameters as a function of the internal concentration (i), k and k' are the slopes of the regressions for Vm and Km versus Q respectively, and MaxVm and MaxKm are the theoretical maximum values of Vm and Km respectively at zero

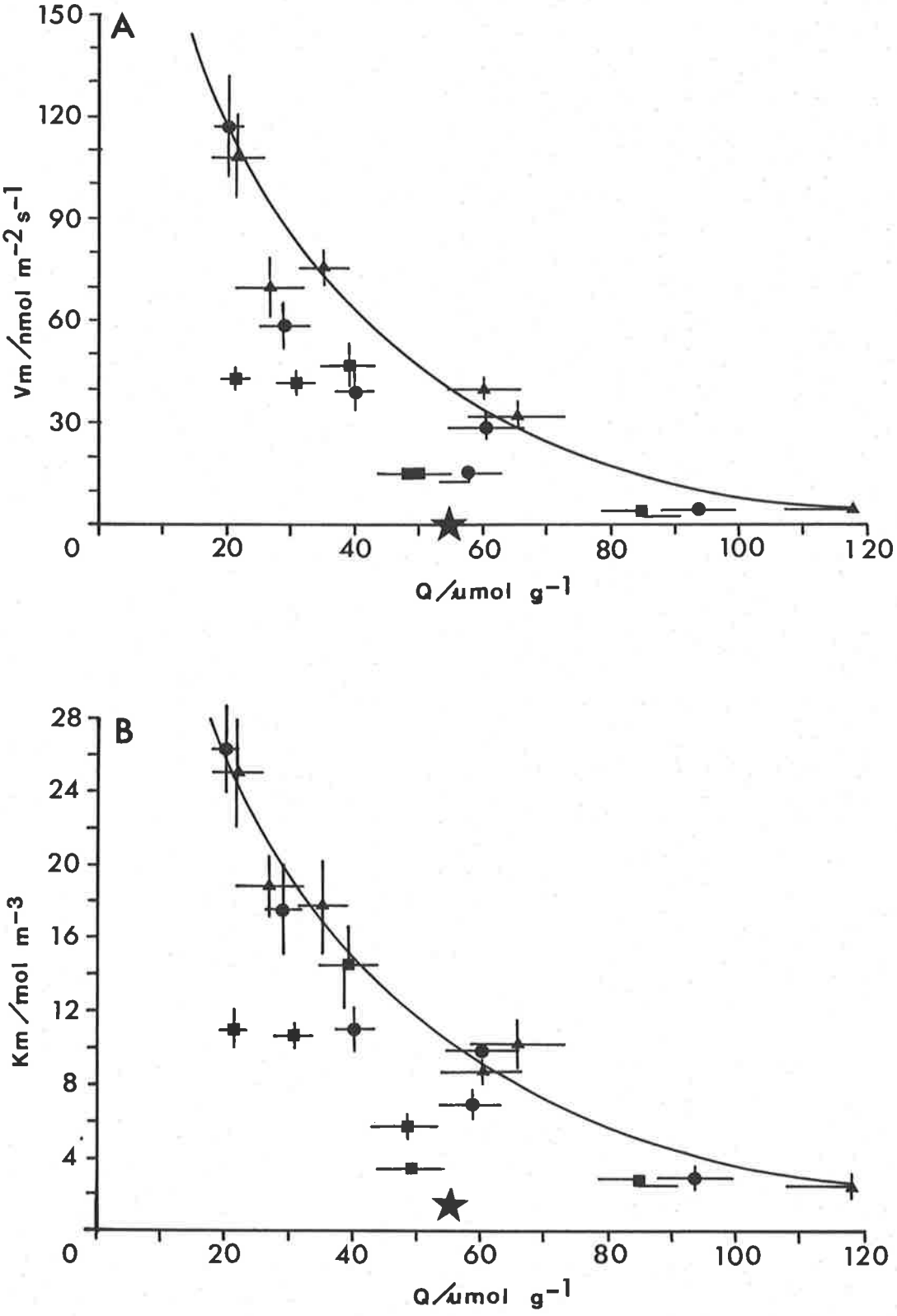

Figure 6.9. Changes in Vm and Km (calculated using the program NONLIN) versus internal total phosphate concentration (D.W., n = 16, C.L.), curves fitted by eye. The symbols are the same as Figure 6.1. (A) Vm versus Q, (B) Km versus Q.

internal concentration. Equations 6.5 and 6.6 can be substituted into the Briggs-Haldane equation, hence

$$V(i) = (MaxVm.e^{ki}\ Cs)(MaxKm.e^{k'i} + Cs)^{-1} \qquad \text{Equ-6.7}$$

where the major difference between Equation 6.7 and that derived by Siddiqi and Glass (1982, Equation 6.1) is the use of the MaxKm as opposed to the MinKm by Siddiqi and Glass. The values of the parameters in Equation 6.7 are given in Table 6.8.

TABLE 6.8. Linear regression of either Vm or Km versus Q.

Treatment	maxKm	k'	r^2	maxVm	k	r^2
Growth-1	21.2	-0.025	0.67	140.9	-0.042	0.91
Growth-3	41.1	-0.027	0.95	223.2	-0.040	0.96
Growth-5	40.0	-0.023	0.98	284.4	-0.034	0.99

Similarly, an expression can be derived relating Equation 6.7 to changes in the D.B.L. with increasing water movement,

$$V(i) = 0.5[Km(i)Kt + CbKt + Vm(i) - \sqrt{(Km(i)Kt + CbKt + Vm(i))^2 - 4KtCbVm(i)}] \qquad \text{Equ-6.8}$$

which is similar in form to the Briggs-Maskell equation.

There was a good correlation between Equation 6.8 and the observed results (Figures 6.4a,b,c) with the r^2 varying from 0.92 to 0.99 (determined using the curve fit program FVKUP modified to fit Equation 6.8). The exceptions were the Growth-3 treatment results for day 10 where the calculated r^2 was 0.72. Figure 6.10 shows that with decreasing Q there was a greater significant difference in influx as predicted. The apparent non-significant difference at high values of Q results from the expanded influx scale.

The calculated differences in the parameters (Table 6.8) for Equation 6.7 correlates with the differences in water movement and also

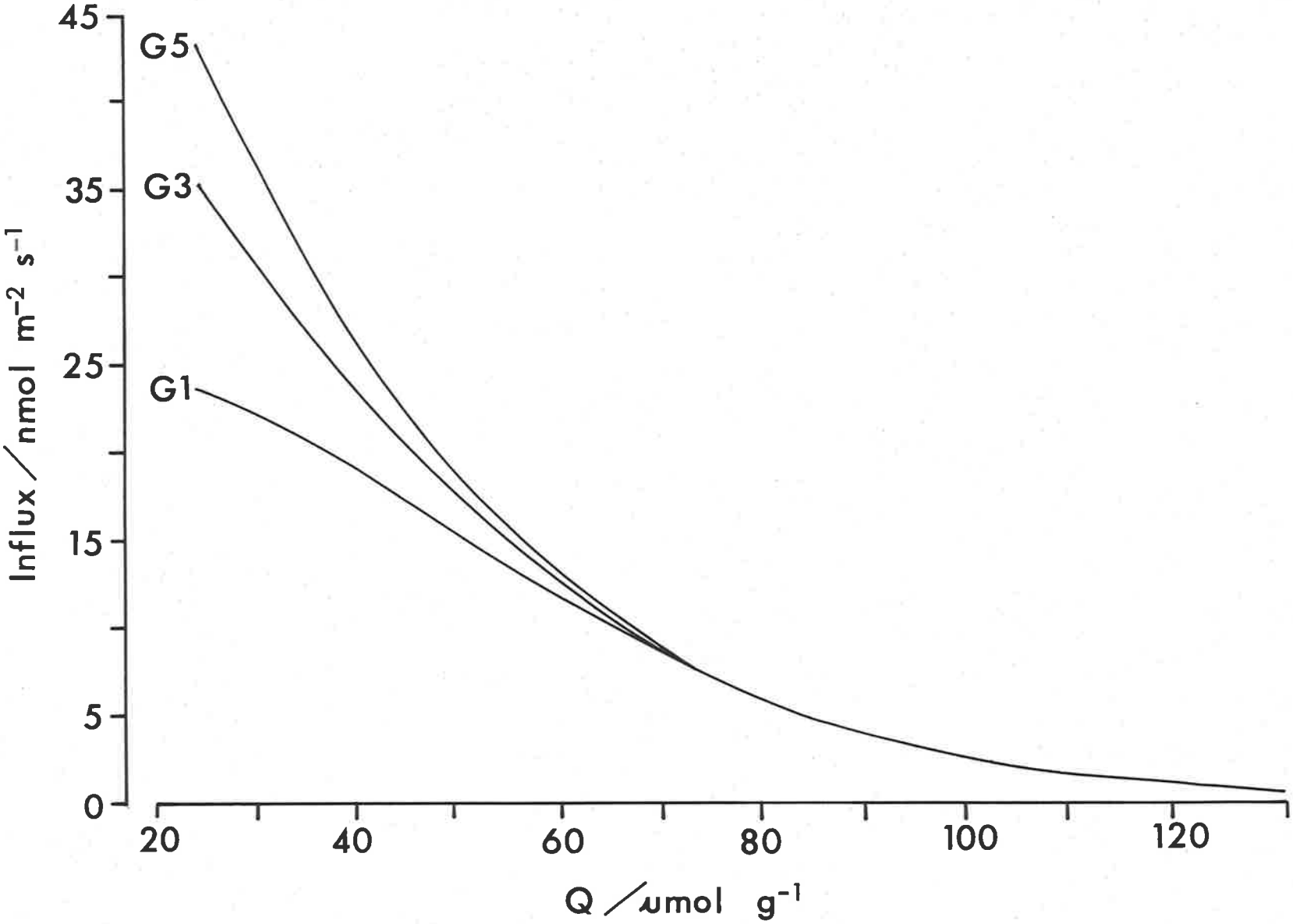

Figure 6.10. Predicted relationship between phosphate influx and internal total phosphate concentration (Q, D.W.) calculated using Equation 6.8. G1 = Growth-1, G3 = Growth-3 and G5 = Growth-5.

varied between different experiments. The argument used to explain the difference between phosphate uptake and influx can also be applied to the observed increase in Km with decreasing Q. Because the metabolic energy available for energy transfer is reduced with declining Q the phosphate carrier system degrades resulting in an apparent increase in Km. Further, the membrane integrity, of which phosphate is an important component, would decline which could explain the linear phase of influx at high [Pi]b (Figures 6.4a,b,c) as this could relate to a diffusion component of influx.

Interestingly, Besford (1979) found an exponential increase in phosphatase activity with declining internal phosphate concentration. Szabo-Nagy, Olah and Erdei (1987) have proposed that the increase in phosphatase activity may play a role in the re-utilization of bound phosphorus within the cytoplasm. No attempt was made to measure phosphatase activity. However the similar response of an exponential increase in phosphatase activity with decreasing Q implies that a similar signal induces both enhanced phosphate influx and increasing synthesis of phosphatase.

The disadvantage of the model of influx predicted by Equation 6.8 is that the parameters MaxVm, MaxKm and the slopes are not constant but depend on other unknown factors associated with their growth in different water velocities.

6.2.3.2. UN-COMPETITIVE INHIBITION MODEL

The observed linear relationship between Km and Vm (Figure 6.8) meant that Km and Vm increase at similar rates, therefore a plot of the reciprocals of influx versus [Pi]b results in approximately parallel slopes for each time period. Dixon and Webb (1964) described this result as characteristic of non-competitive inhibition, sometimes called

anti-competitive inhibition (Dodgson, Spencer and Williams, 1956). Using the enzyme terminology of Dixon and Webb (1964), the enzyme reaction can be depicted by,

$$E + S \underset{k_2}{\overset{k_1}{\rightleftharpoons}} ES \xrightarrow{k_3} E + \text{products}$$

where E is the enzyme, S is the substrate, ES is the enzyme-substrate complex, and k1, k2 and k3 are the equilibrium dissociation constants for the indicated reactions. The reaction velocity (V) is given by,

$$V = k3.e.s[(k2 + k3)/k1 + s]^{-1} \qquad \text{Equ-6.9}$$

where e and s (= Cs) are the enzyme and substrate concentration respectively. The dissociation term was simplified by Briggs-Haldane to,

$$Km = (k2 + k3)/k1 \qquad \text{Equ-6.10}$$

and accounts for the possibility that ES may not always be in equilibrium with E and S. The term Km is therefore not a pure equilibrium constant as it also includes a kinetic element. Also

$$Vm = k3.e \qquad \text{Equ-6.11}$$

therefore Equation 6.9 simplifies to the Briggs-Haldane equation.

For the case when

$$Km = k3/k1 \qquad (k3 >> k2) \qquad \text{Equ-6.12}$$

an inhibition which only effects k3 will produce proportional changes in Vm and Km as experimentally observed. Diagrammatically this can be represented by

$$E + S \underset{k_2}{\overset{k_1}{\rightleftharpoons}} ES \xrightarrow{k_3} E + \text{products}$$
$$k_5 \downarrow\uparrow k_6$$
$$ESI$$

where ESI represents an inhibitor (I) binding with the ES complex. The reaction velocity can be determined from,

$$V(i) = Vm^{*}(1 + Ks^{*}/Cs + i/Ki)^{-1} \qquad \text{Equ-6.13}$$

where Ks is the substrate dissociation constant (k2/k1), Ks^{*} is the apparent Ks, Vm^{*} is the apparent maximum reaction velocity, Ki is the inhibitor dissociation constant (k6/k5), and i represents the concentration of the inhibitor (Ebersole, Guttentag and Wilson, 1943; Dodgson, Spencer and Williams, 1956). For the case of phosphate influx

inhibition by the cellular phosphate concentration then i is equivalent to Q, hence

$$V(Q) = Vm^{*}(1 + Ks^{*}/Cs + (Q - qi)/Ki)^{-1} \qquad \text{Equ-6.14}$$

where qi is the internal phosphate concentration at which zero inhibiton of phosphate influx occurs. The reciprocal of Equation 6.14 is

$$1/V(Q) = [1 + (Q - qi)/Ki](1/Vm^{*}) + (Ks^{*}/Vm^{*})(1/Cs) \qquad \text{Equ-6.15}$$

therefore a plot of 1/V(Q) versus 1/Cs results in a series of parallel lines (slope = Ks^{*}/Vm^{*}) and the x-axis intercept increases by [1 + (Q - qi)/Ki]. Also if 1/V(Q) is ploted against (Q - qi) then Ki can be determined from the slope and was equal to 15.7 ± 1.4 μmol g^{-1} (D.W., n = 19, S.E.). As an approximation qi was approximated to qo.

A Briggs-Maskell type equation can be derived from equation 6.13,

$$V(Q) = (Cb + Ks^{*} + Vm^{*}Rt + CbF - \sqrt{(Cb + Ks^{*} + Vm^{*}Rt + CbF)^{2} - 4Vm^{*}Cb(Rt + RtF)})[2(Rt + RtF)]^{-1} \qquad \text{Equ-6.16}$$

where Rt, the mass transfer resistance is substituted for 1/Kt, and F is equal to (Q - qi)/Ki.

Equation 6.16 gave a similar good fit (r^{2} = 0.89 to 0.99, using a modification of the program FVKUP) to the observed results as Equation 6.8. This model implies that the internal phosphate concentration acts as an inhibitor of the carrier protein, and because this inhibition affects the ES complex the site of inhibition would be within the cell membrane. This agrees with the allosteric model of control postulated by Glass (1976). Parslow, Harrison and Thompson (1985) observed that enhanced ammonium influx in the marine diatom *Thalassiosira* could be explained using an un-competitive model. However, they did not attempt to show how this related to their observed results. Manley (1985), also related enhanced phosphate influx in *Macrocystis* to an inhibitor type

model, but failed to mention the type of inhibition the model referred to.

6.3. TIMING OF THE ENHANCED PHOSPHATE INFLUX SIGNAL

The method described in Section 2.8.1.1.7. was used to determine the time required for the enhanced phosphate influx to decline. Disks of *U. australis* were initially grown for two days in A.S.W. with added Hoagland's solution minus phosphate. Figure 6.11 shows that there was a rapid decline in phosphate influx within the first 30 minutes and thereafter a more gradual decrease in phosphate influx. This gradual decline agrees with the signal for phosphate influx being an initial rapid filling of the internal phosphate pool followed by a slower increase in the internal phosphate pool. Parslow, Harrison and Thompson (1984a) found that the changes in ammonium influx occurred within minutes of additional ammonium being added, and observed that this time scale could not be explained by changes in the membrane characteristics. They proposed that the changes in influx were more likely to result from underlying changes in the number of functional uptake sites.

Use of the un-competitive model of influx does not infer changes in the number of uptake sites and is in agreement with the result for a gradual decline in influx signaled by the filling of the internal phosphate pool. However, more research is required to resolve the timing of the signal within the first minutes of an external spike in the nutrient concentration.

6.4. INFLUX ALONG THE LENGTH OF THE THALLUS

Phosphate influx was measured along the length of rectangular pieces of *U. australis* using the method described in Section 2.8.1.2.1. Because the flow tank required a large volume of seawater (78 litres) which required a large volume of radioactive phosphate, this method was restricted to very few experiments.

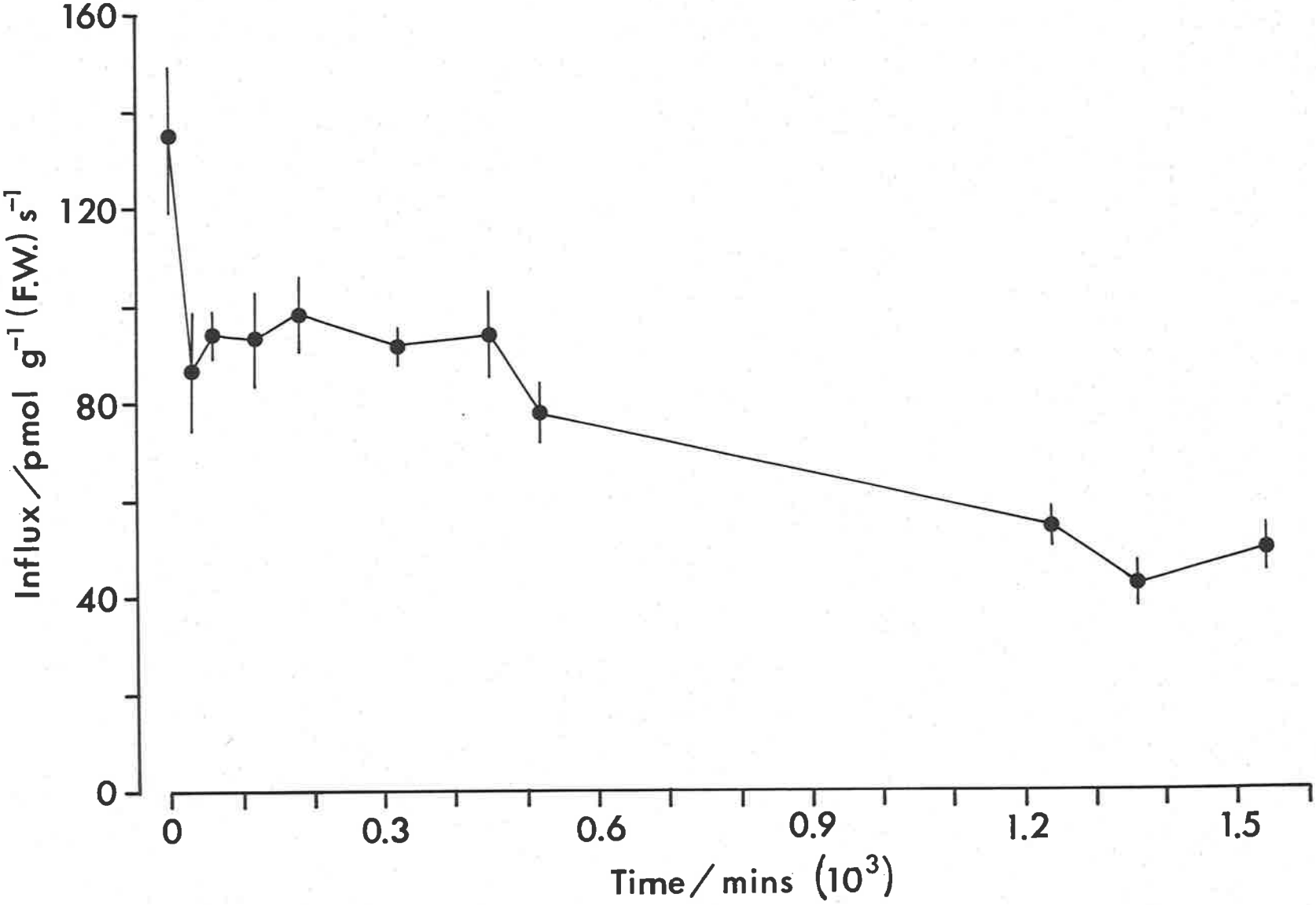

Figure 6.11. Observed decrease in phosphate influx ([Pi]b = 10 mmol m^{-1}) with increased phosphate loading ([Pi]b = 10 mmol m^{-3}) with time (n = 4, C.L.).

TABLE 6.9. Experimental characteristics for the flow tank experiments (S.E., n =10).

Experiment number	Water velocity cm s^{-1}	Q (phosphate) µmol g^{-1} (D.W.)	[Pi]b mmol m^{-3}
1	0.5	30.8 ± 1.6	0.19 ± 0.04
2	0.5	36.8 ± 1.1	0.12 ± 0.06
3	1.0	32.1 ± 0.5	0.09 ± 0.02
4	1.3	38.2 ± 2.3	0.13 ± 0.07

Figure 6.12a shows that phosphate influx decreased with increasing distance from the leading edge for experiments 1-3, but there was only a negligible decrease in experiment 4. The levelling of the influx along the thallus correlated with the changes in the thickness of the phosphate D.B.L., measured with the zinc method.

U. australis exists as a free floating alga at Saint Kilda and therefore does not exhibit the waving action characteristic of plants attached to a solid substrate. Water movement within the Saint Kilda region consists mainly of tidal action due to its locality, apart from periodic storm disturbances. It is reasonable to assume therefore that plants of *U. australis* are influenced by uni-directional water movement during each tidal cycle. The differential phosphate influx found along the length of the *U. australis* thallus indicates that in the field situation plants of *U. australis* take up phosphate at a greater rate near the thallus periphery compared to the inner part of the thallus when the water velocity is below 1.3 cm s^{-1}. Although *Ulva* grows by diffuse cell expansion, the cells near the thallus margins grow faster which would be facilitated by the greater phosphate influx in this region at low water velocities.

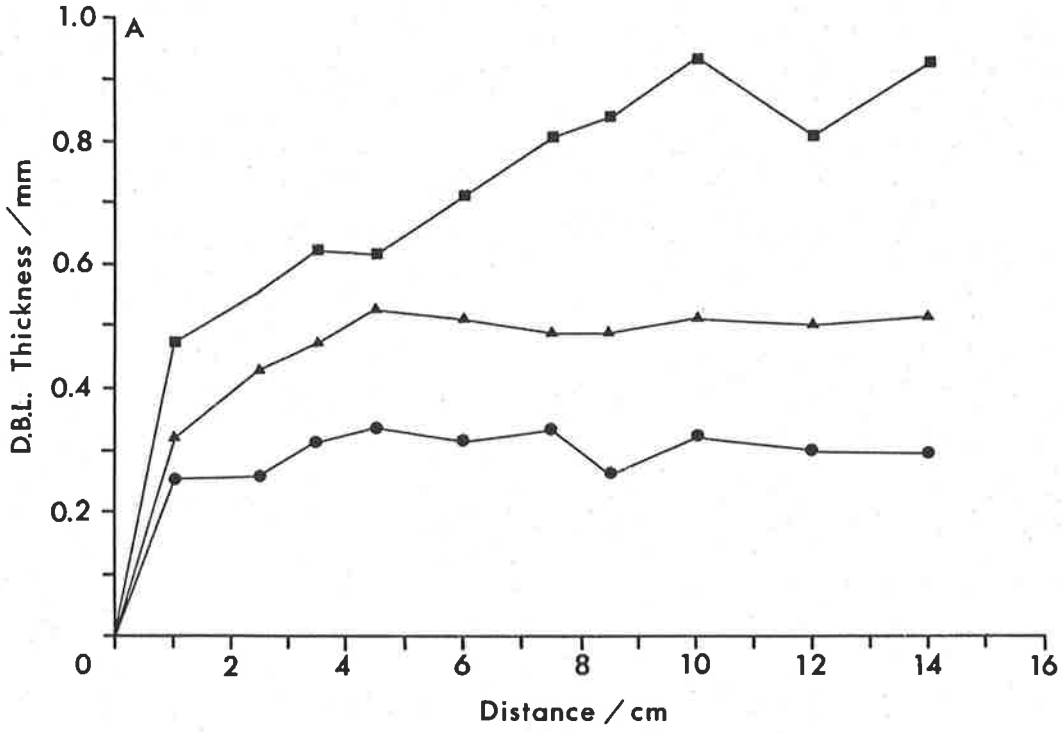

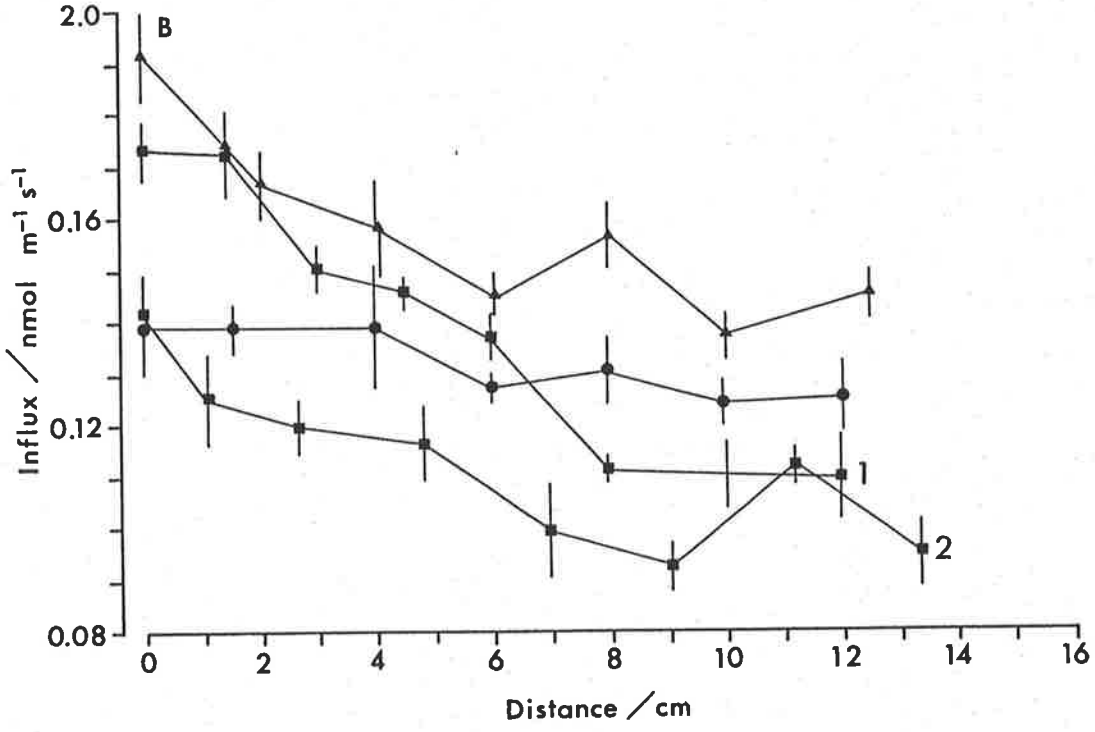

Figure 6.12. (A) Phosphate ($H_2PO_4^-$) D.B.L. thickness along the length of a flat plate, (■) 0.5 cm s^{-1}, (▲) 1.0 cm s^{-1} and (●) 1.3 cm s^{-1}.

(B) Phosphate influx along the length of the plant for Experiment 1 (■), Experiment 2 (■), Experiment 3 (▲) and Experiment 4 (●) (n = 8, C.L.).

6.5. CONCLUSIONS

The enhanced phosphate influx was correlated with changes in the internal phosphate concentration in agreement with an allosteric type model as predicted by previous research (Table 6.1). At low external phosphate concentrations the enhanced phosphate influx rates are modified by apparent increases in efflux, resulting in a decline in net phosphate flux (uptake) with decreasing Q. It was hypothesized that the decrease in internal phosphate concentration resulted in less metabolic energy available for cell maintenance. This resulted in a reduction in the membrane integrity, a decline in nitrogen uptake, a greater efflux potential and a possible degradation of the phosphate carrier. However, the un-competitive model of influx could explain the changes in influx without inferring a change in the carrier. Using the allosteric model it was not necessary to infer an increase in the uptake sites or changes in the affinity of the carrier. The use of a single transport system elicits the least energy consuming mechanism for the acquisition of phosphate. Also the models presented assume the least metabolic changes to transport without having to evoke the synthesis of different transport systems.

The enhancement in phosphate influx was important in maximizing uptake during periods of increased phosphate concentration. Therefore regulation of phosphate influx and metabolism in response to changes in the phosphate supply would be an adaptive advantage in an environment where the growth of *U. australis* is phosphate limited. Thomas and Harrison (1987) have observed an increase in ammonium uptake for macroalgae growing in field conditions. Therefore, the enhanced phosphate influx rate observed under laboratory conditions does have some validity and adaptive significance in the field.

CHAPTER 7. CONCLUSIONS.

The major aim of this work was to examine the interactions between water movement, phosphate influx and growth in an attempt to derive empirically a model to predict the observed results of these interactions. In Chapter 3 it was found that the effect of increasing water movement on short term phosphate influx was to decrease Km. It was predicted that this variation in phosphate influx would influence the growth rate; however, in the experiments described in Chapter 4 it was found that no significant difference in growth occurred between the different water movement treatments. It was concluded that this was because of the dual growth limitation by both phosphate and inorganic nitrogen and the large experimental variance observed between treatments. By preconditioning the plants in a more controlled nutrient and growth environment it was found in Chapter 5 that the rate of growth of *U. australis* increased with increasing water movement. Further, this growth difference could be predicted by relating phosphate influx to internal total phosphate concentration. Nevertheless, the model of growth and phosphate influx used in Chapter 5 could not account for the changes in phosphate uptake at a constant concentration of phosphate in the medium, nor for the observed lag in growth rate when the experimental conditions were changed. The results of Chapter 6 showed that short term phosphate influx increased as the internal total phosphate concentration decreased. This relationship between short term phosphate influx and internal total phosphate concentration was adequately described by two models postulating an allosteric control of phosphate influx by changes in the cellular concentration of phosphate. However, the response of phosphate uptake differed to that for phosphate influx with a decline in phosphate uptake being observed as the internal total phosphate concentration decreased. It was concluded that the

enhanced short term phosphate influx was ecologically only important to plants of *U. australis* during periods when pulses of increased phosphate concentration occur within its immediate environment.

The next sections detail in more depth the conclusions, implications and future lines of research from the research presented within this thesis.

7.1. THE EFFECT OF WATER MOVEMENT ON SHORT TERM PHOSPHATE INFLUX AND PHOSPHATE UPTAKE.

Short phosphate influx was shown to be influenced by changes in water movement relative to disks of *U. australis* (Chapter 3). It has been predicted that the use of the empirical relationships between water velocity and a chemical reaction occurring at the surface of a flat plate (described in Chapter 1) would provide an *a priori* method of determining the extent to which diffusional limitations associated with the presence of a D.B.L. would influence the chemical reaction process. Although these formulae can approximately predict the thickness of the D.B.L. and therefore the magnitude of the diffusional flux to the surface of the object, they failed to predict the effect of water movement on short term phosphate influx. It was concluded in Chapter 3 that the possibility of more than one phosphate ion species diffusing to the plant's surface effectively short circuited the predicted response between $H_2PO_4^-$ influx and water movement. MacFarlane's (1985) model of dual diffusion of both $H_2PO_4^-$ and HPO_4^{2-} through the D.B.L. was the model of phosphate diffusion to the object's surface that gave the best fit to the observed results. In effect what was occurring was that within the D.B.L. the fast equilibrium between $H_2PO_4^-$ and HPO_4^{2-} was effectively increasing the concentration of $H_2PO_4^-$ at the plants surface. By combining the parallel resistances of both $H_2PO_4^-$ and HPO_4^{2-} it was possible to predict the effect of water movement on phosphate influx using the Briggs-Maskell equation.

For a nutrient which occurs in solution at equilibrium with other related nutrient species it is necessary to know the speed of equilibrium, and the individual resistances for each nutrient species to establish the overall resistance within the boundary layer. For this reason the use of the theoretical D.B.L. formulae cannot not be used solely to predict the outcome between water movement and influx. Further, because each nutrient has a different diffusion coefficient its D.B.L. thickness and hence its resistance will differ from other nutrients. Therefore a plant growing in seawater would be surrounded by a diffusion boundary layer for each nutrient that was transported across its membrane.

In Chapter 6 it was shown that short term phosphate influx could increase 50 fold in response to phosphate starvation. The magnitude of short term phosphate influx was also dependent on the growth status of the plant when phosphate was non-limiting to growth (hysteresis phenomenon). The enhancement of phosphate influx by phosphate starvation and its dependence on the plant's growth status could explain why the phosphate influx results of Chapter 3 (Vm = 1 to 2 nmol m^{-2} s^{-1}) in comparison to the results of previous studies (for example, *Ulva rigida*, Vm = 15 nmol m^{-2} s^{-1}, MacFarlane, 1985 and *Macrocystis pyrifera*, Vm = 14 nmol m^{-2} s^{-1}, Manley, 1985) varied to such a large degree. This clearly emphasizes the danger in applying results determined only under one set of environmental conditions to possible ecological implications, and as a species comparison between alternative research efforts.

In Chapter 3 it was hypothesized that the charge balance across the membrane would result in a deficiency of protons at the membrane surface which could affect the equilibrium reaction between the different phosphate ion species. A model derived to test this hypothesis underestimated the observed phosphate influx, and it was concluded that the proton concentration at the surface was sufficient to be

non-limiting to the observed phosphate influx. Nevertheless, the enhanced phosphate influx results observed in Chapter 6 would require an even greater surface concentration of protons. The maximum possible proton diffusion flux to the plant's surface, assuming zero proton concentration at the surface, is 1 to 2 nmol m^{-2} s^{-1}, approximately the same magnitude as observed for phosphate influx in Chapter 3 but significantly less than the observed maximum phosphate flux in Chapter 6. Clearly, the proton concentration at the site of phosphate influx is being maintained at non-limiting concentrations, with the most likely hypothesis being that a fast proton uniport exists in the vicinity of the site of phosphate influx creating a localized acid patch at the membrane surface. The cellular anatomy (Figure 2.1) of *U. australis* shows that the cells are surrounded by a mucilaginous sheath with the possibilty that acid alkaline banding could occur at different areas of the membrane surface. Postulating the existence of a proton uniport is not hard to conceive as it could function for a variety of reasons (e.g. balance other nutrient fluxes, cytoplasmic pH control).

The D.B.L. theory assumes for the case of a flat plate that the surface area of the D.B.L. is equivalent to the plate's surface area. This assumption holds for calculation of the D.B.L. resistance for different water velocities using the zinc method. However, because of the mucaliginous sheath, the membrane surface is not equivalent in surface area to the surface area of the D.B.L.. The assumption in applying the D.B.L. theory for a flat plate was that the membrane surface for each cell immediately adjacent to the plant's surface was the site at which phosphate influx occurred. This assumption apparently held as the observed phosphate influx results could be approximated using the D.B.L. theory for a flat plate. Nevertheless, it is possible that phosphate or other nutrients could diffuse through the mucilaginous sheath and be incorporated through the side of the cells. It is

interesting to speculate that this mucilaginous sheath, with a predicted slower diffusion coefficient for nutrients, could provide an anatomical mechanism for separating different nutrient flux sites on the membrane surface. The possibility exits for future research into a possible pH gradient parallel to the membrane surface of multi-cellular macroalgae, and whether this can be correlated with specific nutrient fluxes. Further, the possibility exists that *U. australis* could overcome the proton deficiency at its surface by allocating greater metabolic expenditure to the proton uniport and therefore overcoming the D.B.L. limitations to proton diffusion flux.

The anomaly in the phosphate transport results was the reciprocal relationship between phosphate influx and uptake at ecologically relevant phosphate concentrations (Phosphate uptake referred to the net phosphate taken up during the growing period). It was concluded that control of phosphate efflux is important in the overall phosphate transport process when plants were starved of phosphate. Further, it was speculated that the increased efflux correlated with the decline in cellular phosphate available for energy transfer processes which are important for maintaining cellular metabolism. Nevertheless, higher seawater phosphate concentrations, typical of the patch type phenomenon of nutrient concentration within the environment (Scavia et. al., 1984), resulted in an increase in the rate of phosphate uptake. More research is required to determine the benefits to metabolism, of an enhanced phosphate uptake during patches of high phosphate concentration, especially considering the varying opinions as to the benefit it has for microalgae (Currie, 1984).

7.2. THE EFFECT OF WATER MOVEMENT ON GROWTH RATE.

The implication from the results of Chapter 3 was that plants growing in different water movement environments would have differing

phosphate influx capabilities, and therefore if phosphate limits growth this should result in a different growth rate for each water movement treatment. It was found that the attempt to predict the effect of water movement on growth rate using the Monod model of growth (1942) in conjunction with the Briggs-Maskell equation failed for two main reasons. Firstly, the Monod model does not account for the growth rate being dependent on the tissue phosphate concentration and therefore cannot predict the growth rate when the system is not at steady state. Secondly, the growth conditions prior to the experimental start did not result in either growth being phosphate limited and did not provide uniform experimental plant material with respect to growth rate.

However, when plants were grown under more uniform and controlled conditions and selected for experimental use based on their growth rate (i.e. larger growth status), then the predicted difference in growth rate between water movement treatments was observed. Significantly, the difference in growth rate observed between different water movement treatments could be approximately simulated by combining the Briggs-Maskell equation for short term phosphate influx and substituting this into the mass balance equation which incorporated the Droop model of growth.

The water velocity required to achieve a growth saturation response was between 2 to 4 cm s^{-1}. *U. australis* plants growing at Saint Kilda probably only experience water velocities less than this between tidal periods. Therefore, further research is needed into measuring the changes and magnitude of water velocities within the marine environment. Attempts to determine water movement variations using the clod card method of Doty (1971) at Saint Kilda failed because the structure used to hold the clod cards in place rapidly became fouled with *U. australis*. Nevertheless, the results did show approximately that the water movement was highly variable at different regions within the bay. This

observation could explain the large degree of variance observed in parameter measurements for plants collected from the field, as the plants collected were not necessarily coming from a homogeneous environment.

7.3. EXPERIMENTAL IMPLICATIONS FOR THE APPLICATION OF MODELS.

The use of the mass balance equation in combination with the Briggs-Maskell equation approximately predicted the effect of water movement on growth. An improvement in predicting the phosphate influx could be achieved by modifying the Briggs-Maskell equation to incorporate either the exponential model or un-competitive model of phosphate influx. The decline in phosphate uptake correlated with the decline in tissue phosphate concentration, but this was not always the case as it was possible to observe a decrease in tissue phosphate concentration without a subsequent decline in phosphate uptake. The inability to predict the changes in phosphate uptake observed and the observed variation in growth lag response meant that the application of the different models varied between experiments, and as a consequence so did the model constants (e.g. qo).

Theoretically the aim of any model is to predict the plant's response under all conditions. Therefore, while individual components of the model could predict their own particular processes, the combination of the models could not accurately explain the observed experimental responses for the matrix of possible physiological and environmental states that could occur.

One of the problems with using models is the reliance on parameters derived without any knowledge as to their mechanistic implications. For example, the use of Vm and Km in the models formulated to explain the enhancement of phosphate influx, were determined by the fit of the Briggs-Haldane equation (program NONLIN) which cannot predict

the observed enhancement, but the values were still able to be used with success in the enhanced phosphate models (the values of Km and Vm determined using NONLIN were approximately equivalent to the values determined by eye).

The large experimental variation inherent in using plants collected from the field emphasized the need to precondition plants for a sufficient length of time to reduce this variation. Further, the results showed that the method of preconditioning was also important in determining the plant's response to the experimental parameters. This variation is an important ecological phenomenon, but, it restricts the use of empirically derived models and their associated constants to very restricted application. Therefore, it would help to be able to incorporate a larger range of interaction parameters (e.g. light, tissue age) into any wide ranging model on algal growth before these types of models can be used to predict growth rates in the field. The developement of such models could have considerable significance in determining management practices for cultivation, and harvest of wild and cultured algal stocks, and the preservation of existing marine flora.

7.4. ECOLOGICAL IMPLICATION OF THE OBSERVED INTERACTION BETWEEN WATER MOVEMENT, PHOSPHATE INFLUX OR UPTAKE, TISSUE PHOSPHATE CONCENTRATION AND GROWTH RATE.

Table 7.1 shows the observed interactions between the measured parameters and water movement, phosphate starvation and growth status. The interactions between the different processes studied and the model constants also, have shown the importance of studying the metabolism of plants under realistic conditions. For example, the increase in Km emphasizes that it is not possible to correctly predict the success of

one species in inter species competition for nutrients by comparing Km values for different species (Healey, 1980).

Table 7.1. Parameter interaction summary in brief.

Parameter	Increasing Water Movement	Phosphate Starvation	Increasing Growth Status
Pi Influx	increases	increases	increases
Pi Uptake	increases	varies	increases
Growth rate	increases	decreases	increases
qo	apparent decrease	-	decreases
μmq	constant	-	increases
Km	decreases	increases	increases
Vm	constant	increases	increases

The plant's ability to alter its environmental tolerance (e.g. variation in qo, safety factor), and therefore increase its probability of survival without wasting energetic resources on surplus metabolic activity, is an important component of any model that attempts to predict whole plant responses to the environment.

It can be concluded, then, that to be able to accurately model water movement, phosphate uptake and growth of *U. australis* it is necessary to determine the considerable amount of interaction that occurs between the different processes that influence metabolism. However, the effect of water movement can be of extreme importance to plant nutrition, when the D.B.L. is limiting to nutrient transport.

CHAPTER 8. REFERENCES

Agar, J. N., 1947. Diffusion and convection at electrodes. Discussions of the Faraday Society, 1, 26-37. Allen, T. F. H., 1977. Scale in microscopic algal ecology: a neglected dimension. *Phycologia*, 16, 253-257.

Anderson, M., and Charters, A. C., 1982. A fluid dynamics study of seawater flow through the bushy algal macrophyte *Gelidium nudifrons*. *Limnology Oceanography*, 27, 399-412.

Andrake, W., 1980. The effect of water motion on the growth and morphology of *Corallina officinalis* Corallinaceae Rhodophyta. *Journal of Phycology*, 16, 3.

Arnon, D. I., 1949. Copper enzymes in isolated chloroplasts. Polyphenoloxidase in *Beta vulgaris*. *Plant Physiology*, 24, 1-15.

Barry, P. H., and Diamond, J.M., 1984. Effects of unstirred layers on membrane phenomena. *Physiological Reviews*, 64, 763-872.

Beer, S., and Eshel, A., 1983. Photosynthesis of *Ulva sp.* : II: Utilization of CO2 and HCO3- when submerged. *Journal of Experimental Marine Biology Ecology*, 70, 97-106.

Beevers, R. E., and Burns, D. J. W., 1980. Phosphorus uptake, storage and utilization by fungi. *Advances in Botanical Research*, 8, 127-219.

Besford, R. T., 1979. Quantitative aspects of leaf acid phosphatase activity and the phosphorus status of tomato plants. *Annals of Botany*, 44, 153-161.

Bieleski, R. L., 1973. Phosphate pools, phosphate transport, and phosphate availability. *Annual Review of Plant Physiology*, 24, 225-252.

Birch, P. B., Gordon, D. M., and McComb, A. J., 1981. Nitrogen and phosphorus nutrition of *Cladophora* in the Peel-Harvey estuarine system, Western Australia. *Botanica Marina*. 24, 381-387.

Bircumshaw, L. L., and Riddiford, A. C., 1952. Transport control in heterogeneous reactions. *Quarterly Review*, 6, 157-185.

Bird, K. T., Habig, C., and DeBusk, T., 1982. Nitrogen allocation and storage patterns in *Gracilaria tikvahiae* (Rhodophyta). *Journal of Phycology*, 18, 344-348.

Bird, R., Stewart, W. E., and Lightfoot, E. N., 1960. *Transport phenomena*. Wiley and Sons, New York.

Blasius, H., 1908. Grenzschichten in Flussigkeiten mit kleiner Reibung. *Z.Mat, Physik.*, 1.

Blum, J. J., 1966. Phosphate uptake by phosphate-starved *Euglenia*. *Journal of General Physiology*, 49, 1125-1137

Boalch, G. T., 1961. Studies on *Ectocarpus* in culture II: Growth and nutrition of bacteria free culture. *Journal of Marine Biology Association U. K.*, 41, 287-304.

Borstlap, A. C., 1981. Invalidity of the multiphasic concept of ion absorption in plants. *Plant, Cell and Environment*, 4, 189-195.

Borstlap, A. C., 1983. The use of model-fitting in the interpretation of 'dual' uptake isotherms. *Plant Cell and Environment*, 6, 407-416.

Bottom, D. L., 1981. A flow through system for field measurements of production by marine macroalgae. *Marine Biology*, 64, 251-257.

Bowling, D. J. F., and Dunlop, J., 1978. Uptake of phosphate by white clover. I. Evidence for an electrogenic phosphate pump. *Journal of of Experimental Botany*, 29, 1139-1146.

Briggs, G. E., and Haldane, I. B. S., 1925. *Journal of Biochemistry*, 19, 338ff.

Briggs, G. E., and Robertson, R. N., 1948. Diffusion and absorption in disks of plant tissue. *New Phytology*, 47, 265-283.

Breeze, V. G., Wild, A, Hopper, M. J., and Jones, L. H. P., 1984. The uptake of phosphate by plants from flowing nutrient solution. *Journal of Experimental Botany*, 35, 1210-1221.

Brown E. J., and Button D. K., 1979. Phosphate-limited growth kinetics of *Selenastrum capricornutum* (Chlorophyceae). *Journal of Phycology*, 15, 305-311.

Buggeln , R. B., 1978. Physiological investigations on *Alaria esculenta* Laminariales Phaeophyceae. IV: Inorganic and organic nitrogen in the blade. *Journal of Phycology*, 14, 156-160.

Butler, J. N., 1964. *Solubility and pH Calculations*. Addison-Wesley, U.S.A.

Canelli E., and Fuhs G.W., 1976. Effect of the sinking rate of two diatoms (*Thalassiosira sp.*) on uptake from low concentrations of phosphate. *Journal of Phycology*, 12, 93-99.

Cebeci, T., and Smith A. M. O., 1974. *Analysis of Turbulent boundary layers*. Academic Press, New York.

Chamberlain, J. A., and Graus, R. R., 1975. Water flow and hydromechanical adaptations of branched reef corals. *Bulletin of Marine Science*, 25, 112-125.

Chapman, A. R. O., 1973. Phenetic variability of stipe morphology in relation to season, exposure, and depth in the non-digitate complex of *Laminaria* Lamour (Phaeophyta), Laminar. *Phycologia*, 12, 53-57 .

Chapman, A. R. O., and Craigie, J. S., 1977. Seasonal growth in *Laminaria longicruris*, relations with dissolved inorganic nutrients and internal reserves of nitrogen. *Marine Biology*, 40, 197-205.

Chapman, A. R. O., Markham, J. W., and Luning, K., 1978. Effects of nitrate concentration on the growth and physiology of *Laminaria saccharina* (Phaeophyta) in culture. *Journal of Phycology*, 14, 195-198.

Charters, A. C., 1940. Transition between laminar and turbulent flow by transverse contamination. *Technical Notes Of the National Advisory Commission of Aeronautics Washington*, 891.

Charters, A. C., and Anderson, S. M., 1980. Low-Velocity water tunnel for biological research. *Journal of Hydronautics*, 14, 3-4.

Charters, A. C., Neushul, M., and Barilotti, C., 1969. The functional morphology of *Eisenia arborea*. *Proceedings International Seaweed Symposium*, 689-105.

Charters, A. C., Neushul, M., and Coon, D., 1973. The effect of water motion on algal spore adhesion. *Limnology Oceanography*, 18, 884-899.

Chen, M., 1974. Kinetics of phosphorus absorption by *Corynebacterium bovis*. *Journal of Microbial Ecology*, 1, 164-175.

Clarke S. M., and Womersley H. B. S., 1981. Cross-fertilization and hybrid development of forms of the brown alga Hormosira banksii (Turner) Decaisne. *Australian Journal of Botany*, 29, 497-505.

Colquhoun D., 1971. *Lectures on biostatistics: An introduction to statistics with applications in biology and medicine*. Clarendon Press, Oxford.

Conover, J. T., 1968. The importance of natural diffusion gradients and transport of substances related to benthic marine plant metaboloism. *Botanica Marina*, 11, 1-9.

Coon, D. A., Neushul, M., and Charters, A. C., 1972. The settling behaviour of marine algal spores. *Proceedings International Seaweed Symposium*, 7, 237-242.

Cooper, L. H. N., 1937. On the ratio of nitrogen to phosphorus in the sea. *Journal of Marine Biology Association U. K.*, 22, 177-182.

Cousens, R., 1981. Variation in annual production by *Ascophyllum nodosum* (L). LeJolis with degree of exposure to wave action. *Proceedings International Seaweed Symposium*, 10, 253-258.

Cousens, R., 1982. The effect of exposure to wave action on the morphology and pigmentation of *Ascophyllum nodosum* in south-eastern Canada. *Botanica Marina*, 25, 191-196.

Cowen, R. K., Agegian, C. R., and Foster, M. S., 1982. The maintenance of community structure in a central California giant kelp forest. *Journal of Experimental Marine Biology*, 64, 189-201.

Cummins, J. T., Strand, J. A., and Vaughan, B. E., 1969. The movement of H+ and other ions at the onset of photosynthesis in *Ulva*. *Biochimica et Biophysica Acta*, 173, 198-205.

Cunningham, A., and Maas, P., 1978. Time lag and nutrient storage effects in the transient growth response of *Chlamydomonas reinhardii* in nitrogen-limited batch and continuous culture. *Journal of of General Microbiology*, 104, 227-231.

Currie, D. J., 1984. Microscale nutrient patches: do they matter to the phytoplankton? *Limnology Oceanography*, 29, 211-214.

Currie, D. J., 1986. Does orthophosphate uptake supply sufficient phosphorus to phytoplankton to sustain their growth? *Canadian Journal of Fisheries and Aquatic Science*, 43, 1482-1487.

Dainty, J., 1963. *Water relations of Plant cells*. Advances in Botanical Research. ed. R. O. Preston, Academic Press, New York.

Dainty, J., and House, C. R., 1966. 'Unstirred layers' in frog skin. *Journal of Physiology*, 182, 66-78.

Darwin, F., and Pertz, D. F. M., 1896. On the effect of water currents on the assimilation of aquatic plants. *Cambridge Philosophical Society Proceedings*, 9, 76-90.

Dawes, C. J., Chen, C. P., Jewett-Smith, J., Marsh, A., and Watts, S. A., 1984. Effect of phosphate and ammonium levels on photosynthetic and respiratory responses of the red alga *Gracilaria verrucosa*. *Marine Biology*, 78, 325-328.

Dayton, P. K., 1971. Competition, disturbance, and community organization: The provision and subsequent utilization of space in a rocky intertidal community. *Ecological Monographs*, 41, 351-389.

Dayton, P. K., Currie, V., Gerrodette, T., Keller, B. D., Rosenthal, R., and Ventresca, D., 1984. Patch dynamics and stability of some California kelp communities. *Ecology Monographs*, 54, 253-289.

Dean, T. A., and Jacobsen, F. R., 1984. Growth of juvenile *Macrocystis pyrifera* (Laminariales) in relation to environmental factors. *Marine Biology*, 83, 301-311.

DeBoer, J. A., Guigli, H. J., Israel, T. L., and D'Elia, C. F., 1978. Nutritional studies of two red algae . I. Growth rate as a function of nitrogen source and concentration. *Journal of Phycology*, 14, 261-266.

DeBusk, T. A., Blakeslee, M., and Ryther, J. H., 1986. Studies on the outdoor cultivation of *Ulva lactuca* L. *Botanica Marina*, 29, 381-386.

DeBusk, T. A., and Ryther, J. H., 1984. Effects of seawater exchange, pH and carbon supply on the growth of *Gracilaria tikvahiae* (Rhodophyceae) in large scale culture. *Botanica Marina*, 27, 357-362.

D'Elia, C and DeBoer, J., 1978. Nutritional studies of two red algae. II. Kinetics of ammonium and nitrate uptake. *Journal of Phycology*, 14, 266-272.

Dethier, M. N., 1984. Disturbance and recovery in intertidal pools: Maintenance of mosaic patterns. *Ecology Monographs*, 54, 99-118.

Dickson ,A. G., and Riley, J. P., 1979.The estimation of acid dissociation constants in seawater media from potentiometric titrations with strong base. II: The dissociation of phosphoric acid. *Marine Chemistry*, 7, 106-109.

Dixon, M., and Webb, E. C., 1964. *Enzymes*. Academic Press, New York.

Dodgson, K. S., Spencer, B. and Williams, K., 1956. Examples of anti-competitive inhibition. *Nature*, 177, 432-433.

Dortch, Q., and Conway, H. L., 1984. Interactions between nitrate and ammonium uptake variation with growth rate, nitrogen source and species. *Marine Biology*, 79, 151-164.

Doty, M. S., 1971a. Measurement of water movement in reference to benthic algal growth. *Botanica Marina*, 14, 32-35.

Doty, M. S., 1971b. Antecedent event influence on benthic marine algal standing crop in Hawaii. *Journal of Experimental Marine Biology Ecology*, 6, 161-166.

Dowd J. E., and Riggs D. S., 1965. A comparison of estimates of Michaelis-Menten kinetic constants from various linear transformations. *Journal of Biology Chemistry*, 240, 863-869.

Drew, E. A., 1983. Physiology of *Laminaria*. 1. Use of exised lamina discs in short and long term experiments. *Marine Ecology*, 4, 211-226.

Droomgoole, F. I., 1978. The effects of oxygen on dark respiration and apparent photosynthesis of marine macroalgae. *Aquatic Botany*, 4, 281-297.

Droop M. R., 1973. Some thoughts on nutrient limitation in algae. *Journal of Phycology*, 9, 264-272.

Dufkova, V., 1984. E.D.T.A. in algal culture media. Archives *Hydrobiology*, 67, 479-492.

Dugdale, D. C., 1967. Nutrient limitation in the sea: dynamics, identification and significance. *Limnology Oceanography*, 12, 685-695.

Duggleby R. G., 1981. A nonlinear regression program for small computers. *Analytical Biochemistry*, 110, 9-18.

Dunlop, J., and Bowling., 1978. Uptake of phosphate by white clover. II. The effect of pH on the electrogenic phosphate pump. *Journal of Experimental Botany*, 29, 1147-1153.

Ebeling, A. W., Laur, D. R., and Rowley, R. J., 1985. Severe storm disturbances and reversal of community structure in a southern California kelp forest. *Marine Biology*, 84, 287-294.

Ebersole, E. R., Guttentag, C., and Wilson, P. W., 1943. Nature of carbon monoxide inhibition of biological nitrogen fixation. *Archives of Biochemistry*, 3, 399-418.

Eckmam, J. E., 1983. Hydrodynamic processes affecting benthic recruitment. *Limnology and Oceanography*, 28, 241-257.

Engasser, J. M., and Horvath, C., 1974. Inhibition of bound Enzymes. II Characterization of product inhibition and accumulation. *Biochemistry*, 13, 3849-3854.

Everitt, C. T., Redwood, W. R., and Haydon, D. A., 1969. Problems of boundary layers in the exchange diffusion of water across bimolecular lipid membranes. *Journal of Theoretical Biology*, 22, 20-32.

Falco, J. W., Kerr, P. C., Barron, M. B., and Brockway, D. L., 1975. The effect of mass transport on biostimulation of algal growth. *Ecology Modelling*, 1, 117-131.

Fage, A., and Townend, H. C. H., 1932. An examination of turbulent flow with an ultramicroscope. *Proceedings of the Royal Society of London (A)*, 135, 656-677.

Falkner, G., Horner, F., and Simonis, W., 1980. The regulation of the energy-dependent phosphate uptake by the blue-green alga *Anacystis nidulans*. *Planta*, 149, 138-143.

Falkner, G., Strasser, P., and Graffius, D., 1984. Phosphate uptake by blue green algae in vitro and in a lake during an algal bloom: Useful applications of a force-flow relationship. *Hydrobiologia*, 108, 265-271.

Fick, A., 1855. On liquid diffusion. *Philosophical Magazine (fourth series)*, 10, 30-39.

Findlay, G. P., Hope, A. B., Pitman, M. G., and Walker, N. A., 1971. Ionic relations of marine algae: III *Chaetomorpha*: Membrane electrical properties and chloride fluxes. *Australian Journal of Biology Science*, 24, 731-745.

Fonseca, M. S., Zieman, J. C., Thayer, G. W., and Fisher, J. S., 1983. The role of current velocity in structuring eelgrass (*Zostera marina* L.) meadows. *Estuarine, Coastal and Shelf Science*, 17, 367-380.

Fortes, M. D., and Luening, K., 1980. Growth rates of North Sea macroalgae in relation to temperature, irradiance and photoperiod. *Helgolander wiss Meeresunters*, 34, 15-29.

Fuhs, G. W., 1969. Phosphorus content and rate of growth in the diatoms Cyclotella nana and *Thalassiosira fluviatilis*. *Journal of Phycology*, 5, 312-321.

Fujita, R. M., 1985. The role of nitrogen status in regulating transient ammonium uptake and nitrogen storage by macroalgae. *Journal of Experimental Marine Biology Ecology*, 92, 283-301.

Fujita, R. M., and Goldman, J. C., 1985. Nutrient flux and growth of the red alga *Gracilaria tikvahiae* McLachlan (Rhodophyta). *Botanica Marina*, 28, 265-268.

Gantt, E., 1981. Phycobilisomes. *Annual Review of Plant Physiology*, 32, 327-347.

Gaur, K., Ramakrishna, T., Subbarayn, D.P. 1982. Ecologyogical studies on *Ulva lactuca* L from Veraval, India. *Hydrobiologia*, 89, 78-89.

Gavis, J., 1976. Munk and Riley revisited: nutrient diffusion transport and rates of phytoplankton growth. *Journal of Marine Research*, 34, 161-179.

Gerard, V. A., 1982. Growth and utilization of internal nitrogen reserves by the giant kelp *Macrocystis pyrifera* in a low-nitrogen environment. *Marine Biology*, 66, 27-35.

Gerard, V. A., 1982a. In situ Water Motion and Nutrient Uptake by the giant kelp *Macrocystis pyrifera*. *Marine Biology*, 69, 51-54.

Gerard, V. A., 1982b. In situ rates of nitrate uptake by giant kelp *Macrocystis pyrifera* (L) C. G. Agardh: tissue differences, environmental effects and predictions of nitrogen-limited growth. *Journal of Experimental Marine Biology. Ecology*, 62, 211-224.

Gerard, V. A., 1987. Hydrodynamic streamlining of *Laminaria saccharina* Lamour. in response to mechanical stress. *Journal of Experimental Marine Biology and Ecology*, 107, 237-244.

Gerard, V. A., and Mann, K. H., 1979. Growth and production of *Laminaria longicrus* (Phaeophyta) populations exposed to different intensities of water movement. *Journal of Phycology*, 15, 33-41.

Gerloff, G. C., and Krombholz, P. H., 1966. Tissue analysis as a measure of nutrient availability for the growth of angiospermaquatic plants. *Limnology Oceanography*, 11, 529-537.

Glass, A. D. M., 1976. Regulation of potassium absorption in barley roots: An allosteric model. *Plant Physiology*, 58, 33-37.

Glass, A. D. M., 1977. Regulation of K+ influx in barley roots: Evidence for direct control by internal K+. *Australian Journal of Plant Physiology*, 4, 313-318.

Goldman, J. C., 1977. Steady state growth of phytoplankton in continous culture: Comparison of internal and external nutrient equations. *Journal of Phycology*, 13, 251-258.

Gordon, D. M., Birch, P. B., and McComb, A. J., 1981. Effects of Inorganic Phosphorous and nitrogen on the growth of an estuarine *Cladophora* in culture. *Botanica Marina*, 24, 93-106.

Gotham, I. J., and Rhee, G. Y., 1981. Comparative kinetic studies of phosphate-limited growth and phosphate uptake in phytoplankton in continuous culture. *Journal of Phycology*, 17, 257-265.

Grace, J., 1977. *Plant response to wind*. Academic Press, New York.

Graus, R. R., Chamberlain, J. A., and Boker, A. M., 1977. Structural modification of corals in relation to waves and currents. *Studies in Geology*, 4, 135-153.

Green, B. R., 1977. The effects of natural and synthetic sea water media on the growth and reproduction of *Acetabularia*. *Phycologia*, 16, 87-94.

Green, K., and Otori, T., 1970. Direct measurements of membrane unstirred layers. *Journal of Physiology*, 207, 93-102.

Guerin, J. M., and Bird, K. T., 1987. Effects of aeration period on the productivity and agar quality of *Gracilaria*. *Aquaculture*, 64, 105-110.

Gutkneckt, J., Bisson, M. A., and Tosteson, F. C., 1977. Diffusion of carbon dioxide through lipid bilayer membranes: Effects of carbonic anhydrase, bicarbonate and unstirred layers. *Journal of General Physiology*, 69, 779-794.

Gutknect, J., and Tosteson D. C., 1973. Diffusion of weak acids across lipid bilayer membranes effects of chemical reactions in the unstirred layers. *Science*, 182, 1258-1261.

Hagen, C. E., and Hopkins, H. T., 1955. Ionic species in orthophosphate uptake by barley roots. *Plant Physiology*, 30, 193-199.

Hanisak, M. D., 1987. Cultivation of *Gracilaria* and other macroalgae in Florida for energy production. In Seaweed Cultivation for renewable resources. Eds. K. T., Bird, and P. H., Benson. *Developments in aquaculture and fisheries science*, 16, 191-218.

Hartmann, L., 1967. Influence of turbulence on the activity of bacterial slimes. *Journal of Water Pollution Control Federation*, 39, 958-964.

Hatcher, B. G., 1977. An apparatus for measuring photosynthesis and respiration of intact large marine algae and comparison of results with those from experiments with tissue segments. *Marine Biology*, 43, 381-385.

Hay, M. E., 1981. The functional morphology of Turf-forming seaweeds: Persistence in stressful marine habitats. *Ecology*, 62, 739-750.

Haydon, D. A., and Hladky, S. B., 1972. Ion transport across lipid membranes. *Quarterly Review Biophysics*, 5, 187-282.

Healey, F. P., 1975. Physiological indicators of nutrient deficiency in algae. *Environment Canada Technical Report*, 58533.

Healey, F. P., 1980. Slope of the Monod equation as an indicator of advantage in nutrient competition. *Microbial Ecology*, 5, 281-286.

Hill, R., and Whittingham, C. P., 1955. *Photosynthesis*. Methuen and Co. Ltd., London.

Hone, P. W., 1982. Growth stimulation of Ulva rigida C. Agardh influenced by water movement and external nutrient concentration. *Honours Thesis, University of Adelaide.*

Howarth, R. W., and Cole, J. J., 1985. Molybdenum availability, nitrogen limitation, and phytoplankton growth in natural waters. *Science*, 229, 653-655.

Huguenin, J. E., 1976. An examination of problems and potentials for future large-scale intensive seaweed culture systems. *Aquaculture*, 9, 313-342.

Hunt, R., 1982. *Plant Growth Analysis. User's Instructions For The Spline Program with Second Derivatives and Compound Second Derivatives.* NERC, Unit of Comparative Plant Ecology, University of Sheffield.

Hurlbert, S. H., 1984. Pseudoreplication and the design of ecological field experiments. *Ecology Monographs*, 54, 187-211.

Jackson, G. A., 1977. Nutrients and production of giant kelp *Macrocystis pyrifera* off southern California. *Limnology and Oceanography*, 22, 979-995.

Jackson, G. A., and Winant, C. D., 1983. Effect of kelp forest on coastal currents. *Continental Shelf Research*, 2, 75-80.

James, W. O., 1928. Experimental researches on vegetable assimilation and respiration. XIX: The effect of variations of carbon dioxide supply upon the rate of assimilation. *Proceedings Royal Society (B)*, 10, 31-42.

Johansson, O., and Wedborg, M., 1979. Stability constants of phosphoric acid in seawater of 5-40% salinity and temperatures of 5-25°C. *Marine Chemistry*, 8, 57-69.

Jones, W. E., 1959. Experiments on some effects of certain environmental factors on *Gracilaria verrucosa* (Hudson) Papenfuss. *Journal of Marine Biology Ass. U. K.*, 38, 153-167.

Jones, W. E., and Demetropoulos, A., 1968. Exposure to wave action: Measurements of an important ecological parameter on rocky shores of Anglesey. *Journal of Experimental Marine Biology Ecology*, 2, 46-63.

Kain, J. M., 1982. Morphology and growth of the giant kelp *Macrocystis pyrifera* in New Zealand and California. *Marine Biology*, 67, 143-157.

Kautsky, L., 1982. Primary production and uptake kinetics of ammonium and phosphate by *Enteromorpha compressa* in an ammonium sulphate industry outlet area. *Aquatic Botany*, 12, 23-40.

Kelly, D. J., 1980. Growth rates of *Ulva rigida*, a newly recorded species in Florida. *Fla. Sci*, 43, 15.

Kester, D. R., and Pytkowicz, R. M., 1967. Determination of the apparent dissociation constants of phosphoric acid in seawater. *Limnology and Oceanography*, 12, 243-252.

King, C. V., and Braverman, M. M., 1932. The rate of solution of zinc in acids. *Journal of American Chemical Society*, 54, 1744-1757.

King, R. J., and Schramm, W., 1976. Determination of photosynthetic rates for the marine algae *Fucus vesiculosus* and *Laminaria digitata*. *Marine Biology*, 37, 209-213.

Koehl, M. A. R., and Wainwright, S. A., 1977. Mechanical adaptations of a giant kelp. *Limnology and Oceanography*, 22, 1067-1071.

Krom, M. D., and Berner, R. A., 1980. The diffusion coefficients of sulphate, ammonium, and phosphate ions in anoxic marine sediments. *Limnology and Oceanography*, 25, 327-337.

Kuhl, A., 1974. Phosphorus. In algal physiology and biochemistry. *Botanical Monographs*, 10, 636-654.

Kunikane, S., Kaneko, M., and Maehara, R., 1984. Growth and nutrient uptake of green alga, *Scenedesmus dimorphus*, under a wide range of nitrogen/phosphorus ratio. I: Experimental study. *Water Research*, 18, 1299-1311.

Kuwabara, J. S., Davis, J. A. and Chang, C. C. Y., 1986. Algal growth response to particle-bound orthophosphate and zinc. *Limnology and Oceanography*, 31, 503-511.

Kuwabara, J. S., and North, W. J., 1980. Culturing microscopic stages of *Macrocystis pyrifera* (Phaeophyta) in Aquil a chemically defined medium. *Journal of Phycology*, 16, 546-549.

Kylin, A., 1964. An outpump balancing phosphate-dependent sodium uptake in *Scenedesmus*. *Biochemistry, biophysics Research Communication*, 16, 497-500.

LaBarbera, M., 1984. Feeding currents and particle capture mechanisms in suspension feeding animals. *American Zoology*, 24, 71-84.

Lapointe, B. E., 1981. The effects of light and nitrogen on growth, pigment content, and biochemical composition of *Gracilaria foliifera* var augustissima (Gigartinales, Rhodophyta). *Journal of Phycology*, 17, 90-95.

Lapointe, B. E., 1985. Strategies for pulsed nutrient supply to *Gracilaria* cultures in the Florida Keys: Interactions between concentration and frequency of nutrient pulses. *Journal of Experimental Marine Biology Ecology*, 93, 211-222.

Lapointe, B. E., 1986. Phosphorus-limited photosynthesis and growth of *Sargassum natans* and *Sargassum fluitans* (Phaeophyceae) in the western North Atlantic. *Deep Sea Research*, 33, 391-399.

Lapointe, B. E., 1987. Phosphorus- and nitrogen -limited photosynthesis and growth of *Gracilaria tikvahiae* (Rhodophyceae) in the Florida Keys: an experimental field study. *Marine Biology*, 93, 561-568.

Lapointe, B. E., Niell, F. X., and Fuentes, J. M., 1981. Community structure succession and production of seaweeds associated with mussel rafts in the Ria-De-Arosa north western Spain. *Marine Ecology Progress Series*, 5, 243-254.

Lapointe, B. E., and Ryther, J. H., 1979. The effects of Nitrogen and seawater flow rate on the growth and biochemical composition of *Gracilaria foliifera* var augustissima in mass outdoor cultures. *Botanica Marina*, 22, 529-537.

Lapointe, B. E., and Tenore, K. R., 1981. Experimental outdoor studies with Ulva fasciata Detile. I: Interaction of light and nitrogen on nutrient uptake, growth, and biochemical composition. *Journal of Experimental Marine Biology Ecology*, 53, 135-152.

Laties, G. G., 1969. Dual mechanisms of salt uptake in relation to compartmentation and long distance transport. *Annual Review of Plant Physiology*, 20, 879-116.

Lee, R. B., 1982. Selectivity and kinetics of ion uptake by barley plants following nutrient deficiency. *Annuals Botany*, 50, 429-449.

Lefebvre, D. D., and Glass, A. D. M., 1982. Regulation of phosphate influx in barley roots: Effects of phosphate deprivation and reduction of influx with provision of orthophosphate. *Physiologia Plantarum*, 54, 199-206.

Lehman, J. T., 1978. Enhanced transport of inorganic carbon into algal cells and its implications for the biological fixation of carbon. *Journal of Phycology*, 14, 33-42.

Lehman, J. T., Botkin, D. B., and Likens, G. E., 1975. The assumptions and rationales of a computer model of phytoplankton population dynamics. *Limnology and Oceanography*, 20, 343-364.

Lehman, J. T., and Scavia, D., 1982. Microscale patchiness of nutrients in plankton communities. *Science*, 216, 729-730.

Levich, B., 1947. The theory of concentration polarisation. *Faraday Society Discussions*, 1, 37-45.

Levich, V. G., 1962. *Physiochemical hydrodynamics*. Prentice Hall, Engelwood Cliffs. 1962.

Leyton, L., 1975. *Fluid behaviour in biological systems*. Clarendon Press, Oxford.

Li, V,- H., and Gregory, S., 1974. Diffusion of ions in seawater and in deep-sea sediments. *Geochimica et Cosmochimica Acta*, 38, 703-714.

Lieb, W. R., and Stein, W. D., 1974. Testing and characterizing the simple carrier. *Biochimica et Biophysica Acta*, 373, 178-196.

Littler, M. M., 1979. Effects of battle volume, thallus weight, oxygen saturation levels and water movement on apparent photosynthetic rates in marine algae. *Aquatic Botany*, 7, 21-34.

Littler, M. M., 1980. Morphological form and photosynthetic performances of marine macroalgae: Tests of a functional/form hypothesis. *Botanica Marina*, 23, 161-165.

Littler, M. M., and Littler, D. S., 1980. The evaluation of thallus form and survival strategies in benthic marine macroalgae: Field and laboratory tests of a functional form model. *American Naturalist*, 116, 25-44.

Littler, M. M., Littler, D. S., and Taylor, P. R., 1983. Evolutionary strategies in a tropical barrier reef system: functional-form groups of marine macroalgae. *Journal of Phycology*, 19, 229-237.

Littler, M. M., Murray, S. N., and Arnold, K. E., 1979. Seasonal variations in net photosynthetic performance and cover of intertidal macrophytes. *Aquatic Botany*, 7, 35-46.

Livansky, K., 1982. CO2 transport in cultures of autrophic algae. *Archives fur Hydrobiologie Supplement*, 63, 101-109.

Lommen, P. W., Schwintzer, C. R., Yocum, C. S., and Gates, D. M., 1971. A model describing photosynthesis in terms of gas diffusion and enzyme kinetics. *Planta*, 98, 195-220.

MacFarlane, J. J., 1985. Diffusion and uptake of nutrients by aquatic macrophytes. *Ph.D. Thesis, The University of Adelaide.*

MacFarlane, J. J., and Raven, J. A., 1985. External and internal CO2 transport in *Lemanea*: Interactions with the kinetics of Ribulose biphosphate carboxylase. *Journal of Experimental Botany*, 36, 610-622.

MacFarlane, J. J., and Smith, F. A., 1982. Uptake of methylamine by *Ulva rigida*: Transport of cations and diffusion of free base. *Journal of Experimental Botany*, 33, 195-207.

Madsen, T. V., and Sondergaard, M., 1983. The effects of current velocity on the photosynthesis of *Callitriche stagnalis* Scop. *Aquatic Botany*, 15, 187-194.

Madsen. T. V., and Warncke, E., 1983. Velocities of currents around and within submerged aquatic vegetation. *Archive Hydrobiologie*, 97, 389-394.

Mahan, B. H., 1975. *University Chemistry*. Adison-Wesley, Reading, Massachusetts.

Manley, S. L., 1985. Phosphate uptake by blades of *Macrocystis pyrifera* (Phaeophyta). *Botanica Marina*, 28, 237-244.

Manley, S. L., and North, W. J., 1984. Phosphorus and the growth of juvenile *Macrocystis pyrifera* (Phaeophyta) sporophytes. *Journal of Phycology*, 20, 389-393.

Mann, K. H., 1971. Relation between stipe length, environment, and the taxonomic characters of *Laminaria*. *Journal of Fisheries Research Board of Canada*, 28, 778-780.

Markl, H., 1977. CO2 transport and photosynthetic productivity of a continuous culture of algae. *Biotechnology and Bioengineering*, 19, 1851-1862.

Maskell, E. J., 1928. Experimental research on vegetable assimilation and respiration. 18 : The relation between stomatal opening and assimilation - A critical study of assimilation. *Proceedings Royal Society London (B)*, 102, 488-533.

Matsumoto, F., 1959. Studies on effects of environmental factors on the growth of "nori" (*Porphyra tenera*) with special reference to water current. *Journal of the Faculty of Fish and Animal Husbandry Hiroshima University*, 2 ,249-333.

McIntire, C. D., 1966. Some effects of current velocity on periphyton communities in laboratory streams. *Hydrobiologia*, 27, 559-570.

McPharlin, I. R., and Bieleski, R. l., 1987. Phosphate uptake by *Spirodela* and *Lemna* during early phosphorus deficiency. *Australian Journal of Plant Physiology*, 14, 561-572.

Menzel, D. W., and Corwin, N., 1965. The measurement of total phosphorous in seawater based on the liberation of organically bound fractions by persulfate oxidation. *Limnology and Oceanography*, 10, 280-282.

Merzkirch, A., 1974. *Flow Visualization*. Academic Press, New York.

Michaelis, L., Menten, M. L., 1911. *Biochem. Z.*, 35, 386.

Mierle, G., 1985. Kinetics of phosphate transport by *Synechococcus leopoliensis* (Cyanophyta): Evidence for diffusion limitation of phosphate uptake. *Journal of Phycology*, 21, 177-181.

Milgram, J. H., 1978. Waves and wave force. *Marine Science Communications*, 4, 347-374.

Millero, F. J., 1983. The estimation of the pk*HA of acids in seawater using the Pitzer equations. *Geochimica et Cosmochimica Acta*, 47, 2121-2129.

Monod, J., 1942. *Recherche sur la croissance des cultures bacteriennes*. Hermann, Paris.

Morgan, K. C., and Simpson, F. J., 1981. Cultivation of *Palmaria* (Rhodymenia) palmata : effect of high concentrations of nitrate and ammonium on growth and nitrogen uptake. *Aquatic Botany*, 11, 167-171.

Morris, J. G., 1968. " A Biologist's Physical Chemistry". Edward Arnold. London.

Mshigeni, K. E., 1979. The economic algal genus *Eucheuma* (Rhodophyta, Gigartinales): Observations on the morphology and distribution ecology of Tanzanian species. *Botanica Marina*, 22, 437-445.

Mshigeni, K. E., and Magingo, F. S. S., 1982. Studies on the morphology, distribution ecology and ecophysiology of Acrocystis nana Zanardinis in Tanzania. *Botanica Marina*, 25, 1-7.

Muller, H., 1970. Das Wachstum von Nitzschia actinastroides (Lemm.) v. Gorr im Chemostaten bei limitierender Phosphatkonzentration. *Ber. Dtsch. Bot. Ges.*, 83, 537-544.

Munk, W. K., and Riley, G. A., 1952. Absorption of nutrients by aquatic plants. *Journal of Marine Research*, 11, 215-240.

Murphy, J., and Riley, J. P., 1962. A modified single solution method for the determination of phosphate in natural waters. *Analytica Chimica Acta*, 27, 31-36.

Myers, J., 1944. The growth of *Chlorella pyrenoidosa* under various culture conditions. *Plant Physiology*, 19, 576-589.

Myers, V. B., and Iverson, R. I., 1981. *Phosphorus and nitrogen limited phytoplankton productivity in northeastern Gulf of Mexico coastal estuaries. In Estuaries and Nutrients*. Eds B. J. Nielson and L. E. Cronin. Humana Press, Clifton, N. J.

Nandi, S. K., Pant, R. C., and Nissen P., 1987. Multiphasic uptake of phosphate by corn roots. *Plant Cell and Environment*, 10, 463-474.

Nernst, W., 1904. Theorie der Reaktionsgeschwindigigkeit in heterogenen Systemen. *Zeitschrift fur Physikalische Chemie*, 47, 52-55.

Neushul, M., 1972. *Functional interpretation of benthia marine algal morphology. In: contributions to the systematics of benthic marine algae of the north Pacific.* Eds. I. A. Abott and M. Kurogi, Japanese Society of Phycology, Kobe.

Nissen, P., 1973. Multiphasic uptake in plants. I: Phosphate and Sulfate. *Physiologia Plantarum*, 28, 304-316.

Norton, T. A., 1969. Growth form and environment in *Saccorhiza polyschides*. *Journal of Marine Biological Association, U. K.*, 49, 1025-1045.

Norton, T. A., 1973. Orientated growth of *Membranipora membranacea* (L.) on the thallus of *Saccorhiza polyschides* (Lightf.) *Batt. Journal of Experimental Marine Biology Ecology*, 13, 91-95.

Norton, T. A., and Fettler, R., 1981. The settlement of *Sargassum muticum* propagules in stationary and flowing water. *Journal of Marine Biology Association U. K.*, 61, 929-940.

Norton, T. A., Mathieson, A. C., and Neushul, M., 1982. A review of some aspects of form and function in seaweeds. *Botanica Marina*, 25, 501-510.

Owens, M., and Maris, P. J., 1964. Some factors affecting the respiration of some aquatic plants. *Hydrobiologia*, 23, 533-543.

Oza, R. M., 1978. Studies on Indian *Gracilaria*. IV: Seasonal variation in agar and gel strength of *Gracilaria corticata* occurring on the coast of Veraval. *Botanica Marina*, 21, 165-168.

Oza, R. M., and Rao, S. P., 1977. Effects of different culture media on growth and sporulation of laboratory raised germlings of *Ulva fasciata*. *Botanica Marina*, 20, 427-432.

Paine, R. T., and Levin, S. A., 1981. Intertidal landscapes: Disturbance and the dynamics of pattern. *Ecology Monographs*, 51, 145-178.

Parker, H. S., 1981. Influence of relative water motion on the growth, amonium uptake and carbon and nitrogen composition of *Ulva lactuca*, *Marine Biology*, 63, 309-318.

Parker, H. S., 1982. Effects of simulated current on the growth rate and nitrogen metabolism of *Gracilaria tikvahiae* (Rhodophyta). *Marine Biology*, 69, 137-145.

Parslow, J. S., Harrison, P. J., and Thompson, P. A., 1984a. Development of rapid ammonium uptake during starvation of batch and chemostat cultures of the marine diatom *Thalassiosira pseudonana*. *Marine Biology*, 83, 43-50.

Parslow, J. S., Harrison, P. J., and Thompson, P. A., 1984b. Saturated uptake kinetics : transient response of the marine diatom *Thalassiosira pseudonana* to ammonium, nitrate, silicate or phosphate starvation. *Marine Biology*, 83, 51-59.

Parslow, J. S., Harrison, P. J., and Thompson, P. A., 1985. Interpreting rapid changes in uptake kinetics in the marine diatom *Thalassiosira pseudonana* (Hustedt). *Journal of Experimental Marine Biology Ecology*, 91, 53-64.

Parsons, I. T., and Hunt, R., 1981. Plant growth analysis : a program for the fitting of lengthy series of data by the method of B-splines. *Annals Botany*, 48, 341-352.

Pasciak, W. J., and Gavis, J., 1974. Transport limitation of nutrient uptake in phytoplankton. *Limnology and Oceanography*, 19, 881-888.

Pasciak, W. J., and Gavis, J., 1975. Transport limited nutrient uptake rates in *Ditylum brightwellii*. *Limnology and Oceanography*, 20, 604-617.

Peckol, P., and Searles, R. B., 1983. Effects of seasonality and disturbance on population development in a Carolina continental shelf community. *Bulletin of Marine Science*, 33, 67-86.

Perry, M. J., 1976. Phosphate utilization by an oceanic diatom in phosphorus-limited chemostat culture and in the oligotrophic waters of the central North Pacific. *Limnology and Oceanography*, 21, 88-107.

Polle, E. O., and Jenny, H., 1971. Boundary layer effects in ion absorption by roots and storage organs of plants. *Physiologia Plantarum*, 25, 219-224.

Poorter, H., and Lewis, C., 1986. Testing differences in relative growth rate : A method avoiding curve fitting and pairing. *Physiologia Plantarum*, 76, 223-226.

Prandtl, L., 1905. *"Über Fluss gkeitsbewegung bei sehr kleiner Reibung." Verhandlungen des III: Internationalen Mathematiker-Kongresses.* Leipzig.

Probyn, T. A., and Chapman, A. R. O., 1982. Nitrogen uptake characteristics of *Chordaria flagelliformis* (Phaeophyta) in batch mode and continuous mode experiments. *Marine Biology*, 71, 129-133

Probyn, T. A., and Chapman, A. R. O., 1983. Summer growth of *Chordaria. flagelliformis* (O. F. Muell.) C. Ag. : physiological strategies in a nutrient stressed environment. *Journal of Experimental Marine Biology Ecology*, 73, 243-271.

Provasoli, L., 1958. Effect of plant hormones on *Ulva*. Biology Bulletin Marine Biology Laboratory, 114, 375-384.

Provasoli. L., McLaughlin, J. J., and Droop, M. R., 1957. The development of artificial media for marine algae. *Arch. Mikrobiology*, 25, 392.

Purcell, E. M., 1977. Life at low Reynolds number. *American Journal of Physics*, 45, 3-11.

Pytkowicz, R. M., 1967. Carbonate cycle and the buffer mechanism of recent oceans. *Geochimica et Cosmochimica Acta*, 31, 63-73.

Ramus, J., 1972. Differentiation of the green alga *Codium fragile*. *American Journal of Botany*, 59, 478-482.

Ramus, J., 1972. Differentiation of the green alga *Codium fragile*. *American Journal of Botany*, 59, 478-482.

Ramus, J., 1983. A physiological test of the theory of complementary chromatic adaptation. II: Brown, green and red seaweeds. *Journal of Phycology*, 19, 173-178.

Ramus, J., and Rosenberg, G., 1980. Diurnal photosynthetic performance of seaweeds measured under natural conditions. *Marine Biology*, 56, 21-28.

Raven, J. A., 1974a. Phosphate transport in *Hydrodictyon africanum*. *New Phytologist*, 73, 421-432.

Raven, J. A., 1974b. Energetics of active phosphate influx in *Hydrodictyon africanum*. *Journal of Experimental Botany*, 25, 221-229.

Raven, J. A., 1980. Nutrient transport in microalgae. *Advances in Microbiology Physiology*, 21, 47-226.

Raven, J. A., 1981. Nutritional strategies of submerged benthic plants : the aquisition of C, N and P by rhizophytes and haptophytes. *New Phytologist*, 188, 1-30.

Raven, J., Beardall, J., and Griffiths, H., 1982. Inorganic c-sources for *Lamanea*, *Cladophora* and *Ramuncalius* in a fast flowing stream: Measurements of gas exchange and of carbon isotope ratio and their ecological implications. *Oecologia*, 53, 68-78.

Raven, J. A., and Smith, F. A., 1980. Intracellular pH regulation in the giant-celled marine alga *Chaetomorpha darwinii*. *Journal of Experimental Botany*, 31, 1357-1370.

Raymont, J. E., 1963. *Plankton and productivity in the oceans*. MacMillan, New York.

Rees, G., and Jones, E. B. G., 1984. Observations on the attachment of spores of marine fungi. *Botanica Marina*, 27, 145-160.

Reynolds, O., 1883. An experimental investigation of the circumstances which determine whether the motion of water shall be direct or sinuous, and of the law of resistance. *Transactions of the Royal Society of London*, 174, 935-982.

Rhee, G. Y., 1973. A continuous culture study of phosphate uptake, growth rate and polyphosphate in *Scenedesmus sp. Journal of Phycology*, 9, 495-506.

Rice, D. L., 1984. A simple mass transport model for metal uptake by marine macroalgae growing at different rates. *Journal of Experimental Marine Biology Ecology*, 82, 175-182.

Riedl, R., 1971. *Water movement: Animals*. In Marine Ecology, Vol. 1 Environmental factors pt. 2. Ed. O, Kinne, Wiley-Interscience, New York.

Ritchie, R. J., and Larkum, A. W. D., 1984. Chloride transport in *Enteromorpha intestinalis* (L.) Link. *New Phytologist*, 97, 319-345.

Ritchie, R. J., and Larkum, A. W. D., 1985. Potassium transport in *Entermorpha intestinalis* (L.) Link. *Journal of Experimental Botany*, 36, 63-78.

Roberson J. A., and Crowe, C. T., 1965. *Engineering Fluid Mechanics*. Rudolph Steiner Press, London.

Roberts, H. H., and Suhayda, J. N., 1983., Wave-current interactions on a shallow reef (Nicaragua, Central America). *Coral Reefs*, 1, 209-214.

Rohsenow, W. M., and Choi, H. Y., 1961. *Heat, Mass, and momentum transfer*. Prentice Hall, Engelwood Cliffs, New Jersey.

Rosell, K. -G., and Srivastava, L. M., 1984. Seasonal variation in the chemical constituents of the brown algae *Macrocystis integrifolia* and *Nereocystis luetkeana*. *Canadian Journal of Botany*, 62, 2229-2236.

Rosenberg, G., Probyn, T. A., and Mann, K. H., 1984. Nutrient uptake and growth kinetics in brown seaweeds: Response to continuous and single additions of ammonium. *Journal of Experimental Marine Biology Ecology*, 80, 125-146.

Rosenberg, G., and Ramus, J., 1981. Ecological growth strategies in the seaweeds *Gracilaria foliifera* (Rhodophyceae) and Ulva sp. (Chlorophyceae): The rate and timing of growth. *Botanica Marina*, 24, 583-589.

Rosenberg, G., and Ramus, J., 1982a. Ecological growth strategies in the seaweeds *Gracilaria foliifera* (Rhodophyceae) and *Ulva sp.* (chlorophyceae) : photosynthesis and antenna composition. *Marine Ecology Progress Series*, 8, 233-241.

Rosenberg, G., and Ramus, J., 1982b. Ecological growth strategies in the seaweeds *Gracilaria foliifera* (Rhodophyceae) and *Ulva sp.* (chlorophyceae) : Soluble nitrogen and reserve carbohydrate. *Marine Biology*, 66, 251-259.

Rosenberg, G., and Ramus, J., 1984. Uptake of inorganic nitrogen and seaweed surface area : volume ratios. *Aquatic Botany*, 19, 65-72.

Ruttner, F., 1926. Bemerkungen, uber den Sauerstoffgehalt der Gewasser dessen respiratorischen Wert. *Naturwissenschaften*, 14, 1237-1239.

Ryther, J. H., 1983. Marine biomass research in Florida. *Soil and Crop Science Society, Florida Proceedings*, 42, 40-48.

Ryther, J. H., Corwin, N., DeBusk, T. A., and Williams, L. D., 1981. Nitrogen uptake and storage by the red alga *Gracilaria tikvahiae* (McLachlan, 1979). *Aquaculture*, 26, 107-115.

Sanders, D., 1986. Generalized kinetic analysis of ion-driven cotransport systems : II Random Ligand binding as a simple explanation for non-Michaelian kinetics. *Journal of Membrane Biology*, 90, 67-87.

Santelices, B., 1977. Water movement and seasonal algal growth in Hawaii. *Marine Biology*, 43, 225-236.

Santelices, B., Castilla. J. C., Cancino, J., and Schmiede, P., 1980. Comparative ecology of *Lessonia nigresceus* and *Durvillaea antarctica* Phaeophyta in central Chile. *Marine Biology*, 59, 119-132.

Santelices, B., and Ojeda. F. P., 1984. Recruitment, growth and survival of *Lessonia nigrexens* (Phaeophyta) at various tidal levels in exposed habitats of central Chile. *Marine Ecology Progress Series*, 19, 73-82.

Scavia, D., Fahnenstiel, G. L., Davis, J. A., and Kreis (Jr.), R. G., 1984. Small-scale nutrient patchiness: Some consequences on a new encounter mechanism. *Limnology and Oceanography*, 29, 785-793.

Schjorring, J. K., and Jensen, P., 1984a. Phosphorus nutrition of barley, buckwheat and rape seedlings. I: Influence of seed-borne P, and external P levels on growth, P content and 32P/31P - fractionation in shoots and roots. *Physiologia Plantarum*, 61, 577-583.

Schjorring, J. K., and Jensen, P., 1984b. Phosphorus nutrition of barley, buckwheat and rape seedlings. II: Influx and efflux of phosphorus by intact roots of different P status. *Physiologia Plantarum*, 61, 584-590.

Schlichting, J., 1968. *Boundary layer theory*. McGraw-Hill, New York.

Schonbeck, M. W., and Norton, T. A., 1978. Factors controlling the upper limits of fucoid algae on the shore. *Journal of Experimental Marine Biology Ecology*, 31, 303-313.

Schonbeck, M. W., and Norton, T. A., 1980. The effects on the growth of fucoid algae of some synthetic materials used in the construction of culture apparatus. *Botanica Marina*, 23, 433-434.

Schumacher, G. J., and Whitford, L. A., 1965. Respiration and P32 uptake in various species of freshwater algae as affected by a current. *Journal of Phycology*, 1, 78-80.

Sentenac, H., and Grignon, C., 1985. Effect of pH on orthophosphate uptake by corn roots. *Plant Physiology*, 77, 136-141.

Sentenac, H., and Grignon, C., 1987. Effect of H+ excretion on the surface pH of corn root cells evaluated by using weak acid influx as a pH probe. *Plant Physiology*, 84, 1367-1372.

Sha'afi, R. I., Rich, G. T., Sidel, V. W., Bossert, W., and Solomon, A. K., 1967. The effect of the unstirred layer on human red cell water permeability. *Journal of General Physiology*, 50, 1377-1399.

Shivji, M. S., 1985. Interactive effects of light and nitrogen on growth and chemical composition of juvenile *Macrocystis pyrifera* (L) C. Ag. (Phaeophyta) Sporophytes. *Journal of Experimental Marine Biology Ecology*, 89, 81-96.

Shaw, T. I., 1960. The mechanisms of iodide accumulation by the brown seaweed *Laminaria digitata*. II: Respiration and iodide uptake. *Proceedings of the Royal Society of London, Series B*, 152, 109-117.

Siddiqi, M. Y., and Glass, A. D. M., 1982. Simultaneous consideration of tissue and substrate potassium concentration in K+ uptake kinetics : A model. *Plant Physiology*, 69, 283-285.

Smith, F. A., 1966. Active phosphate uptake by *Nitella translucens*. *Biochimica et Biophysica Acta*, 126, 94-99.

Smith, F. A., and Walker, N. A., 1980. Photosynthesis by aquatic plants: Effects of unstirred layers in relation to assimilation of CO2 and HCO3- and to carbon isotopic discimination. *New Phytologist*, 86, 245-259.

Smith R. E. H., Harrison, W. G., and Harris, L., 1985. Phosphorus exchange in marine microplankton communities near Hawaii. *Marine Biology*, 86, 75-84.

Smith, R. E. H., and Kalff, J., 1982. Size-dependent phosphorus uptake kinetics and cell quota in phytoplankton. *Journal of Phycology*, 18, 275-284.

Smith, S. V., 1984. Phosphorus versus nitrogen limitation in the marine environment. *Limnology and Oceanography*, 29, 1149-1160.

Smulders, A. P., and Wright, E. M., 1971. The magnitude of nonelectrolyte selectivity in the gall bladder epithelium. *Journal of Membrane Biology*, 5, 297-138.

Sober, H. A., 1968. *Handbook Of Chemistry*. The Chemical Rubber Co., Cleveland, Ohio.

Sokal, R. R., and Rohlf, F. J., 1969. *Biometry*. W. H. Freeman and Co. San Francisco.

Sommer, U., 1984. The paradox of the plankton : Fluctuations of phosphorus availability maintain diversity of phytoplankton in flow - through cultures. *Limnology and Oceanography*, 29, 633-636.

Sourina, A., 1982. Form and function in marine phytoplankton. *Biology Review*, 57, 347-394.

Sousa, W. P., 1979a. Disturbance in marine intertidal boulder fields: The non-equilibrium maintenance of species diversity. *Ecology*, 60, 1225-1239.

Sousa, W. P., 1979b. Experimental investigations of disturbance and ecological succession in a rocky intertidal algal community. *Ecological Monographs*, 49, 227-254.

Sperling, J. A., and Grunewald, R., 1969. Batch culturing of thermophilic benthic algae and phosphorus uptake in a laboratory stream model. *Limnology and Oceanography*, 14, 944-949.

Sperling, J. A., and Hale, G. M., 1973. Patterns of radiocarbon uptake by a thermophitic blue-green alga under varying conditions of incubation. *Limnology and Oceanography*, 18, 658-662.

Steffensen, D. A., 1976. The effect of nutrient enrichment and temperature on the growth in culture of *Ulva lactuca* L. *Aquatic Botany*, 2, 337-351.

Strickland, J. D. A., and Parsons, T. R., 1965. A manual of seawater analysis. *Fisheries Research Board Canada*, Bulletin 125, 1-203.

Subbaramaiah, K., 1970. Growth and reproduction of *Ulva fasciata* Delile in nature and in culture. *Botanica Marina*, 13, 25-27.

Sundene, O.,1962. Growth in the sea of *Laminaria digitata* sporophytes from culture. *Nytt Magazin for Botanik* , 9, 5-24.

Sundene, O., 1964. The ecology of *Laminaria digitata* in Norway in view of transport experiments. *Nytt Magazine for Botanikk*, 11, 83-107.

Szabo-Nagy, A., Olah, Z., and Erdei, L., 1987. Phosphatase induction in roots of winter wheat during adaptation to phosphorus deficiency. *Physiologia Plantarum*, 70, 544-552.

Taylor .P. R., and Hay, M. E., 1984. Functional morphology of intertidal seaweeds: Adaptive significance of aggregate vs. solitary forms. *Marine Ecology Progress Series*, 18, 295-302.

Terekhove, T. K., 1973. Effect of surf strength and current speed on the development of White Sea fucoid algae. *Journal of Hydrobiology*, 8, 13-18.

Thirb, H. H., and Benson-Evans, K., 1982. The effect of different current velocities on the red alga *Lemanea* in a laboratory stream. *Archives Hydrobiologia*. 96, 65-72.

Thomas, T. E., and Harrison, P. J., 1985. Effect of nitrogen supply on nitrogen uptake, accumulation and assimilation in *Porphyra perforata* (Rhodophyta). *Marine Biology*, 85, 269-278.

Thomas, T. E., and Harrison, P. J., 1987. Rapid ammonium uptake and nitrogen interactions in five intertidal seaweeds grown under field conditions. *Journal of Experimental Marine Biology Ecology*, 107, 1-8.

Thomson, A. B. R., and Dietschy, J. M., 1977. Derivation of the equations that describe the effects of unstirred water layers on the kinetic parameters of active transport in the intestine. *Journal of Theoretical Biology*, 64, 277-294.

Tilman, D., 1977. Resource competition between Planktonic algae: An experimental and theoretical approach. *Ecology*, 58, 338-348.

Tilman, D., and Kilham, S. S., 1976. Phosphate and silicate growth and uptake kinetics of the diatoms *Asterionella formosa* and *Cyclotella meneghiniana* in batch and semi-continuous culture. *Journal of Phycology*, 12, 375-383.

Tobias, C. W., Eisenberg, M., and Wilke, C. R., 1952. Diffusion and convection in electrolysis: A theoretical review. *Journal of Electrochemical Society*, 99, 359-365.

Topinka, J. A., 1978 .Nitrogen uptake by *Fucus spiralis* (Phaeophyceae). *Journal of Phycology*, 14, 241-247.

Turpin, D. H., and Harrison, P. J., 1979. Limiting nutrient patchiness and its role in phytoplankton ecology. *Journal of Experimental Marine Biology Ecology*, 39, 151-166.

Ullrich-Eberius, C. I., 1973. Die pH - Abhangigkeit der Aurfnahme von H2PO4-, SO4--, Na+, und K+ und ihre gegenseitige beeinflussung bei *Ankistrodesmus braunii*, *Planta*, 109, 161-176.

Ullrich-Eberius, C. I., Novacky, A., Fischer, E., and Luttge, U., 1981. Relationship between energy-dependent phosphate uptake and the electrical membrane potential in *Lemna gibba* G. *Plant Physiology*, 67, 797-801.

Ullrich-Eberius, and C. I., Simonis, W., 1970a. Der Einflub von Natrium- und Kaliumionen auf die Photophosphorylierung bei *Ankistrodesmus braunii*. *Planta*, 92, 358-373.

Ullrich-Eberius, and C. I., Simonis, W., 1970b. Der Einflub von Natrium- und Kaliumionen auf die Phosphataufnahme bei *Ankistrodesmus braunii*. *Planta*, 93, 214-226.

Ullrich-Eberius, C. I., and Yingchol, Y., 1974. Phosphate uptake and its pH dependence in halophytic and glycophytic algae and higher plants. *Oecologia*, 17, 17-26.

Vahl, O., 1971. Growth and density of *Patina pellecida* L. (Gastropoda: Prosobranchia) on *Laminaria hyperborea* (Gunneries) from western Norway. *Ophelia*, 9, 31-50.

Vahl, O., 1972. On the position of *Patina pellucida* gastropoda on the frond of *Laminaria hyperborea*. *Ophelia*, 10, 1-9.

Valiela, I., 1984. *Marine ecological processes*. Springer-Verlag, New York.

Vange, M. S., Holmern, K., and Nissen, P., 1974. Multiphasic uptake of sulfate by barley roots. I: Effects of analogues, phosphate, and pH. *Plant Physiology*, 68, 1433-1438.

Velimirov, B., and Griffiths, C. L., 1979. Wave-induced kelp movement and its importance for community structure. *Botanica Marina*, 22, 169-172.

Vermaat, J. E., and Sand-Jensen, K., 1987. Survival, metabolism and growth of *Ulva lactuca* under winter conditions: a laboratory study of bottle necks in the life-cycle. *Marine Biology*, 95, 55-61.

Vetter, K. J., 1967. *Electrochemical kinetics: Theoretical and experimental aspects*. Academic Press, New York.

Vielstich, W., 1953. Der Zusammenhang zwischen Nernstscher Diffusionsschicht und Prandtlscher Stromungsgrenzschicht. *Zeitschrift fur Elektrochemie*, 57, 646-655.

Vilenkin, B. Ya., and Pertsov, N. A., 1985. Convective mass exchange on surface of unicellular algae. *D. K. B. S. A. S.*, 277, 429-431.

Vogel, S., 1981. *Life in moving fluids: The physical biology of flow*. Willard Grant, Boston, Massachusettes.

Vogel, S., and LaBarbera, M., 1978. Simple flow tanks for research and teaching. *Bioscience*, 28, 638-643.

Vogel, S., and London, C., 1985. Fluid mechanics of the thallus of an intertidal red alga, *Halosaccion glandiforme*. *Biology Bulletin*, 168, 161-174.

Von Karman, T., 1954. *Aerodynamics*. McGraw-Hill, New York.

Waite, T., and Mitchell, R., 1972. The effect of nutrient fertilization on the benthic alga *Ulva lactuca*. *Botanica Marina*, 15, 151-156.

Wagner, C., 1949. The role of natural convection in electrolytic processes. *Transcript of the Electrochemical Society*, 95, 161-173.

Walker, N. A., Smith, F. A., and Cathers, I. R., 1980. Bicarbonate assimiliation by fresh-water *Charophytes* and higher plants. I: Membrane transport of bicarbonate ions is not proven. *Journal of Membrane Biology*, 57, 51-58.

Wallentinus, I., 1978. Productivity studies on Baltic macroalgae. *Botanica Marina*, 21, 365-380.

Wallentinns, I., 1984. Comparisons of nutrient uptake rates for Baltic macroalgae with different thallus morphologies. *Marine Biology*, 80, 215-225.

Watts, C. J., and. Nduku, W. K., 1981. Loss of nutrients from water samples by filtration and its affect on algal bioassay procedures. *Journal of Limnology Society South Africa*, 6, 77-81.

Werner, I., and Weise, G., 1982. Biomass production of submerged macrophytes in a selected stretch of the river Zschopan (South G. D. R) with special regard to orthophosphate incorporation. *International Review Ges. Hydrobiolie*, 67, 45-62.

West, K. R., and Pitman, M. G., 1967. Ionic relations and ultrastructure in *Ulva lactuca*. *Australian Journal of Biology Science*. 20, 901-914.

Westlake, D. F. 1967. Some effects of low-velocity currents on the metabolism of aquatic macrophytes. *Journal of Experimental Botany*, 18, 187-205.

Wheeler, P. A., 1979. Uptake of methylamine (an ammonium analogue) by *Macrocystis pyrifera* (Phaeophyta). *Journal of Phycology*, 15, 12-17.

Wheeler, P. A., and North, W. J., 1981. Effect of nitrogen supply on nitrogen content and growth rate of juvenile *Macrocystis pyrifera* (Phaeophyta) sporophytes. *Journal of Phycology*, 16, 577-582.

Wheeler, W. N., 1976. Ecological studies in kelp forests factors influencing productivity. *Journal of Phycology*, 12, 14.

Wheeler, W. N., 1977. The interrelationship between light, water velocity and macronutrients in the productivity of the giant kelp *Macrocystis*. *Proceedings International Seaweed Symposium*, 9.

Wheeler, W. N., 1980. Effect of boundary layer transport on the fixation of carbon by the giant kelp *Macrocystis pyrifera*. *Marine Biology*, 56, 103-110.

Wheeler, W. N., 1981. Laboratory and field studies of photosynthesis in the marine crop plant *Macrocystis*. *Proceedings International Seaweed Symposium*, 8, 264-271.

Wheeler, W. N., and Neushul, M., 1981. *The Aquatic Environment in Physiological plant ecology. I: Responses to the physical environment*. Eds. O. L. Lange, P. S. Nobel, C. B. Osmond and H. Zeigler, Springer-Verlag, Berlin, Heidelberg, London.

Wheeler, W. N., and Weidner, M., 1983. Effects of external inorganic nitrogen concentration on metabolism, growth and activities of key carbon and nitrogen assimilatory enzymes of *Laminaria*. *Journal of Phycology*, 19, 92-96.

Wheeler, W. N., and Srivastava, L. M., 1984. Seasonal nitrate physiology of *Macrocystis integrifolia* Bory. *Journal of Experimental Marine Biology Ecology*, 76, 35-50.

Whitfield, M., 1975. The extension of chemical models for seawater to include trace components at 25 C and 1 atm. pressure. *Geochimica et Cosmochimica Acta*, 39, 1545-1557.

Whitford, L. A., 1960. The current effect and growth of freshwater algae. *Transactions of the American Microscopy Society*, 79, 302-309.

Whitford, L. A., and Kim, C. S., 1966. The effect of light and water movement on some species of marine algae. *Revue Algologique*, 8, 251-254.

Whitford, L. A., and Schumacher, G. J., 1961. Effect of current in mineral uptake and respiration by freshwater algae. *Limnology and Oceanography*, 6, 423-425.

Whitford, L. A., and Schumacher, G. J., 1964. Effect of a current on respiration and mineral uptake in *Spirogyra* and *Oedogonium*. *Ecology*, 45, 168-170.

Wilke, C. R., Eisenberg, M., and Tobias, C. W., 1953. Correlation of Limiting Currents under Free Convection Conditions. *Journal of the Electrochemical Society*, 100, 513-523.

Williams, J. B., and Kutchai, H., 1986. Use of a membrane-bound fluorophore to characterize diffusion boundary layers around human erythrocytes. *Biophysics Journal*, 49, 453-458.

Wilson, F. A., and Dietschy, J. M., 1974. The intestinal unstirred layer : its surface area and effect on active transport kinetics. *Biochimica et Biophysica Acta*. 363, 112-126.

Wilson, J. W., Hunt, R., and Hand, D. W., 1986. Philosophical aspects of measurements, equations and interferences in plant growth studies. *Annals of Botany*, 58, 73-80.

Winne, D., 1973. Unstirred layer, source of biased Michaelis constant in membrane transport. *Biochimica et Biophysica Acta*, 298, 27-31.

Winne, D., 1977. Correction of the apparent Michaelis constant, biased by an unstirred layer, if a passive transport component is present. *Biochimica et Biophysica Acta*, 464, 118-126.

Womersley, H. B. S., 1984. *The marine benthic flora of Southern Australia, Part 1*. South Australian Goverment Printer, Adelaide.